

MODELING OF SO₂ EMISSIONS FROM
YATAĞAN POWER PLANT

739094

by

Ulaş İm

B.S. in Env. E., Yıldız Technical University, 2000

Submitted to the Institute of Environmental Sciences in partial fulfillment of
the requirements for the degree of

Master of Science

In

Environmental Technologies

Boğaziçi University

2003

TC YÜKSEKÖĞRETİM KURULU
DOKÜMANTASYON MERKEZİ

739094

MODELING OF SO₂ EMISSIONS FROM
YATAĞAN POWER PLANT

APPROVED BY:

Prof. Dr. Orhan Yenigün.....

(Thesis Supervisor)

Prof. Dr. Selahattin İncecik.....

Assist. Prof. Dr. Nadim Copty.....

DATE OF APPROVAL: 10.09.2003.....

ACKNOWLEDGEMENTS

I would like to forward my appreciations and thanks to Prof. Dr. Orhan YENİGÜN for his help, courage and support during my thesis.

I would like to express my sincere gratitude to my jury members Prof. Dr. Selahattin İNCECİK, and Assist. Prof. Nadim COPTY for spending their valuable time and for their help and support throughout my thesis.

I would like to thank Mr. Mark GARRISON for his help and support for the technical parts of my thesis and for spending his valuable time.

Finally, I wish to dedicate this thesis to my beloved parents Kıvılcım ARSLAN and Ömer İM, and also my dearest friend Esra ORUÇ for the support, love and courage that they give throughout my thesis and life.

ABSTRACT**MODELING OF SO₂ EMISSIONS FROM
YATAĞAN POWER PLANT**

The meteorological model, CALMET, and its plume dispersion model, CALPUFF, were used in order to simulate the dispersion of SO₂ emitted from Yatağan Power Plant and its effect on Yatağan district in the episodic event on December 2 and 3, 2000. CALMET was used to predict the hourly meteorological fields for 96 hours, starting from December 1, 2000, to December 4, 2000, while CALPUFF was used to predict the hourly ground level SO₂ concentrations over a region of 15 km x 15 km grid with 1 km resolution. The meteorological data were obtained from two meteorological stations: surface data from Yatağan Meteorological Station, and upper air data from Isparta Meteorological Station. The emission data was taken from Yatağan Power Plant. It is found that south westerly and light winds and the nighttime surface inversion layers lead to accumulation of pollutants over Yatağan district. The results are compared with the measurements done by Local Environmental Authorities of Muğla. The simulation results indicate that the maximum ground level concentrations were found northeast from the source, which agrees with experimental measurement. On the other hand, the magnitude of results obtained with the model shows some differences compared with experimental measurements. The SO₂ concentration levels are calculated to be very high in the morning hours of December 2 and 3, 2000. Overall, the results indicate that Yatağan district suffered seriously on these days. The sensitivity analysis showed that the concentrations are directly proportional to the emission rates, but wind speed is the most significant meteorological parameter on air pollution modeling compared to other meteorological parameters.

ÖZET

YATAĞAN TERMİK SANTRALİNDEN KAYNAKLANAN SO₂ EMİSYONLARININ MODELLENMESİ


Bu çalışmada, 2 ve 3 Aralık 2000 tarihlerinde, Yatağan Termik Santralinden kaynaklanan SO₂ kirliliği, CALMET meteoroloji modeli ve CALPUFF duman dağılım modeli kullanılarak modellenmiştir. CALMET 96 saatlik meteorolojik alanları, CALPUFF da saatlik SO₂ konsantrasyonlarını tahmin etmek için kullanılmıştır. Model alanı doğu – batı ve kuzey – güney yönlerinde 15' er km olarak seçilmiş ve alan 1 km'lik gridlere ayrılmıştır. Meteorolojik datalar, yer seviyesi dataları Yatağan Meteoroloji İstasyonu, sondaj dataları ise Isparta Meteoroloji İstasyonundan alınmıştır. Emisyon verileri Yatağan Termik Santralinden alınmıştır. Sonuç olarak, güney batıdan, düşük hızlarla esen rüzgarlar ve gece saatlerinde oluşan inversiyon tabakalarının, kirleticilerin yüksek konsantrasyonlarda, Yatağan ilçesi üzerinde hapis olmasına sebep olmasına sebep olduğu çıkarılmıştır. Model sonuçları, Muğla İl Çevre Müdürlüğü'nce yapılan ölçüm sonuçları ile karşılaştırılmıştır. Model sonuçlarına göre, kirleticiler, kaynağın kuzey doğu tarafında birikmiştir ve bu sonuç, ölçümlerce de doğrulanmıştır. Ancak, model sonuçları ile ölçüm sonuçları arasında, büyüklük açısından farklar görülmüştür. 2 ve 3 Aralık 2000 günlerinin sabah saatlerinde, SO₂ konsantrasyonlarının yüksek değerlere ulaştığı görülmüş ve Yatağan ilçesinin bu kirlilikten ciddi bir biçimde etkilendiği sonucuna varılmıştır. Hassasiyet analizleri, konsantrasyonların emisyonlarla doğru orantili olduğunu, ancak rüzgar hızının, diğer meteorolojik parametrelere kıyasla çok daha önemli bir parametre olduğunu ortaya koymuştur.

TABLE OF CONTENTS

ACKNOWLEDGEMENTS	iii
ABSTRACT	iv
ÖZET	v
LIST OF FIGURES	ix
LIST OF TABLES	xx
LIST OF SYMBOLS	xxi
1. INTRODUCTION	1
2. THEORETICAL BACKGROUND ON AIR POLLUTION MODELING	
2.1. Fundamentals of Air Pollution Modeling	3
2.2. Plume Rise	5
2.2.1. Stack Downwash	6
2.2.2. Buoyancy Flux Parameter	6
2.2.3. Unstable – Neutral Buoyancy Plume Rise	6
2.2.4. Stability Parameter	7
2.2.5. Stable Buoyancy Plume Rise	7
2.2.6. Gradual Rise – Buoyancy Conditions	8
2.2.7. Unstable – Neutral Momentum Plume Rise	8
2.3. Meteorology of Air Pollution	
2.3.1. Planetary Boundary Layer	8
2.3.2. Mixed Layer	10
2.3.3. Residual Layer	12
2.3.4. Stable Boundary Layer	13
2.4. PBL Parameters	
2.4.1. PBL Height	14
2.4.2. The Mixing Height	15
2.4.3. The Roughness Length	15
2.4.4. Monin – Obukhov Length	15
2.4.5. Stability and the Pasquill Stability Classes	16

2.5. Transport and Dispersion of Air Pollutants	
2.5.1. Wind	18
2.5.2. Effect of Direction	19
2.5.3. Effect of Speed	19
2.5.4. Turbulence	20
2.6. Basic Equations of Atmospheric Fluid Mechanics	21
2.6.1. The Gaussian Plume Model	24
2.7. Dry and Wet Deposition	26
2.7.1. Dry Deposition	26
2.7.2. Wet Deposition	27
2.8. The Atmospheric Chemistry of Sulphur in Power Station Plumes	29
8.1. Gas – Phase Oxidation of Sulphur Dioxide	29
8.2. Removal of Sulphur by Wet and Dry Deposition	29
3. OVERVIEW OF THE MATHEMATICAL MODEL	31
3.1. CALMET	31
3.1.1. Data Requirements of CALMET	33
3.1.2. Technical Description of the CALMET Meteorological Model	34
3.2. CALPUFF	37
3.2.1. Major Features and Options of CALPUFF	37
3.2.2. Data requirements of CALPUFF	39
3.3. CALPOST	40
4. STUDY AREA AND SOURCE CHARACTERISTICS	
4.1. Topographical Data	41
4.2. Meteorological Data	43
4.3. Source Characteristics	44
5. RESULTS AND DISCUSSION	
5.1. Simulation of the Episodic Event on 2 nd and 3 rd of December 2000	46
5.2. Simulations of Different Scenarios	68
5.2.1. Simulation of Scenario 1	68
5.2.2. Simulation of Scenario 2	82

5.2.3. Simulation of Scenario 3	95
5.3. Sensitivity Analysis	114
6. Conclusions and Recommendations	118
REFERENCES	120
REFERENCES NOT CITED	122
APPENDIX I	123
APPENDIX II	127
APPENDIX III	140
APPENDIX IV	158
APPENDIX V	159
APPENDIX VI	160
APPENDIX VII	161
APPENDIX VIII	162



LIST OF FIGURES

Figure 2.1. Major parts of the Planetary Boundary Layer (PBL)	10
Figure 2.2. Typical daytime profiles of mean virtual potential temperature, wind speed, water vapor mixing ratio, and pollutant concentration	11
Figure 2.3. A relationship between L and z_0 for various Pasquill stability classes	18
Figure 2.4. Eulerian and Lagrangian reference systems for the atmospheric motion	22
Figure 2.5. The Gaussian plume in a wind – oriented coordinate system	25
Figure 2.6. Conceptual framework of wet deposition processes	28
Figure 4.1. Contour map of the modeling area	42
Figure 4.2. 3D view of the modeling area	42
Figure 4.3. Land use types of the modeling region	43
Figure 5.1. Original Case: Wind field for the modeling area at 07:00 on December 1, 2000	47
Figure 5.2. Wind field for the modeling area at 15:00 on December 1, 2000	47
Figure 5.3. Wind field for the modeling area at 23:00 on December 1, 2000	48
Figure 5.4. Wind field for the modeling area at 07:00 on December 2, 2000	48

Figure 5.5. Wind field for the modeling area at 15:00 on December 2, 2000	49
Figure 5.6. Wind field for the modeling area at 23:00 on December 2, 2000	49
Figure 5.7. Wind field for the modeling area at 07:00 on December 3, 2000	50
Figure 5.8. Wind field for the modeling area at 15:00 on December 3, 2000	50
Figure 5.9. Wind field for the modeling area at 23:00 on December 3, 2000	51
Figure 5.10. Wind field for the modeling area at 07:00 on December 4, 2000	51
Figure 5.11. Wind field for the modeling area at 15:00 on December 4, 2000	52
Figure 5.12. Wind field for the modeling area at 23:00 on December 4, 2000	52
Figure 5.13. Concentration distribution for the modeling area at 07:00 on December 1, 2000	55
Figure 5.14. Concentration distribution for the modeling area at 15:00 on December 1, 2000	56
Figure 5.15. Concentration distribution for the modeling area at 23:00 on December 1, 2000	56
Figure 5.16. Concentration distribution for the modeling area at 07:00 on December 2, 2000	57
Figure 5.17. Concentration distribution for the modeling area at 15:00 on December 2, 2000	57

Figure 5.18. Concentration distribution for the modeling area at 23:00 on December 2, 2000	58
Figure 5.19. Concentration distribution for the modeling area at 07:00 on December 3, 2000	58
Figure 5.20. Concentration distribution for the modeling area at 15:00 on December 3, 2000	59
Figure 5.21. Concentration distribution for the modeling area at 23:00 on December 3, 2000	59
Figure 5.22. Concentration distribution for the modeling area at 07:00 on December 4,2000	60
Figure 5.23. Concentration distribution for the modeling area at 15:00 on December 4, 2000	60
Figure 5.24. Concentration distribution for the modeling area at 23:00 on December 4, 2000	61
Figure 5.25. Concentration distribution (μgm^{-3}) at 07 :00 on December 1, 2000	61
Figure 5.26. Concentration distribution (μgm^{-3}) at 15 :00 on December 1, 2000	62
Figure 5.27. Concentration distribution (μgm^{-3}) at 23 :00 on December 1, 2000	62
Figure 5.28. Concentration distribution (μgm^{-3}) at 07 :00 on December 2, 2000	63
Figure 5.29. Concentration distribution (μgm^{-3}) at 15 :00 on December 2, 2000	63

Figure 5.30. Concentration distribution (μgm^{-3}) at 23 :00 on December 2, 2000	64
Figure 5.31. Concentration distribution (μgm^{-3}) at 07 :00 on December 3, 2000	64
Figure 5.32. Concentration distribution (μgm^{-3}) at 15 :00 on December 3, 2000	65
Figure 5.33. Concentration distribution (μgm^{-3}) at 23 :00 on December 3, 2000	65
Figure 5.34. Concentration distribution (μgm^{-3}) at 07 :00 on December 4, 2000	66
Figure 5.35. Concentration distribution (μgm^{-3}) at 15 :00 on December 4, 2000	66
Figure 5.36. Concentration distribution (μgm^{-3}) at 23 :00 on December 4, 2000	67
Figure 5.37. The maximum concentrations over Yatağan during the simulation period	67
Figure 5.38. Scenario 1: Concentration distribution for the modeling area at 07:00 on December 1, 2000	69
Figure 5.39. Concentration distribution for the modeling area at 15:00 on December 1, 2000	69
Figure 5.40. Concentration distribution for the modeling area at 23:00 on December 1, 2000	70
Figure 5.41. Concentration distribution for the modeling area at 07:00 on December 2, 2000	70

Figure 5.42. Concentration distribution for the modeling area at 15:00 on December 2, 2000	71
Figure 5.43. Concentration distribution for the modeling area at 23:00 on December 2, 2000	71
Figure 5.44. Concentration distribution for the modeling area at 07:00 on December 3, 2000	72
Figure 5.45. Concentration distribution for the modeling area at 15:00 on December 3, 2000	72
Figure 5.46. Concentration distribution for the modeling area at 23:00 on December 3, 2000	73
Figure 5.47. Concentration distribution for the modeling area at 07:00 on December 4, 2000	73
Figure 5.48. Concentration distribution for the modeling area at 15:00 on December 4, 2000	74
Figure 5.49. Concentration distribution for the modeling area at 23:00 on December 4, 2000	74
Figure 5.50 Concentration distribution (μgm^{-3}) at 07:00 on December 1, 2000	75
Figure 5.51 Concentration distribution (μgm^{-3}) at 15:00 on December 1, 2000	75
Figure 5.52 Concentration distribution (μgm^{-3}) at 23:00 on December 1, 2000	76
Figure 5.53 Concentration distribution (μgm^{-3}) at 07:00 on December 2, 2000	76

Figure 5.54 Concentration distribution (μgm^{-3}) at 15:00 on December 2, 2000	77
Figure 5.55 Concentration distribution (μgm^{-3}) at 23:00 on December 2, 2000	77
Figure 5.56 Concentration distribution (μgm^{-3}) at 07:00 on December 3, 2000	78
Figure 5.57 Concentration distribution (μgm^{-3}) at 15:00 on December 3, 2000	78
Figure 5.58 Concentration distribution (μgm^{-3}) at 23:00 on December 3, 2000	79
Figure 5.59 Concentration distribution (μgm^{-3}) at 07:00 on December 4, 2000	79
Figure 5.60 Concentration distribution (μgm^{-3}) at 15:00 on December 4, 2000	80
Figure 5.61 Concentration distribution (μgm^{-3}) at 23:00 on December 4, 2000	80
Figure 5.62. The maximum concentrations over Yatağan for Scenario 1	81
Figure 5.63. Scenario 2: Concentration distribution for the modeling area at 07:00 on December 1, 2000	82
Figure 5.64. Concentration distribution for the modeling area at 15:00 on December 1, 2000	83
Figure 5.65. Concentration distribution for the modeling area at 23:00 on December 1, 2000	83
Figure 5.66. Concentration distribution for the modeling area at 07:00 on December 2, 2000	84

Figure 5.67. Concentration distribution for the modeling area at 15:00 on December 2, 2000	84
Figure 5.68. Concentration distribution for the modeling area at 23:00 on December 2, 2000	85
Figure 5.69. Concentration distribution for the modeling area at 07:00 on December 3, 2000	85
Figure 5.70. Concentration distribution for the modeling area at 15:00 on December 3, 2000	86
Figure 5.71. Concentration distribution for the modeling area at 23:00 on December 3, 2000	86
Figure 5.72. Concentration distribution for the modeling area at 07:00 on December 4, 2000	87
Figure 5.73. Concentration distribution for the modeling area at 15:00 on December 4, 2000	87
Figure 5.74. Concentration distribution for the modeling area at 23:00 on December 4, 2000	88
Figure 5.75. Concentration distribution (μgm^{-3}) at 07:00 on December 1, 2000	88
Figure 5.76. Concentration distribution (μgm^{-3}) at 15:00 on December 1, 2000	89
Figure 5.77. Concentration distribution (μgm^{-3}) at 23:00 on December 1, 2000	89

Figure 5.78. Concentration distribution (μgm^{-3}) at 07:00 on December 2, 2000	90
Figure 5.79. Concentration distribution (μgm^{-3}) at 15:00 on December 2, 2000	90
Figure 5.80. Concentration distribution (μgm^{-3}) at 23:00 on December 2, 2000	91
Figure 5.81. Concentration distribution (μgm^{-3}) at 07:00 on December 3, 2000	91
Figure 5.82. Concentration distribution (μgm^{-3}) at 15:00 on December 3, 2000	92
Figure 5.83. Concentration distribution (μgm^{-3}) at 23:00 on December 3, 2000	92
Figure 5.84. Concentration distribution (μgm^{-3}) at 07:00 on December 4, 2000	93
Figure 5.85. Concentration distribution (μgm^{-3}) at 15:00 on December 4, 2000	93
Figure 5.86. Concentration distribution (μgm^{-3}) at 23:00 on December 4, 2000	94
Figure 5.87. Maximum concentration levels over Yatağan for Scenario 2	94
Figure 5.88. Scenario 3: Wind field for the modeling area at 07:00 on December 1, 2000	95
Figure 5.89. Wind field for the modeling area at 15:00 on December 1, 2000	96
Figure 5.90. Wind field for the modeling area at 23:00 on December 1, 2000	96
Figure 5.91. Wind field for the modeling area at 07:00 on December 2, 2000	97
Figure 5.92. Wind field for the modeling area at 15:00 on December 2, 2000	97

Figure 5.93. Wind field for the modeling area at 23:00 on December 2, 2000	98
Figure 5.94. Wind field for the modeling area at 07:00 on December 3, 2000	98
Figure 5.95. Wind field for the modeling area at 15:00 on December 3, 2000	99
Figure 5.96. Wind field for the modeling area at 23:00 on December 3, 2000	99
Figure 5.97. Wind field for the modeling area at 07:00 on December 4, 2000	100
Figure 5.98. Wind field for the modeling area at 15:00 on December 4, 2000	100
Figure 5.99. Wind field for the modeling area at 23:00 on December 4, 2000	101
Figure 5.100. Concentration distribution for the modeling area at 07:00 on December 1, 2000	101
Figure 5.101. Concentration distribution for the modeling area at 15:00 on December 1, 2000	102
Figure 5.102. Concentration distribution for the modeling area at 23:00 on December 1, 2000	102
Figure 5.103. Concentration distribution for the modeling area at 07:00 on December 2, 2000	103
Figure 5.104. Concentration distribution for the modeling area at 15:00 on December 2, 2000	103
Figure 5.105. Concentration distribution for the modeling area at 23:00 on December 2, 2000	104

Figure 5.106. Concentration distribution for the modeling area at 07:00 on December 3, 2000	104
Figure 5.107. Concentration distribution for the modeling area at 15:00 on December 3, 2000	105
Figure 5.108. Concentration distribution for the modeling area at 23:00 on December 3, 2000	105
Figure 5.109. Concentration distribution for the modeling area at 07:00 on December 4, 2000	106
Figure 5.110. Concentration distribution for the modeling area at 15:00 on December 4, 2000	106
Figure 5.111. Concentration distribution for the modeling area at 23:00 on December 4, 2000	107
Figure 5.112. Concentration distribution (μgm^{-3}) at 07:00 on December 1, 2000	107
Figure 5.113. Concentration distribution (μgm^{-3}) at 15:00 on December 1, 2000	108
Figure 5.114. Concentration distribution (μgm^{-3}) at 23:00 on December 1, 2000	108
Figure 5.115. Concentration distribution (μgm^{-3}) at 07:00 on December 2, 2000	109
Figure 5.116. Concentration distribution (μgm^{-3}) at 15:00 on December 2, 2000	109
Figure 5.117. Concentration distribution (μgm^{-3}) at 23:00 on December 2, 2000	110

Figure 5.118. Concentration distribution (μgm^{-3}) at 07:00 on December 3, 2000	110
Figure 5.119. Concentration distribution (μgm^{-3}) at 15:00 on December 3, 2000	111
Figure 5.120. Concentration distribution (μgm^{-3}) at 23:00 on December 3, 2000	111
Figure 5.121. Concentration distribution (μgm^{-3}) at 07:00 on December 4, 2000	112
Figure 5.122. Concentration distribution (μgm^{-3}) at 15:00 on December 4, 2000	112
Figure 5.123. Concentration distribution (μgm^{-3}) at 23:00 on December 4, 2000	113
Figure 5.124. Maximum concentrations levels over Yatağan for Scenario 3	113
Figure 5.125. Concentration levels over Yatağan district on December 2 at 15:00	116
Figure 5.126. Concentration levels over Yatağan district on December 2 at 15:00	117
Figure 5.127. Concentration levels over Yatağan district on December 2 at 15:00	117
Figure 5.128. Concentration levels over Yatağan district on December 2 at 15:00	117

LIST OF TABLES

Table 2.1. Roughness lengths for various surfaces	16
Table 2.2. Estimation of Pasquill Stability Classes	17
Table 3.1. Major features of CALMET Meteorological Model	33
Table 3.2. Major features of CALPUFF	38
Table 3.3. The input data used by CALPUFF	39
Table 4.1. Specifications of lignite used in the plant	44
Table 4.2. Emission characteristics of Yatağan Power Plant	45
Table 5.1. Concentration levels over Yatağan district on December 2 at 15:00	114
Table 5.2. Concentration levels over Yatağan district on December 2 at 15:00	114
Table 5.3. Concentration levels over Yatağan district on December 2 at 15:00	115
Table 5.4. Concentration levels over Yatağan district on December 2 at 15:00	115

LIST OF SYMBOLS

C	Pollutant concentration
C	Pollutant concentration
C_{DN}	Neutral drag coefficient
c_p	specific heat at constant pressure
d	Inside – stack top diameter
D	Molecular diffusivity
d_p	Particle diameter
f	Coriolis parameter
F	Pollutant deposition flux
F	Buoyancy flux parameter
Fr	Froude number
g	Acceleration due to gravity
h	Stack height
H	Effective plume height
k	von Karman constant
K	Thermal conductivity
K_x	Eddy diffusivity coefficient along the x direction
K_y	Eddy diffusivity coefficient along the y direction
K_z	Eddy diffusivity coefficient along the z direction
L	Monin – Obukhov length
N	Brunt – Vaisala frequency
Q	Heat generated by any sources in the fluid
Q^*	Net radiation
Q_e	Latent heat flux
Q_f	Anthropogenic heat flux
Q_g	the storage / soil heat flux
Q_h	Sensible heat flux
R	Removal term
S	Source term
T	Ambient air temperature

T_s	Stack gas temperature
u	Wind speed
x	Source – to – receptor distance
x^*	Horizontal distance at which atmospheric turbulence begins to dominate entrainment
x_f	Horizontal distance from the stack
u	Wind component along x axis
U	Internal energy per unit mass
u^*	Friction velocity
u_a	Wind speed at anemometer height
u_z	Wind speed at vertical height z above ground
v	Wind component along y axis
v_s	Stack gas exit velocity
V_d	Deposition velocity
w	Wind component along z axis
W_g	Wet deposition rate of gases
W_p	Wet deposition rate of particles
w^*	Convective velocity scale
z_0	Roughness length
z_a	Anemometer height
z_i	PBL height
$\Delta\theta / \Delta z$	Change in potential temperature with height
ρ	Air density
γ_d	Dry adiabatic lapse rate
γ	Atmospheric lapse rate
ε	Average height of the obstacles in the study area
∇	Gradient operator
μ	Fluid viscosity
δ_{ij}	Kronecker delta
Φ	Heat generated per unit volume and time as a result of viscous dissipation
Λ	Washout coefficient

ψ_1	Potential temperature lapse in layer above h_t
θ	Temperature jump at the top of the mixed layer
ψ_m	Stability correction function



1. INTRODUCTION

The impacts of air pollution are usually estimated through the use of air quality simulation models. These models are usually distinguished by type of source, pollutant, transformations and removal, distance of transport, and averaging time. Air pollution modeling is widely used in studying the relationship between air quality, emission sources and meteorology. In its simplest form, a model requires two types of data inputs: information on the source or sources including pollutant emission rate, and meteorological data such as wind velocity and turbulence. The model then simulates mathematically the pollutant's transport and dispersion, and depending on the aim, its chemical and physical transformations and removal processes. The model output is air pollutant concentration for a particular time period, usually at specific receptor locations.

Power plants play an important role in emitting a significant fraction of SO₂ to the atmosphere. Several scientists have studied the SO₂ pollution produced by power plants before (Garcia and Leon, 1999; Hewitt C. N., 2001; Ames *et al.*, 2002). The Yatağan Power Plant has lead to episodic events in recent years. The plant is located in a very complex topography and close to Yatağan district. The mountains surrounding the region behave as natural barriers that trap the pollutants in the region as well as light winds and stable conditions that lead to surface inversions. Therefore, Yatağan seriously suffers from the SO₂ pollution produced by Yatağan Power Plant.

Such a case has happened on December 2 and 3, 2000. Light winds and surface inversions resulted with the accumulation of SO₂ over Yatağan district and lead to ground level concentrations reaching values around 8 to 9 times higher than the limits prescribed in legislations.

In this study, the episodic case is simulated using the CALPUFF modeling system. The system includes three main programs: the meteorological model CALMET, the dispersion model CALPUFF, and the post processing model CALPOST. The CALPUFF modeling system was developed by Sigma Research Corporation (now part of Earth Tech. Inc.) and sponsored by California Air Resources Board.

The meteorological data are obtained from two meteorological stations, surface data from Yatağan Meteorological Station, and upper air data from Isparta Meteorological Station. The meteorological data were then processed by CALMET Meteorological Model, and wind fields were produced. These fields are then used as input to the CALPUFF Dispersion Model. The emission data required by CALPUFF are obtained from Yatağan Power Plant.

This study presents the simulation of the dispersion of SO₂ under light winds and stable conditions and provides a basis for the prediction of the results of possible future scenarios.



2. THEOROTICAL BACKGROUND ON AIR POLLUTION MODELING

2.1. Fundamentals of Air Pollution Modeling

In order to build new facilities or expand existing ones without harming the environment, it is desirable to assess the air pollution impact of a facility prior to its construction, rather than construct and monitor to determine the impact whether it is necessary to retrofit additional controls. Potential air pollution impact is usually estimated through the use of air quality simulation models. These models are usually distinguished by type of source, pollutant, transformations and removal, distance of transport, and averaging time.

In its simplest form, a model requires two types of data inputs: information on the source or sources including pollutant emission rate, and meteorological data such as wind velocity and turbulence. The model then simulates mathematically the pollutant's transport and dispersion, and depending on the aim, its chemical and physical transformations and removal processes. The model output is air pollutant concentration for a particular time period, usually at specific receptor locations (Stern *et al.*, 1988).

Air pollution modeling is a unique tool for most of the air pollution studies. Air pollution modeling is widely used on studying the relationship between air quality, emission sources and meteorology. These models involve the conservation of mass equation that describes advection, turbulence, diffusion, chemical reactions, and emissions of pollutants. The models are a unique tool for:

- establishing emission control legislation; i.e. determining the maximum allowable emission rates that will meet fixed air quality standards
- evaluating proposed emission control techniques and strategies; i.e. evaluating the impacts of future control
- selecting locations of future sources of pollutants in order to minimize their environmental impacts

- planning the control of air pollution episodes; i.e. defining intermediate intervention strategies, (such as warning systems short – term emission reduction strategies) to avoid severe air pollution episodes in a certain region
- assessing responsibility for existing air pollution levels; i.e. evaluating present source – receptor relationships.

Models can be divided into

- physical models – small scale, laboratory representations of the phenomena (e.g., wind tunnel, water tank)
- mathematical models – a set of analytical / numerical algorithms that describe the physical and chemical aspects of the problem

Mathematical models can be

- deterministic models, based on fundamental mathematical descriptions of atmospheric processes, in which effects (i.e., air pollution) are generated by causes (i.e., emissions)
- statistical models, based upon semiempirical statistical relations among available data and measurements

It is important to clarify what air quality modeling is and what it is not. Air quality modeling is only a tool; it is not the solution of the air pollution problem. Modeling and monitoring studies constitute only a relatively inexpensive activity whose results, in the best case, provide useful information for possible future implementations of much more expensive emission reduction and control strategies.

Simulation modeling techniques can be applied to all aspects of the air pollution problem; such as: (1) to evaluate emission rates, (2) to describe to phenomena that take place in the atmosphere, and (3) to quantify adverse pollution effects (damage computation) in a certain region.

Practical application of air quality models requires

- analysis of the problem
- selection of the appropriate model(s)
- application of the selected model(s)

The analysis of the problem requires the identification of

- the type of pollutant (reactive or nonreactive)
- the averaging time of interest (e.g., instantaneous concentrations, for odor problems; one – hour averages, for short – term cases; or annual averages, for long term analyses)
- the characteristics of the domain (e.g., simple flat terrain cases or complex orography)
- the computational limitations (e.g., simple assumptions or more complex formulations, depending on the available computational facilities)

Finally, the optimal application of a deterministic model for control strategy analysis should incorporate its calibration and evaluation with local air quality monitoring data, in order to determine its applicability and minimize forecasting errors (Zannetti P., 1990).

2.2. Plume Rise

Gases emitted from stacks rise higher than the stack top when they are either of lower density than the surrounding air (buoyancy rise) or ejected at a velocity high enough to give the exit gases upward kinetic energy (momentum rise). Buoyancy rise is sometimes called *thermal rise* because the most common cause of lower density is higher temperature. Exceptions are emissions of gases of higher density than the surrounding air and stack downwash. To estimate effective plume height, equations of Briggs are used. The wind speed u in the following equations is the measured or estimated wind speed at the physical stack top.

2.2.1. Stack Downwash

The lowering below the stack top of portions of the plume by vortices shed downwind of the stack is simulated by using a value h' , m, in place of the physical stack height h . This is somewhat less than the physical height when the stack gas exit velocity v_s is less than 1.5 times the wind speed u , m s^{-1} (Stern *et al.*, 1984):

$$\begin{aligned} h' &= h \text{ for } v_s \geq 1.5 u \\ &= h + 2 d [(v_s / u) - 1.5] \text{ for } v_s < 1.5 u \end{aligned} \quad (2.1)$$

where d is the inside – stack top diameter, m. h' value is used with the buoyancy or the momentum plume rise equations. If stack downwash is not considered, h is substituted for h' in the equations.

2.2.2. Buoyancy Flux Parameter

For most plume rise estimates, the value of the buoyancy flux parameter F in m^4s^{-3} is needed:

$$F = g v_s d^2 (T_s - T) / (4 T_s) = 2.45 v_s d^2 (T_s - T) / T_s \quad (2.2)$$

where g is the acceleration due to gravity, about 9.806 m s^{-2} , T_s is the stack gas temperature in $^{\circ}\text{K}$, T is the ambient air temperature in $^{\circ}\text{K}$ (Stern *et al.*, 1984).

2.2.3. Unstable – Neutral Buoyancy Plume Rise

The final effective plume height, H , is stack height plus plume rise. Where buoyancy dominates, the horizontal distance x_f from the stack to where the final plume rise occurs is assumed to be $3.5 x^*$, where x^* is the horizontal distance, in km, at which atmospheric turbulence begins to dominate entrainment.

For unstable and neutral stability situations, and for F less than 55, H , in m, and x_f , in km, are (Stern *et al.* 1984);

$$H = h' + 21.425 F^{3/4} / u ; x_f = 0.048 F^{5/8} \quad (2.3a)$$

For F equal to or greater than 55, H and x_f are (Stern *et al.*, 1984):

$$H = h' + 38.71 F^{3/4} / u ; x_f = 0.119 F^{5/8} \quad (2.3b)$$

2.2.4. Stability Parameter

For stable conditions, the stability parameter is calculated by (Stern *et al.*, 1984):

$$s = g (\Delta\theta / \Delta z) / T \quad (2.4)$$

where $(\Delta\theta / \Delta z)$ is the change in potential temperature with height.

2.2.5. Stable Buoyancy Plume Rise

For stable conditions when there is wind, H and x_f are (Stern *et al.*, 1984):

$$H = h' + 2.6 (F / us)^{1/3} ; x_f = 0.00207 us^{-1/2} \quad (2.5a)$$

For calm conditions, the stable buoyancy rise is (Stern *et al.*, 1984):

$$H = h' + 4 F^{1/4} / s^{3/8} \quad (2.5b)$$

Under stable conditions, the lowest value of Equation 2.5a or 2.5b is usually taken as the effective stack height.

The wind speed that yields the same rise from Equation 2.5a as that from Equation 2.5b for calm conditions is (Stern *et al.*, 1984):

$$u = 0.2746 F^{1/4} s^{1/8} \quad (2.6)$$

2.2.6. Gradual Rise – Buoyancy Conditions

Plume rise for distances closer to the source than the distance to the final rise can be estimated from (Stern *et al.*, 1984):

$$H = h' + 160 F^{1/3} x^{2/3} u \quad (2.7)$$

where x is the source – to – receptor distance, km. If this height exceeds the final effective plume height, that height should be substituted.

2.2.7. Unstable – Neutral Momentum Plume Rise

If the stack gas temperature is below or only slightly above the ambient temperature, the plume rise due to momentum will be greater than that due to buoyancy. For unstable and neutral situations (Stern *et al.*, 1984):

$$H = h + 1.5[v_s^2 d^2 T / (4 T_s u)]^{1/3} s^{-1/6} \quad (2.8)$$

This equation is most applicable when v_s / u exceeds 4 (Stern *et al.*, 1984). Since momentum plume rise occurs quite close to the source, the horizontal distance to the final plume rise is considered to be zero.

2.3. Meteorology of Air Pollution

2.3.1. Planetary Boundary Layer

Most air pollution phenomena occur in the lower part of the atmosphere called the planetary boundary layer, or PBL. The planetary boundary layer (which is sometimes called “The Friction Layer”) is defined as “the region in which the atmosphere experiences surface effects through vertical exchanges of momentum, heat and moisture” (Zannetti P., 1990).

Traditionally, the PBL is divided vertically into various layers, each characterized by different “scaling” parameters. Even in ideal conditions (i.e., a horizontally homogeneous and

clear PBL), this vertical differentiation by layers is difficult, especially in the “stable” nighttime boundary layer, where, however, some progress in understanding its structure has been made.

The boundary layer is directly influenced by the Earth’s surface, responding to such forcings as frictional drag force, solar heating and radiation. Each of these effects generates turbulence of various sized eddies, which can be as deep as the boundary layer itself. The meteorological factors that influence air pollution phenomena are:

- the height above the ground,
- atmospheric stability,
- horizontal wind speed and direction,
- atmospheric vertical motion caused by pressure differences or complex terrain effects,
- temperature inversion.

Over oceans, the boundary layer depth varies relatively slowly in space and time. The sea surface temperature changes little over a diurnal cycle because of the tremendous mixing within the top of the ocean. Also, water has a large heat capacity, meaning that it can absorb large amounts of heat from the sun with relatively little temperature change. Thus, a slowly varying sea surface temperature means a slowly varying forcing into the bottom of the boundary layer.

Over both land and oceans, the general nature of the boundary layer is to be thinner in high -pressure regions than in low – pressure regions (Figure 2.1). The subsidence and low – level horizontal divergence associated with synoptic high pressure moves boundary layer air out of the high towards lower pressure regions. The shallower depths are often associated with cloud - free regions. If clouds are present, they are often fair – weather cumulus or stratocumulus clouds.

In low pressure regions, the upwards motions carry boundary layer air away from the ground to large altitudes throughout the troposphere. It is difficult to define a boundary - layer top for these situations. Cloud base is often used as an arbitrary cut – off for boundary layer

studies in these cases. Thus, the region studied by boundary layer meteorologists may actually be thinner in low pressure regions than in high pressure ones.

2.3.2. Mixed Layer

The turbulence in the mixed layer (ML) is usually convectively driven, although a nearly well – mixed layer can form in regions of strong winds. Convective sources include heat transfer from a warm ground surface, and radiative cooling from the top of the cloud layer. The first situation creates thermals of warm air rising from the ground, while the second creates thermals of cool air sinking from cloud top. Both can occur simultaneously when a cool stratocumulus topped mixed layer is being advected over warmer ground.

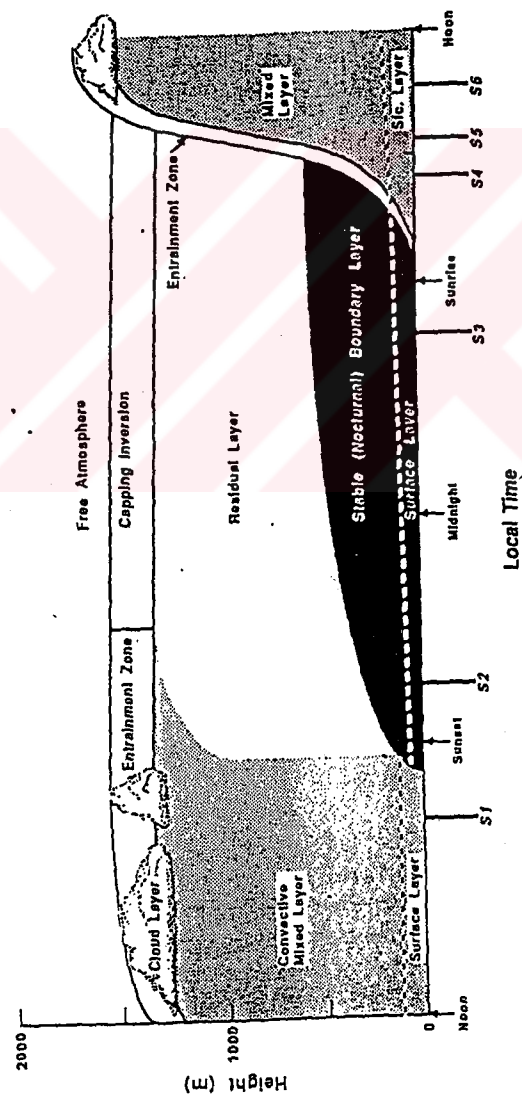


Figure 2.1. Major parts of the Planetary Boundary Layer (PBL) (Stull, 1988).

On initially cloud – free days, however, mixed layer growth is tied to solar heating of the ground. Starting about a half hour after sunrise, a turbulent ML begins to grow in depth. This ML is characterized by intense mixing in statically unstable situation where thermals of warm air rise from the ground. The ML reaches to its maximum depth in late afternoon. It grows by entraining, or mixing down into it, the less turbulent air from above.

The resulting turbulence tends to mix heat, moisture, and momentum uniformly in the vertical. Pollutants emitted from smoke stacks exhibit a characteristic looping as those portions of the effluent emitted into warm thermals begin to rise.

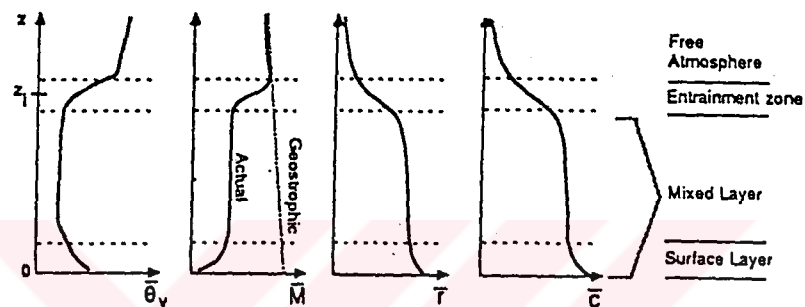


Figure 2.2. Typical daytime profiles of mean virtual potential temperature, wind speed, water vapor mixing ratio, and pollutant concentration (Stull, 1988).

Virtual potential temperature profiles are nearly adiabatic in the middle portion of the ML. In the surface layer, one often finds a super adiabatic layer adjacent to the ground. A stable layer at the top of the ML acts as a lid to the rising thermals, thus restraining the domain of turbulence. It is called the *entrainment zone*.

At times this capping stable layer is strong enough to be classified as a temperature inversion; that is, the absolute temperature increases with height. It is frequently called *inversion layer* regardless of the magnitude of the stability. The most common symbol for ML depth is z_i , which represents the average height of the inversion base.

The middle portion of the ML frequently has nearly constant wind speed and direction. Wind speeds decrease towards zero near the ground, resulting in a wind speed profile that is

nearly logarithmic with height in the surface layer. Wind directions cross the isobars at increasingly large angles as the ground is approached, with 45 degree angles not uncommon near the surface.

Mixing ratios tend to decrease with height, even within the center portion of the ML. This reflects the evaporation of soil and plant moisture from below, and the entrainment of drier air from above.

Most pollutant sources are near the Earth's surface. Thus, pollutant concentrations can build up in the ML while free atmosphere (FA) concentrations remain relatively low. Pollutants are transported by eddies such as thermals; therefore, the inability of thermals to penetrate very far into the stable layer means that the stable layer acts as a lid to the pollutants too. Trapping of pollutants below such an inversion layer is common in high – pressure regions, and sometimes leads to pollution alerts in large communities.

As the tops of the highest thermals reach greater and greater depths during the course of the day, the highest thermals might reach *lifting condensation level*, if sufficient moisture is present. High or middle overcast can reduce the insolation at ground level, which reduces the intensity of thermals. On these days, the ML may exhibit slower growth, and may even become nonturbulent or neutrally – stratified if the clouds are thick enough.

2.3.3. Residual Layer

About half hour before sunset, the thermals cease to form, in the absence of cold air advection, allowing turbulence to decay formerly well – mixed layer. The resulting layer of air sometimes called the residual layer (RL) because its initial mean state variables and concentration variables are the same as those of the recently – decayed mixed layer.

In the absence of advection, passive tracers dispersed into the daytime mixed layer will remain aloft in the RL during the night. The RL is neutrally stratified, resulting in turbulence that is nearly of equal intensity in all directions. As a result, smoke plumes emitted into the RL tend to disperse at equal rates in the vertical and lateral directions, creating a cone - shaped plume.

Nonpassive pollutants may react with other constituents during the night to create compounds that were not originally emitted from the ground. Sometimes gaseous chemicals may react to form aerosols or particulates which can precipitate out. The RL often exists for a while in the mornings before being entrained into the new ML. During this time, solar radiation may trigger photochemical reactions among the constituents in the RL.

Variables such as virtual potential temperature usually decrease slowly during the night because of radiation divergence. This cooling rate is on the order of $1\text{ }^{\circ}\text{C/d}$ (Stull, 1988). The cooling rate is more – or – less uniform throughout the depth of RL, thus allowing the RL virtual potential temperature profile to remain nearly adiabatic. When the top of the next day's ML reaches the base of the RL, the ML growth becomes very rapid.

The RL does not have direct contact with the ground. During the night, the nocturnal stable layer gradually increases in thickness by modifying the bottom of the RL. Thus, the remainder of the RL is not affected by turbulent transport of the surface – related properties and hence does not really fall within the definition of the boundary layer.

2.3.4. Stable Boundary Layer

As the night progresses, the bottom portion of the residual layer is transformed by its contact with the ground into a stable boundary layer. This is characterized by statically stable air with weaker, sporadic turbulence. Although the wind at the ground level frequently becomes lighter or calm at night, the winds aloft may accelerate to supergeostrophic speeds in a phenomenon that is called the low – level jet of nocturnal jet.

The statically stable air tends to suppress turbulence, while developing nocturnal jet enhances wind shears that tend to generate turbulence. As a result, turbulence sometimes occurs in relatively short bursts that can cause mixing throughout the stable boundary layer (SBL). During the nonturbulent periods, the flow becomes essentially decoupled from the surface.

As opposed to the daytime ML which has a clearly defined top, the SBL has a poorly defined top that smoothly blends into the RL above. The top of the ML is defined as the base

of the stable layer, while the SBL top is defined as the top of the stable layer or the height where turbulence intensity is a small fraction of its surface value.

Pollutants emitted into the stable layer disperse relatively little in the vertical. They disperse more rapidly or fan out in the horizontal. This behavior is called fanning.

Winds exhibit a very complex behavior at night. Just above ground level the wind speed often becomes light or even calm. At altitudes on the order of 200 m above ground, the wind may reach $10 - 30 \text{ ms}^{-1}$ in the nocturnal jet. Another few hundred meters above that, the wind speed is smaller and closer to its geostrophic value. The strong shears below the jet are accompanied by rapid change in the wind direction, where the lower level winds are directed across the isobars towards low pressure.

2.4. PBL Parameters

2.4.1. PBL Height

The PBL height (z_i) is determined by the top of the ground – based nighttime inversion (in stable conditions) or the bottom of the first elevated inversion (unstable conditions). In neutral conditions, z_i can be computed by Equation 2.9, unless an elevated inversion is lower than this computed value, in which case, z_i is the bottom of the elevated inversion. In unstable conditions, z_i can be computed by Equation 2.10. In stable conditions, z_i can be approximated, at mid – latitudes, by the value $2.4 \cdot 10^3 u_*^{3/2}$.

$$z_i \cong h = \text{const} \frac{u_*}{f} \quad (2.9)$$

where $\text{const} = 0.15$ to 0.25 , u_* is the friction velocity, and f is the Coriolis parameter.

$$h(t) = \left[\frac{2 \int H dt}{c_p \rho (\gamma_d - \gamma)} \right]^{1/2} \quad (2.10)$$

where H is the surface heat flux, ρ is the air density, c_p is the specific heat at constant pressure, γ_d is the dry adiabatic lapse rate, and γ is the atmospheric lapse rate.

2.4.2. The Mixing Height

The mixing height is defined as the depth of the surface boundary layer in which thermally – generated or shear – generated turbulence is found.

In neutral or unstable conditions, the mixing height, h , is $\approx z_i$. In stable conditions, h can be approximated by Equation 2.11.

$$h_{eq} = const \sqrt{\frac{u_*}{f}} L \quad (2.11)$$

where L is the Monin – Obukhov length, and $const = 0.4$ (Garratt, 1982).

2.4.3. The Roughness Length

Roughness length, z_0 , is a parameter to describe the degree of roughness of the earth's surface. The roughness length is based on the size and distance between objects in a group. The roughness length is important in determining wind shears over a surface, and influences turbulence development in the PBL. The value of roughness length can be obtained from Table 2.1, or approximated by the Equation 2.12.

$$z_0 = \frac{\epsilon}{30} \quad (2.12)$$

where ϵ is the average height of the obstacles in the study area.

2.4.4. Monin – Obukhov Length

Monin – Obukhov length, L , is a fundamental scaling quantity in the surface layer theory. It is a measure of relative importance of mechanical and thermal forcing on atmospheric turbulence. Simply, it is the height above the ground at which the production of

Table 2.1. Roughness lengths for various surfaces (Seinfeld and Pandis, 1998)

Type of Surface	z_0 (m)
Very smooth (ice, mud flats)	10^{-5}
Snow	10^{-3}
Smooth sea	10^{-3}
Level desert	10^{-3}
Lawn	10^{-2}
Uncut grass	0.05
Fully grown root crops	0.1
Tree covered	1
Low - density residential	2
Central business district	5 – 10

turbulence by both mechanical and thermal forces is equal. When L is large and negative, mechanical forces dominate over thermal forces. On a windy day with little sunshine, L might have a value of -150 m. When L is small and negative, the turbulence is driven by convection. At night, when L is positive, the temperature stratification tends to suppress the mechanical generation of turbulence. Monin – Obukhov length also provides a measure of the stability of surface layer. For positive L values, the atmosphere is stable, for negative L , it is unstable, and finally for infinite L , the atmosphere is neutral.

2.4.5. Stability and the Pasquill Stability Classes

The atmospheric resistance to vertical motion is called stability. If a fluid particle is denser than the particles below, the fluid particle tends to sink. After the particle has sunk, the original space occupied by the particle has to be filled by other particles from the surroundings. This atmospheric condition is called unstable. If the particle is less dense than the ones below, hydrostatic force will prevent any vertical motion. This atmospheric condition is then called stable. If the particle has the same density as the neighboring particles, the particle is in a state of equilibrium. This kind of atmosphere is called neutral.

The importance of atmospheric stability in atmospheric dilution process is that it determines the rate of dilution from a source. An unstable atmosphere implies a higher turbulence level in the atmosphere. Hence, more rapid mixing would be observed. A stable atmosphere implies that pollutants tend to stay relatively undispersed at an equilibrium level for a long period of time. In general, an unstable atmosphere is considered to be ideal ground for pollutant dispersal.

Stable atmospheres are usually observed in the winter when the ground is frozen and wind speed is less than 1 ms^{-1} . In high pressure systems, the subsiding air is compressed and warmed up while the surface temperature cools off by radiational cooling. The temperature increases with height instead of decreasing with height in normal situation. This inverted temperature condition is called an inversion.

The Monin – Obukhov length, L , is not a parameter that is routinely measured. Recognizing the need for a readily usable way to define atmospheric stability based on routine observations, Pasquill (1961) introduced the concept of stability classes defined in Table 2.2. These classes have proved very useful in atmospheric diffusion calculations.

Table 2.2. Estimation of Pasquill Stability Classes (Seinfeld and Pandis, 1998)

Surface Wind Speed at 10m (m s^{-1})	Solar Radiation			Nighttime Cloud Cover Fraction	
	Strong	Moderate	Slight	$\geq \frac{4}{8}$	$\leq \frac{3}{8}$
< 2	A	A – B	B		
2 – 3	A – B	B	C	E	F
3 – 5	B	B – C	C	D	E
5 – 6	C	C – D	D	D	D
> 6	C	D	D	D	D

where A denotes extremely unstable, B moderately unstable, C slightly unstable, D neutral, E slightly stable, and F moderately stable.

Golder (1972) established a relation between the Pasquill stability classes, the roughness length z_0 , and L (Figure 2.3).

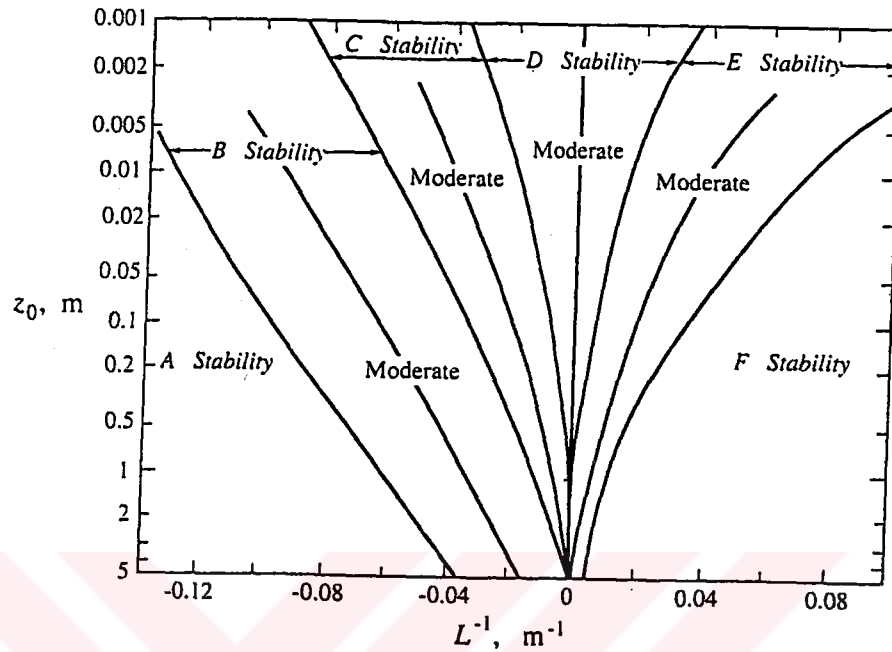


Figure 2.3. A relationship between L and z_0 for various Pasquill stability classes (Seinfeld and Pandis, 1998)

2.5. Transport and Dispersion of Air Pollutants

2.5.1. Wind

Wind is a velocity, a vector quantity having a direction and speed. Although the wind vector can occur in three dimensions, it is common only to consider the horizontal components of the wind. By convention, the wind direction is the direction from the wind comes. For airport observations, the wind is reported with a resolution of 10 degrees. North is 0 degrees or 360 degrees and east is 90 degrees (Turner, 1994). The horizontal wind is motion in response to both the horizontal pressure gradient and the horizontal temperature gradient.

2.5.2. Effect of Direction

The effect of wind direction is to determine the direction of transport of released pollutants. Because wind direction is the direction from which the wind blows, a west wind would cause pollution to move towards the east from source.

Air pollutant concentrations from point sources are probably more sensitive to wind direction than any other parameter. If the wind is blowing directly toward a receptor, a shift in direction of as little as 5° (the approximate accuracy of a wind direction measurement) causes concentrations at the receptor to drop about 10% under unstable conditions, about 50% under neutral conditions, and about 90 % under stable conditions. The direction of plume transport is very important in source impact assessment where there are sensitive receptors or two or more sources, and in trying to assess the performance of a model through comparison of measured air quality with model estimates (Stern et al., 1984).

2.5.3. Effect of Speed

For pollution releases that are continuous, the pollutants are diluted right at the point of release, such as the stack top. The resulting concentrations in the plume are inversely proportional to the wind speed; double the wind speed, the concentration in the plume becomes half of that with the lighter wind (Turner, 1994).

Because there is a frictional effect on the wind by the ground's surface and the roughness elements on the surface, the wind slows at heights close to the ground. The resulting slowing of wind near the ground or increase with height away from the ground is frequently approximated mathematically with the power – law wind profile (Turner, 1994).

The power – law is:

$$u_z = u_a \left(\frac{z}{z_a} \right)^p \quad (2.13)$$

where u_z is the wind speed at vertical height z above ground (m s^{-1}), u_a is the wind speed at anemometer height (m s^{-1}), z is the vertical height above ground (m), z_a is the anemometer height (m), and p is an exponent that is dependent primarily on atmospheric stability, which varies from around 0.07 for unstable conditions to about 0.55 for stable conditions (Turner, 1994).

One of the effects of the wind speed is to dilute continuously released pollutants at the point of emission. Whether a source is at the surface or elevated, this dilution takes place in the direction of plume transport.

Wind speed also affects the travel time from source to receptor; halving of the wind speed will double the travel time. For buoyant sources, plume rise is affected by wind speed: the stronger the wind, the lower the plume (Stern *et al.*, 1984).

2.5.4. Turbulence

Turbulence is a highly irregular motion of the wind. The atmosphere does not flow smoothly but random, rapidly varying, and erratic. The uneven flow superimposed on the mean flow has swirls or eddies in a wide range of sizes.

There are basically two different causes of turbulent eddies. Eddies set in motion by air moving past objects are the result of mechanical turbulence. Parcels of superheated air rising from the heated earth's surface, and the slower descent of a larger portion of the atmosphere surrounding these more rapidly rising air parcels, result in thermal turbulence (Stern *et al.*, 1984).

Fluctuations due to mechanical turbulence tend to be quite regular, that is, eddies of nearly constant size are generated. The eddies generated by thermal turbulence are both larger and more variable in size than those due to mechanical turbulence.

The most important mixing process in the atmosphere which causes the dispersion of pollutants is called *eddy diffusion*. The atmospheric eddies cause a breaking apart of atmospheric parcels which mixes polluted air with relatively unpolluted air, causing polluted

air at lower and lower concentrations to occupy successively larger volumes of air. Eddy or turbulent dispersion is most efficient when the scale of the eddy is similar to that of the pollutant puff or plume being diluted. Smaller eddies are effective only at tearing at the edges of the pollutant mass. On the other hand, larger eddies will usually only transport the mass of polluted air as a whole.

The size and influence of eddies on the vertical expansion of continuous plumes have been related to vertical temperature structure. Strong lapse rate is decrease of temperature with height in excess of the adiabatic lapse rate. Weak lapse is decrease of temperature with height at a rate between the dry adiabatic lapse rate and the isothermal condition (no change of temperature with height).

Atmospheric turbulence is responsible for the transport of heat, water vapor and trace gases and aerosols from the surface to atmosphere as a whole. In order to understand these processes, basic equations of atmospheric fluid mechanics have to be described.

2.6. Basic Equations of Atmospheric Fluid Mechanics

Air pollution diffusion can be numerically simulated by several techniques, which are divided into two categories, as Lagrangian models and Eulerian models. The basic difference between the Eulerian and Lagrangian view is illustrated in Figure 2.5., in which The Eulerian reference system is fixed while the Lagrangian reference system follows the average atmospheric motion.

Lagrangian models describe fluid elements that follow the instantaneous flow. Lagrangian models use the Lagrangian derivative d/dt , which gives the total change in any value with time. A Lagrangian model simulates the movement of an air parcel and changes that it goes through in time.

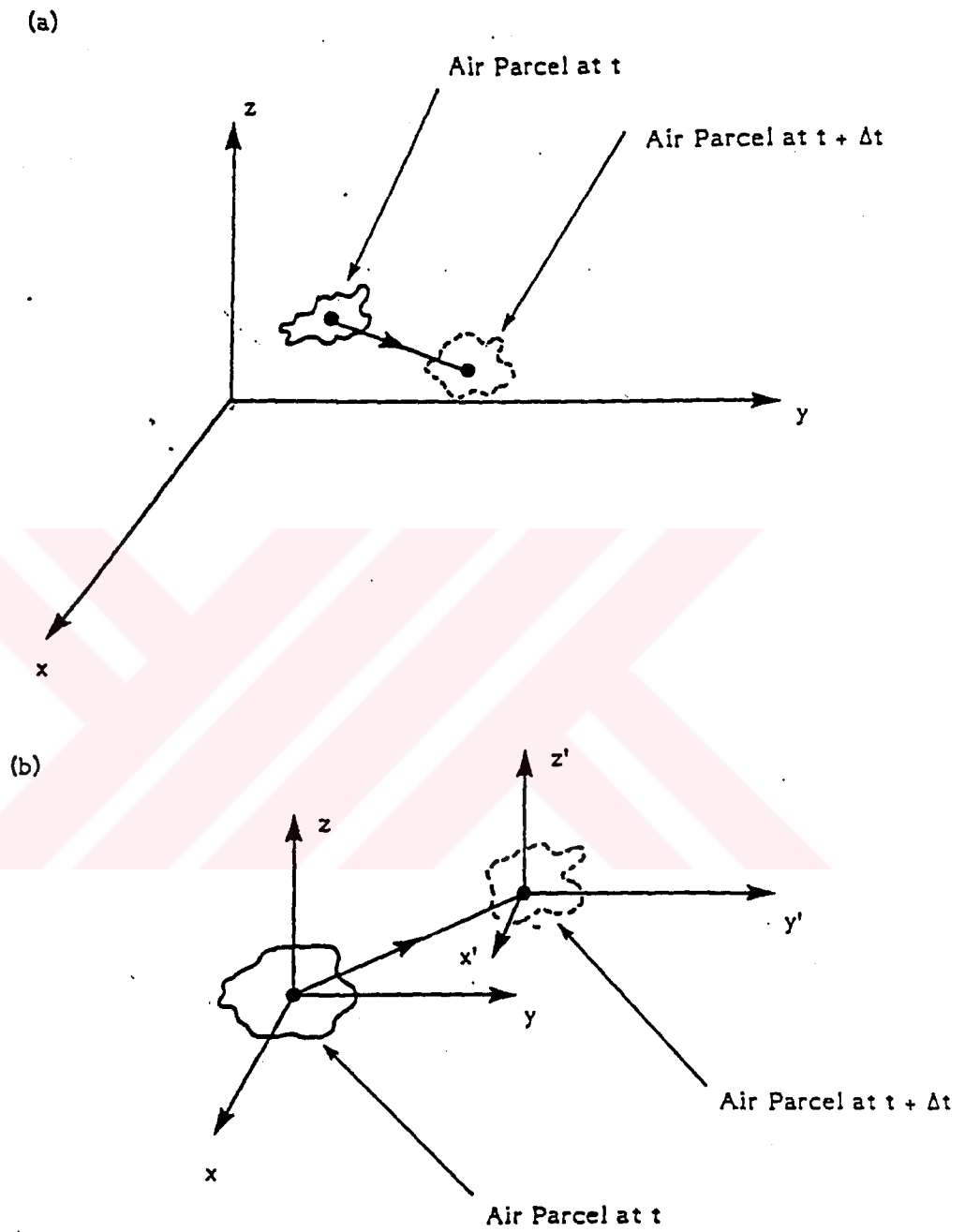


Figure 2.4. Eulerian (a) and Lagrangian (b) reference systems for the atmospheric motion (Zannetti P., 1990).

The Eulerian approach is based on the conservation of mass of a single pollutant species of $c(x, y, z, t)$.

$$\frac{\partial c}{\partial t} = -V\nabla c + D\nabla^2 c + S \quad (2.14)$$

where $D\nabla^2 c$ is the molecular diffusion term; D is the molecular diffusivity, $\nabla^2 = \partial^2 / \partial x^2 + \partial^2 / \partial y^2 + \partial^2 / \partial z^2$ is the Laplacian operator, and ∇ is the gradient operator. As seen above, Eulerian models use the Eulerian derivative, $\partial / \partial t$, which is also called as partial derivative. In an Eulerian model, the user does not follow an air parcel, yet the reference is fixed, therefore, concentration is on a fixed location that does not move.

The concentration of each species, at each instant, must satisfy a material balance taken over a volume element. Thus, any accumulation of the material over time, when added to the net amount of convected out of the volume element, must be balanced by an equivalent amount of material that is produced by chemical reactions in the element, that is emitted into it by sources, and that enters by molecular diffusion.

For an ideal gas, p and ρ are related by the equation of state:

$$p = \frac{\rho RT}{M_a} \quad (2.15)$$

The equations of continuity and motion for a compressible, Newtonian fluid in a gravitational field are

$$\frac{\partial \rho}{\partial t} + \frac{\partial}{\partial x_i} (\rho u_i) = 0 \quad (2.16)$$

$$\frac{\partial u_i}{\partial t} + u_j \frac{\partial u_i}{\partial x_j} = -\frac{\partial p}{\rho_0 \partial x_i} + \frac{\mu}{\rho_0} \frac{\partial^2 u_i}{\partial x_j^2} + \frac{gT}{T_0} \delta_{i3} \quad (2.17)$$

where $u_i(x_1, x_2, x_3, t)$ is the fluid velocity component in direction i , μ is the fluid viscosity, and δ_{ij} is the Kronecker delta, defined by $\delta_{ij} = 1$ if $i = j$, and $\delta_{ij} = 0$ if $i \neq j$.

The energy equation is

$$\rho \left(\frac{\partial U}{\partial t} + u_j \frac{\partial U}{\partial x_j} \right) = k \frac{\partial^2 T}{\partial x_j^2} - p \frac{\partial u_j}{\partial x_j} + \Phi + Q \quad (2.18)$$

where U is the internal energy per unit mass, k is the thermal conductivity, Φ is the heat generated per unit volume and time as a result of viscous dissipation, and Q represents the heat generated by any sources in the fluid (Seinfeld and Pandis, 1998).

After incorporating the mean (time averaged) and fluctuating components of velocity, temperature and pressure, the final forms of the above equations are obtained as below:

$$\frac{\partial \bar{u}_i}{\partial x_i} = 0 \quad (2.19)$$

$$\frac{\partial}{\partial t}(\rho_0 \bar{u}_i) + \frac{\partial}{\partial x_j}(\rho_0 \overline{u_i u_j}) = -\frac{\partial \bar{p}}{\partial x_i} + \frac{\partial}{\partial x_j} \left(\mu \frac{\partial \bar{u}_i}{\partial x_j} - \rho_0 \overline{u'_i u'_j} \right) + \frac{g}{T_0} \overline{\theta \delta_{i3}} \quad (2.20)$$

$$\rho_0 c_p \left(\frac{\partial \bar{\theta}}{\partial t} + \overline{u_j \frac{\partial \bar{\theta}}{\partial x_j}} \right) = \frac{\partial}{\partial x_j} \left(k \frac{\partial \bar{\theta}}{\partial x_j} - \rho_0 c_p \overline{u'_j \theta'} \right) \quad (2.21)$$

Dispersion of pollutants in the atmosphere is governed by the basic atmospheric diffusion equation. Under non-isotropic conditions, the atmospheric diffusion equation satisfying the equation of continuity can be written as in Equation 2.22.(Sharan *et al.*, 1996).

$$\frac{\partial C}{\partial t} + u \frac{\partial C}{\partial x} + v \frac{\partial C}{\partial y} + w \frac{\partial C}{\partial z} = \frac{\partial}{\partial x} \left[K_x \frac{\partial C}{\partial x} \right] + \frac{\partial}{\partial y} \left[K_y \frac{\partial C}{\partial y} \right] + \frac{\partial}{\partial z} \left[K_z \frac{\partial C}{\partial z} \right] + S + R \quad (2.22)$$

where C is the pollutant concentration, S represents the source term, R is the removal term, and u , v and w are the wind components and K_x , K_y and K_z are the eddy diffusivity coefficients along the x , y and z directions, respectively.

2.6.1. The Gaussian Plume Model

The Gaussian plume model is the most common air pollution model. It is based on a simple formula that describes the three – dimensional concentration field generated by a point source under stationary meteorological and emission conditions. The Gaussian plume model is

visualized in Figure 2.6. In a general reference system, the Gaussian plume formula is expressed in Equation 2.23.

$$c = \frac{Q}{2\pi\sigma_y\sigma_z u} \exp\left[-\frac{1}{2}\left(\frac{y}{\sigma_y}\right)^2\right] * \left\{ \exp\left[-\frac{1}{2}\left(\frac{z-H}{\sigma_z}\right)^2\right] + \exp\left[-\frac{1}{2}\left(\frac{z+H}{\sigma_z}\right)^2\right] \right\} \quad (2.23)$$

where Q is the emission rate, u is the wind speed, σ_z is the standard deviation of vertical distribution of plume concentration, x is the downwind distance, y is the crosswind distance, and z is the receptor height above ground.

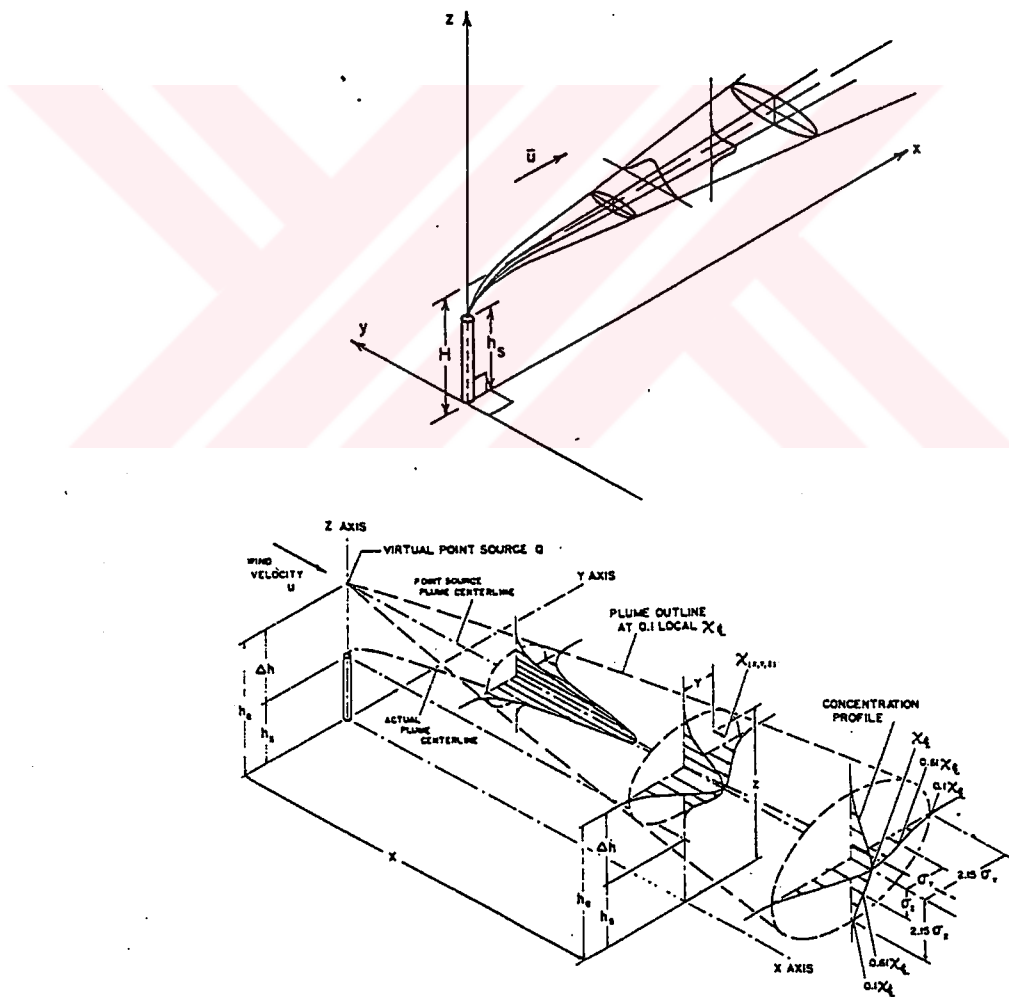


Figure 2.5. The Gaussian plume in a wind – oriented coordinate system (Zannetti P., 1990)

2.7. Dry and Wet Deposition

Deposition phenomena are the way in which atmosphere cleans itself. The process is efficient as only a few gases (most notably CO₂) shows signs of global increase in spite of large emission of pollutants from both natural and anthropogenic sources. Atmospheric deposition takes place via two pathways: wet deposition and dry deposition. Wet deposition is the result of precipitation, which removes particles and gases from the atmosphere. Dry deposition is the transfer of particles and gases to the landscape through a number of atmospheric processes in the absence of precipitation (Lavery *et al.*, 2001).

2.7.1. Dry Deposition

Dry deposition is the transport of gaseous and particulate species from the atmosphere onto surfaces in the absence of precipitation. The factors that govern the dry deposition of gaseous species or a particle are the level of atmospheric turbulence, the chemical properties of the depositing species, and the nature of the surface itself.

The level of turbulence in the atmosphere, especially in the layer nearest the ground, governs the rate at which species are delivered down to the surface. For gases, solubility and chemical reactivity may affect uptake at the surface. For particles, size, density and shape may determine whether capture by the surface occurs. The surface itself is a factor in dry deposition. A nonreactive surface may not lead to particle bounce – off. Natural surfaces, such as vegetation, while highly variable and often difficult to describe theoretically, generally promote dry deposition (Seinfeld and Pandis, 1998.).

Dry deposition is commonly measured by the deposition velocity, V_d , which was defined as the ratio between the pollutant deposition flux, F , and the pollutant concentration, c , as in Equation 2.24. In fact, only large particles possess a deposition velocity dominated by gravitational effects.

$$V_d = \frac{F}{c} \quad (2.24)$$

As far as gases are concerned, dry deposition is strongly affected by their chemical interactions with the surface. For particles, deposition velocities have been computed from wind tunnel experiments. As discussed by Nicholson (1998a), for very small particles (i.e., with a diameter less than $0.1 \mu\text{m}$), Brownian motion allows rapid movements across the viscous air layers just above the surface, while the motion of large particles (i.e., with a diameter greater than $1 \mu\text{m}$), is dominated by sedimentation (gravitational) effects where the “terminal” velocity, V_T (or gravitational settling velocity, V_G), increases with the particle size. Intermediate size particles are strongly affected by impaction and interception phenomena, which are difficult to quantify correctly. In particular, particles in size ranging from 0.1 to $1 \mu\text{m}$ have low predicted deposition velocities due to relative weakness of Brownian motion and gravitational settling effects, even though field measurements indicate high deposition rates. Surface roughness play an important role in a stable atmosphere, as it significantly influences the near – surface turbulence, and, in turn, the rate of pollutant transfer to the surface (Zannetti P., 1990).

2.7.2. Wet Deposition

Wet deposition refers to the natural process by which material is scavenged by atmospheric hydrometeors (cloud and fog drops, rain, and snow) and is consequently delivered to the Earth’s surface. A number of different terms are used more or less synonymously with wet deposition including precipitation scavenging, wet removal, washout, and rainout. Washout usually refers to in – cloud scavenging and rainout to below – cloud scavenging by falling rain, snow, and so on.

Mainly, three steps are necessary for wet removal of a material. Specifically, the species (gas or aerosol) must first be brought into the presence of condensed water. Then, the species must be scavenged by the hydrometeors, and finally it needs to be delivered to the Earth’s surface. Furthermore, the compounds may undergo chemical transformations during each one of the above steps. These wet deposition steps are depicted in Figure 2.6. An important point is that almost all processes are reversible. For example, rain may scavenge particles below cloud, but raindrops that evaporate produce new aerosols (Seinfeld and Pandis, 1998.).

Unlike dry deposition, a phenomenon that occurs in the lower layers of the PBL, precipitation scavenging affects all volume element aloft inside the precipitation layer. Following Seinfeld (1986), the wet flux of a pollutant to the surface is given in Equations 2.25 and 2.26.

$$W_g = \int_0^{\infty} \Lambda(z,t)c(x,y,z,t)dz \tag{2.25}$$

for gases and

$$W_p = \int_0^{\infty} \Lambda(d_p; z,t)c(d_p; x,y,z,t)dz \tag{2.26}$$

for particles, where Λ is the washout coefficient and c is the concentration expressed, for particles, as a function of the particle diameter d_p . It must be noted that Λ varies spatially and temporally.

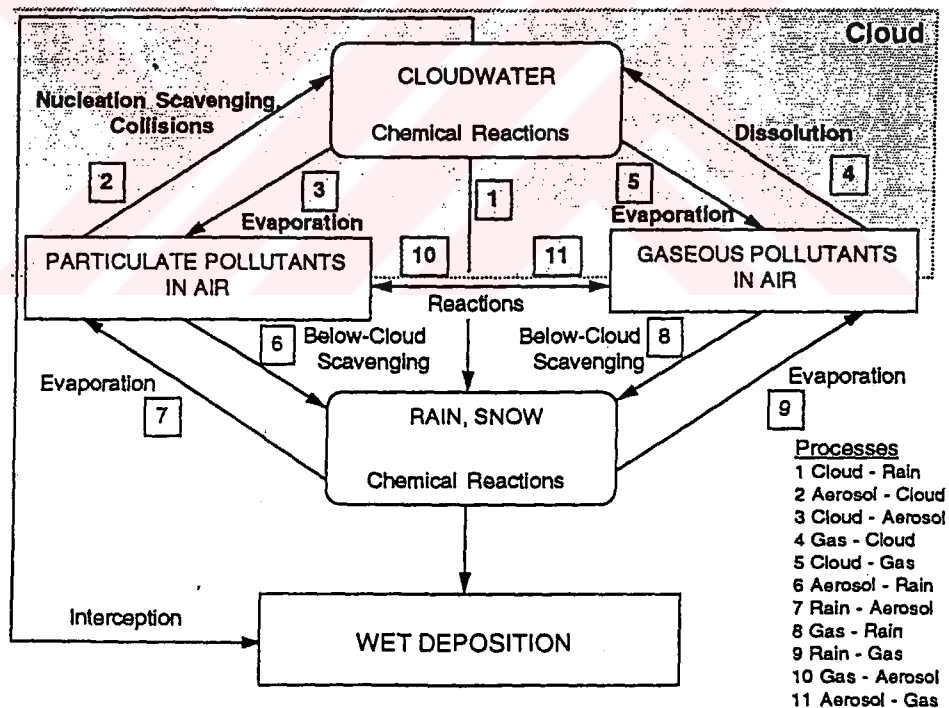


Figure 2.6. Conceptual framework of wet deposition processes (Seinfeld and Pandis, 1998)

2.8. The Atmospheric Chemistry Of Sulphur In Power Station Plumes

Emissions of sulphur compounds from power stations represent a significant fraction of the total emissions of these compounds to the atmosphere. At least 90% of sulphur present in fossil fuel enters the gas phase in the form of sulphur dioxide (SO₂) during combustion, and, unless it is deliberately removed from the flue gas, is emitted to the atmosphere, leading to a global anthropogenic emission of about 65 Tg SO₂ (as S) yr⁻¹ (Hewitt C. N., 2001). Globally, an increasing proportion of this reactive sulphur is emitted from power plants, as power generation becomes more and more concentrated on large units.

2.8.1. Gas – phase oxidation of sulphur dioxide

In the gas phase, SO₂ can potentially be subject to a large number of reactions involving reactive transient oxidants. These reactions are all thermodynamically possible in the atmosphere under ambient conditions of temperature and pressure. Coupled with the wide range of concentrations of these various oxidants in the atmosphere, only very few of these possible reactions play an appreciable role in the oxidation of SO₂ in the atmosphere.

2.8.2. Removal of sulphur by wet and dry deposition

The primary pollutant SO₂, its secondary products H₂SO₄ and SO₄²⁻ are subject to continuous removal from the boundary layer by the process of dry deposition to the Earth's surface. This process may be parameterized by the use of a deposition velocity, the magnitude of which varies from compound to compound and with environmental conditions and the nature of surface. A typical range of deposition velocities reported for various pollutants and surfaces is 0.1 – 2 cm⁻¹ (Hewitt C. N., 2001). Additionally, intermittent deposition may occur for soluble gases and particles by the process of wet deposition. Although wet deposition may be extremely efficient, it is, by its nature, sporadic.

In non – cloudy conditions, SO₂ removal from power station plumes occurs primarily during the daytime by reaction with the OH radical. In cloudy conditions, it will be removed rapidly by reactions in the aqueous phase. Removal rate will normally be lower in a plume than in background air, due to oxidant limitations, in both the gas and aerosol phases, with

plume fringes offering an intermediate oxidation environment. Absolute oxidation rates of SO_2 will vary with plume and background air composition and ambient conditions. In sunny conditions, a maximum SO_2 conversion rate of around $3\% \text{ h}^{-1}$ might be expected (Hewitt C. N., 2001). However, lower rates may be expected in a “normal” power station plume as oxidant supply becomes diminished by consumption of O_3 .



3. OVERVIEW OF THE MATHEMATICAL MODEL

CALMET is a meteorological model that develops hourly wind and temperature fields on a three – dimensional gridded modeling domain, including two – dimensional fields such as mixing height, surface characteristics and dispersion properties.

CALPUFF is a transport and dispersion model that advects puffs” of material emitted from modeled sources, simulating dispersion and transformation processes along the way, using the fields generated by CALMET.

CALPOST processes the output files of CALMET and CALPUFF, producing tabulations that summarize results.

In addition to the three models, the modeling system interfaces to several other models, which is facilitated by several preprocessors and utilities.

3.1. CALMET

The CALMET meteorological model consists of a diagnostic wind field module and micrometeorological modules for over water and overland boundary layers. It is developed to produce hourly fields of three – dimensional winds and various micrometeorological variables from routinely available surface and upper air meteorological observations.

The diagnostic wind field module uses a two – step approach to the computation of wind fields (Douglas and Kessler, 1988). In the first step, an initial – guess wind field is adjusted for kinematic effects of terrain, slope flows and terrain blocking effects, to produce a Step 1 wind field. The kinematic effects of terrain on the horizontal wind components are evaluated by applying a divergence – minimization procedure¹ to the initial guess wind field. Slope flow magnitudes are parameterized in terms of terrain slope, terrain height, domain – scale lapse rate and the time of the day. The thermodynamic blocking effects of terrain on the wind flow are parameterized in terms

¹ Divergence minimization procedure adjusts the horizontal wind component for a fixed vertical velocity field so that at each grid point, the divergence is less than a user – specified maximum value.

of local Froude number (Allwine and Whiteman, 1985). Froude number, Fr , is a dimensionless parameter, which should be used instead of wind speed. For a fixed reference height of 10 m, Fr is directly proportional to the wind speed ($F = 0.1u_{10}$). Froude number is defined in Equation 3.1. (Scire *et al.* 2000).

$$Fr = \frac{u}{(NH)} \quad (3.1)$$

where u is the wind speed, N is the Brunt – Vaisala frequency (Equation 3.2.)

$$N = \sqrt{\frac{g}{-\frac{\rho}{\partial \rho}} \frac{\partial \rho}{\partial z}} \quad (3.2)$$

ρ is the density of air and g is the gravity acceleration. For $0 < Fr < 1$, the atmosphere is strongly stable. If the Froude number at a particular point is less than a critical value and the wind has an uphill component, the wind is adjusted to be tangent to the terrain. The second step consists of an objective analysis procedure to introduce observational data into Step 1 wind field to produce a final wind field. An inverse – distance ($1 / r^2$) scheme is used which gives a higher weight to the observational data in the neighborhood of observational station, while Step 1 wind field takes over the interpolated wind field in regions having no observational data. An option is provided to allow gridded prognostic wind field to be used in CALMET, which may better represent regional flows and certain aspects of sea breeze circulations and slope / valley circulations.

CALMET consists of two boundary layer models for overland and over water applications. For overland surfaces, the energy balance method of Holtslag and van Ulden (1983) is used to compute hourly gridded fields of the heat flux, surface friction velocity, Monin – Obukhov length, and convective velocity scale. Mixing heights are determined from the computed hourly surface heat fluxes and observed temperature soundings. The model also determines the Pasquill – Gifford stability class and optional hourly precipitation rates.

Major features of the CALMET meteorological model are briefly summarized in Table 3.1.

Table 3.1. Major features of CALMET Meteorological Model

.....

Boundary Layer Modules of CALMET

- Overland Boundary Layer – Energy Balance Method
- Over water Boundary Layer – Profile Method
- Produces gridded fields of:
 - Surface Friction Velocity
 - Convective Velocity Scale
 - Monin – Obukhov Length
 - Mixing Height
 - PGT Stability Class
 - Air Temperature (3 – D)
 - Precipitation Rate

Diagnostic Wind Field Module of CALMET

- Slope Flows
 - Kinematic Terrain Effects
 - Terrain Blocking Effects
 - Divergence Minimization
 - Produces Gridded Fields of U, V, W Wind Components
 - Inputs Include Domain – Scale Winds, Observations, and (Optionally) Coarse – Grid Prognostic Model Winds
 - Lambert Conformal Projection Capability
-

3.1.1. Data Requirements of CALMET

CALMET is designed to require only routinely – available surface and upper air meteorological observations, although special data inputs can be accommodated.

CALMET reads hourly surface observations of wind speed, temperature, cloud cover, ceiling height, surface pressure, relative humidity, and precipitation type codes (only if wet removal is to be computed). Missing values of temperature, cloud cover, ceiling height, surface pressure, and relative humidity at surface stations are allowed by the program. The missing values are internally replaced by values at the closest station with non – missing data.

The upper air data required by CALMET include vertical profile of wind speed, wind direction, temperature, pressure, and elevation. If the upper air wind speed, wind direction, or temperature is missing, CALMET will interpolate to replace the missing data. Actually, the interpolation of wind data is performed with the u and v components, so both the wind speed and direction must be present for either to be used. Because the program does not extrapolate upper air data, the top valid level must be at or above the model domain and the lowest (surface) level of the sounding must be valid.

CALMET also requires geophysical data including gridded fields of terrain elevations and land use categories. Gridded fields of other geophysical parameters, such as surface roughness length, albedo, Bowen ratio, a soil heat flux parameter, anthropogenic heat flux, and vegetation leaf area index.

CALMET reads the user's inputs from a "control file" with a default name of CALMET.INP. This file contains the user's selections of the various model options, input variables, output options, etc. The model input parameters are shown in Appendices I, II and III.

3.1.2. Technical Description of the CALMET Meteorological Model

Convective Mixing Height

The daytime mixing height is computed using a modified Carson method based on Maul. Knowing hourly variation in the surface heat flux and the vertical temperature profile from the twice – daily sounding data, the convective mixing height at the time $t +$

dt can be estimated from its value at time t in a stepwise manner, as in Equation 3.3. and 3.4. (Scire *et al.* 2000).

$$h_{t+dt} = \left[ht^2 + \frac{2Q_h(1+E)dt}{\psi_1 \rho c_p} - \frac{2d\theta_t h_t}{\psi_1} \right]^{1/2} + \frac{d\theta_{t+dt}}{\psi_1} \quad (3.3.)$$

$$d\theta_{t+dt} = \left[\frac{2\psi_1 E Q_h d_t}{\rho c_p} \right]^{1/2} \quad (3.4.)$$

where ψ_1 is the potential temperature lapse in layer above h_t , $d\theta$ is the temperature jump at the top of the mixed layer, and E is a constant of 0.15.

The potential temperature lapse rate is determined through a layer above the previous hour's convective mixing height. If only routinely available, twice – daily sounding data are available, the morning (1200 GMT) sounding at the nearest upper air station is used to determine ψ_1 up to 2300 GMT. After 2300 GMT, the afternoon sounding (0000 GMT) is used.

Monin – Obukhov Length

The Monin – Obukhov length, L, is defined in Equation 3.5.

$$L = -\frac{\rho c_p T u_*^3}{kg Q_h} \quad (3.5.)$$

where T is the air temperature, u_* is the surface friction velocity, ρ is the air density, c_p is the specific heat of air at constant pressure, k is the von Karmon constant, g is the acceleration due to gravity, and Q_h is the sensible heat flux.

An initial guess for surface friction velocity assuming neutral conditions is made. This value of u_* is used to estimate L. a new value for u_* is then computed with L. the procedure is repeated until convergence is obtained.

$$u_* = \frac{ku}{\left[\ln\left(\frac{z}{z_0}\right) - \psi_m\left(\frac{z}{L}\right) + \psi_m\left(\frac{z_0}{L}\right) \right]} \quad (3.6.)$$

where z_0 is the surface roughness length, ψ_m is a stability correction function, k is the von Karman constant, and u is the wind speed at height z .

This equation is used to obtain an initial guess for u_* assuming neutral conditions ($L = \text{infinity}$). This value of u_* is then used to estimate L . During stable conditions, Weil and Brower (1983) compute u_* with the method based on Venkatram (1980), as in Equation 3.7.

$$u_* = \frac{C_{DN}u}{2} [1 + \sqrt{C}] \quad (3.7.)$$

$$C = 1 - \frac{4u_0^2}{C_{DN}u^2} \quad (C \geq 0) \quad (3.8.)$$

$$u_0^2 = \frac{\gamma z_m g \theta^*}{T} \quad (3.9.)$$

where C_{DN} is the neutral drag coefficient, γ is a constant (approx. 4.7), and z_m is the measurement height of the wind speed, u .

Boundary Layer Parameters

Over land surfaces, the energy balance method of Holtslag and van Ulden (1983) is used to compute hourly gridded fields of the sensible heat flux, surface friction velocity, Monin – Obukhov length, and convective velocity scale. Mixing heights are determined from the computed hourly heat fluxes and observed temperature soundings.

An energy budget method, based primarily on Holtslag and van Ulden (1983), is used over land surfaces. The energy balance at the surface is written as in Equation 3.10.

$$Q_* + Q_f = Q_H + Q_e + Q_g \quad (3.10.)$$

Where Q^* is the net radiation, Q_f is the anthropogenic heat flux, Q_h is the sensible heat flux, Q_e is the latent heat flux, and Q_g is the storage / soil heat flux.

3.2. CALPUFF

CALPUFF is a multi-layer, multi-species non-steady-state puff dispersion model which can simulate the effects of time-and space-varying meteorological conditions on pollutant transport, transformation, and removal. CALPUFF can use the three dimensional meteorological fields developed the CALMET model.

CALPUFF contains algorithms for near - source effects such as building downwash, transitional plume rise, partial plume penetration, subgrid scale terrain interactions as well as longer-range effects such as pollutant removal (wet scavenging and dry deposition), chemical transformation, vertical wind shear, over water transport and coastal interaction effects.

3.2.1. Major Features and Options of CALPUFF

A full resistance model is provided in CALPUFF for the computation of dry deposition rates of gases and particulate matter as a function of geophysical parameters, meteorological conditions, and pollutant species.

An empirical scavenging coefficient approach is used in CALPUFF to compute the depletion and wet deposition fluxes due to precipitation scavenging. The scavenging coefficients are specified as a function of the pollutant and precipitation type.

CALPUFF includes options for parameterizing chemical transformation effects using the five species scheme (SO_2 , SO_4^- , NO_x , HNO_3 , and NO_3^-) used in the MESOPUFF II model, a modified six - species scheme (SO_2 , SO_4^- , NO , NO_2 , HNO_3 , and NO_3^-) adapted from RIVAD / ARM3 method, or a set of user specified, diurnally - varying transformation rates.

CALPUFF has an optional puff splitting algorithm that allows vertical wind shear effects across individual puffs to be simulated. Differential rates of dispersion and

transport occur on the puffs generated from the original puff, which under some conditions, can substantially increase the effective rate of horizontal growth of plume.

Some of the important features of CALPUFF are briefly summarized in Table 3.2.

Table 3.2. Major features of CALPUFF

-
- **Source types**
 - Point sources (constant or variable emissions)
 - Line sources (constant or variable emissions)
 - Volume sources (constant or variable emissions)
 - Area sources (constant or variable emissions)
 - **Non – steady state emissions and meteorological conditions**
 - Gridded 3 – D fields of meteorological variables
 - Spatially – variable fields of mixing height, friction velocity, convective velocity scale, Monin – Obukhov length, precipitation rate
 - Vertically and horizontally – varying turbulence and dispersion rates
 - Time – dependent source and emissions data
 - **Plume rise**
 - Partial penetration
 - Buoyant and momentum rise
 - Stack tip effects
 - Vertical wind shear
 - Building downwash effects
 - **Dry Deposition**
 - Gases and particulate matter
 - Full treatment of space and time variations of deposition with a resistance model
 - User – specified diurnal cycles for each pollutant
 - **Wet removal**
 - Scavenging coefficient approach
 - Removal rate a function of precipitation intensity and precipitation type

3.2.2. Data requirements of CALPUFF

CALPUFF reads user inputs from a control file with a default name of CALPUFF.INP. A meteorological data file (CALMET.DAT) contains hourly gridded fields of micro – meteorological parameters and three – dimensional wind and temperature fields. The meteorological data file also contains geophysical data such as terrain heights and land use, which are required by both the meteorological model and by CALPUFF model.

The input data used by CALPUFF is briefly summarized in Table 3.3.

Table 3.3. The input data used by CALPUFF

- **Geophysical Data (CALMET.DAT)**

Gridded fields of:

- surface roughness lengths (z_0)
- land use categories
- terrain elevations
- leaf area index

- **Meteorological Data (CALMET.DAT)**

Gridded fields of:

- u, v, w wind components (3 – D)
- air temperature (3 – D)
- surface friction velocity (u_*)
- convective velocity scale (w_*)
- mixing height (z_i)
- Monin – Obukhov length (L)
- PGT stability class
- Precipitation rate

Hourly values of the following parameters at surface meteorological stations:

- air density (ρ_0)
 - air temperature
 - short – wave solar radiation
 - relative humidity
 - precipitation type
-

3.2.CALPOST

The CALPOST program is a postprocessor designed to average and report or wet deposition flux results based on the hourly data contained in the CALPUFF output file. A range of averaging times may be selected, and the results may be reported in a number of different formats. The name and full path of each file is assigned in the control file, CALOST.INP. CALPOST generates an output list file, with a default name of CALPOST.LST, and a set of optional files.

4. STUDY AREA AND SOURCE CHARACTERISTICS

4.1. Topographical Data

Yatağan is a small district of Muğla, which is located in the Aegean part of Turkey. The centrum of Yatağan is located in a valley – like part of the region and surrounded with hills, which behave as natural barriers that trap air pollutants, particularly of the Yatağan Power Plant located in the district.

The simulation area is divided into 15 x 15 x 9 grids with a grid spacing of 1 km for x and y directions and varying resolution in vertical direction with a ceiling height of 1620m. The simulation domain extends from 28.02° E to 28.12° E longitude (592 – 607 km E in UTM zone 35), and from 37.17° N to 37.25° N latitude (4126 – 4141 km N in UTM zone 35) (for UTM coordinate system, see Appendix VIII). The source of the pollution, Yatağan Power Plant, is located in 597.185 km E and 4132.830 km N in UTM zone 35. The gridded receptor system is used in CALPUFF for 15 x 15 grids throughout the modeling area, which calculates the concentrations at a total of 225 receptors.

The terrain heights are read from a topographic map of 1:25000 scale. The average terrain heights are calculated at each grid and processed as the average terrain height of the particular grid in CALMET. The maximum height in the north of the modeling area is 700 m, whereas in the south of the modeling domain is 600 m. The coordinates in kilometers and the terrain heights of the modeling domain are shown in Figure 4.1., and a three-dimensional illustration of the modeling domain is shown in Figure 4.2.

A very significant parameter, in addition to terrain heights, in meteorological modeling is the land use types of the region. Land use types of the area is also read from the topographic map and provided as input to CALMET. An illustration of the land use types of the modeling domain is shown in Figure 4.3. As seen in Figure 4.3., most of the region is covered with forests and agricultural lands, whereas, a small portion of the region is covered with

residential areas and is gathered within the Yatağan Centrum (for land use types, see Appendix VII).

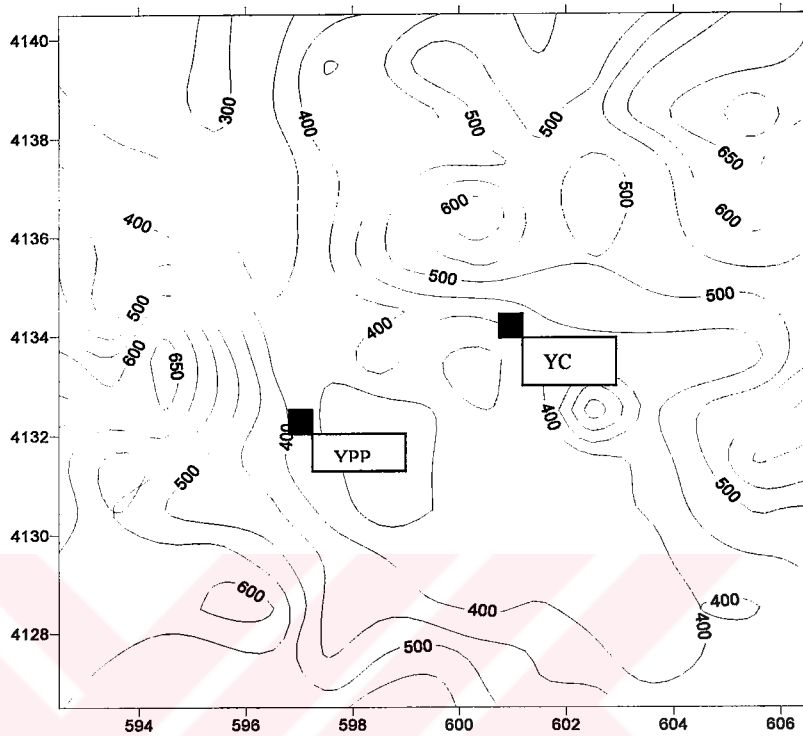


Figure 4.1. Contour map (elevation in meters) of the modeling area.

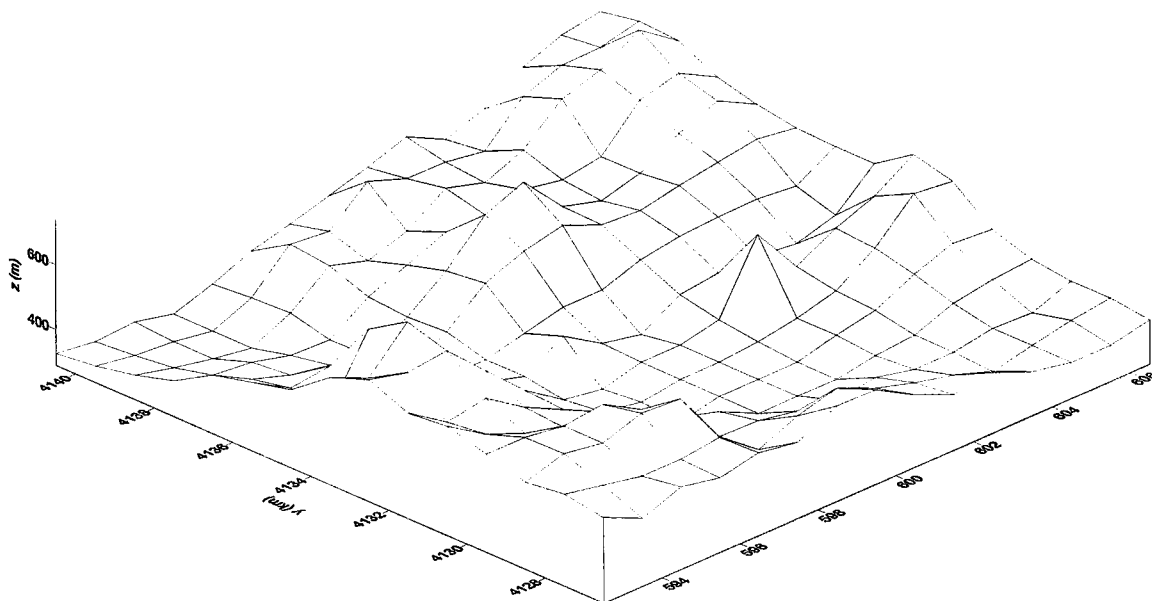


Figure 4.2. 3D view of the modeling area.

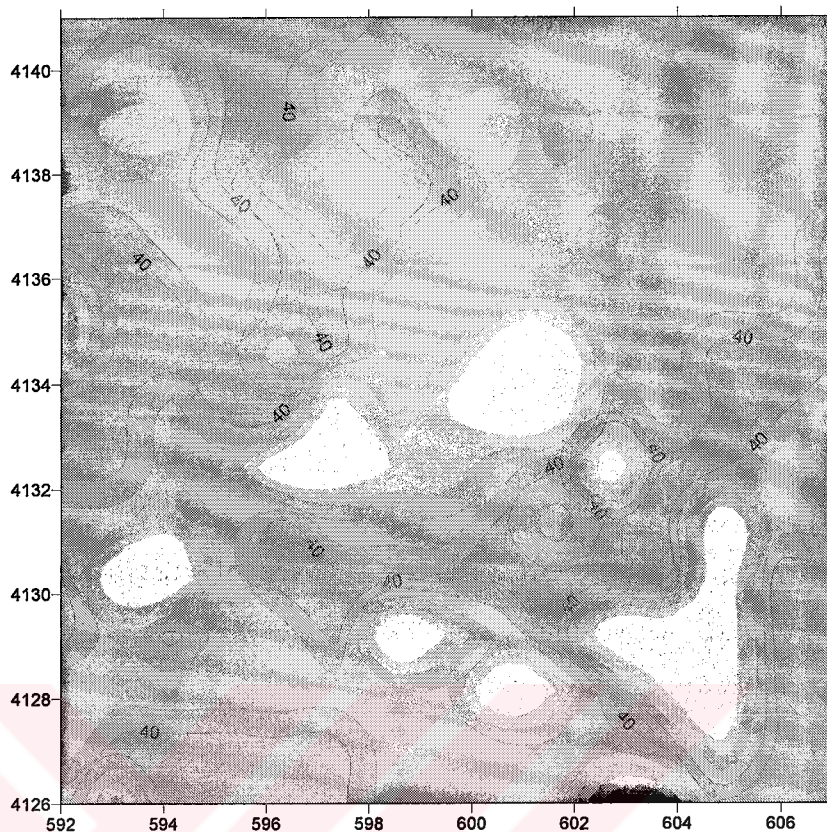


Figure 4.3. Land use types of the modeling region.

(40 – 45 = Forest Land, 20 – 25 = Agricultural Land, 10 – 15 = Urban Land)

4.2. Meteorological Data

Meteorological data used by CALMET is collected from two meteorological stations; hourly surface data is provided from Yatağan Meteorological Station, which is located in 600.375 km E and 4134.350 km N, upper air data is provided from Isparta Meteorological Station, which is located in 817.875 km E and 4179.975 km N.

Surface meteorological data consist of wind speed, wind direction, surface pressure, temperature, cloudiness, relative humidity, and precipitation information. No precipitation is recorded during the modeling period. Winds are generally south – westerly during the day,

especially on the early hours of morning, and vary from north – easterly to north – westerly during the night.

Upper air radiosonde data is taken at 00z and 12z everyday and include wind speed, wind direction, pressure, humidity, and height values for levels between approximately 900 mb to 750 mb.

4.3. Source Characteristics

The Yatağan Power Plant was established for the utilization of a reserve of 800 million tons of low – value lignite resources, which have a low calorific value and is of no use except for electric energy production. The plant is located about 4 km from Milas – Bodrum junction of İzmir - Muğla highway, and 3 km from Yatağan Centrum.

Yatağan Power Plant consists of three units, which are opened to production in 1982, 1983, and 1985, respectively, and each with a capacity of 210 MW. The primary fuel is lignite and the secondary fuel is fuel – oil. Daily lignite consumption, under full – capacity, is 16500 kg / day. The specifications of lignite used in the plant are listed in Table 4.1.

²Table 4.1. Specifications of lignite used in the plant

Calorific Value	(Kcal / kg)	2000
Ash Content	%	28
Moisture Content	%	32
Total Sulphur Content	%	1.93
Volatile Sulphur Content	%	1.13
Efficiency of the plant	%	37.75

² The values are taken from the document named “YATAĞAN POWER PLANT, TECHNICAL SPECIFICATIONS

The total emission rate of SO₂ emitted from the Power Plant is 3804 gs⁻¹. Emission characteristics of each unit of the power plant are given in Table 4.2.

Table 4.2. Emission characteristics of Yatağan Power Plant

.....
Unit 1

SO ₂ Emission Rate	(gs ⁻¹)	1402
Exit Velocity	(ms ⁻¹)	4.10
Exit Temperature	(° C)	163
Stack Height (H)	(m)	120
Max. Stack Diameter	(m)	11.3
Min. Stack Diameter	(m)	6.4

Unit 2

SO ₂ Emission Rate	(gs ⁻¹)	1209
Exit Velocity	(ms ⁻¹)	4.10
Exit Temperature	(° C)	163
Stack Height (H)	(m)	120
Max. Stack Diameter	(m)	11.3
Min. Stack Diameter	(m)	6.4

Unit 3

SO ₂ Emission Rate	(gs ⁻¹)	1193
Exit Velocity	(ms ⁻¹)	4.20
Exit Temperature	(° C)	163
Stack Height (H)	(m)	120
Max. Stack Diameter	(m)	11.3
Min. Stack Diameter	(m)	6.4

.....

5. RESULTS AND DISCUSSION

5.1. Simulation of the Episodic Event on 2nd and 3rd of December 2000

CALMET was used to simulate a 96-hour period, starting from December 1, 2000 at 00:00, to December 4, 2000 at 23:00. The episodic event that has been simulated by CALMET took place around the early hours of morning, on December 2, 2000. The meteorological conditions on December 1, 2000 and December 4, 2000 are simulated in order to prescribe the behavior of the winds, before and after the episodic event. Surface meteorological data were obtained at 10 m above the ground. Temperatures were around 9° C on average, surface pressure was 980 mb on average, and relative humidity was around 73 %. Winds in the modeling period were light winds; varying from 1 to 8 ms⁻¹. Precipitation records show that there was no precipitation during the simulation period. On December 2 and 3, 2000, starting from the early hours of the day to the afternoon hours, wind speeds turned out to be very low, varying from 0.1 to 0.5 ms⁻¹. The upper air profile obtained from radiosonde data from Isparta meteorological station shows that wind speed did not show a linear trend with height, and again, very low wind speeds were observed in the early hours of December 2 and 3, 2000. The CALMET simulation shows that on December 1, 2000, the winds are south – easterly (Figures 5.1. and 5.2.), but after noon, they changed to blow south – westerly (Figure 5.3., 5.4. and 5.5.), and a significant decrease in wind speed to values below 0.5 ms⁻¹ on December 2, 2000, was observed, causing the pollutants to be trapped above the Yatağan town center. After noon, on 2nd of December 2000, although there are no change in wind directions (Figure 5.6.), due to the increase of wind speed to values reaching 8 ms⁻¹, and temperatures increasing to around 10°C, the inversion layer started to disappear and the pollutants dispersed away from the simulation boundary. In the early hours of December 3, 2000, there is a considerable decrease in wind speeds and temperatures, an inversion layer occurred and with the winds blowing south – easterly again (Figures 5.7., and 5.8.), causing the pollutants to be trapped above the district. After noon, the wind speed started to increase again, temperatures increased and the winds changed to be, first, north – westerly (Figure 5.9.), later shifting to south – easterly winds (Figures 5.10, 5.11., and 5.12).

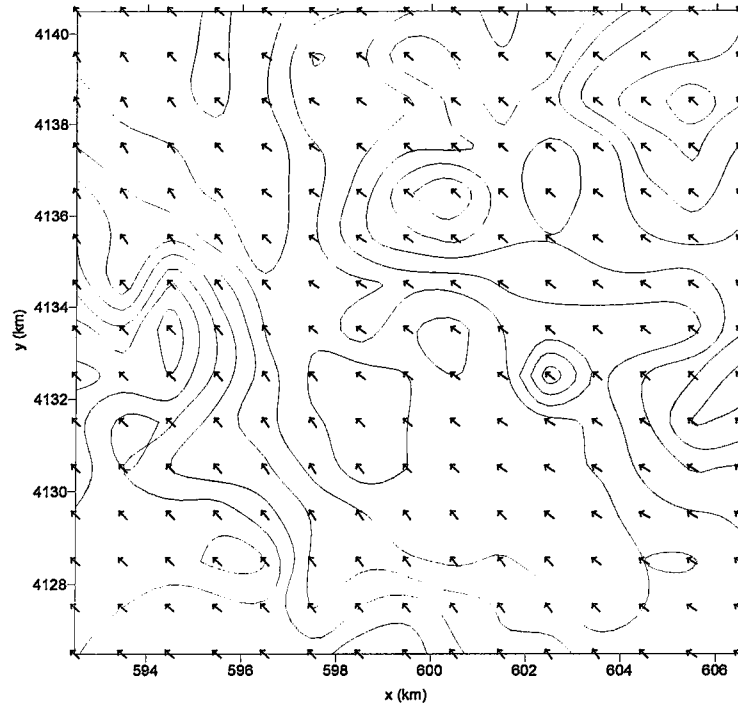


Figure 5.1. Wind field for the modeling area at 07:00 on December 1, 2000

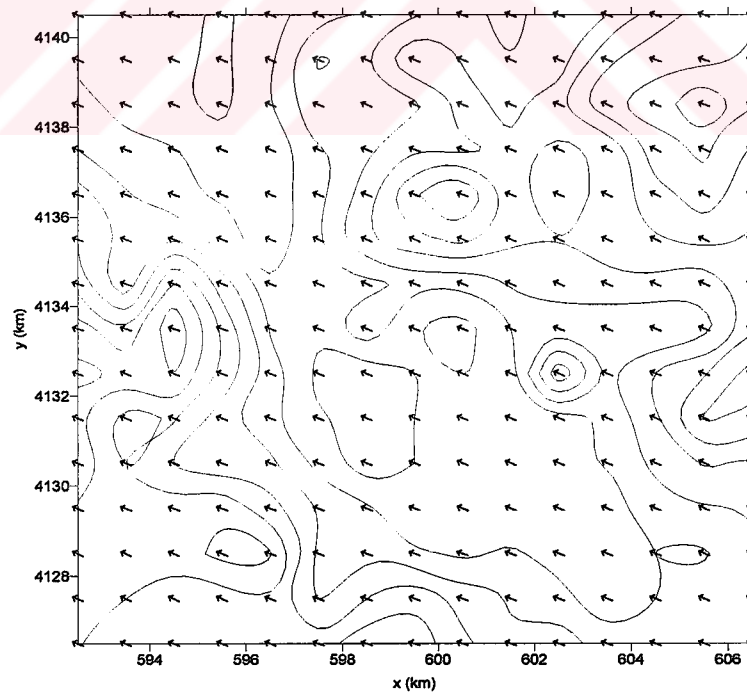


Figure 5.2. Wind field for the modeling area at 15:00 on December 1, 2000

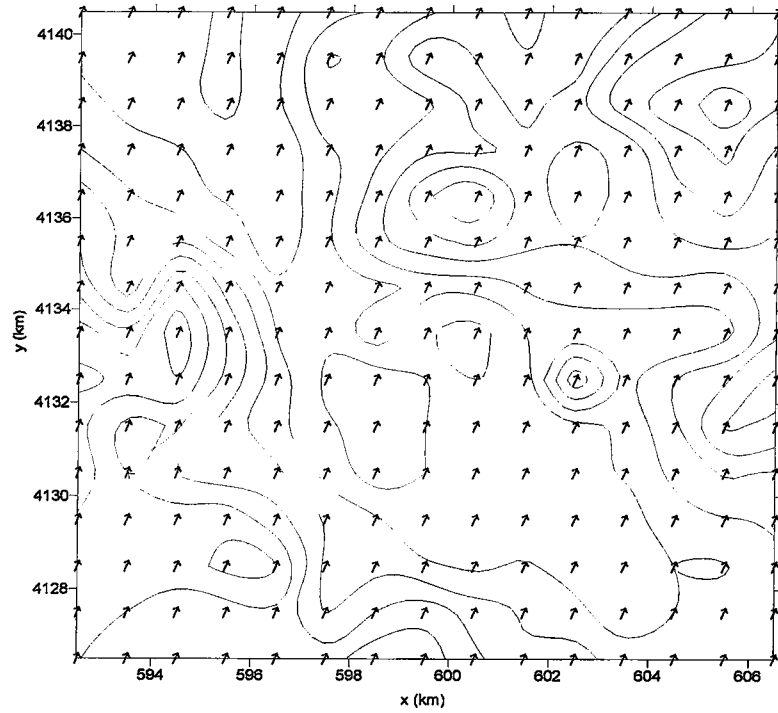


Figure 5.3. Wind field for the modeling area at 23:00 on December 1, 2000

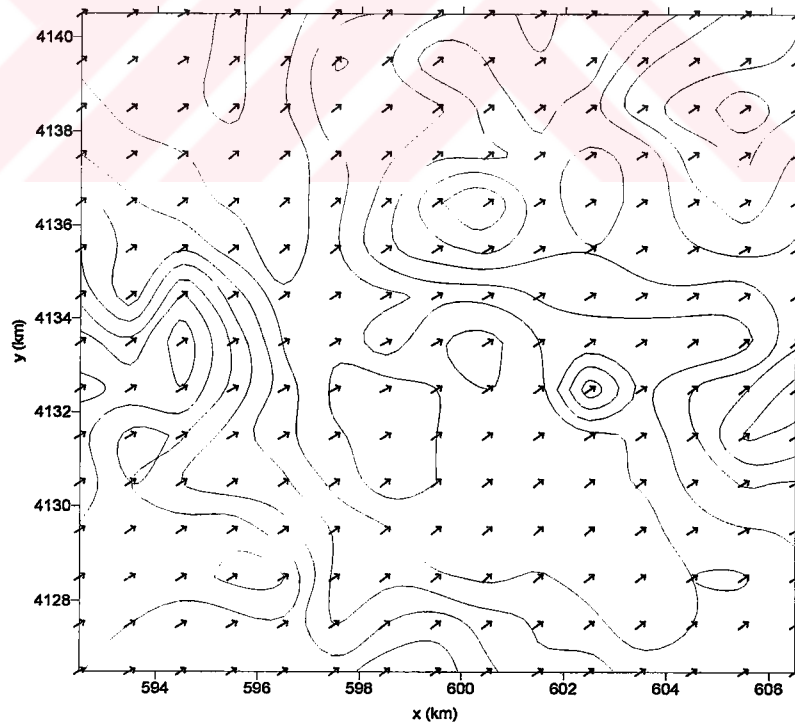


Figure 5.4. Wind field for the modeling area at 07:00 on December 2, 2000

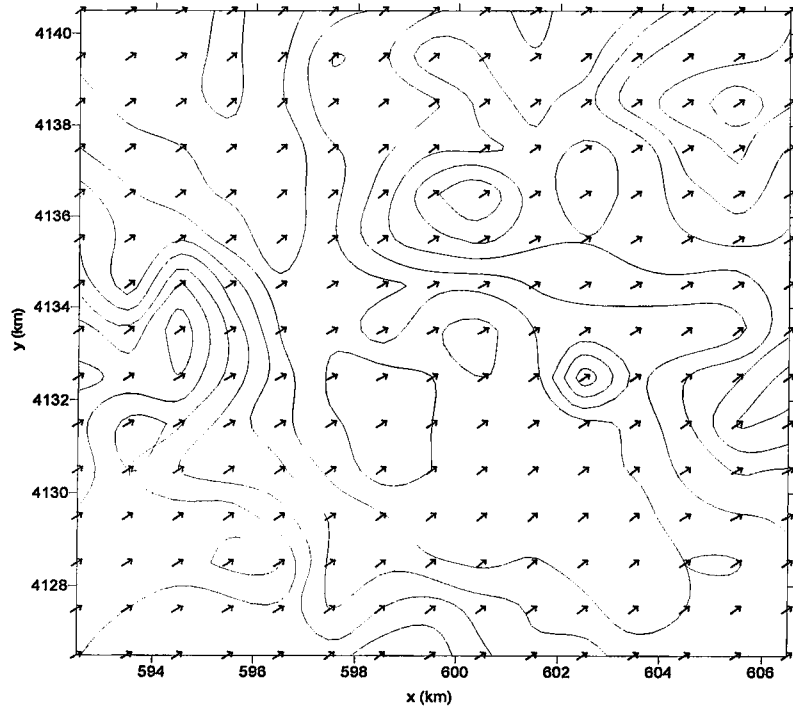


Figure 5.5. Wind field for the modeling area at 15:00 on December 2, 2000

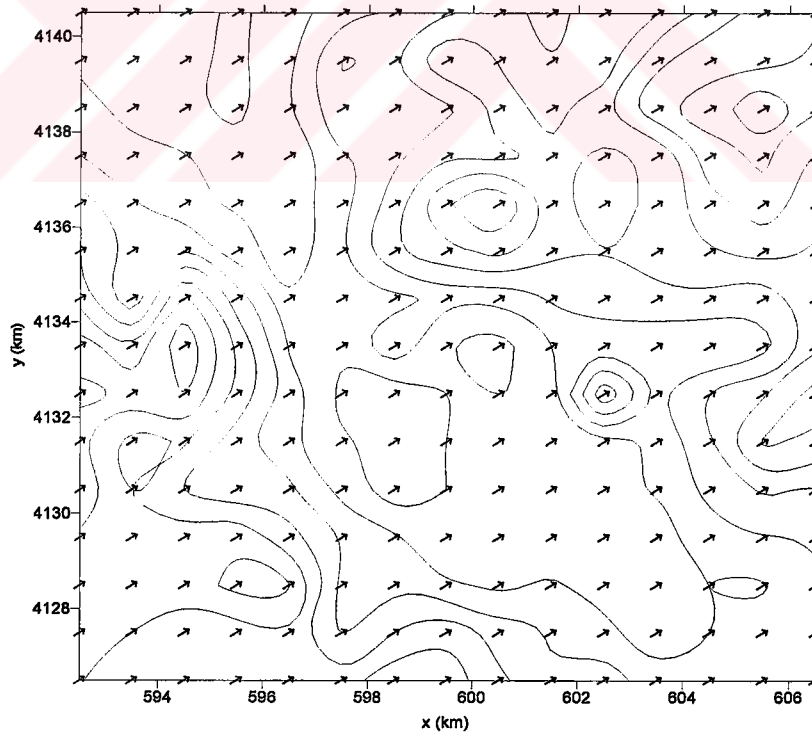


Figure 5.6. Wind field for the modeling area at 23:00 on December 2, 2000

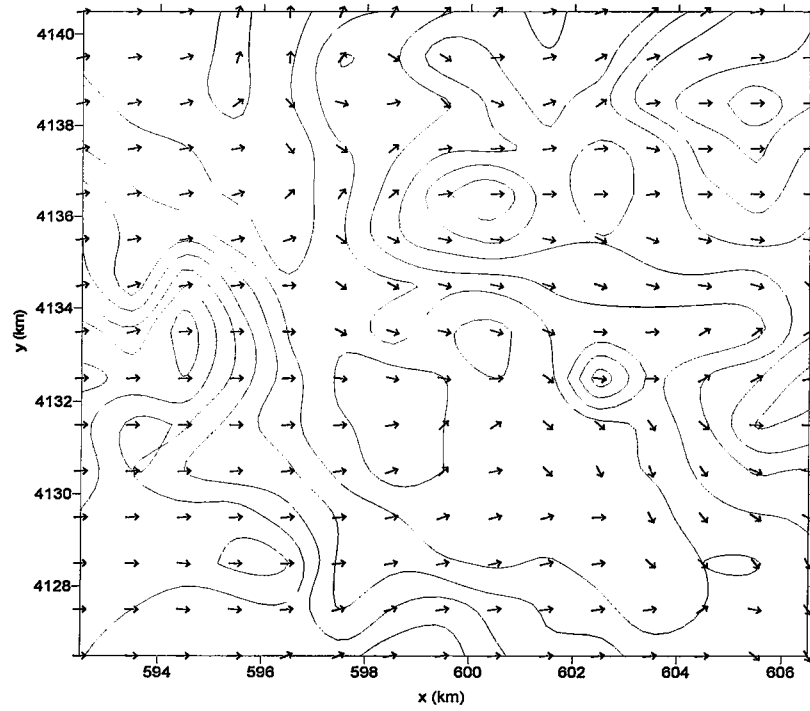


Figure 5.7. Wind field for the modeling area at 07:00 on December 3, 2000

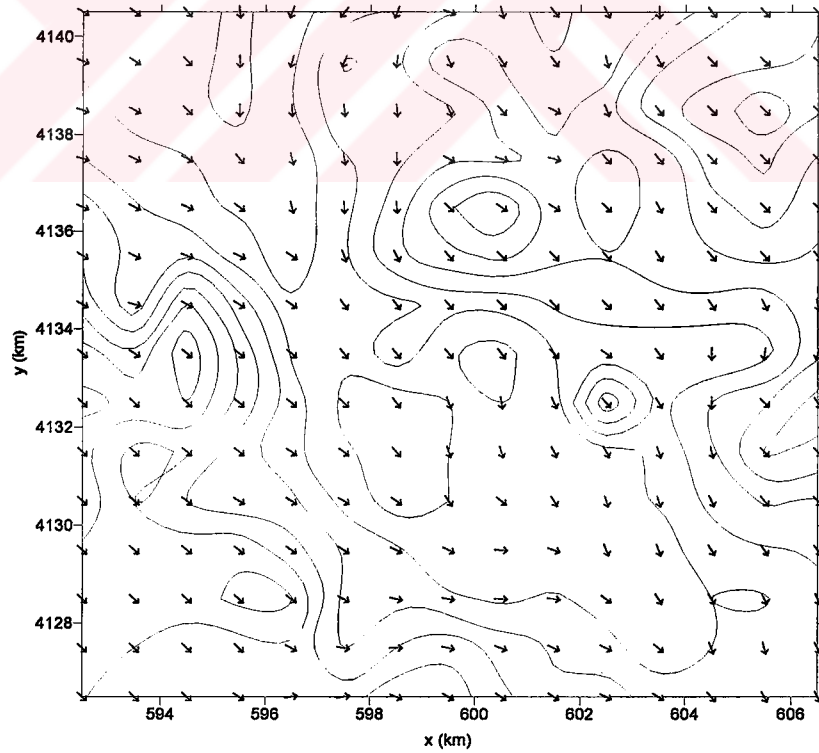


Figure 5.8. Wind field for the modeling area at 15:00 on December 3, 2000

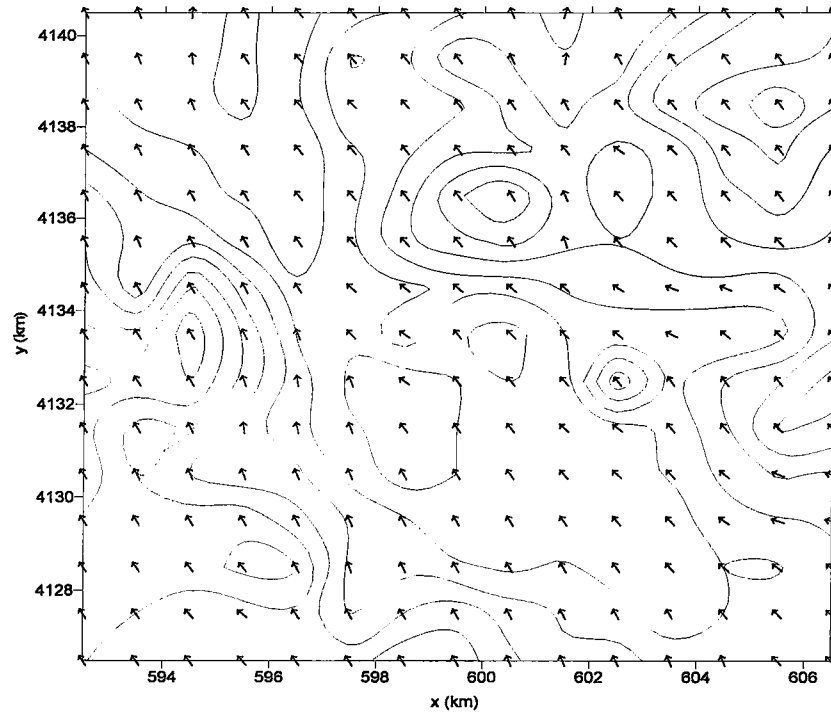


Figure 5.9. Wind field for the modeling area at 23:00 on December 3, 2000

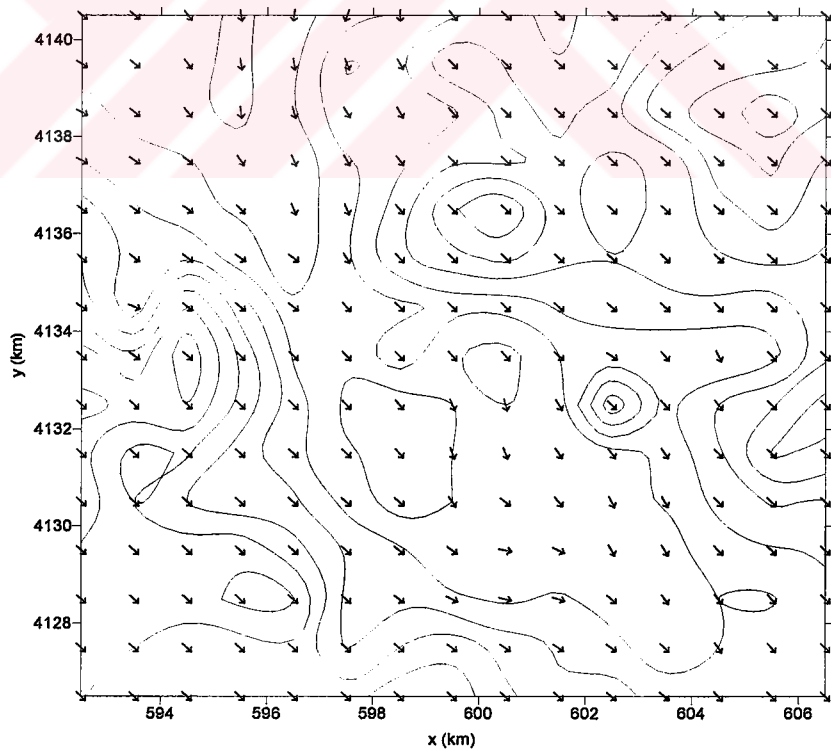


Figure 5.10. Wind field for the modeling area at 07:00 on December 4, 2000

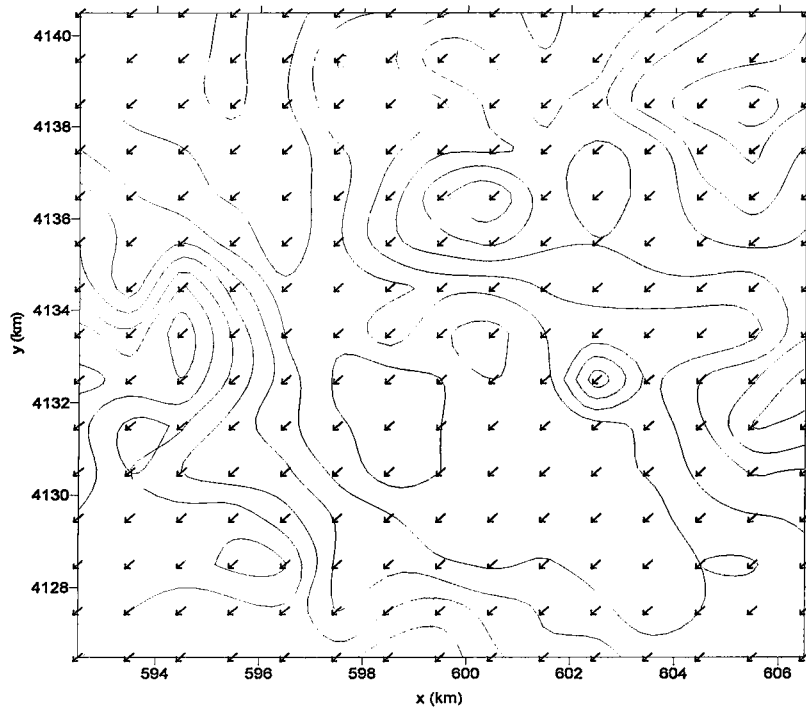


Figure 5.11. Wind field for the modeling area at 15:00 on December 4, 2000

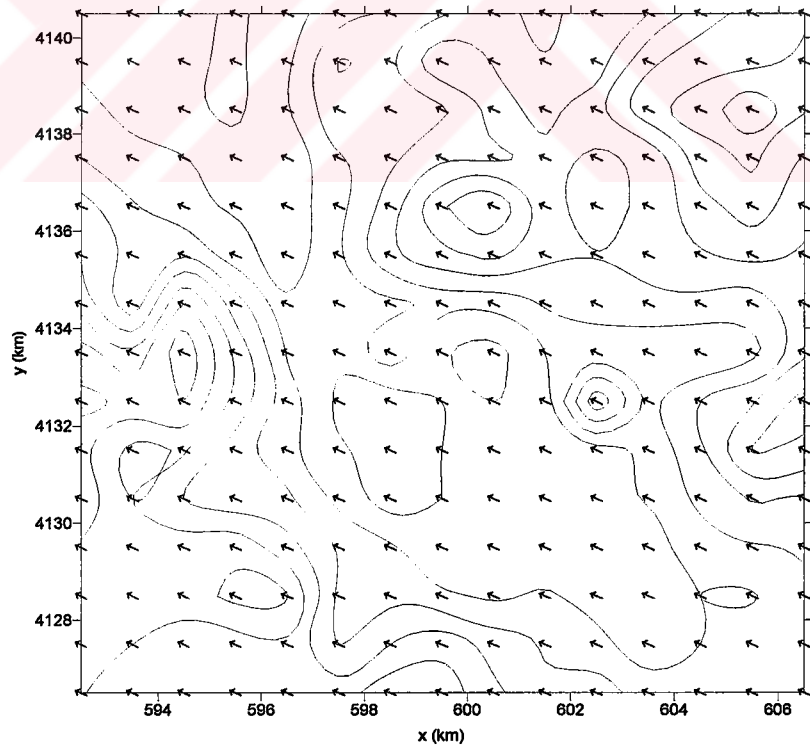


Figure 5.12. Wind field for the modeling area at 23:00 on December 4, 2000

For the simulation of the dispersion of SO₂ emitted from Yatağan Power Plant, CALPUFF was run for 96 hours, starting from December 1, 2000 at 00:00 to December 4, 2000 at 23:00. Since the plant has three units, the source is considered as three point sources emitting SO₂. The emission rates from each unit are 1402, 1209, and 1193 gs⁻¹, respectively. Stack heights are 120 m, exit temperatures are 163° K, and exit velocities are approximately 4.10 ms⁻¹.

The simulation results indicate that maximum ground level concentrations are found northeast from the source, which agrees with experimental observations. On the other hand, the magnitude of results resolved by the model shows some differences compared with experimental measurements. These discrepancies are due to the presence of complex wind patterns and their influence on the pollutant dispersion (Garcia *et al.*, 1999). Wind speeds less than 2 ms⁻¹ are generally considered to be low, as most of the conventional models for dispersion are to some extent, because of their assumptions considering the wind speed falls below 2 ms⁻¹. In most of the Gaussian plume models, when mean wind speed becomes very low (< 2 ms⁻¹) the pollutant concentrations tends to go exceptionally high (Sharan *et al.*, 1996).

According to the results of this simulation, Yatağan town center was highly affected from the SO₂ emissions from Yatağan Power Plant on December 2 and 3, 2000, and the ground level concentrations within this period exceeded the maximum limit of 400 µgm⁻³ that has been prescribed by legislations, and reached to values around 4100 µgm⁻³. The ground level concentrations in each receptor for some selected hours for each day of the simulation are presented in Figures 5.13 through 5.24. With the south – easterly winds, the pollutants were carried to the western part of the domain after 8 hours from the beginning of the simulation, with concentration values varying around 100 µgm⁻³, and a maximum ground level concentration of 39 µgm⁻³ at Yatağan town center (Figure 5.13.). During day time, at noon hours, with wind directions slightly changing, but still south – easterly blowing, and with increasing wind speed, the pollutants continued dispersing through the same region (Figure 5.14.). After 15:00, with winds starting to change direction and become south – westerly, the pollutants first start to disperse over a narrower region around the power plant (Figure 5.15). Starting from the early hours of December 2, 2000, pollutants are carried towards Yatağan

district, and with decreasing wind speeds, pollutants dispersed over a larger region over the town center reaching a maximum ground level concentrations of $974 \mu\text{gm}^{-3}$ (Figure 5.16.). At noon, under stable conditions, with a sharp decrease of wind speed to values below 0.5 ms^{-1} and temperatures falling to 2° C , the pollutants were trapped over Yatağan District with a maximum ground level concentration of $3140 \mu\text{gm}^{-3}$ (Figure 5.17.). After noon, with the increasing wind speed, the pollutants were carried away from the district and ground level concentrations decreased to values around $150 \mu\text{gm}^{-3}$, and a maximum level of $165 \mu\text{gm}^{-3}$ was observed (Figure 5.18). At night and at early hours of December 3, 2000, the wind speed was again subject to some decrease and winds turned out to be westerly, carrying the pollutants towards Yatağan again and causing concentrations over the district increase and reach a maximum level of $510 \mu\text{gm}^{-3}$ (Figure 5.19.). Significant decreases of wind speed to values below 0.5 ms^{-1} in early hours of the morning, despite the change of winds to north – westerly direction, caused pollutants to be trapped over the district again and reached a maximum ground level concentration of $1593 \mu\text{gm}^{-3}$ (Figure 5.20.). After noon, with the winds blowing south – easterly and wind speed increasing, the pollutants are carried away from the simulation area (Figure 5.21.). On December 4, 2000, the ground level concentration of SO_2 over Yatağan district was below $100 \mu\text{gm}^{-3}$ and a maximum value of $73 \mu\text{gm}^{-3}$ was computed (Figures 5.22. through 5.24.).

Inversion heights are calculated by the temperature - height profiles provided from the radiosonde data taken from Isparta Meteorological Station, and the results indicated that night time surface inversion layers were present on 2 and 3 December, 2000, and pollutants were not dispersed due to low mixing heights. The average mixing height is calculated as 323 m and 440 m for 2nd and 3rd of December, respectively.

The maximum concentration during the simulation period in the domain is calculated as $3140 \mu\text{gm}^{-3}$ on the 38th hour of the period, on December 2, 2000, at 13:00, whereas according to the on site measurements recorded by Local Environmental Authority of Muğla (Muğla İl Çevre Müdürlüğü), the highest ground level concentration measured at Yatağan during the simulation period is recorded as $4100 \mu\text{gm}^{-3}$. This difference between the modeled concentration levels and measured concentration levels may originate from the inadequacies with meteorological data incorporated into the model. The fact that the meteorological station

where radiosonde data are obtained from is outside the modeling domain causes the model not to resolve the meteorological conditions during the simulation efficiently. Therefore, data obtained from only one meteorological station inside the modeling area may not permit to adequately resolve the episode. The predicted concentrations are calculated as the maximum average values within 1 hour intervals inside a 1 km x 1 km resolution whereas the on site observations represent the conditions at the particular moment at a particular point. Therefore, a one to one match between the predicted and observed concentrations was not expected.

As can be seen from the figures presenting the ground level concentrations in the domain, peak levels of concentrations occur inside the grid where the power plant is located. Since the overall SO₂ emission from the plant is very high (3804 gs⁻¹), the concentrations calculated by the model within this grid were expected to be high. A more detailed study can be done by dividing the modeling domain to smaller grids in order to understand the behavior of the plume close to the plant better, but since the main interest is concentrated on the effects of this episodic event on the Yatağan district, these peak concentration levels in the power plant grid are not discussed in evaluating the effects of power plant on the region.

The image maps of the ground concentration levels are also provided in Figures 5.25. through 5.36. in order to visualize and understand the dispersion of the pollutants better.

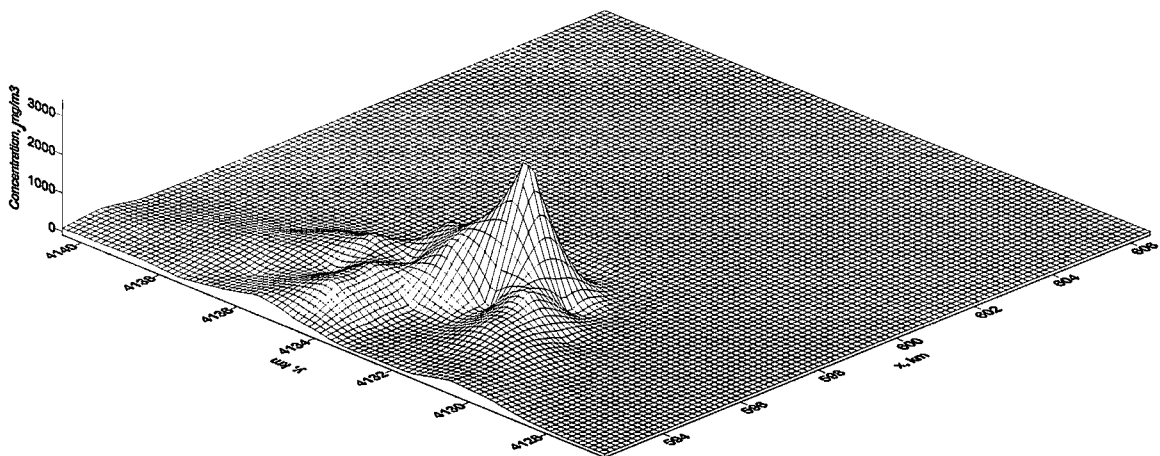


Figure 5.13. Concentration distribution for the modeling area at 07:00 on December 1, 2000

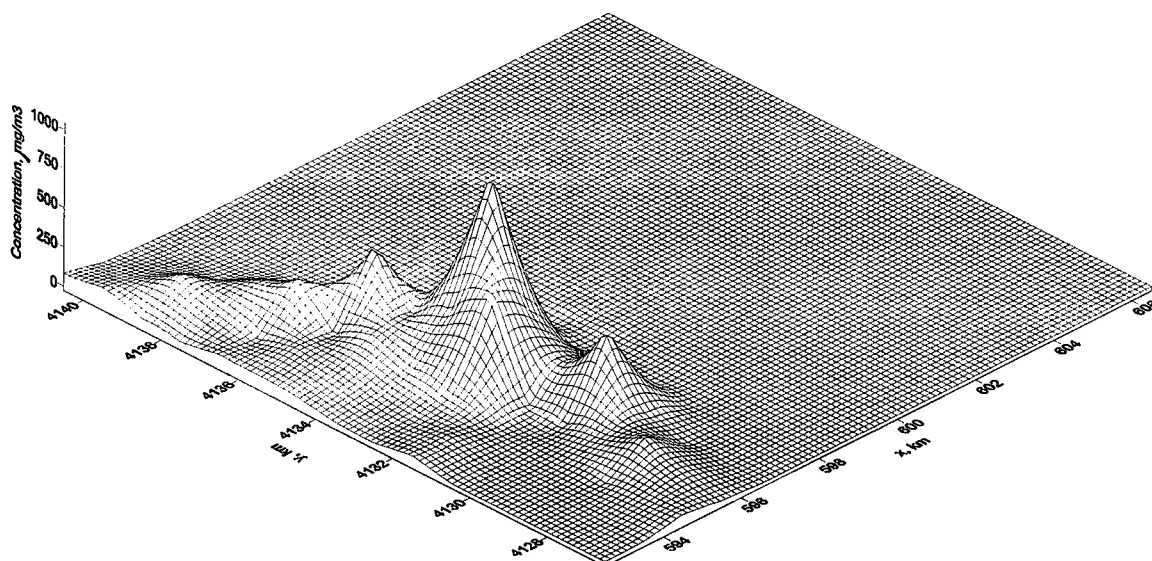


Figure 5.14. Concentration distribution for the modeling area at 15:00 on December 1, 2000

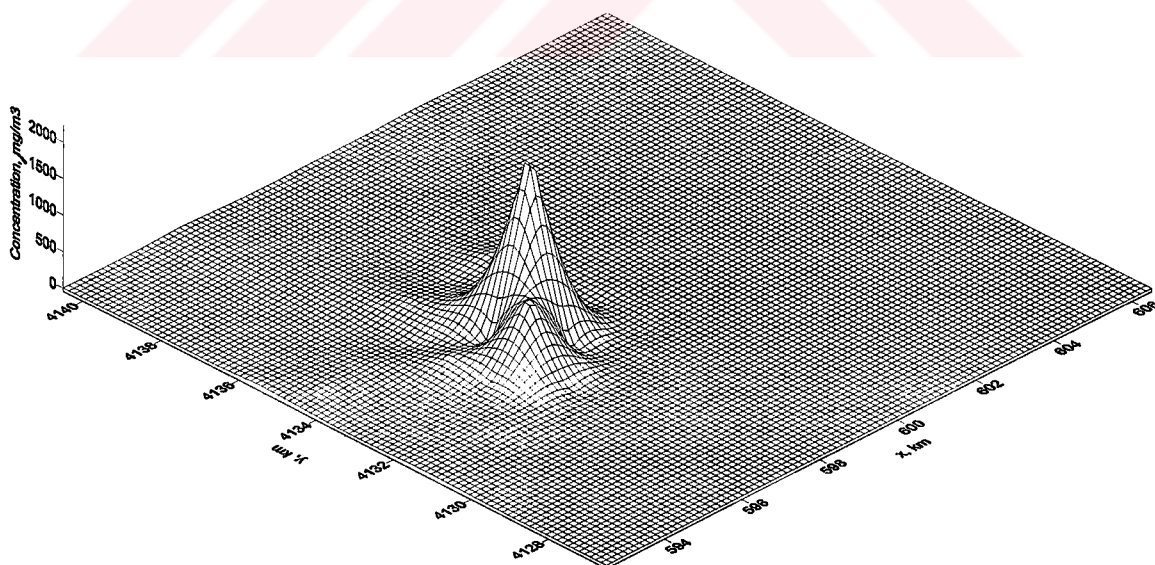


Figure 5.15. Concentration distribution for the modeling area at 23:00 on December 1, 2000

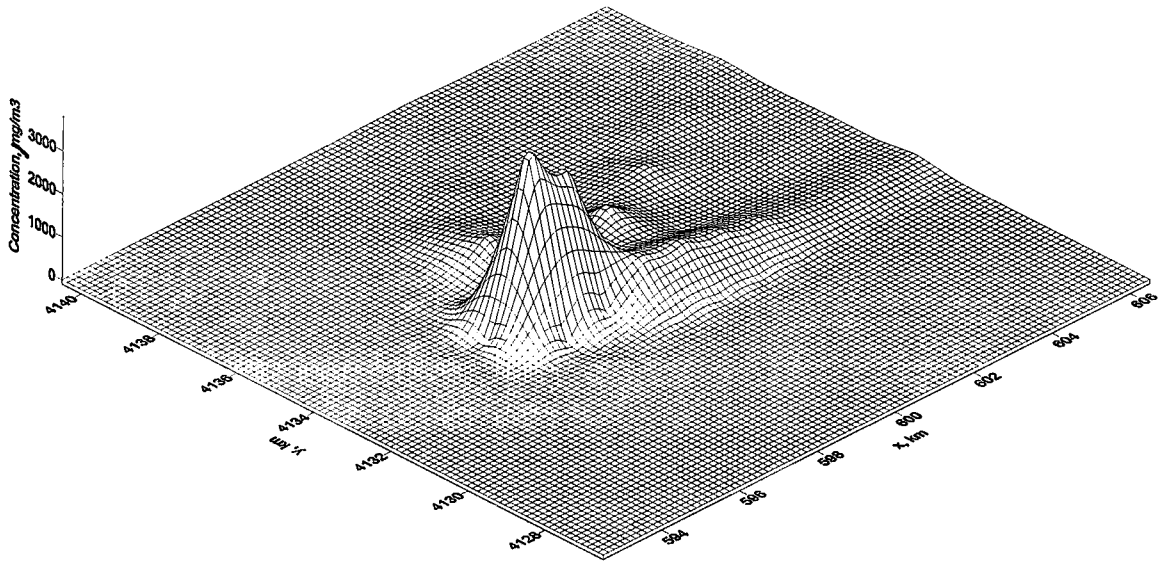


Figure 5.16. Concentration distribution for the modeling area at 07:00 on December 2, 2000

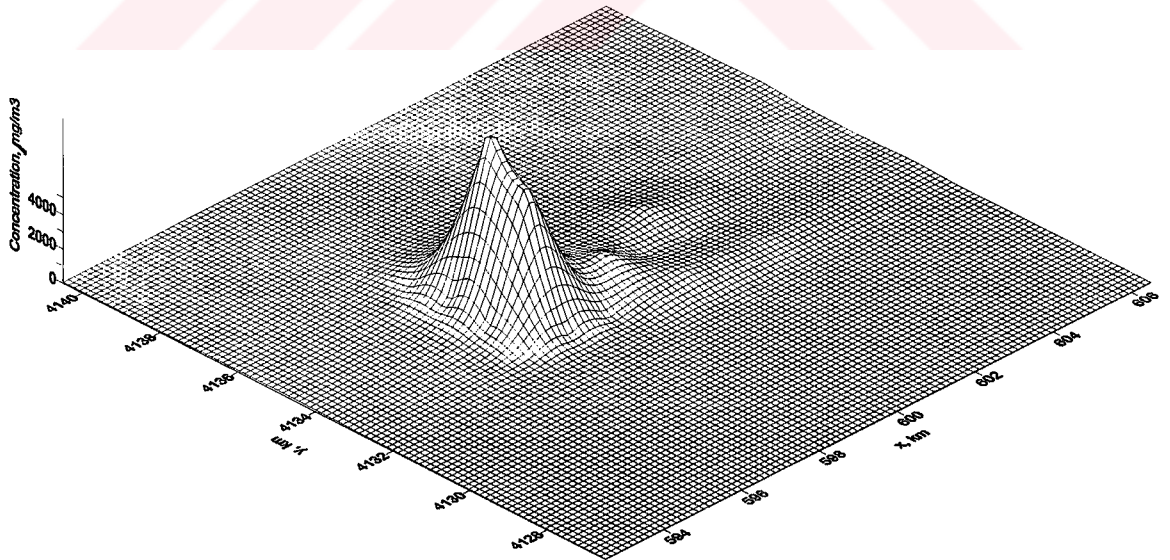


Figure 5.17. Concentration distribution for the modeling area at 15:00 on December 2, 2000

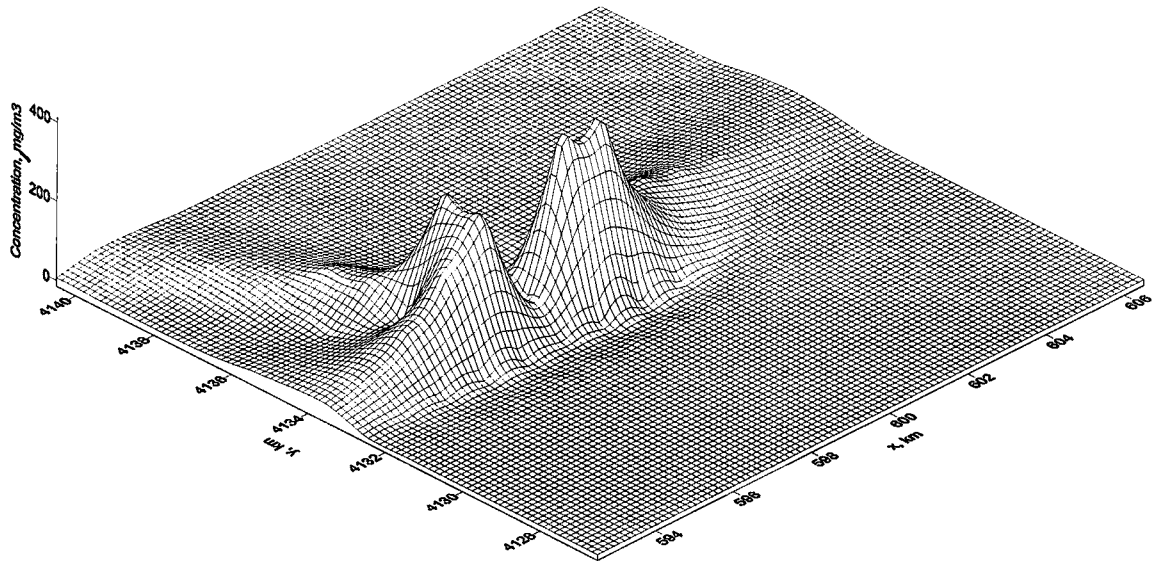


Figure 5.18. Concentration distribution for the modeling area at 23:00 on December 2, 2000

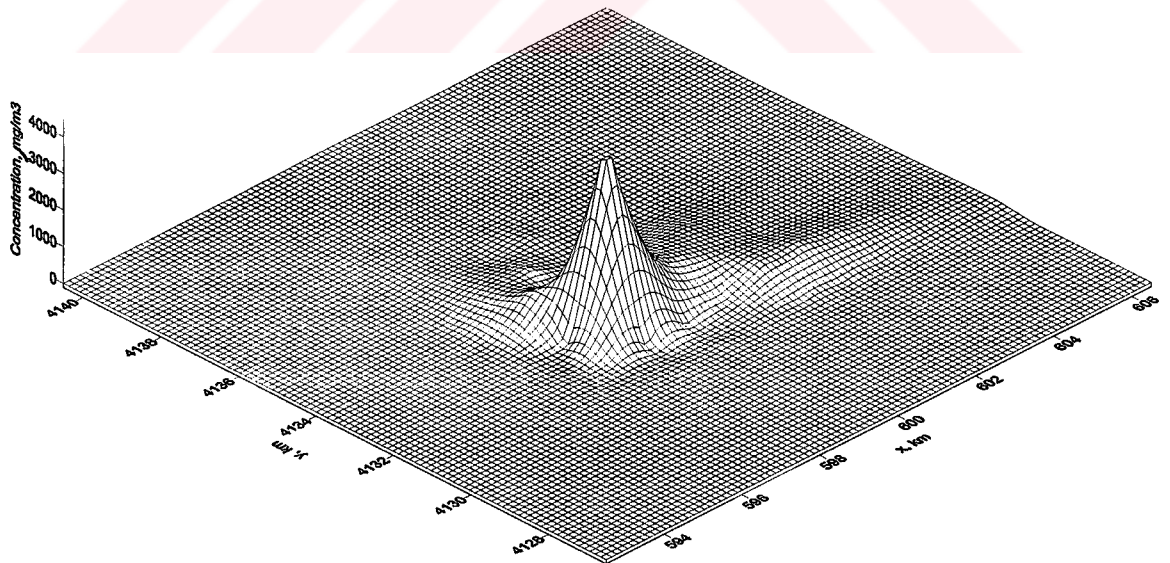


Figure 5.19. Concentration distribution for the modeling area at 07:00 on December 3, 2000

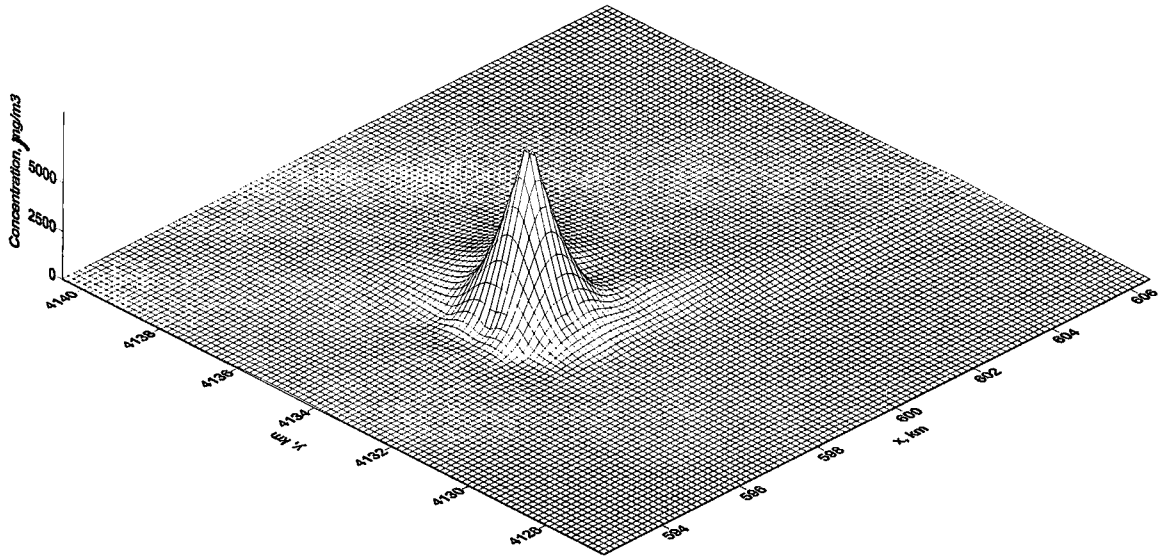


Figure 5.20. Concentration distribution for the modeling area at 15:00 on December 3, 2000

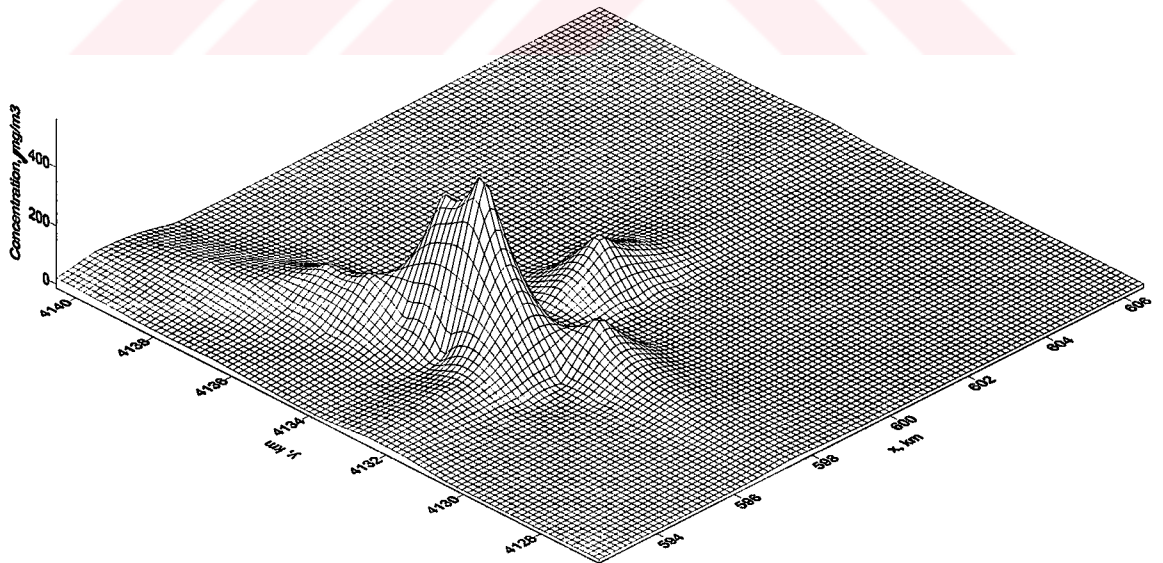


Figure 5.21. Concentration distribution for the modeling area at 23:00 on December 3, 2000

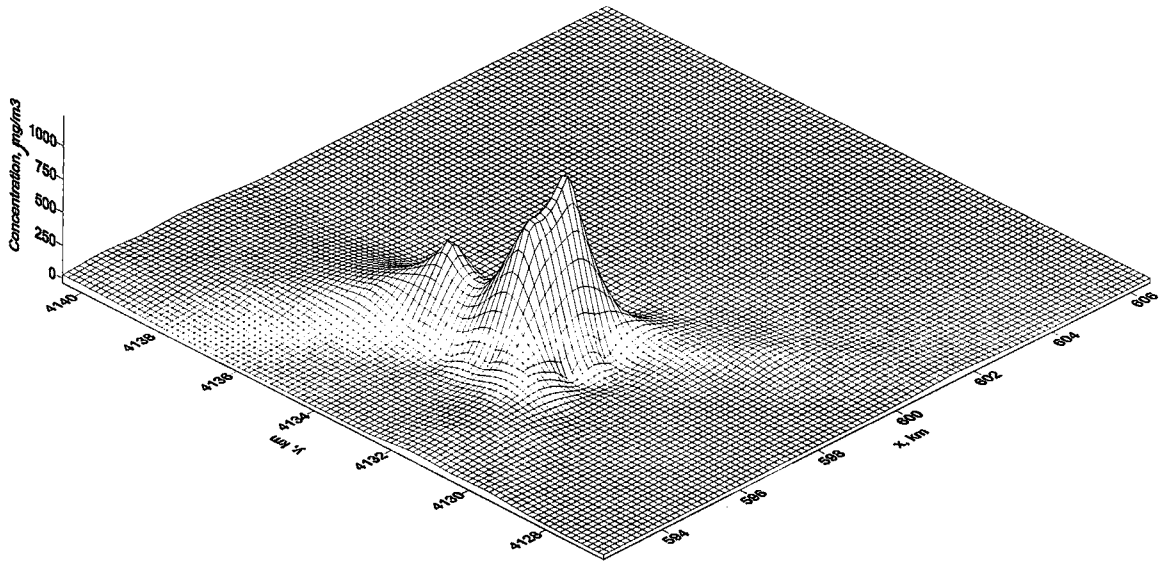


Figure 5.22. Concentration distribution for the modeling area at 07:00 on December 4, 2000

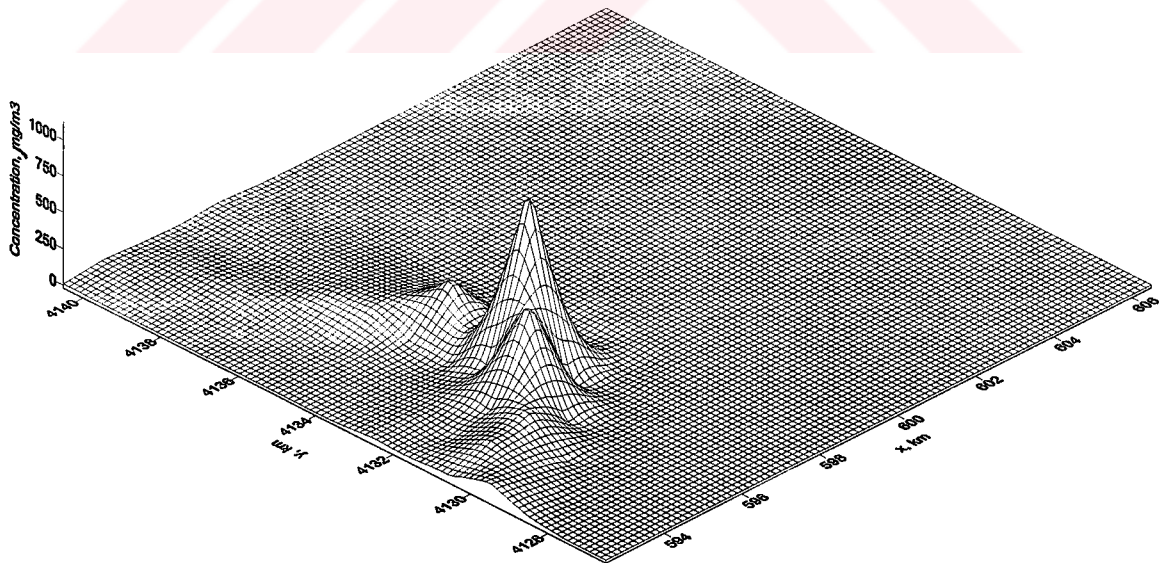


Figure 5.23. Concentration distribution for the modeling area at 15:00 on December 4, 2000

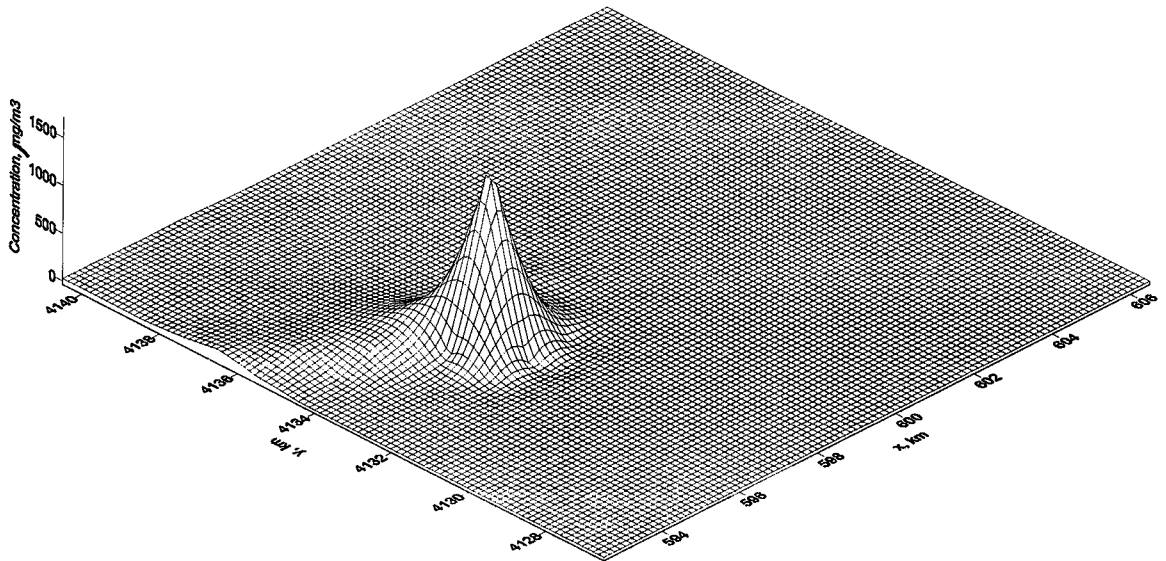


Figure 5.24. Concentration distribution for the modeling area at 23:00 on December 4, 2000

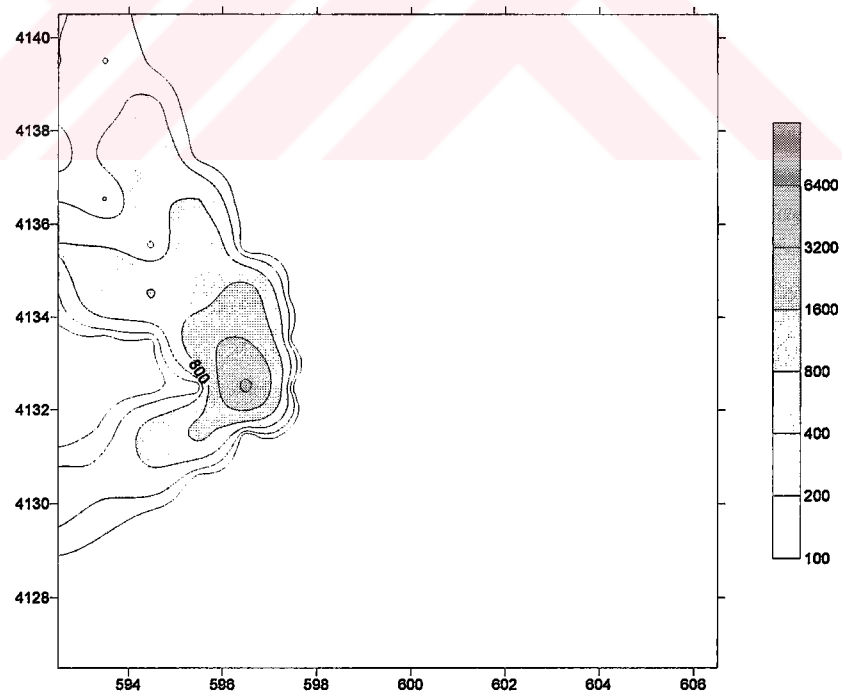


Figure 5.25. Concentration distribution ($\mu\text{g}/\text{m}^3$) at 07 :00 on December 1, 2000.

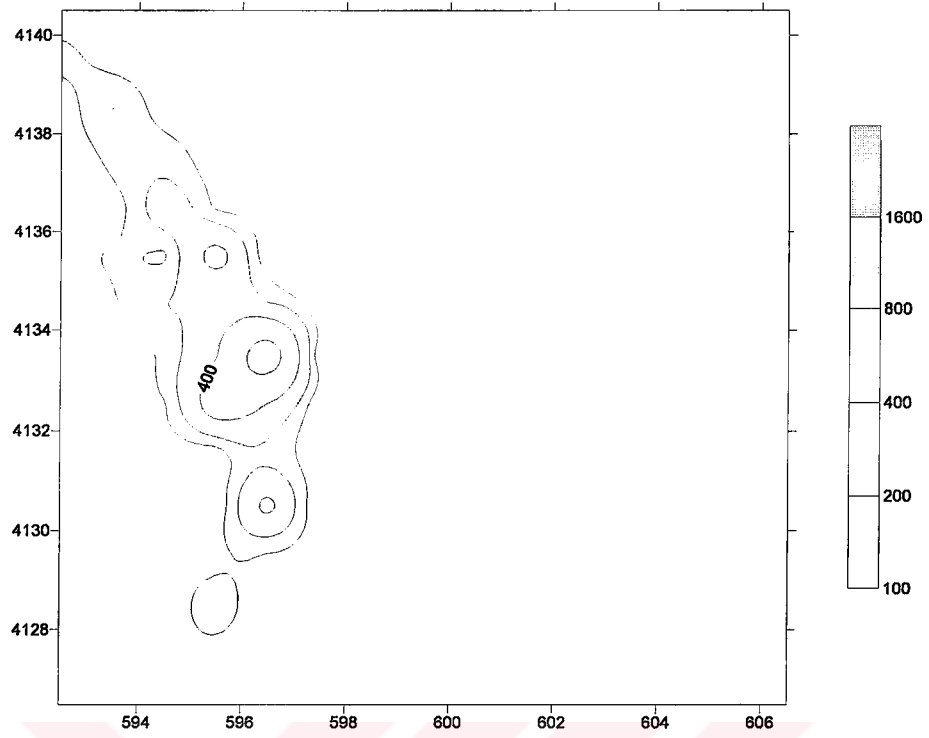


Figure 5.26. Concentration distribution ($\mu\text{g}\text{m}^{-3}$) at 15 :00 on December 1, 2000.

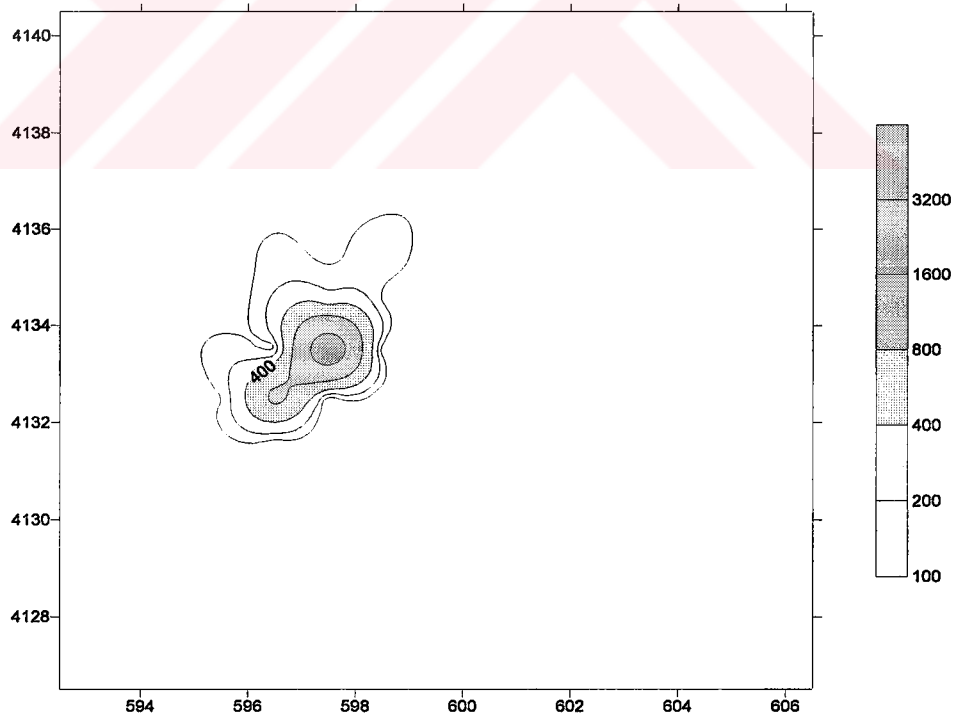


Figure 5.27. Concentration distribution ($\mu\text{g}\text{m}^{-3}$) at 23 :00 on December 1, 2000.

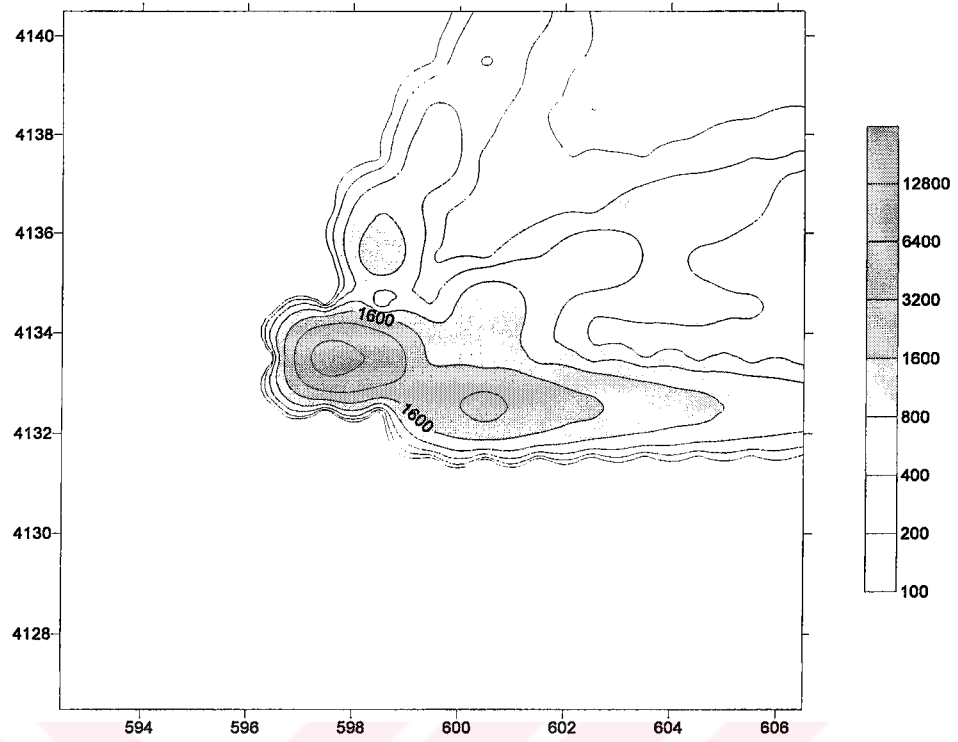


Figure 5.28. Concentration distribution ($\mu\text{g m}^{-3}$) at 07 :00 on December 2, 2000.

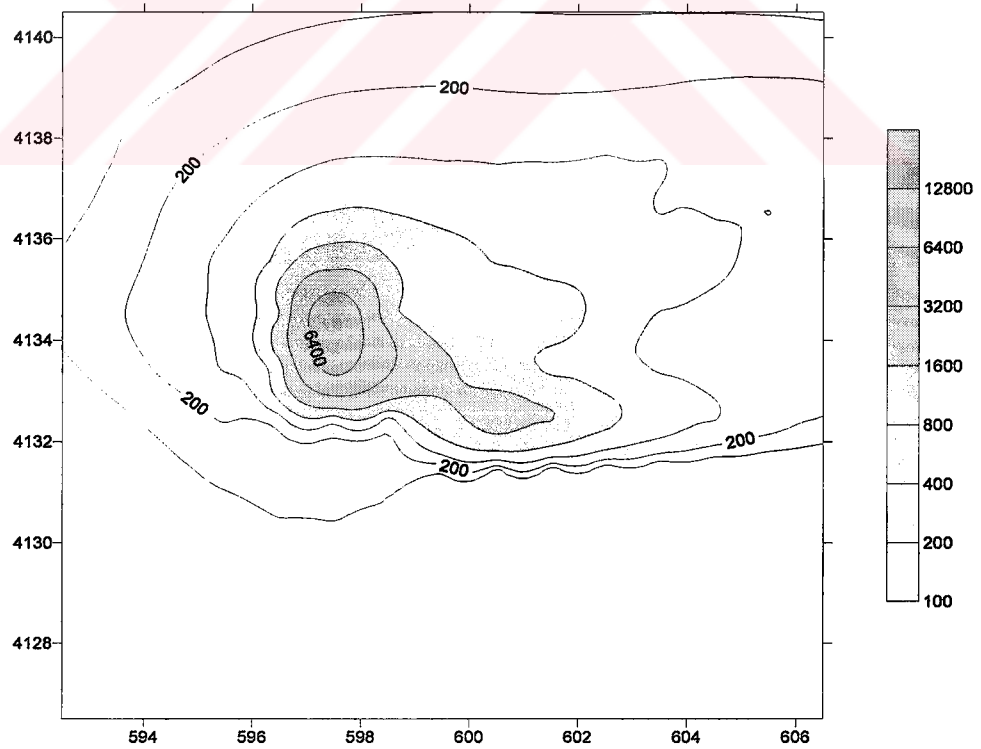


Figure 5.29. Concentration distribution ($\mu\text{g m}^{-3}$) at 15 :00 on December 2, 2000.

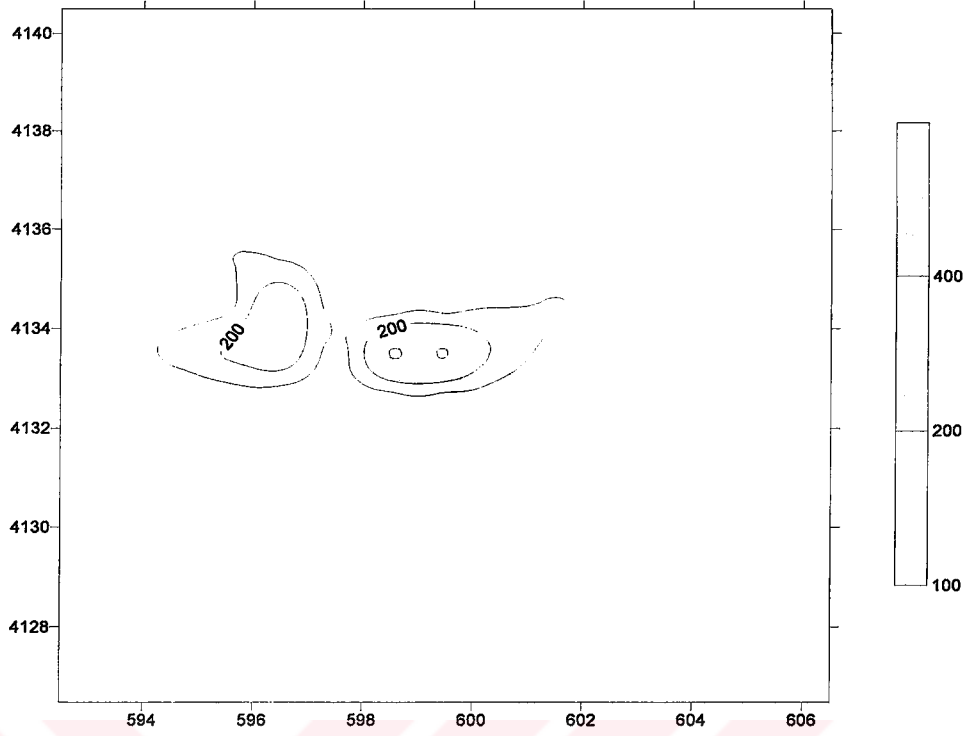


Figure 5.30. Concentration distribution ($\mu\text{g}\text{m}^{-3}$) at 23 :00 on December 2, 2000.

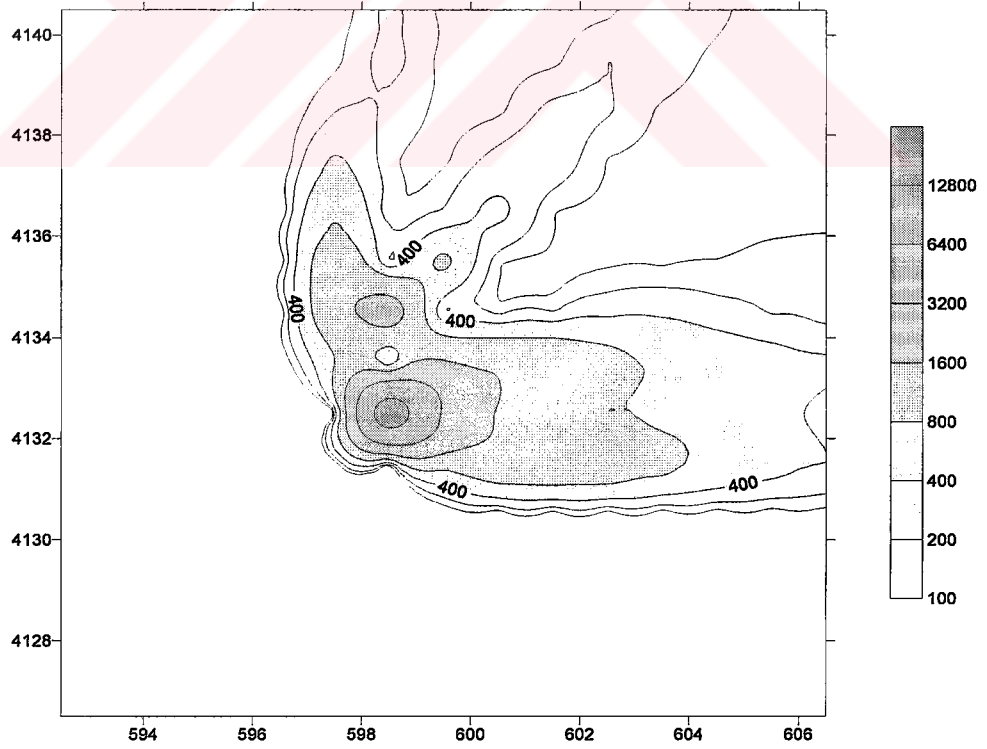


Figure 5.31. Concentration distribution ($\mu\text{g}\text{m}^{-3}$) at 07 :00 on December 3, 2000.

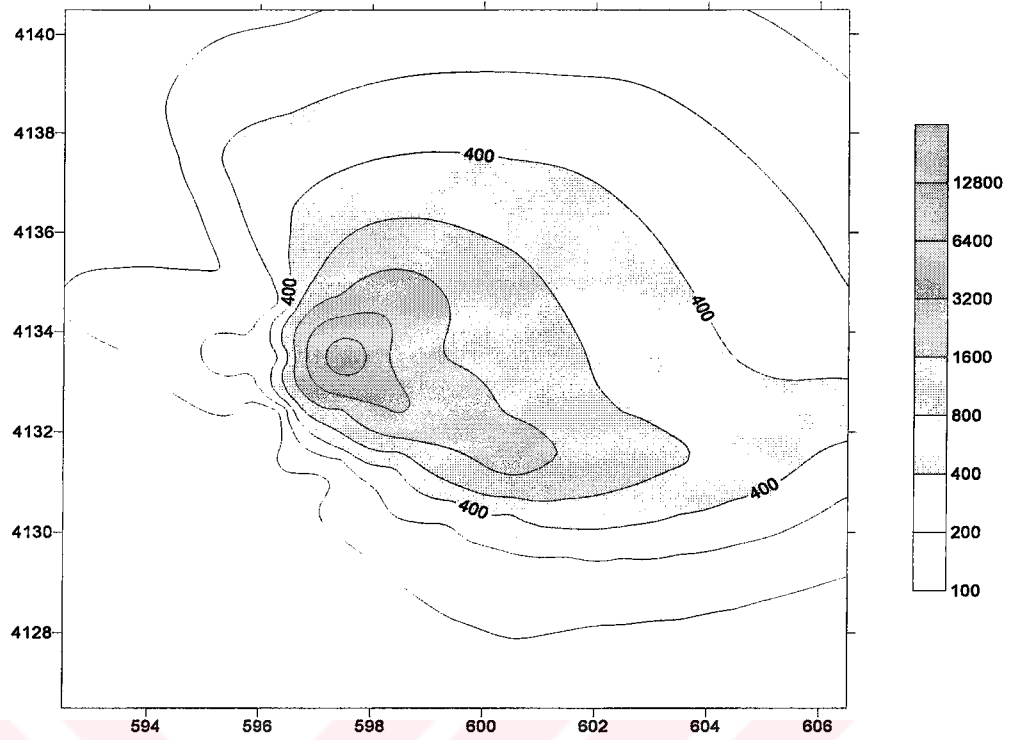


Figure 5.32. Concentration distribution ($\mu\text{g}\text{m}^{-3}$) at 15 :00 on December 3, 2000.

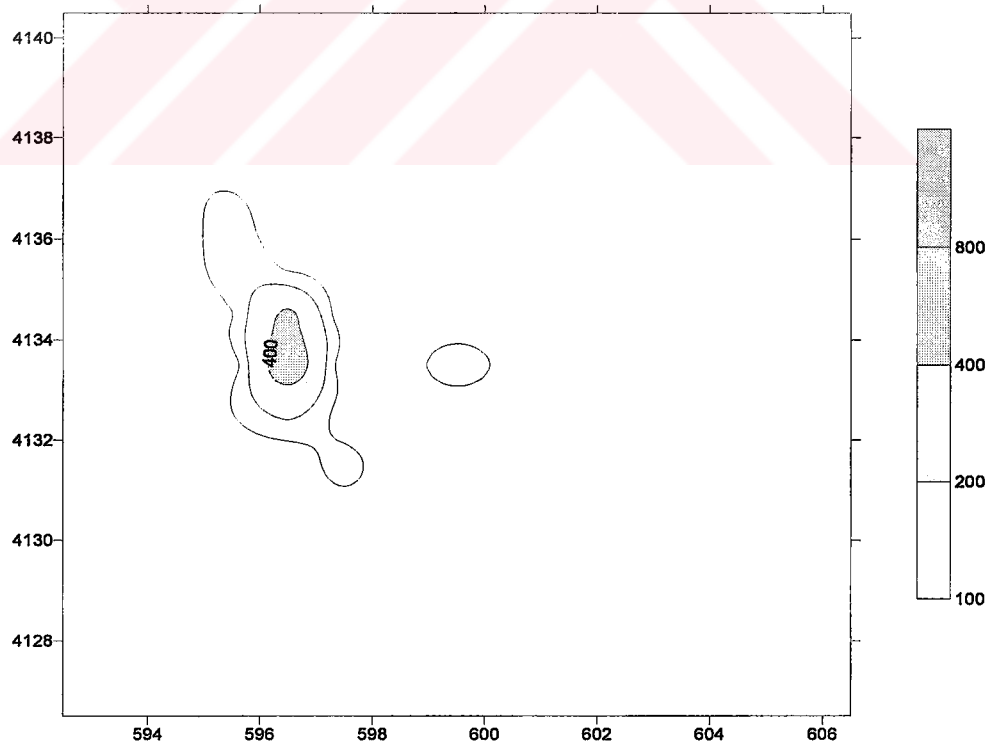


Figure 5.33. Concentration distribution ($\mu\text{g}\text{m}^{-3}$) at 23 :00 on December 3, 2000.

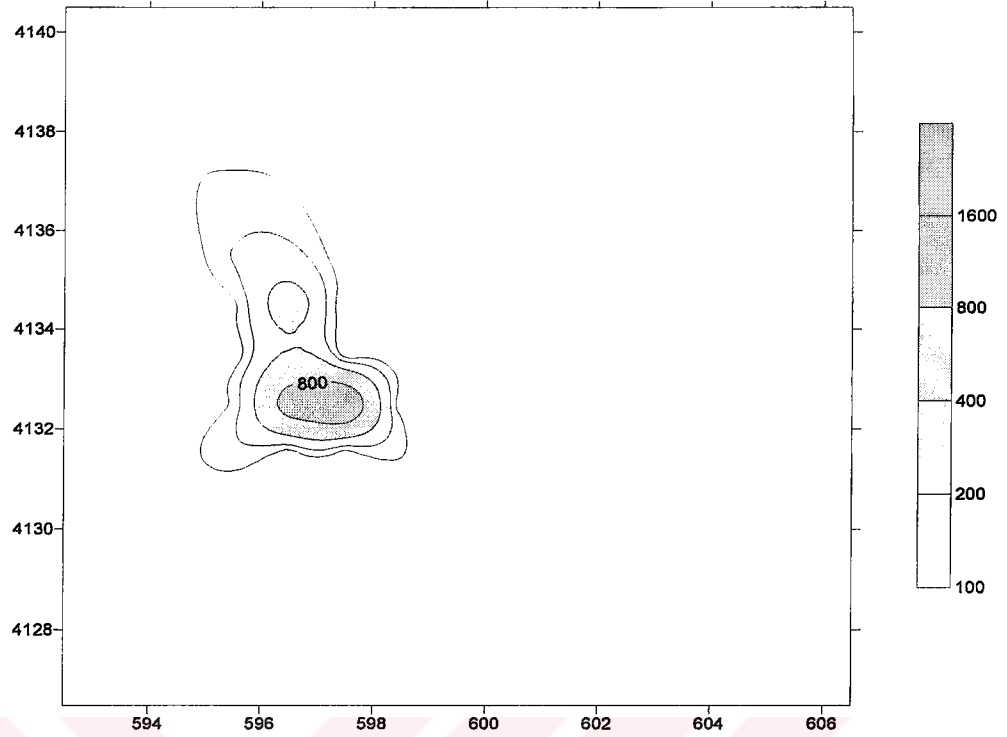


Figure 5.34. Concentration distribution ($\mu\text{g}\text{m}^{-3}$) at 07 :00 on December 4, 2000.

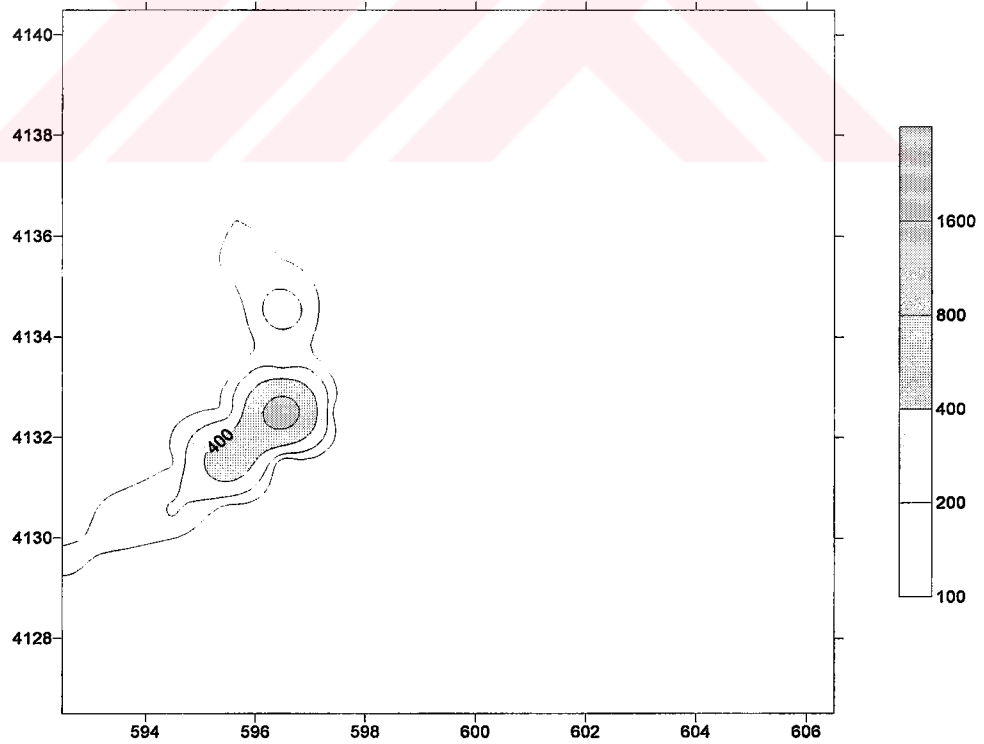


Figure 5.35. Concentration distribution ($\mu\text{g}\text{m}^{-3}$) at 15 :00 on December 4, 2000.

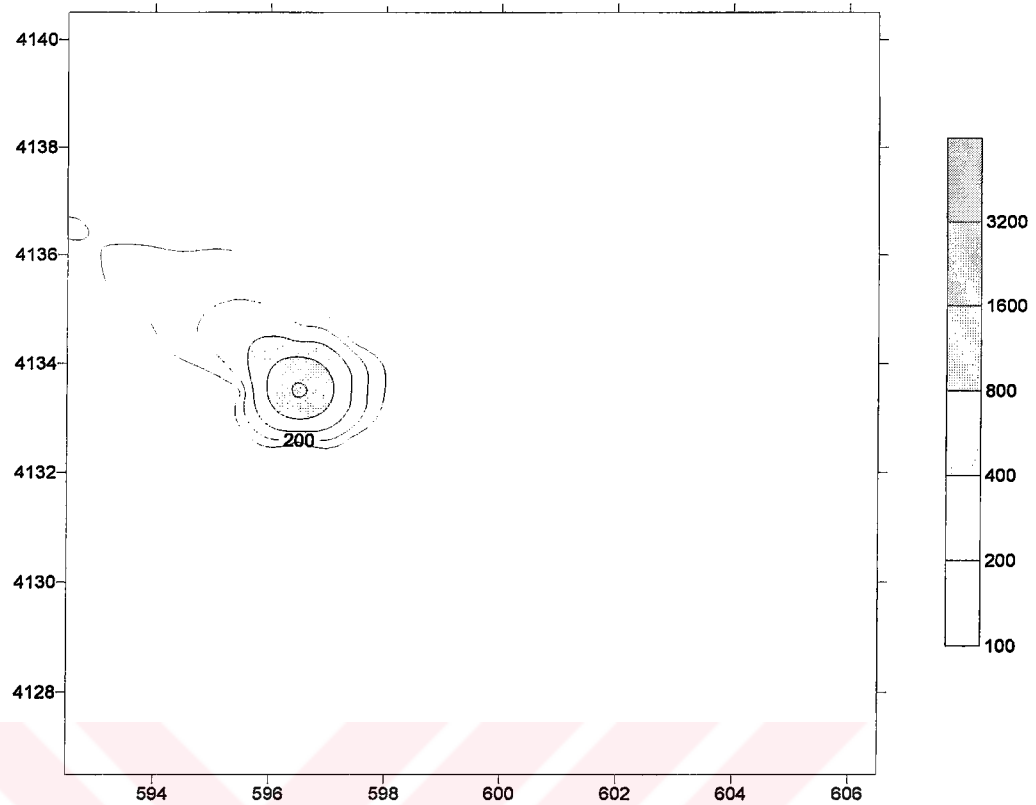


Figure 5.36. Concentration distribution ($\mu\text{g}/\text{m}^3$) at 23 :00 on December 4, 2000.

The maximum ground level concentrations calculated by the model over Yatağan are presented in Figure 5.37.

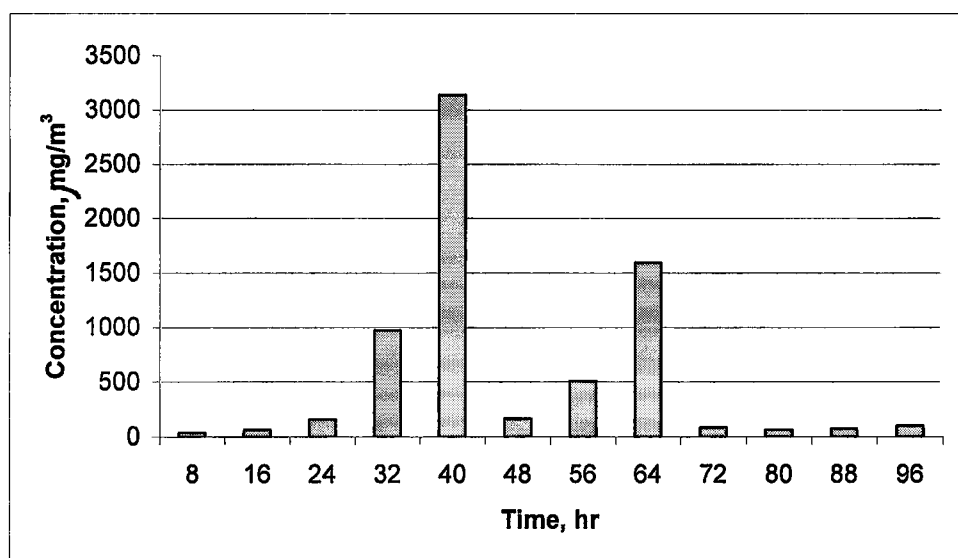


Figure 5.37. The maximum concentrations over Yatağan during the simulation period.

5.2 Simulations of Different Scenarios

Different scenarios are simulated in order to visualize how the pollutants would behave under different meteorological conditions, but same topographical and source characteristics as in the original case. Three scenarios are modeled in which the wind patterns are varied in terms of velocity and direction. In the first two scenarios, the wind speeds were subject to change to higher values and lower values, respectively. In the final scenario, the wind direction was changed. By the results of these three scenarios, the influences of the SO₂ pollution over the modeling domain are discussed.

5.2.1. Simulation of Scenario 1

In this case, it is assumed that winds observed by the surface meteorological station are not light winds causing high levels of pollutants accumulating over Yatağan district, but winds with velocities of 9 ms⁻¹ on average. The wind direction, temperature and other meteorological variables are kept the same as the original case. Figures 5.38. through 5.49 illustrate the predicted concentration levels throughout the simulation period. Image maps are also provided in Figures 5.50 through 5.61. As can be seen from these figures, as the wind speeds increase, the pollutants are well mixed and as a result decrease in the ground level concentrations are observed. The maximum ground level concentration over the district is calculated as 420 µgm⁻³, which is approximately 9 times lower than the level of 3140 µgm⁻³ in the original case. With the higher values of wind speed than in the original case, the maximum ground level concentrations do not exceed the legislation limit of 400 µgm⁻³ except for the 32nd hour of the simulation. The maximum ground level concentrations over Yatağan are presented in Figure 5.62. This simulation indicates that in case of high wind speed, the district of Yatağan would not be seriously affected as in the original case.

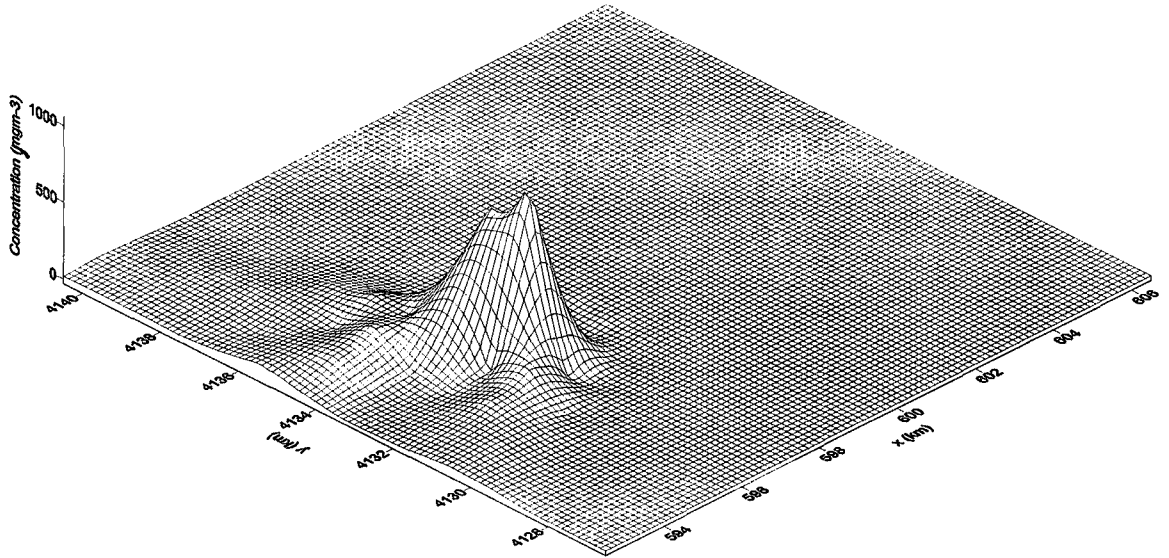


Figure 5.38. Concentration distribution for the modeling area at 07:00 on December 2, 2000

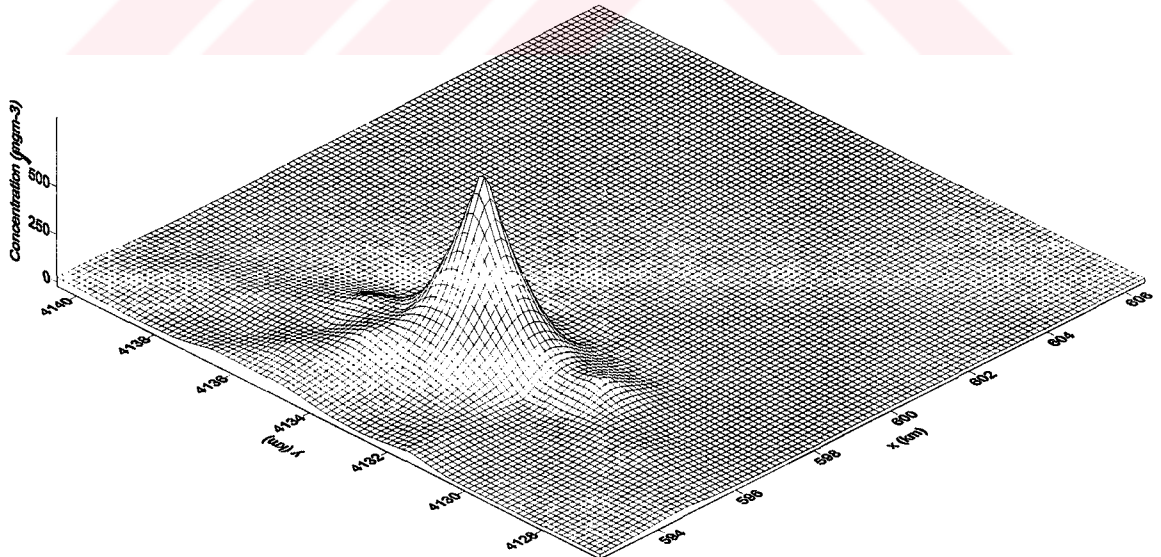


Figure 5.39. Concentration distribution for the modeling area at 15:00 on December 1, 2000

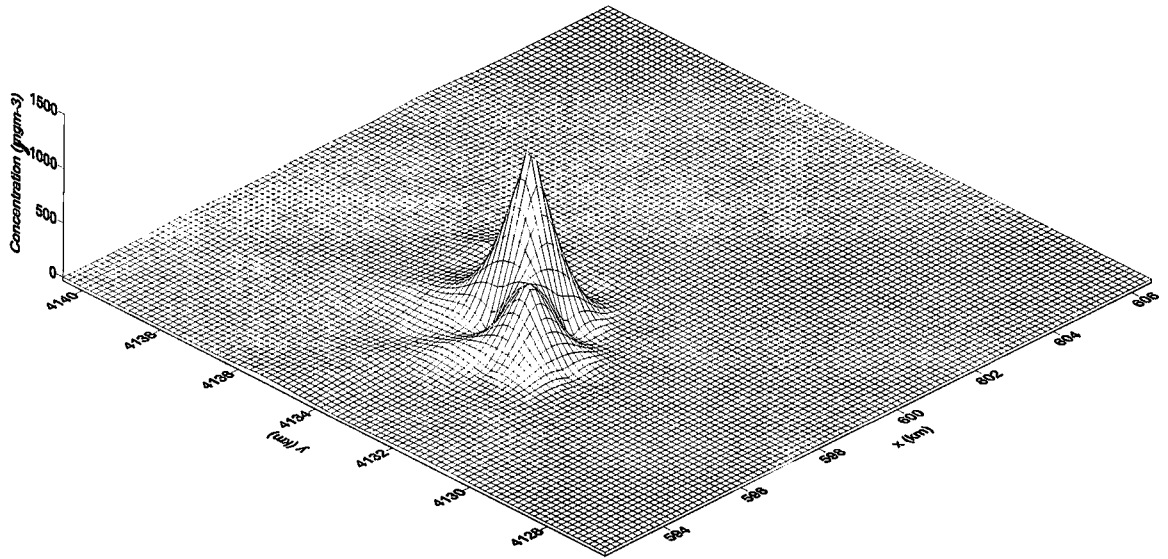


Figure 5.40. Concentration distribution for the modeling area at 23:00 on December 1, 2000

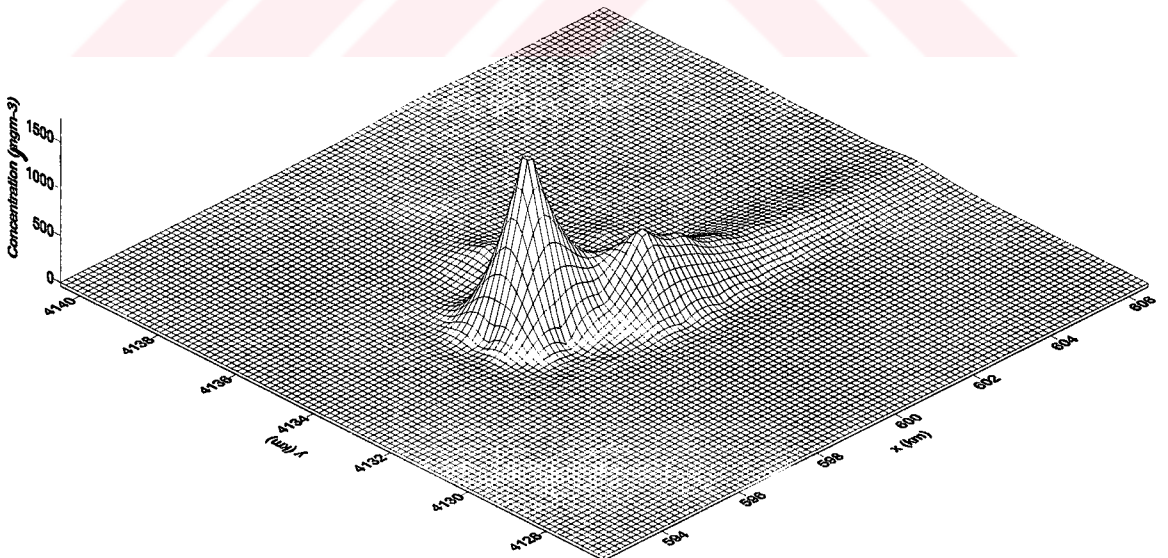


Figure 5.41. Concentration distribution for the modeling area at 07:00 on December 2, 2000

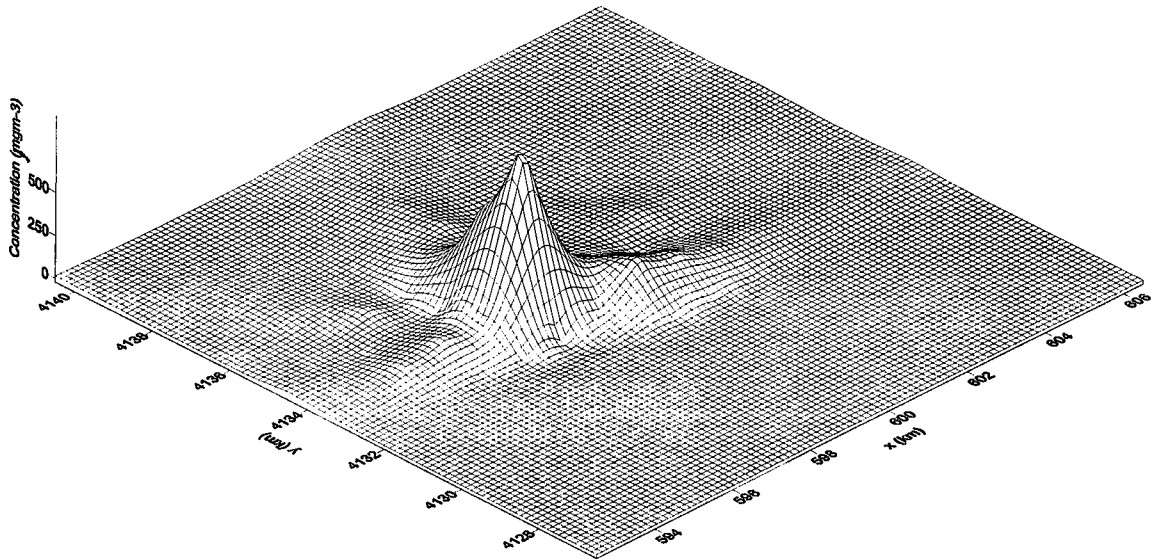


Figure 5.42. Concentration distribution for the modeling area at 15:00 on December 2, 2000

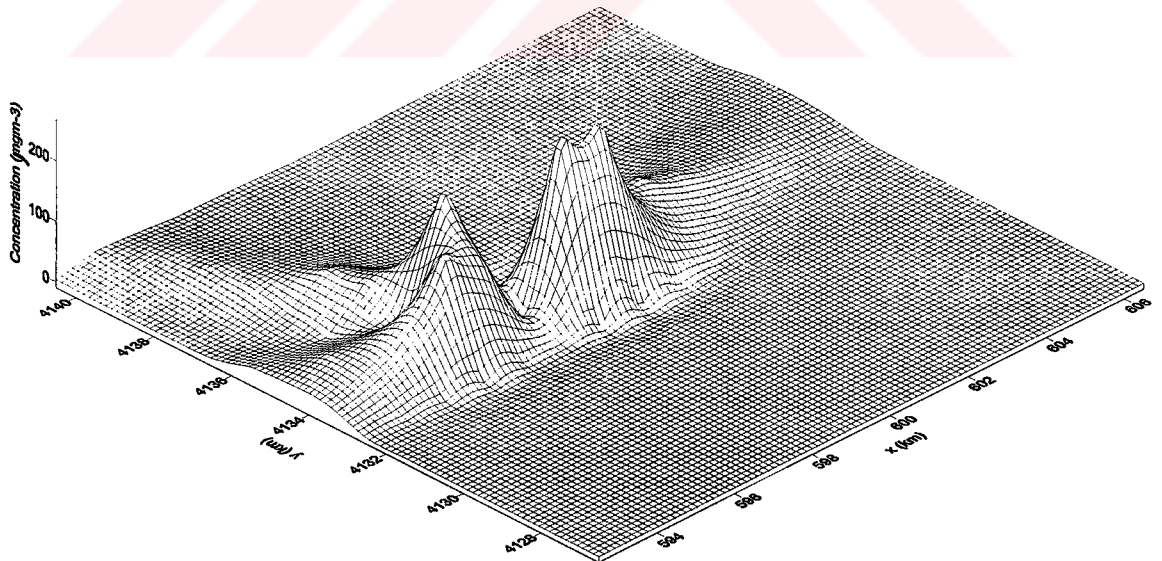


Figure 5.43. Concentration distribution for the modeling area at 23:00 on December 2, 2000

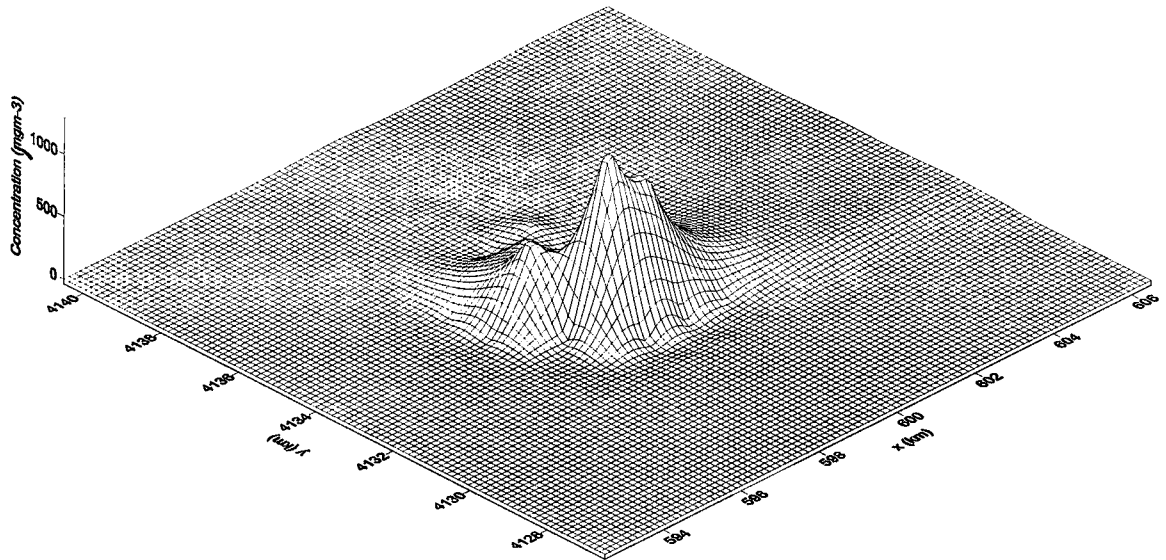


Figure 5.44. Concentration distribution for the modeling area at 07:00 on December 3, 2000

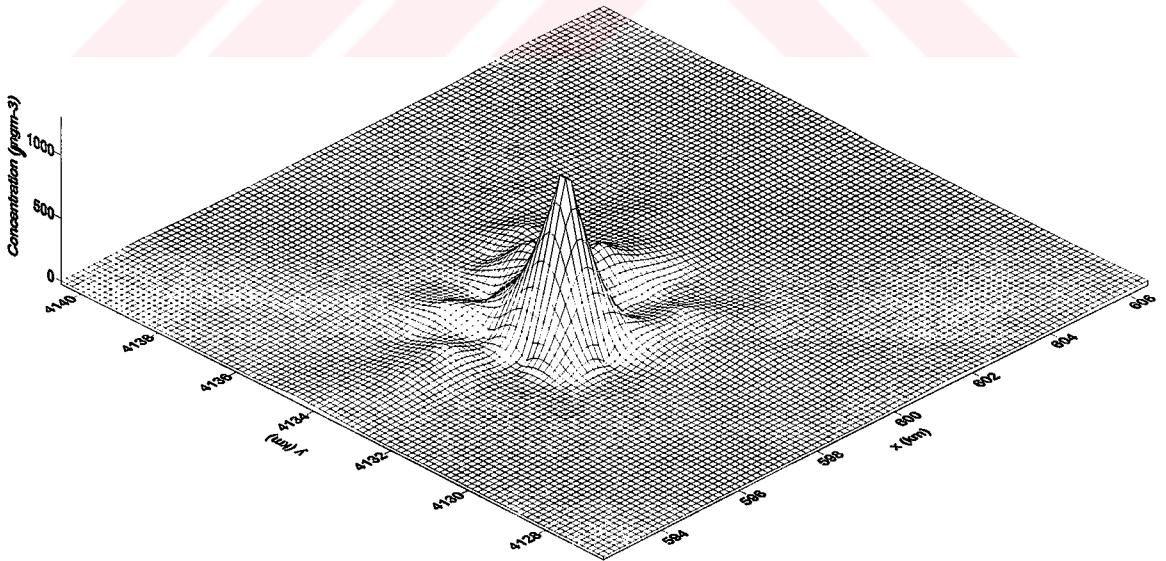


Figure 5.45. Concentration distribution for the modeling area at 15:00 on December 3, 2000

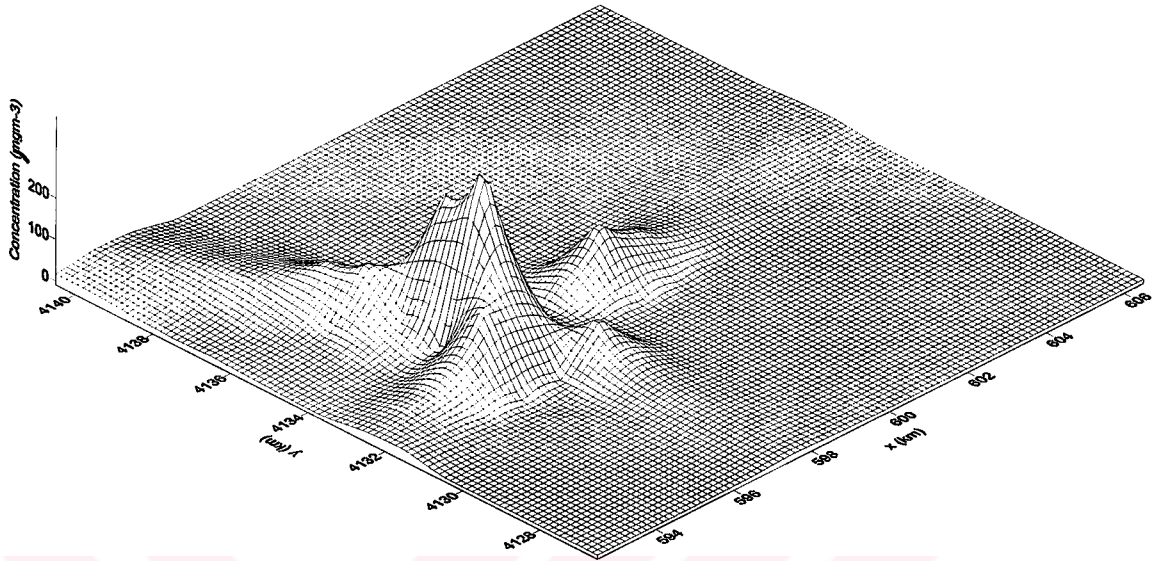


Figure 5.46. Concentration distribution for the modeling area at 23:00 on December 3, 2000

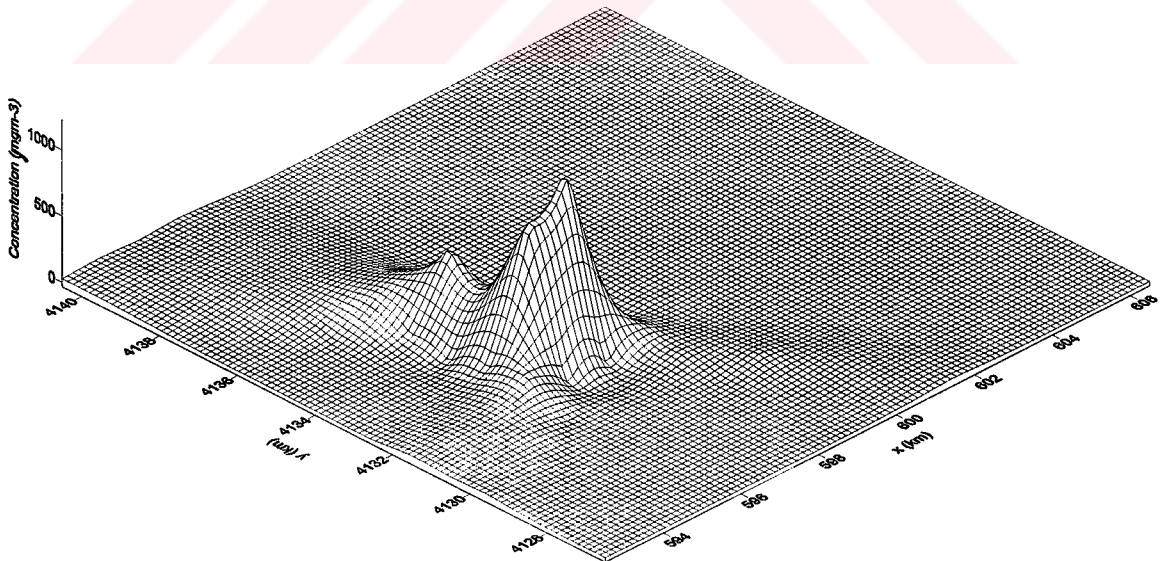


Figure 5.47. Concentration distribution for the modeling area at 07:00 on December 4, 2000

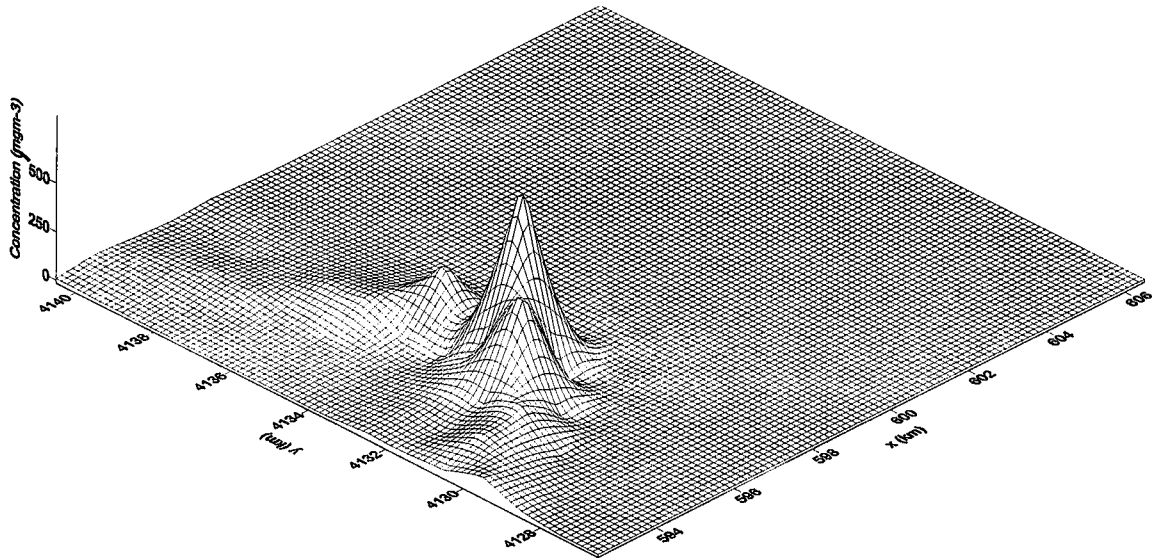


Figure 5.48. Concentration distribution for the modeling area at 15:00 on December 4, 2000

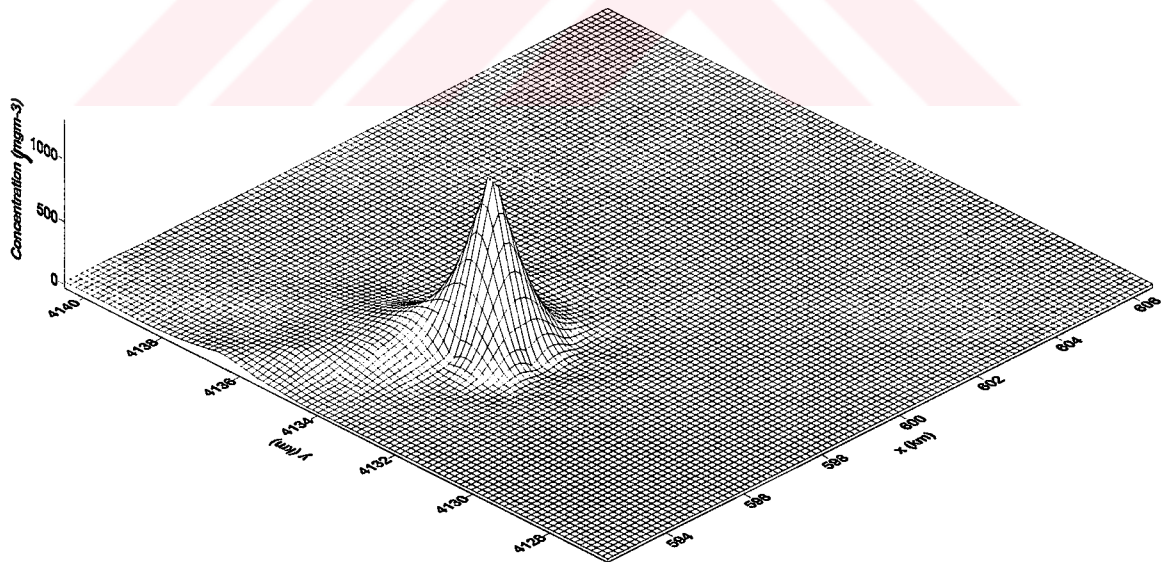


Figure 5.49. Concentration distribution for the modeling area at 23:00 on December 4, 2000

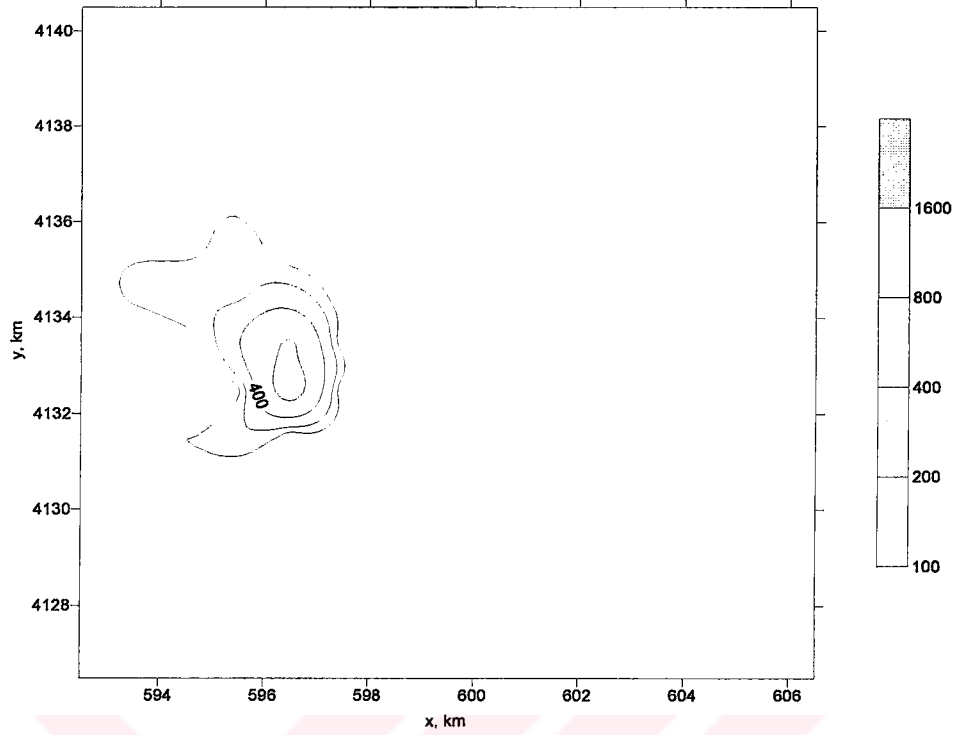


Figure 5.50 Concentration distribution ($\mu\text{g}\text{m}^{-3}$) at 07:00 on December 1, 2000.

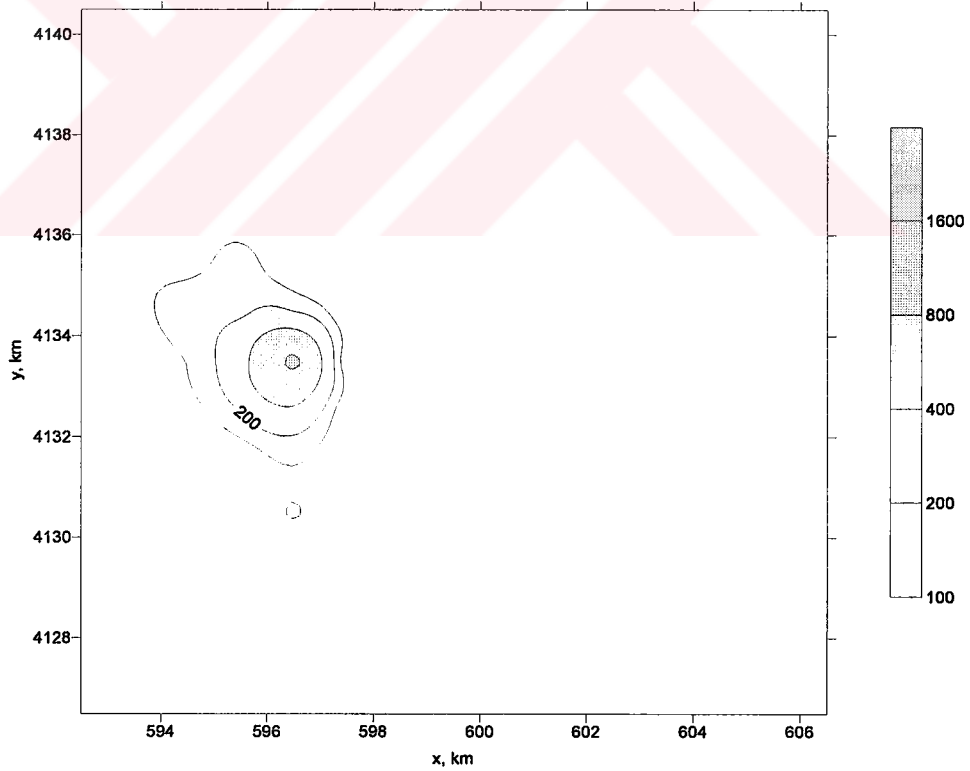


Figure 5.51 Concentration distribution ($\mu\text{g}\text{m}^{-3}$) at 15:00 on December 1, 2000.

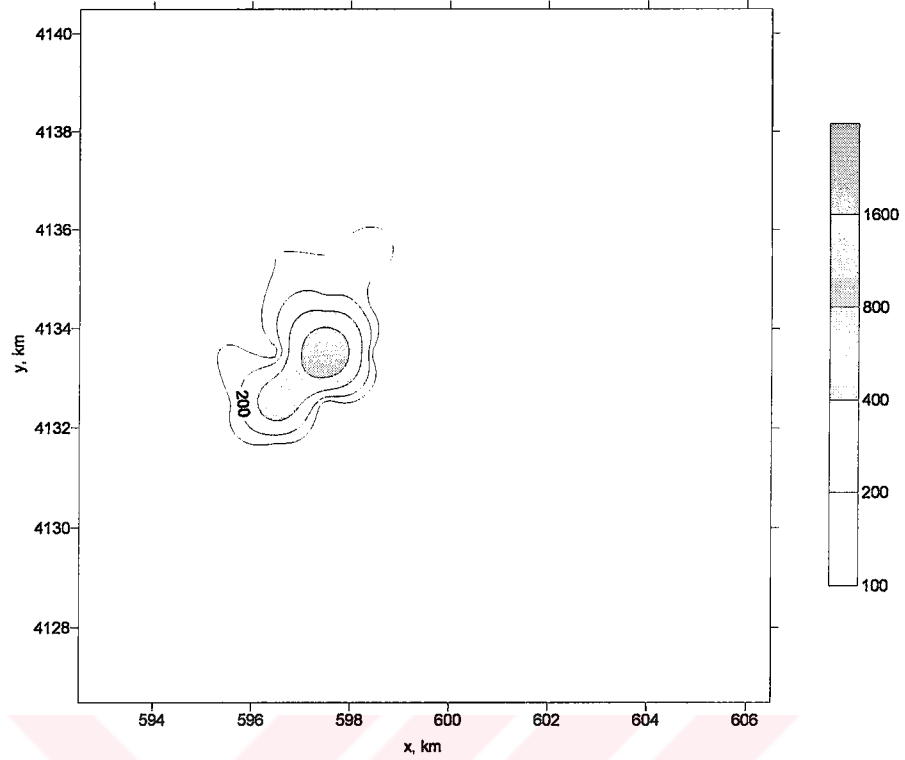


Figure 5.52 Concentration distribution ($\mu\text{g m}^{-3}$) at 23:00 on December 1, 2000.

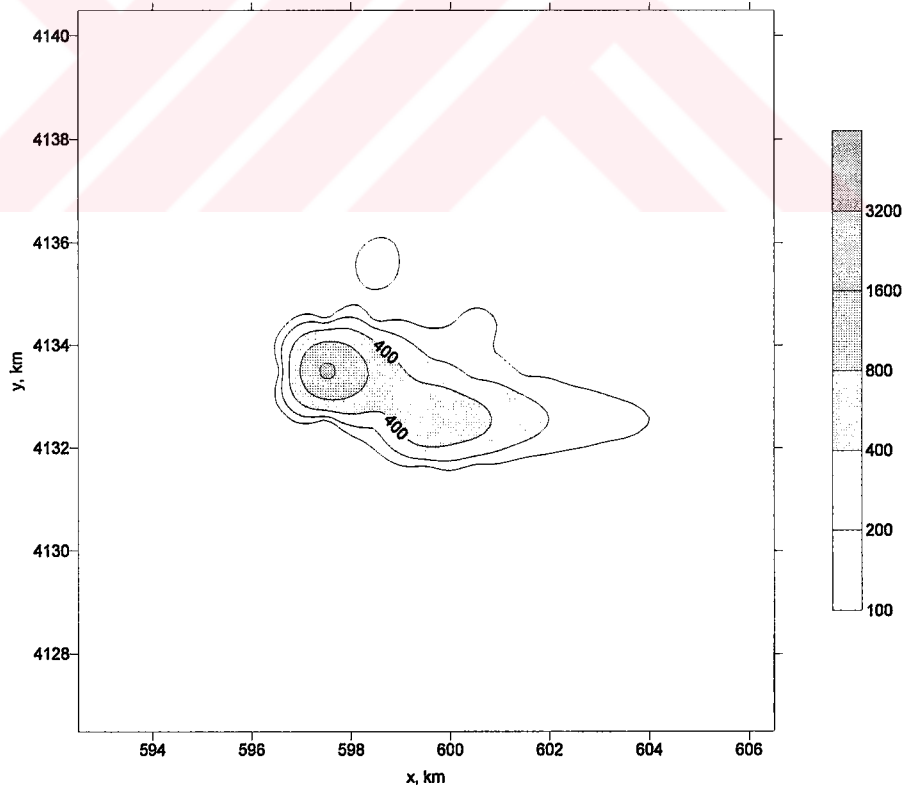


Figure 5.53 Concentration distribution ($\mu\text{g m}^{-3}$) at 07:00 on December 2, 2000.

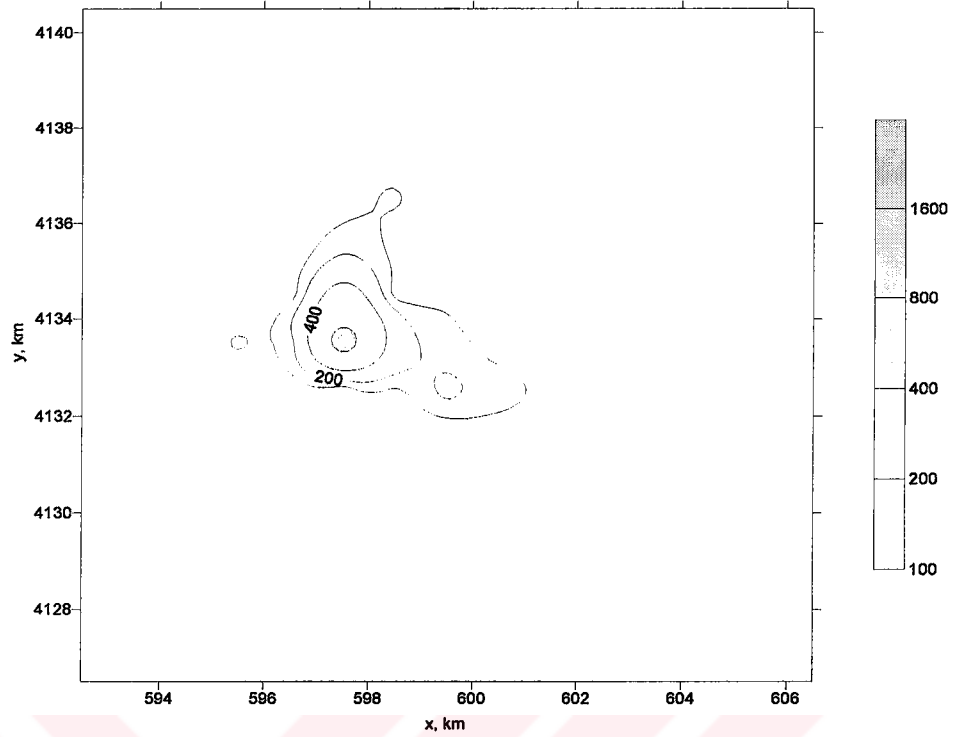


Figure 5.54 Concentration distribution ($\mu\text{g m}^{-3}$) at 15:00 on December 2, 2000.

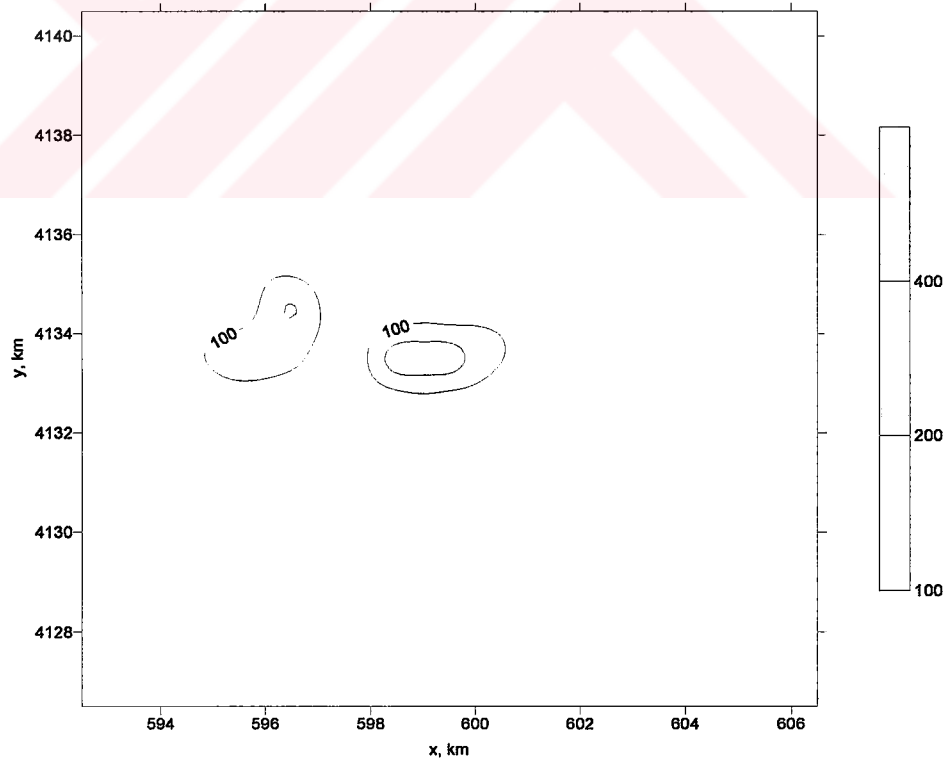


Figure 5.55 Concentration distribution ($\mu\text{g m}^{-3}$) at 23:00 on December 2, 2000.

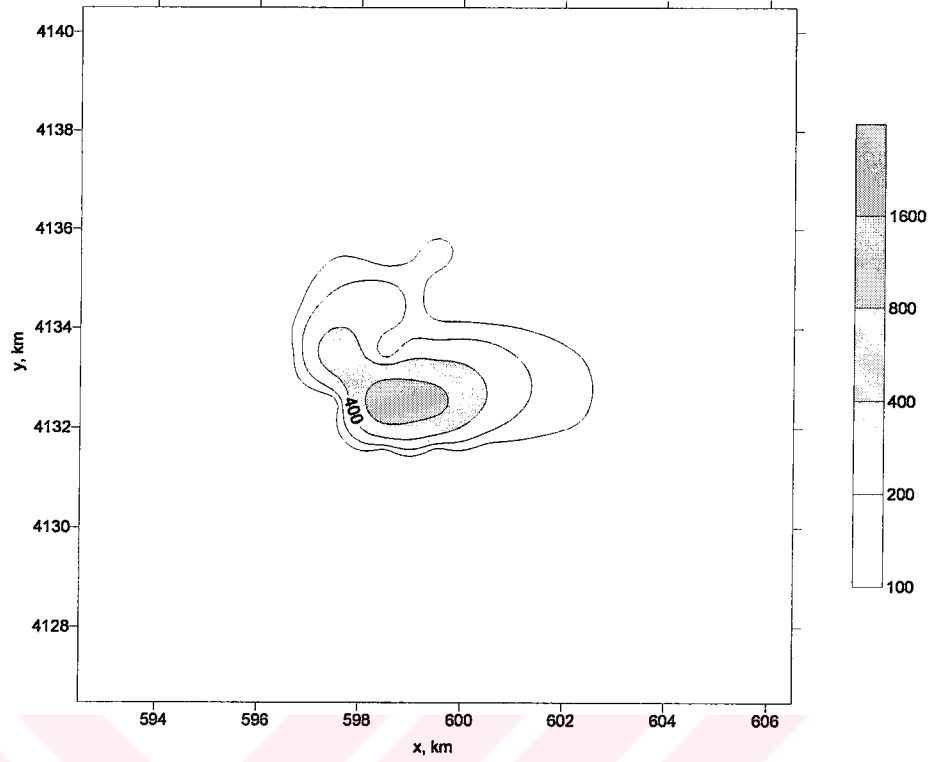


Figure 5.56 Concentration distribution ($\mu\text{g}\text{m}^{-3}$) at 07:00 on December 3, 2000.

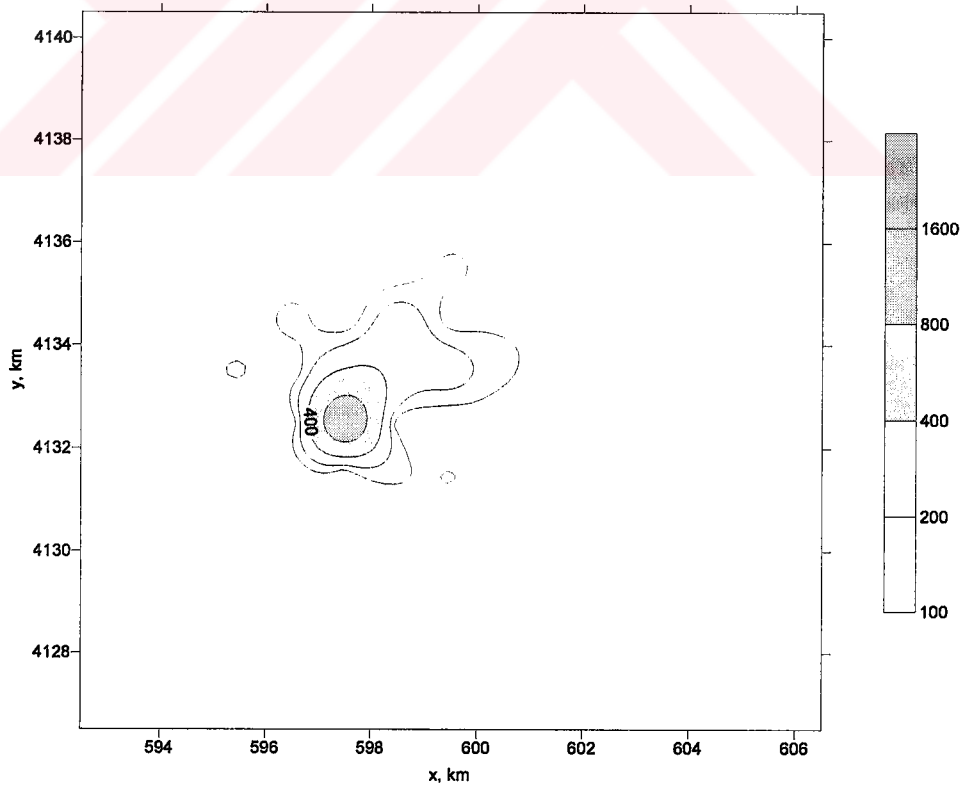


Figure 5.57 Concentration distribution ($\mu\text{g}\text{m}^{-3}$) at 15:00 on December 3, 2000.

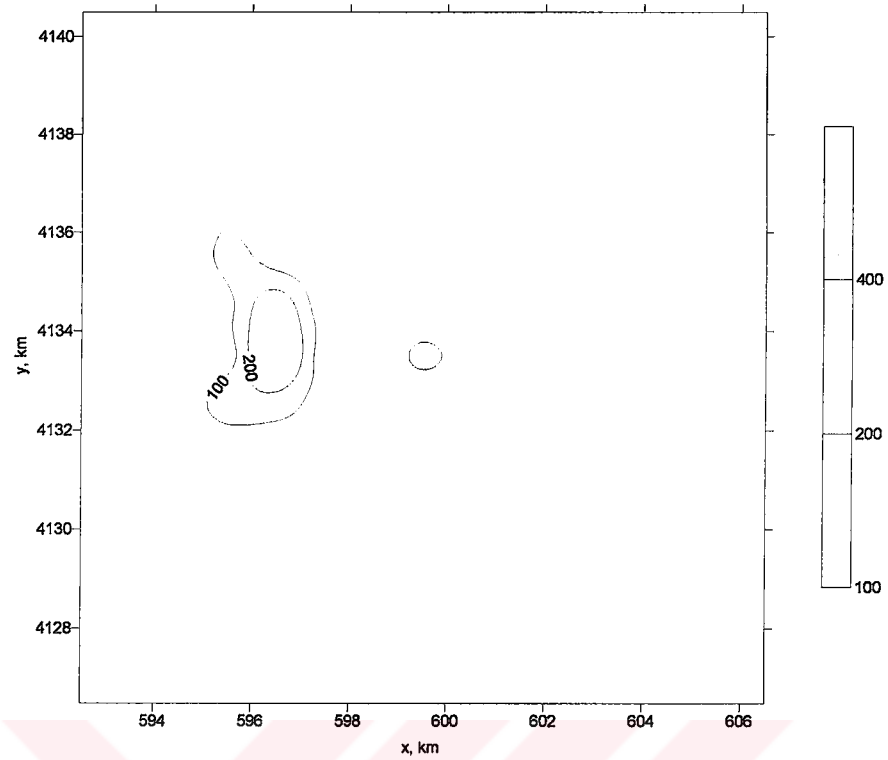


Figure 5.58 Concentration distribution ($\mu\text{g m}^{-3}$) at 23:00 on December 3, 2000.

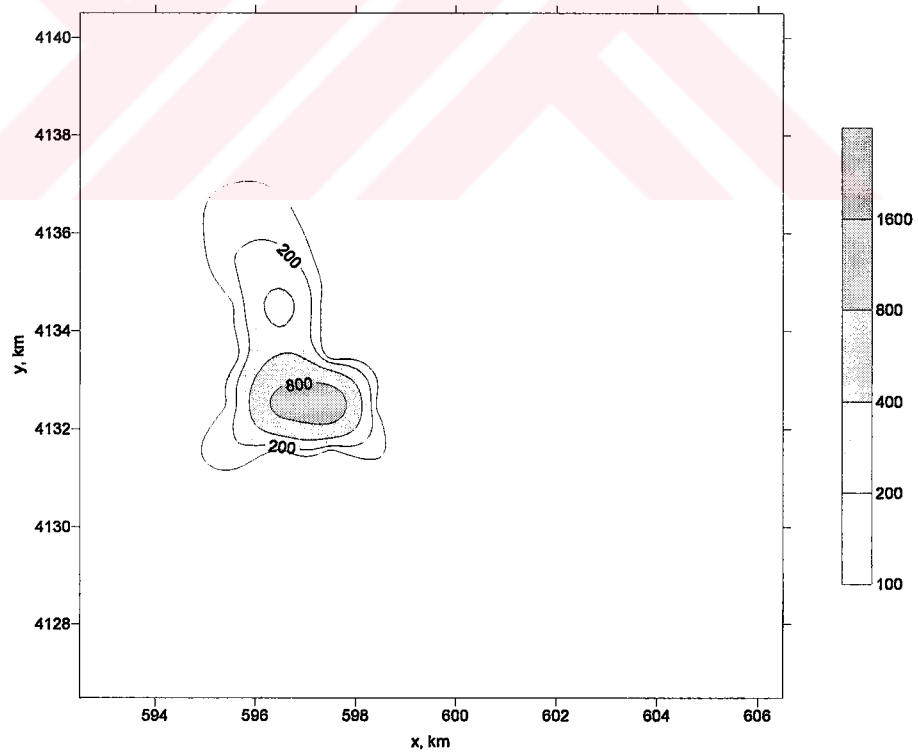


Figure 5.59 Concentration distribution ($\mu\text{g m}^{-3}$) at 07:00 on December 4, 2000.

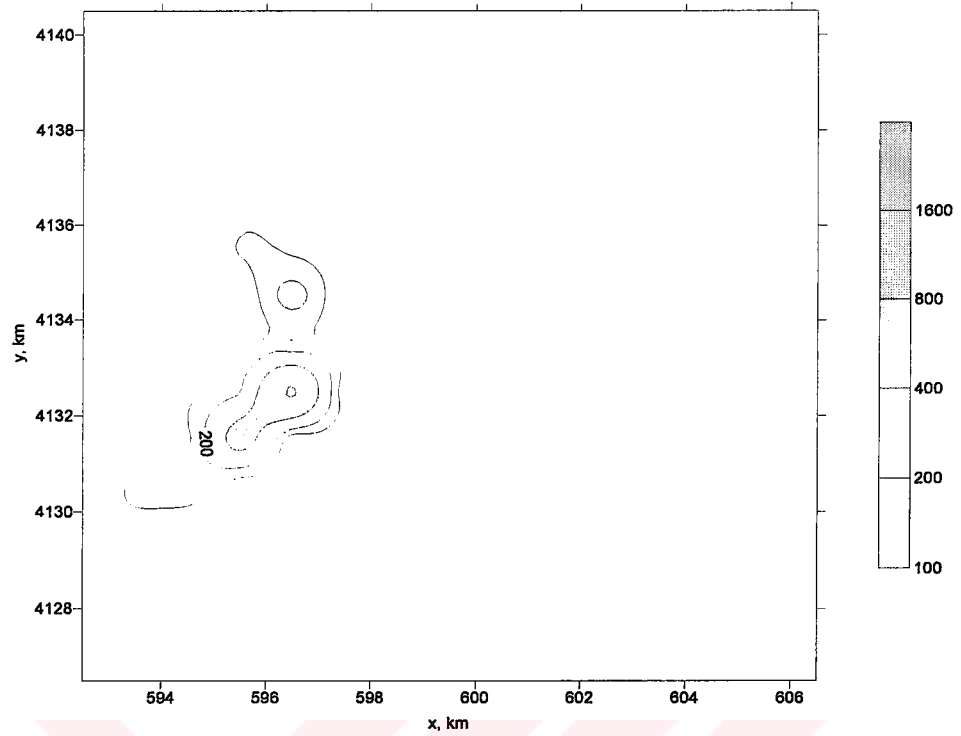


Figure 5.60 Concentration distribution ($\mu\text{g m}^{-3}$) at 15:00 on December 4, 2000.

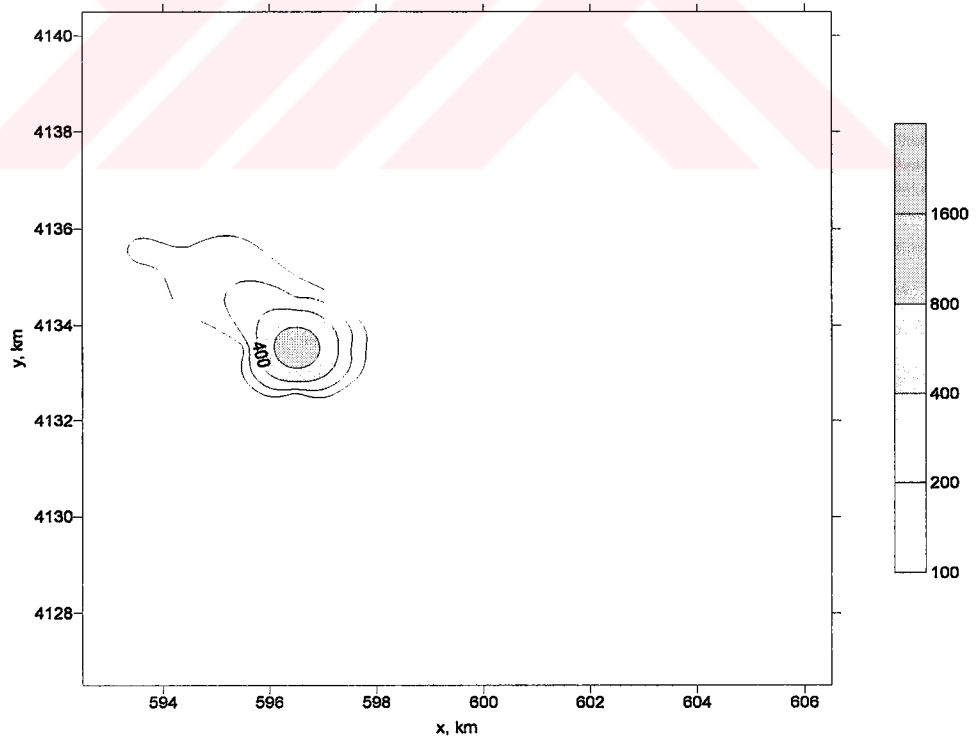


Figure 5.61 Concentration distribution ($\mu\text{g m}^{-3}$) at 23:00 on December 4, 2000.

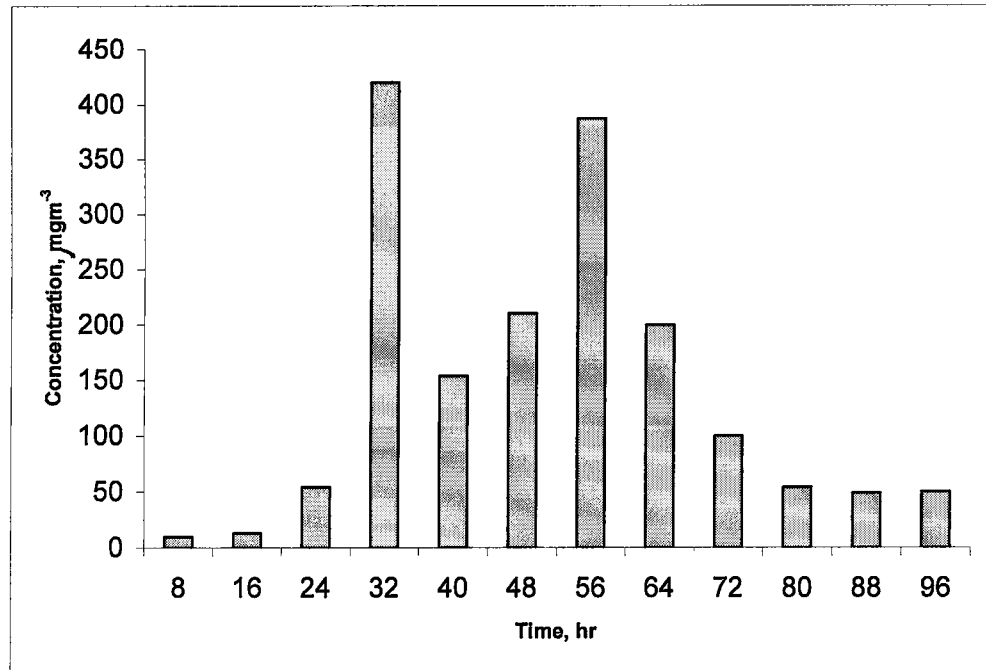


Figure 5.62. The maximum concentrations over Yatağan during the simulation period

5.2.2. Simulation of Scenario 2

In the second scenario, it is assumed that the winds observed by the surface meteorological station at Yatağan are light winds, with an average speed of 1 ms^{-1} . In this case, the pollutants in the atmosphere are subject to very low levels of mixing. The wind direction, temperature and other meteorological parameters are kept the same as the original case. Concentration distributions are presented in Figures 5.63. through 5.74 and image maps are presented in Figures 5.75. through 5.86. Under these very stable conditions, the maximum ground level concentration over Yatağan is calculated as $6500 \mu\text{gm}^{-3}$ at the 32th hour of the simulation period (Figure 5.87.). On the 3rd of December at afternoon hours, with the winds turning south easterly, the pollutants begin to accumulate over the western parts of the modeling area reaching to concentration levels of $1600 \mu\text{gm}^{-3}$. Additionally, at the 56th hour of the simulation, maximum ground level concentration over Yatağan district reaches a level of $5900 \mu\text{gm}^{-3}$. This simulation indicates that in the case of very light winds and stable conditions the ground level concentrations over Yatağan would increase significantly to dangerous levels, approximately 15 times higher than the limit of $400 \mu\text{gm}^{-3}$, and Yatağan would suffer seriously from this episodic event.

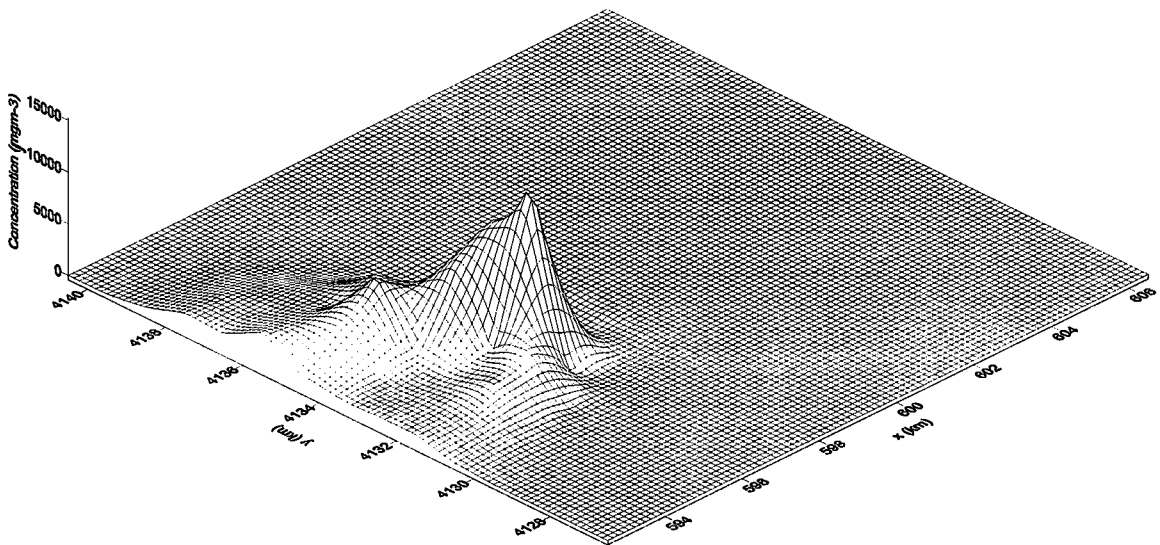


Figure 5.63. Concentration distribution for the modeling area at 07:00 on December 1, 2000.

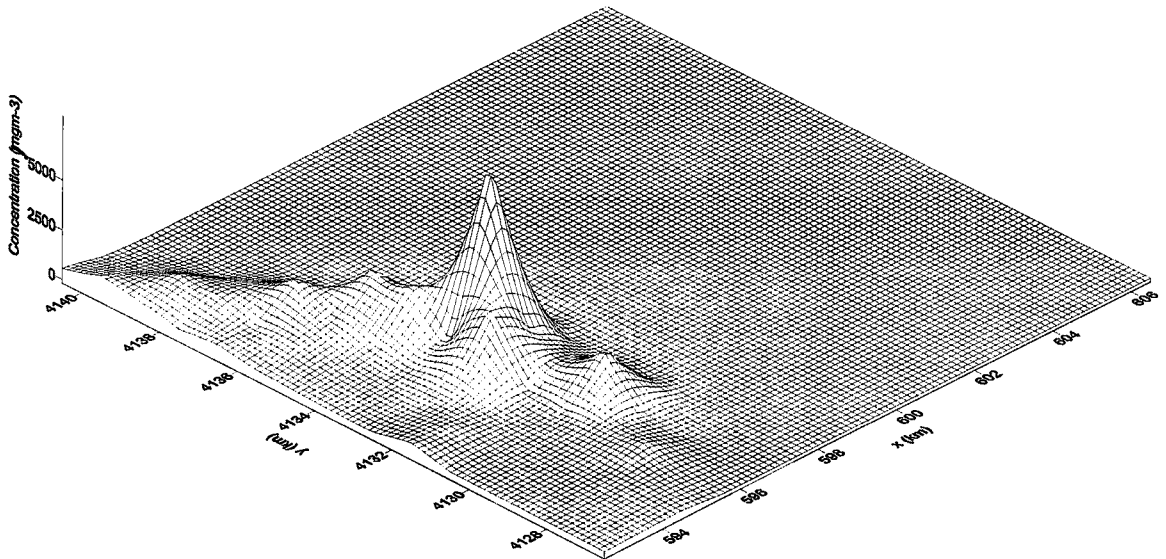


Figure 5.64. Concentration distribution for the modeling area at 15:00 on December 1, 2000.

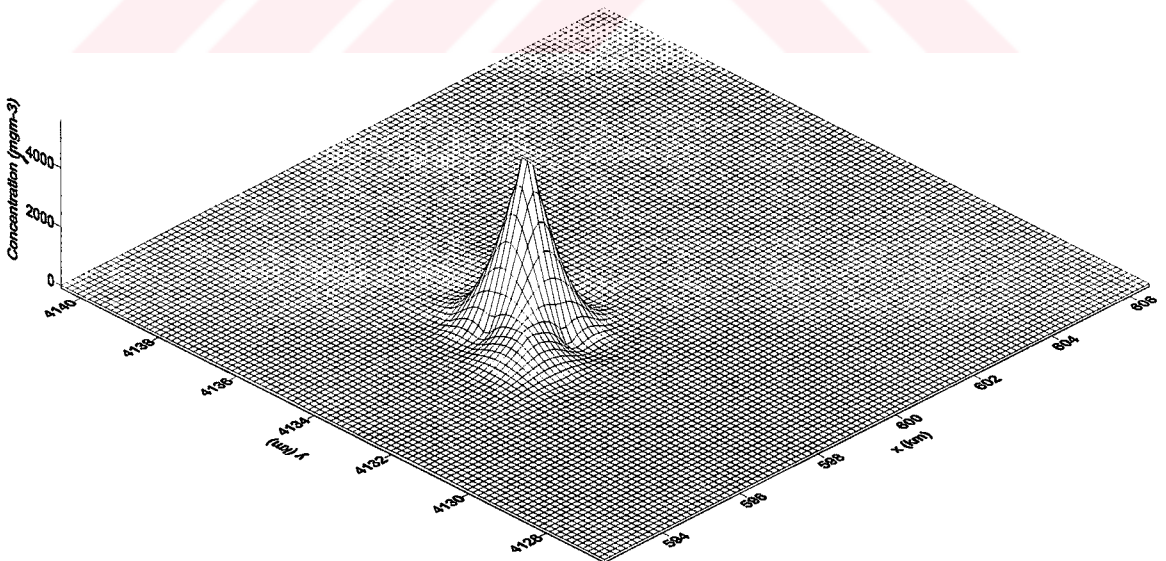


Figure 5.65. Concentration distribution for the modeling area at 23:00 on December 1, 2000.

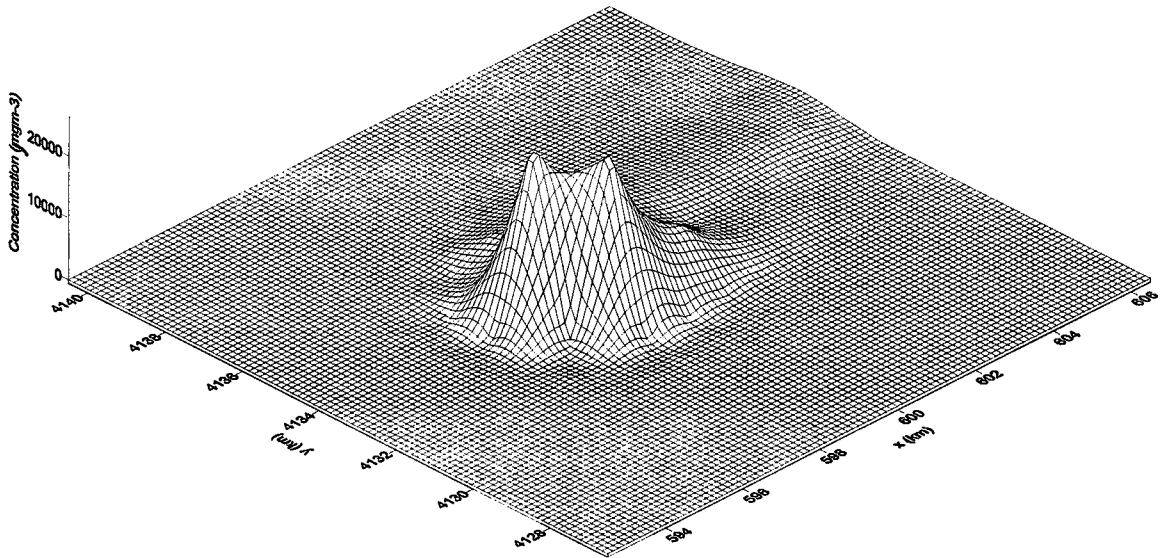


Figure 5.66. Concentration distribution for the modeling area at 07:00 on December 2, 2000.

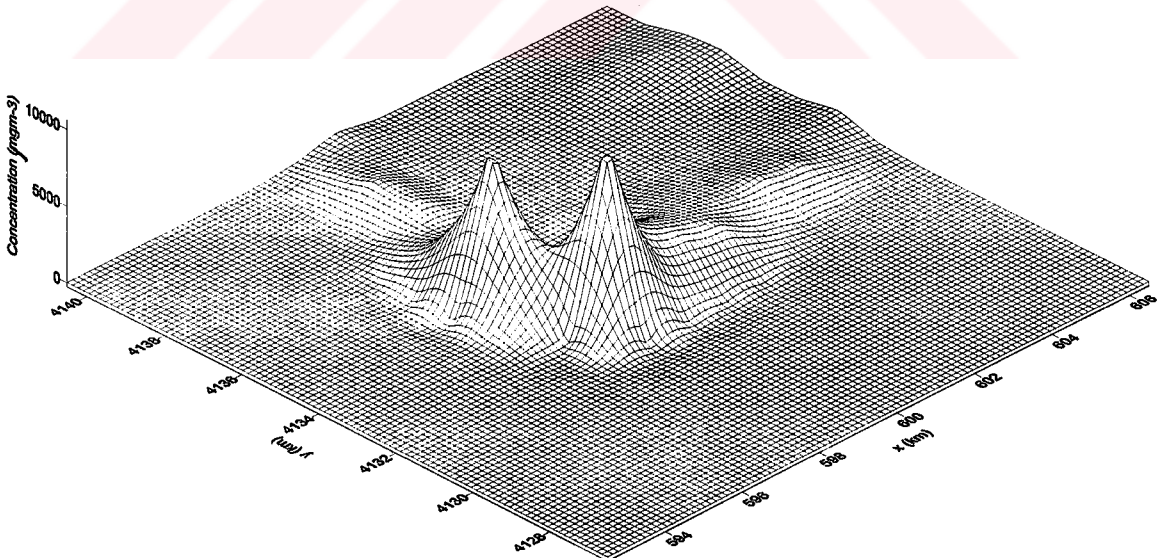


Figure 5.67. Concentration distribution for the modeling area at 15:00 on December 2, 2000.

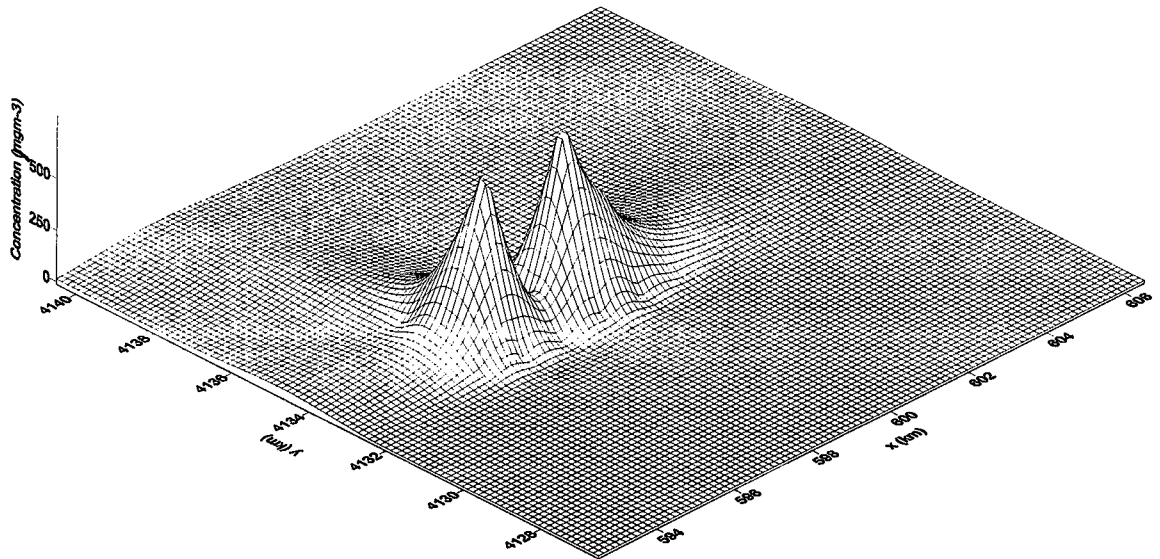


Figure 5.68. Concentration distribution for the modeling area at 23:00 on December 2, 2000.

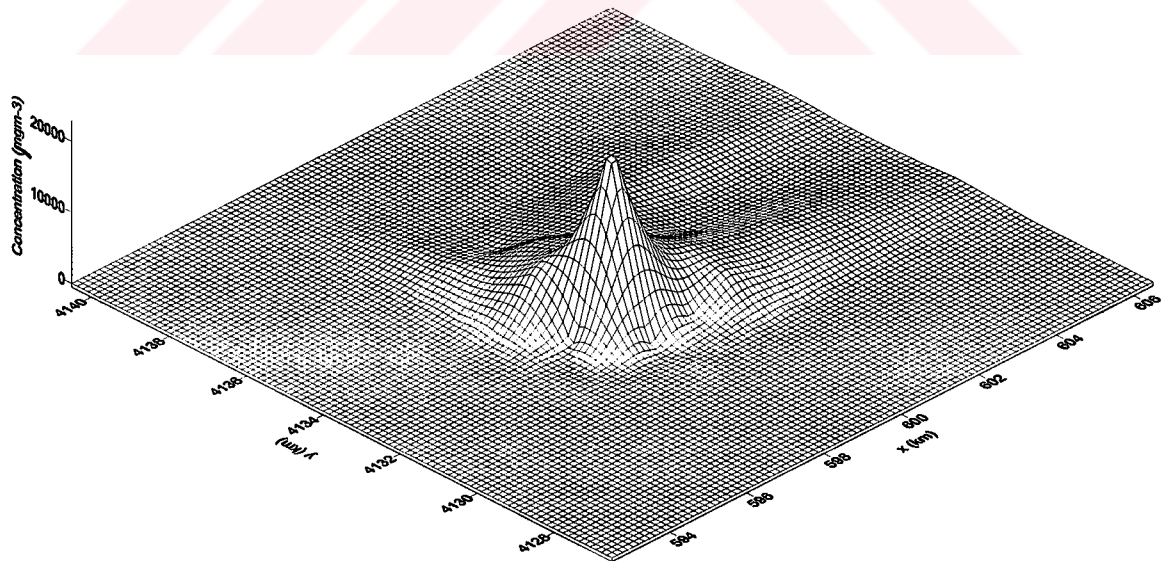


Figure 5.69. Concentration distribution for the modeling area at 07:00 on December 3, 2000.

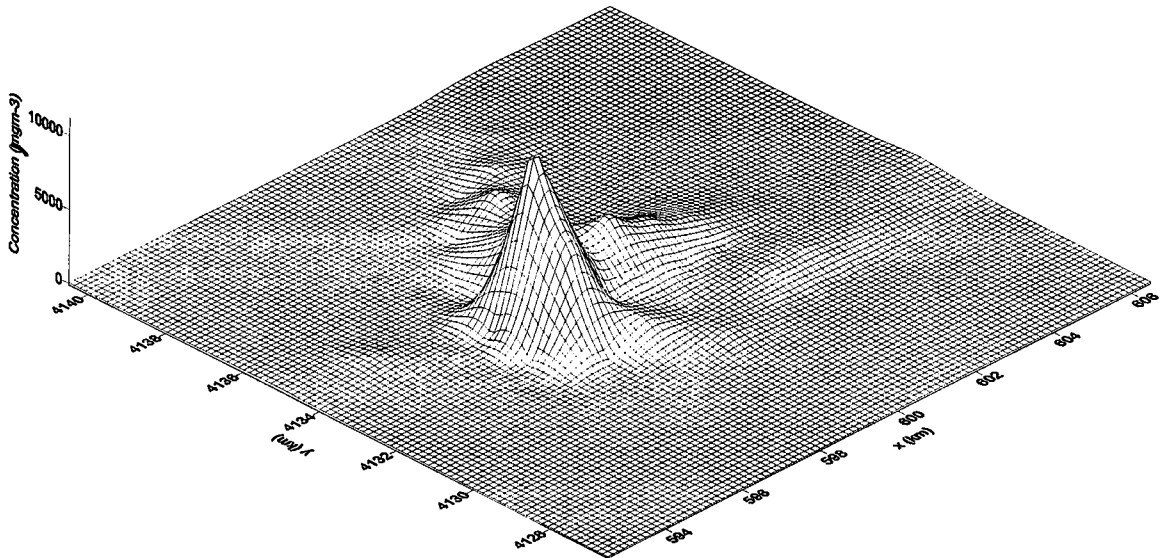


Figure 5.70. Concentration distribution for the modeling area at 15:00 on December 3, 2000.

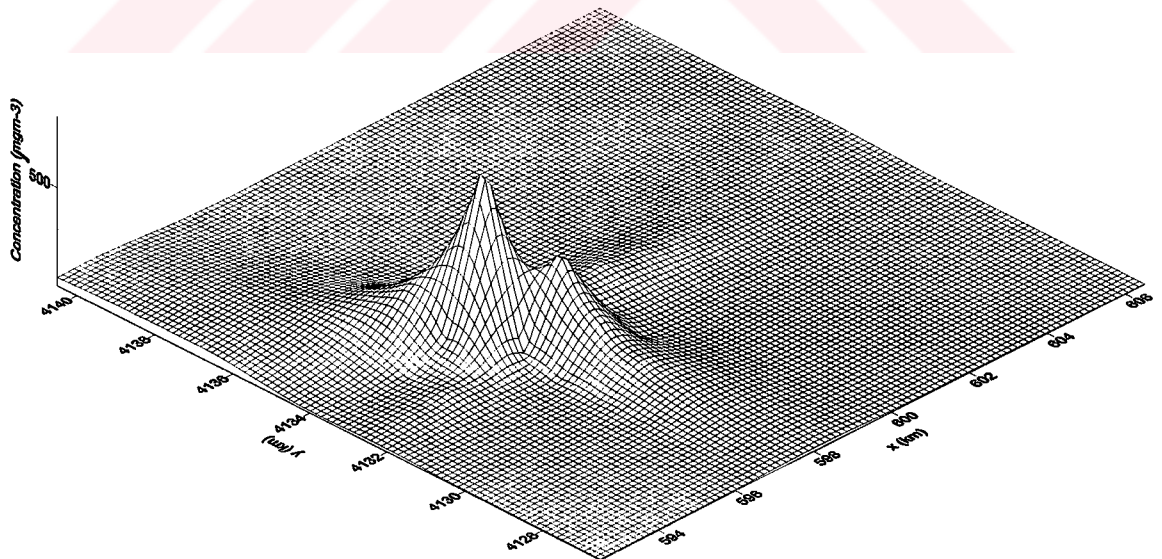


Figure 5.71. Concentration distribution for the modeling area at 23:00 on December 3, 2000.

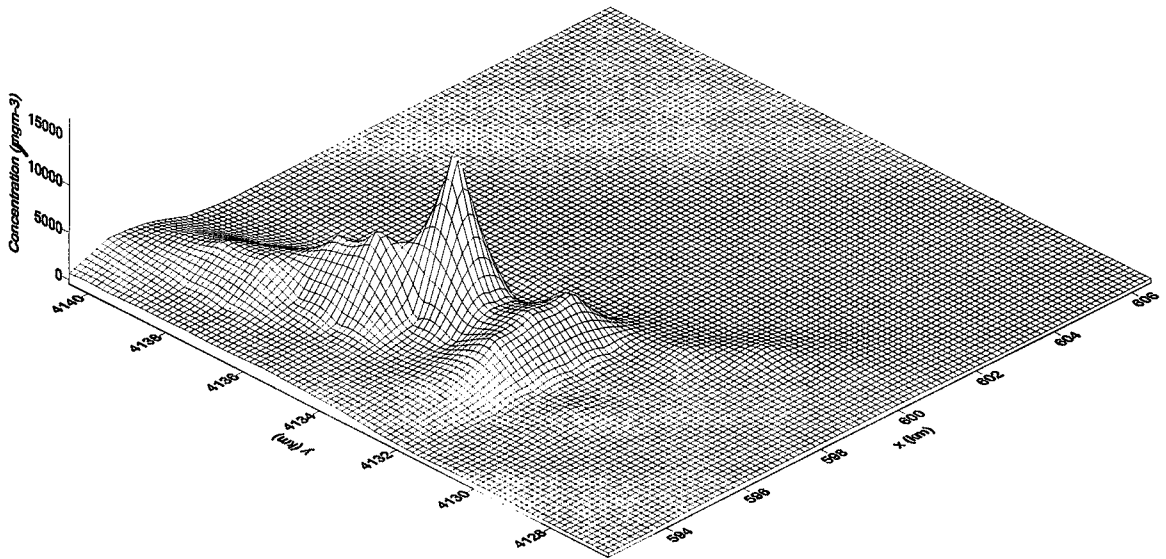


Figure 5.72. Concentration distribution for the modeling area at 07:00 on December 4, 2000.

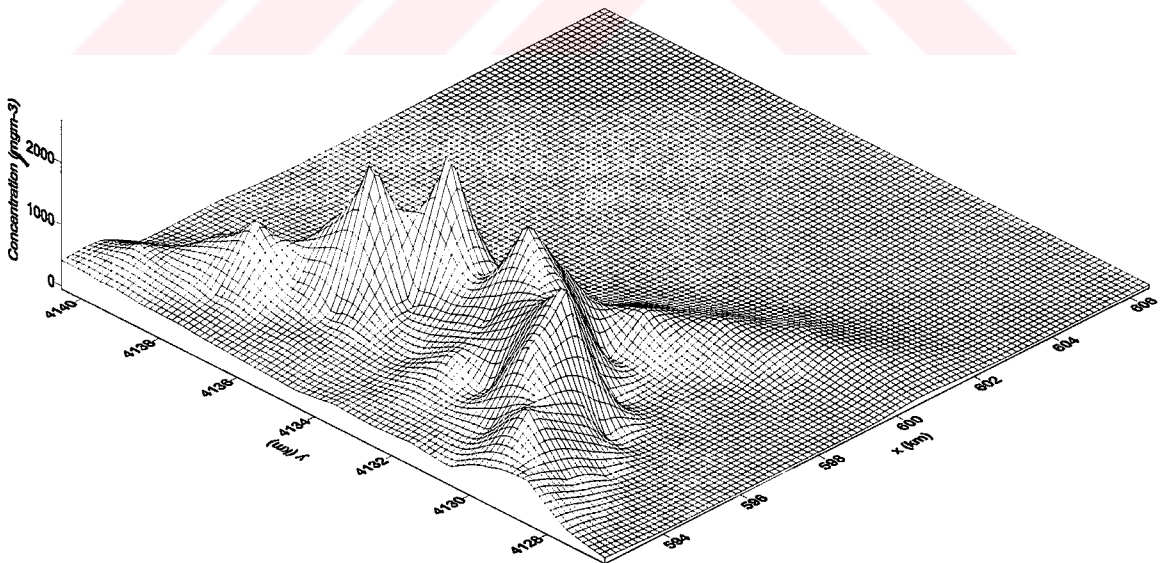


Figure 5.73. Concentration distribution for the modeling area at 15:00 on December 4, 2000.

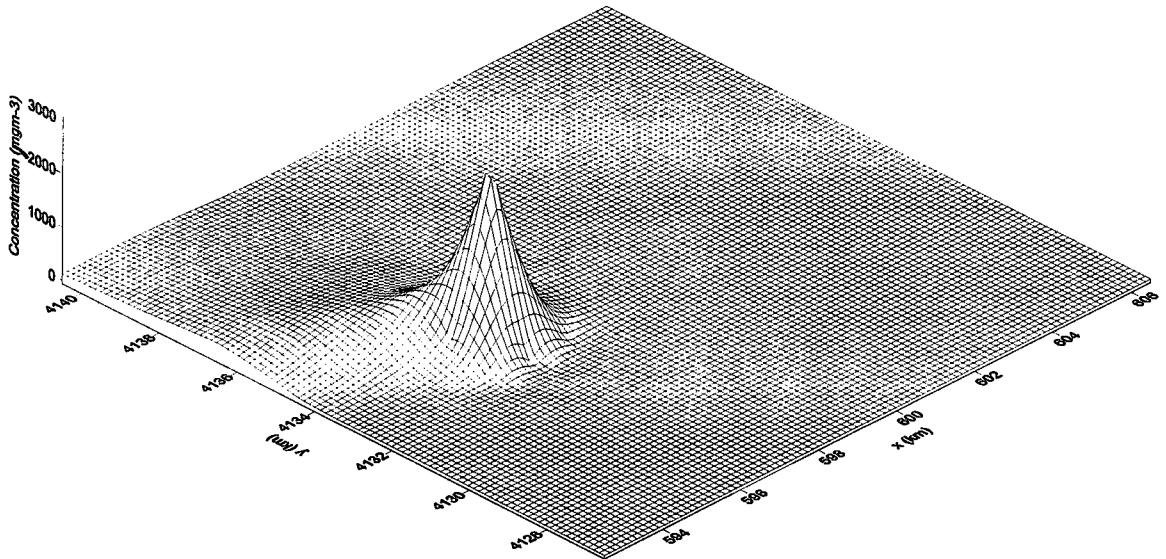


Figure 5.74. Concentration distribution for the modeling area at 23:00 on December 4, 2000.

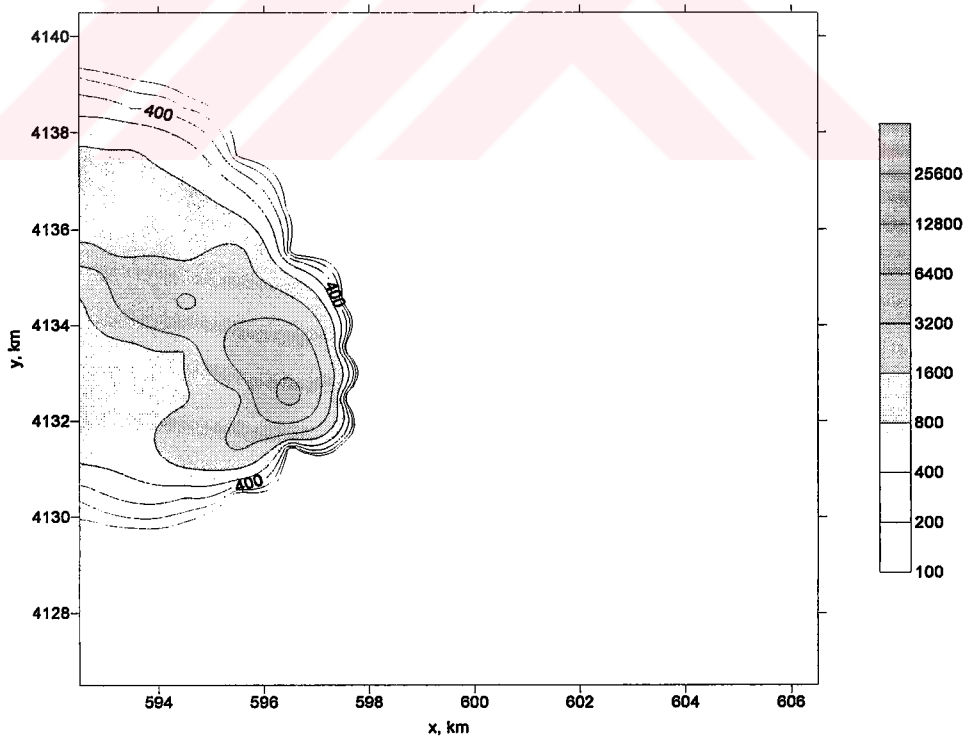


Figure 5.75. Concentration distribution ($\mu\text{g}\cdot\text{m}^{-3}$) at 07:00 on December 1, 2000.

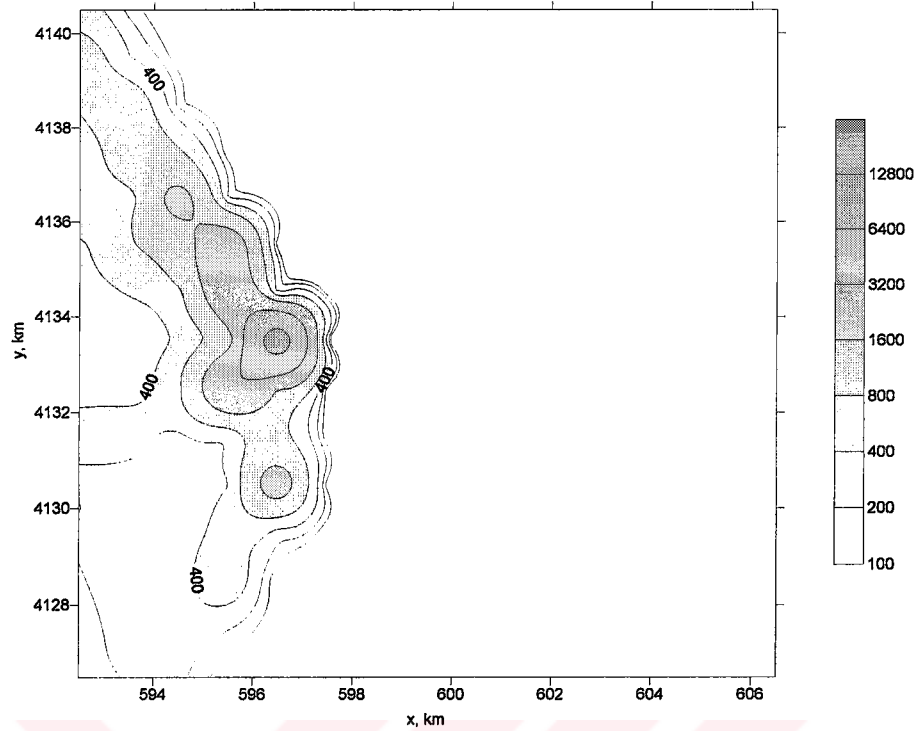


Figure 5.76. Concentration distribution ($\mu\text{g m}^{-3}$) at 15:00 on December 1, 2000.

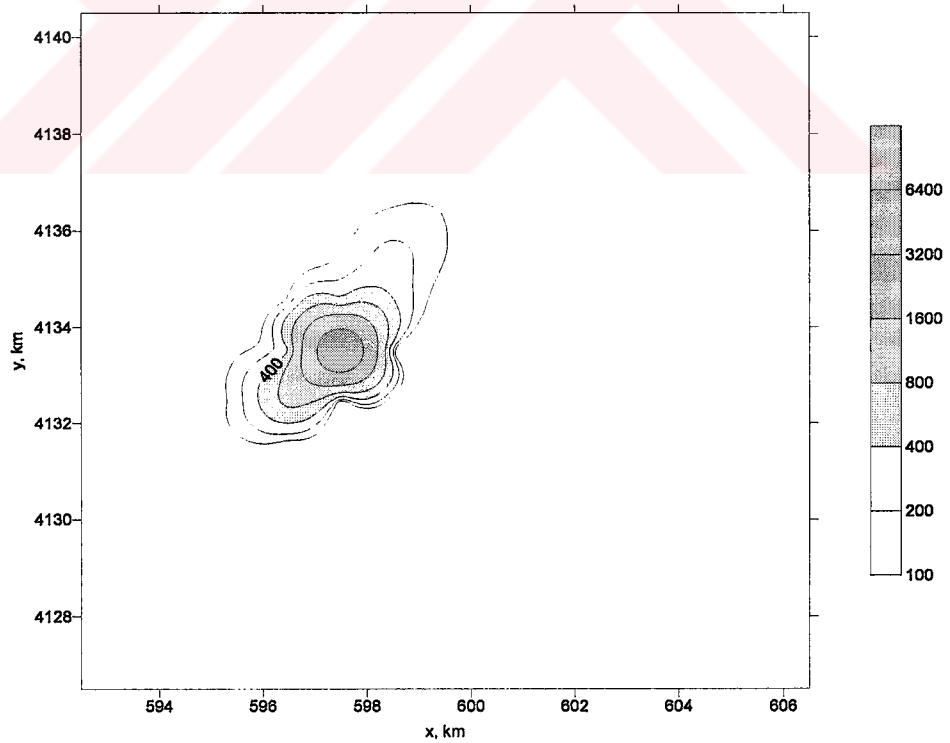


Figure 5.77. Concentration distribution ($\mu\text{g m}^{-3}$) at 23:00 on December 1, 2000.

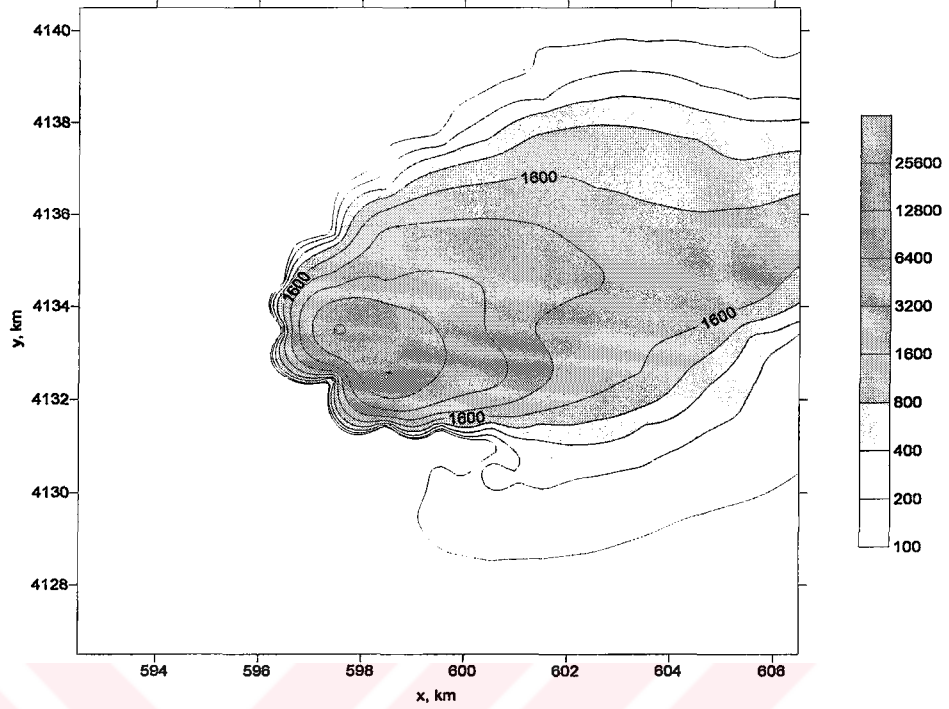


Figure 5.78. Concentration distribution (μgm^{-3}) at 07:00 on December 2, 2000.

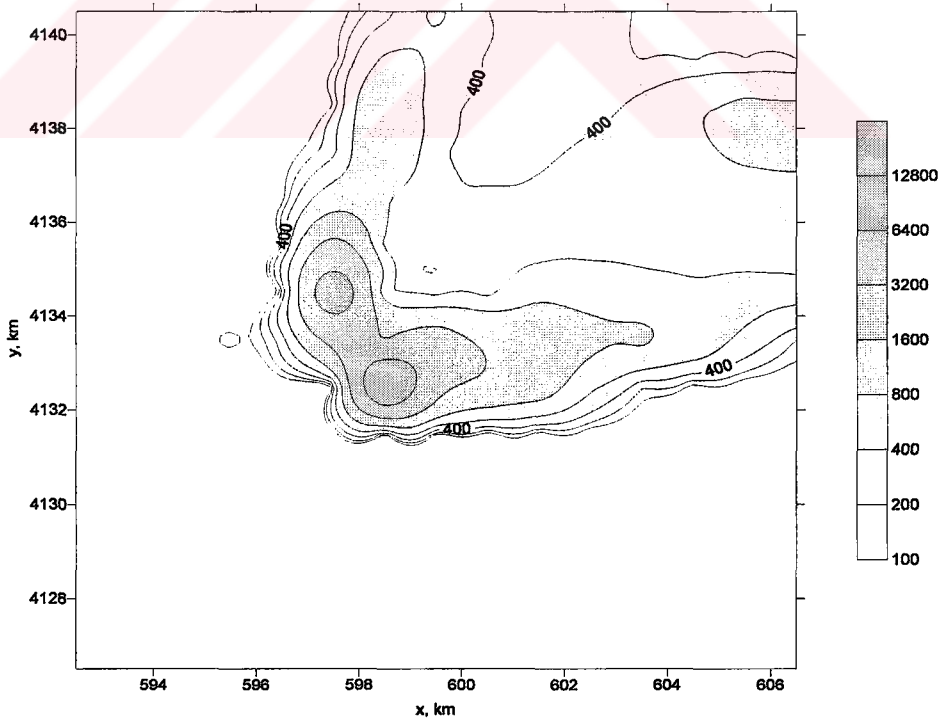


Figure 5.79. Concentration distribution (μgm^{-3}) at 15:00 on December 2, 2000.

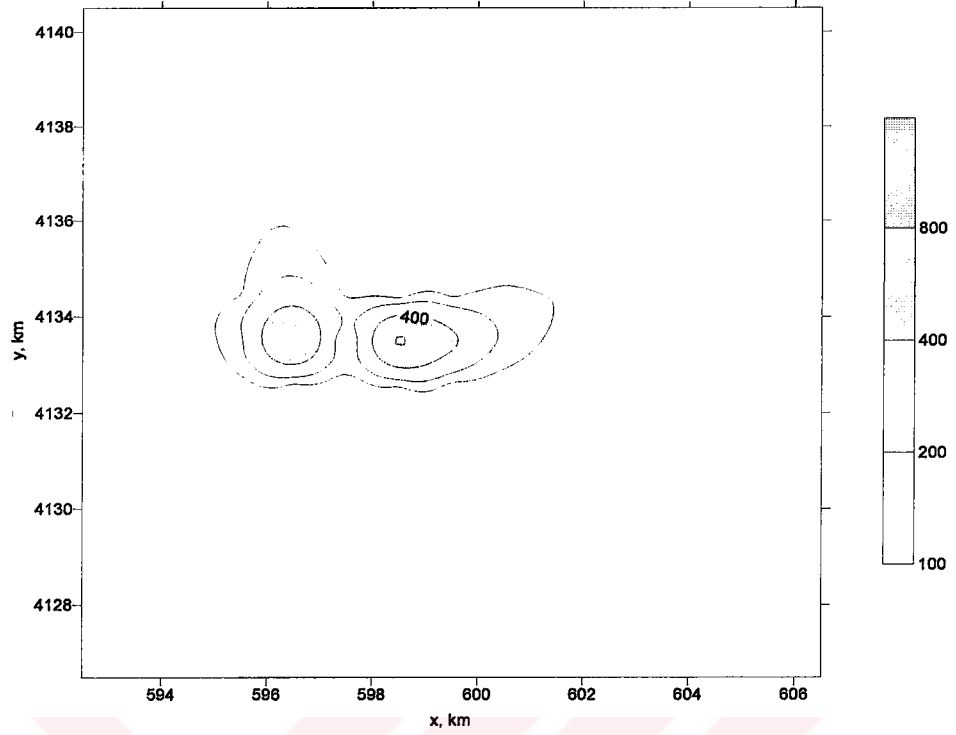


Figure 5.80. Concentration distribution ($\mu\text{g m}^{-3}$) at 23:00 on December 2, 2000.

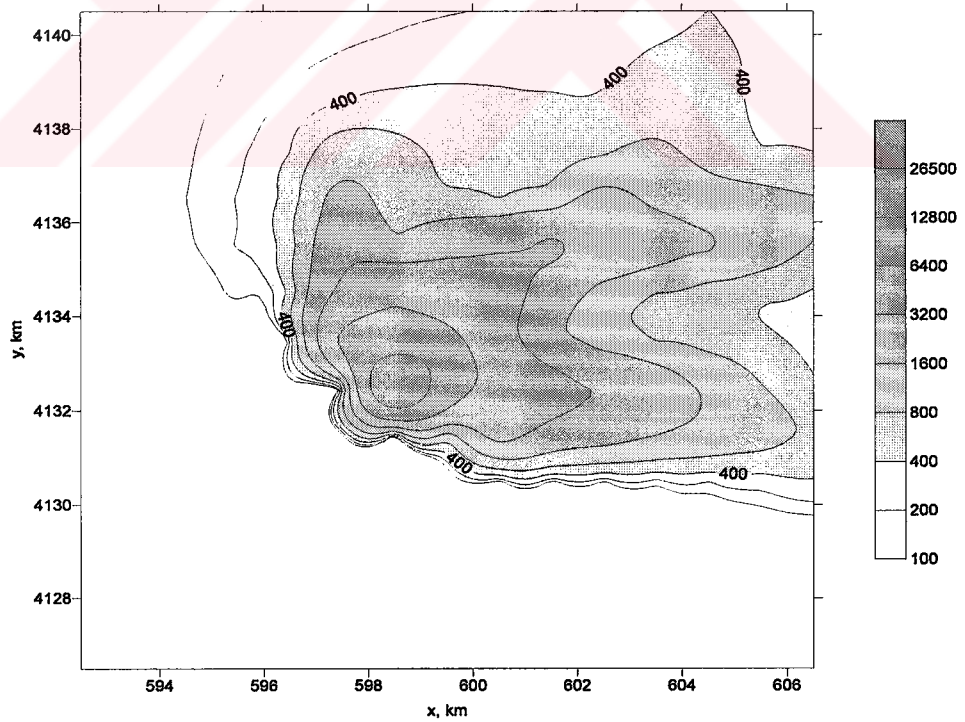


Figure 5.81. Concentration distribution ($\mu\text{g m}^{-3}$) at 07:00 on December 3, 2000.

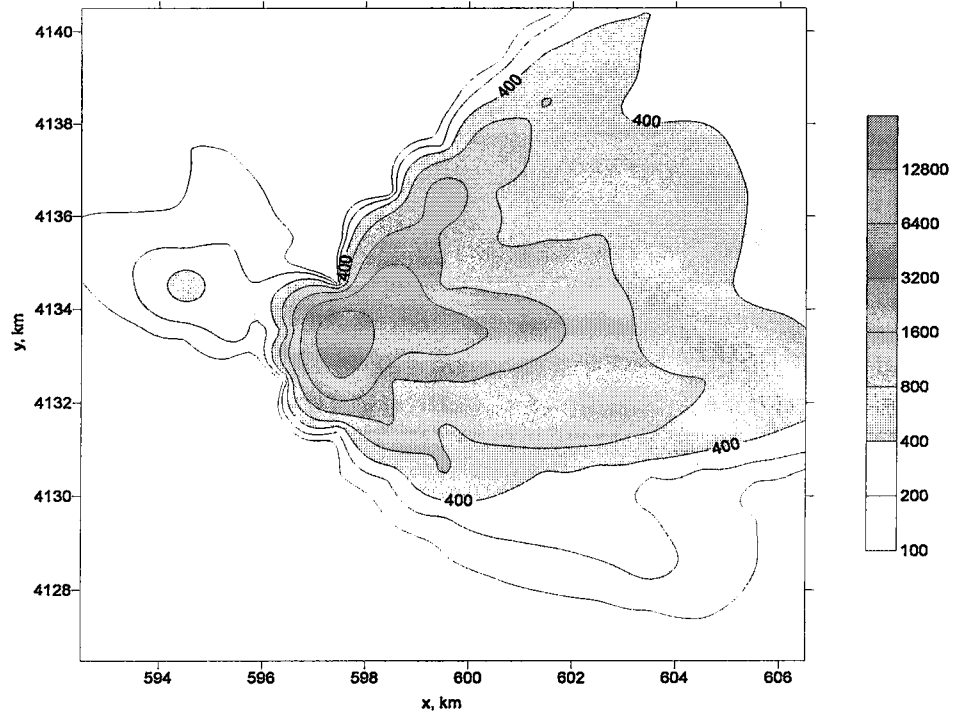


Figure 5.82. Concentration distribution ($\mu\text{g m}^{-3}$) at 15:00 on December 3, 2000.

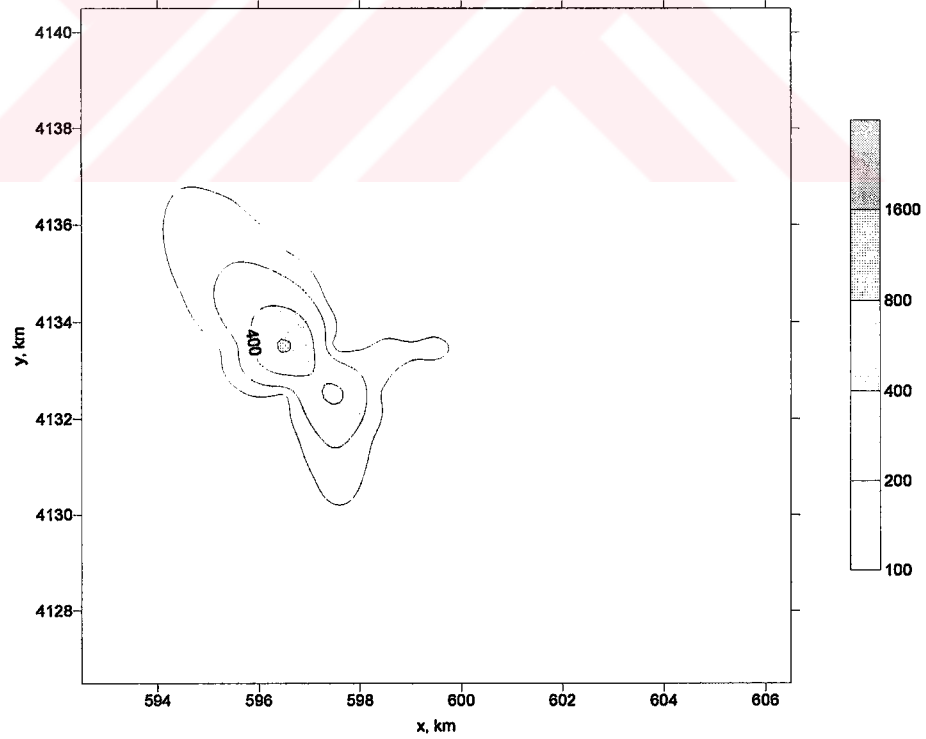


Figure 5.83. Concentration distribution ($\mu\text{g m}^{-3}$) at 23:00 on December 3, 2000.

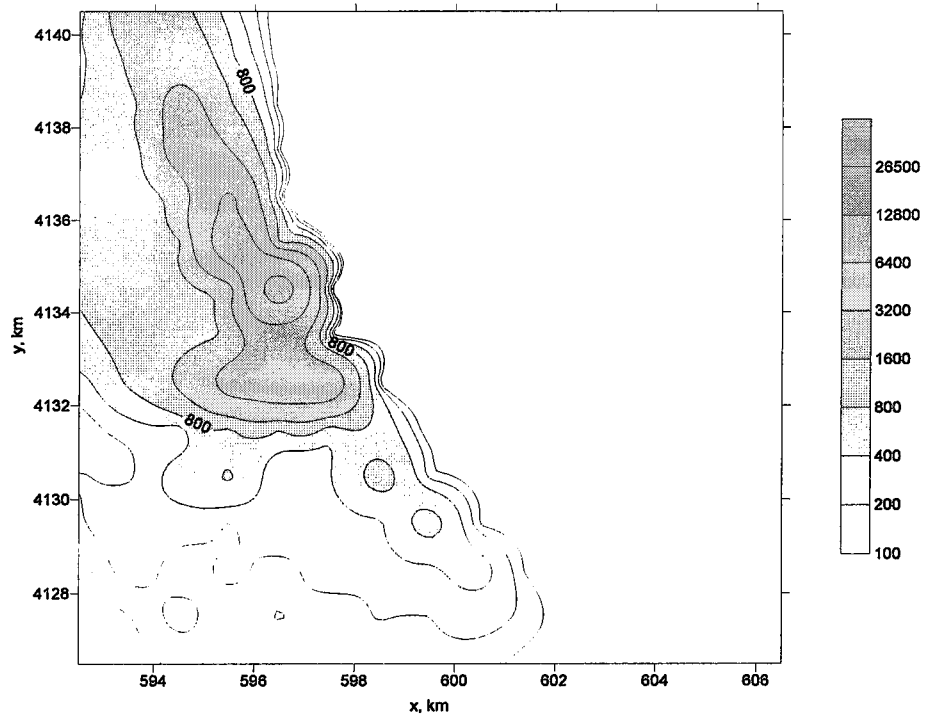


Figure 5.84. Concentration distribution ($\mu\text{g m}^{-3}$) at 07:00 on December 4, 2000.

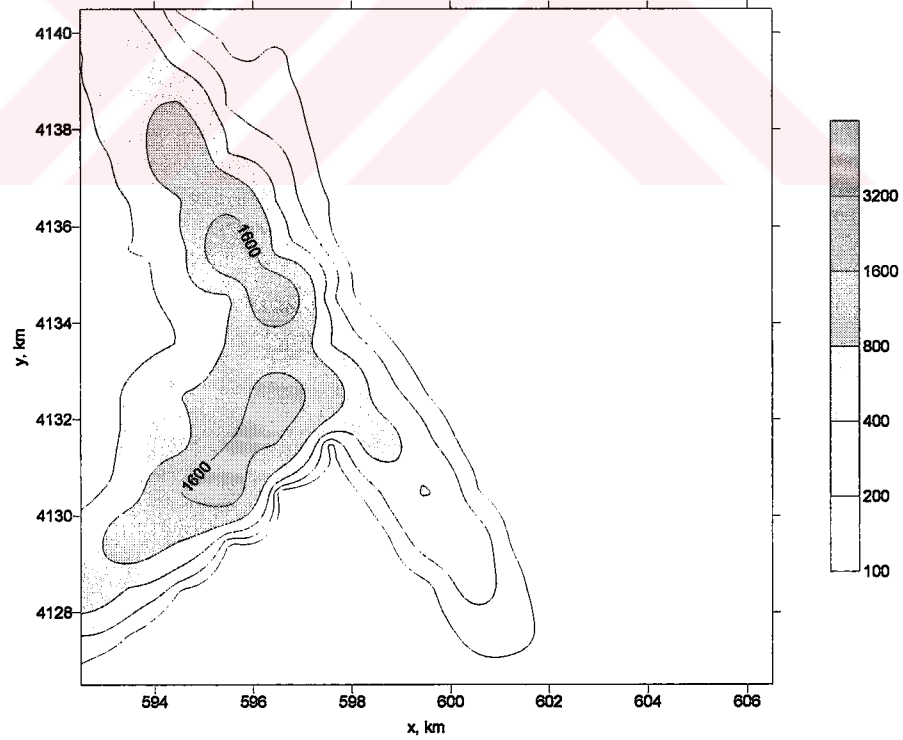


Figure 5.85. Concentration distribution ($\mu\text{g m}^{-3}$) at 15:00 on December 4, 2000.

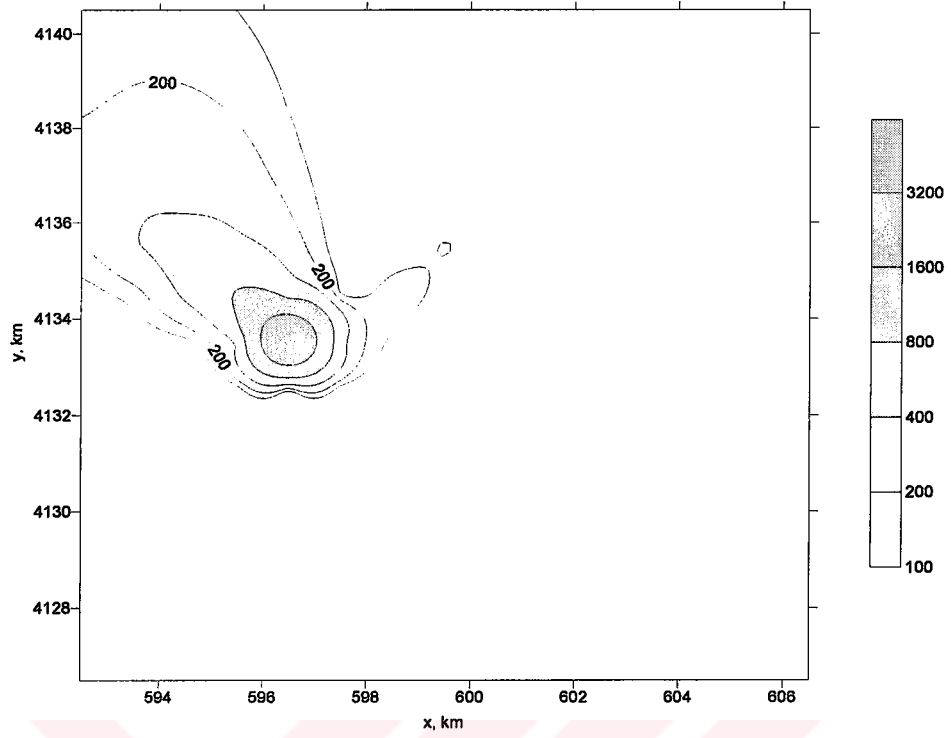


Figure 5.86. Concentration distribution ($\mu\text{g}\text{m}^{-3}$) at 23:00 on December 4, 2000.

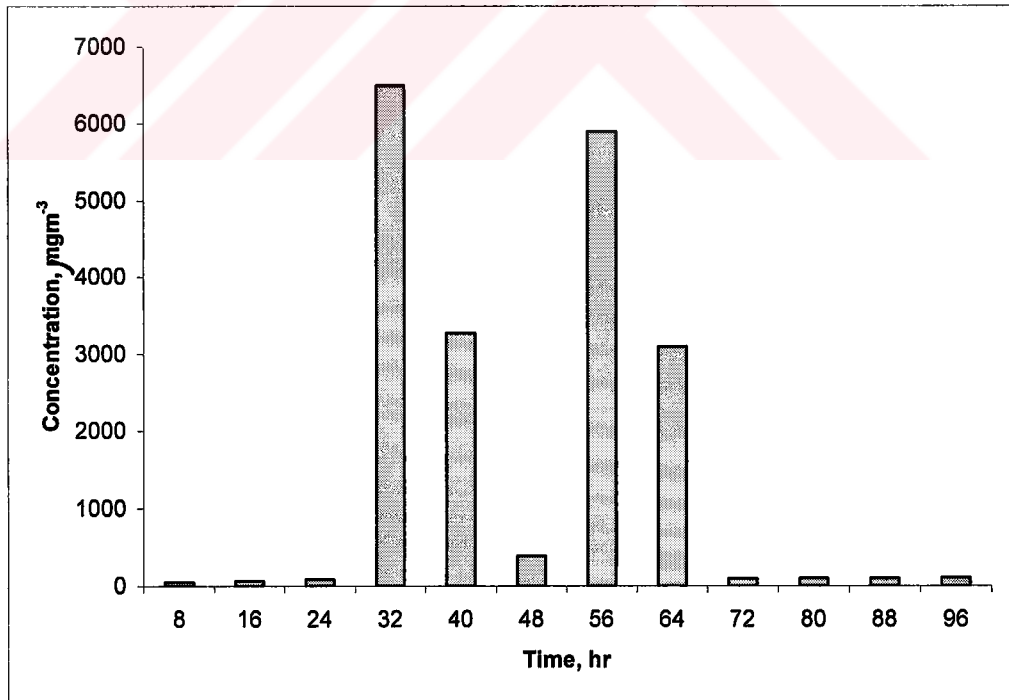


Figure 5.87. Maximum concentration levels over Yatağan for Scenario 2

5.2.3. Simulation of Scenario 3

In the third scenario, it is assumed that the winds observed by the surface meteorological station are north easterly. The wind speed and other meteorological parameters are kept the same as in the original case. The wind fields produced by the model are presented in Figures 5.88. through 5.99. Concentration distributions are presented in Figures 5.100. through 5.111 and image maps are presented in Figures 5.112. through 5.123. Starting from the early hours of December 2, 2000, the pollutants disperse in a larger region and spread over the southwestern region of the modeling area. The highest ground level concentration calculated in the modeling area is $1670 \mu\text{gm}^{-3}$ and found about 1 km south west from the power plant . The highest ground level concentrations are observed around the southwest region of the modeling area. The highest ground level concentration over Yatağan district is calculated as $250 \mu\text{gm}^{-3}$ at the 32nd hour of the simulation period (Figure 5.124.). This simulation indicates that in case of the governing winds being north easterly, the ground level concentrations over the district would not exceed the maximum limits, however, the southwestern region of the modeling area would be seriously affected by the pollution.

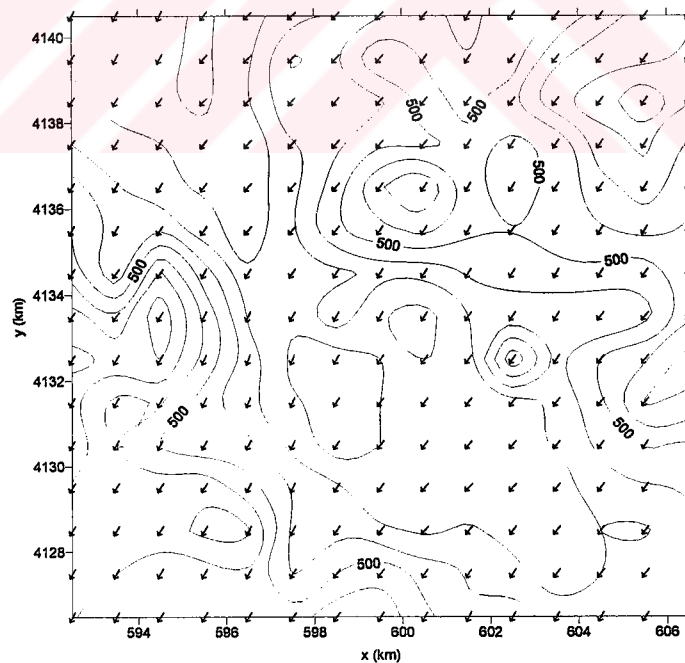


Figure 5.88. Wind field for the modeling area at 07:00 on December 1, 2000

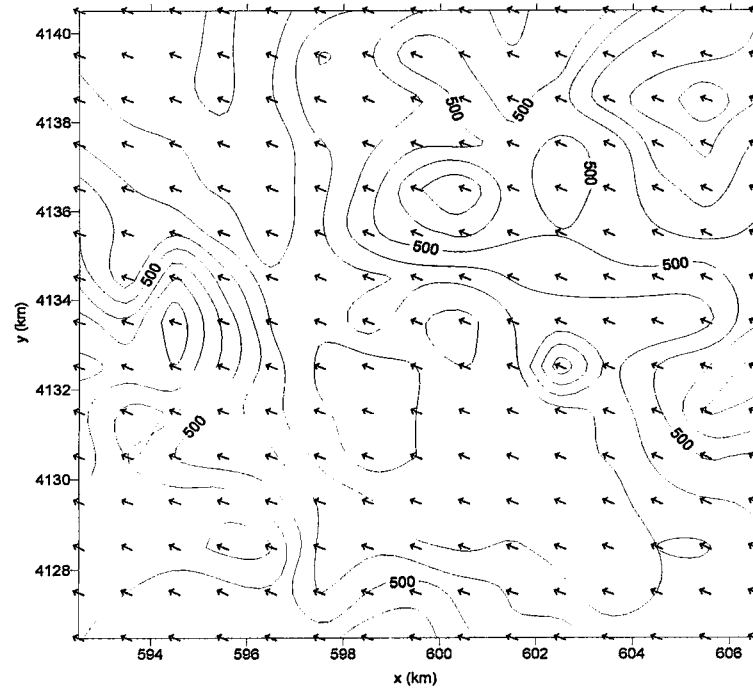


Figure 5.89. Wind field for the modeling area at 15:00 on December 1, 2000

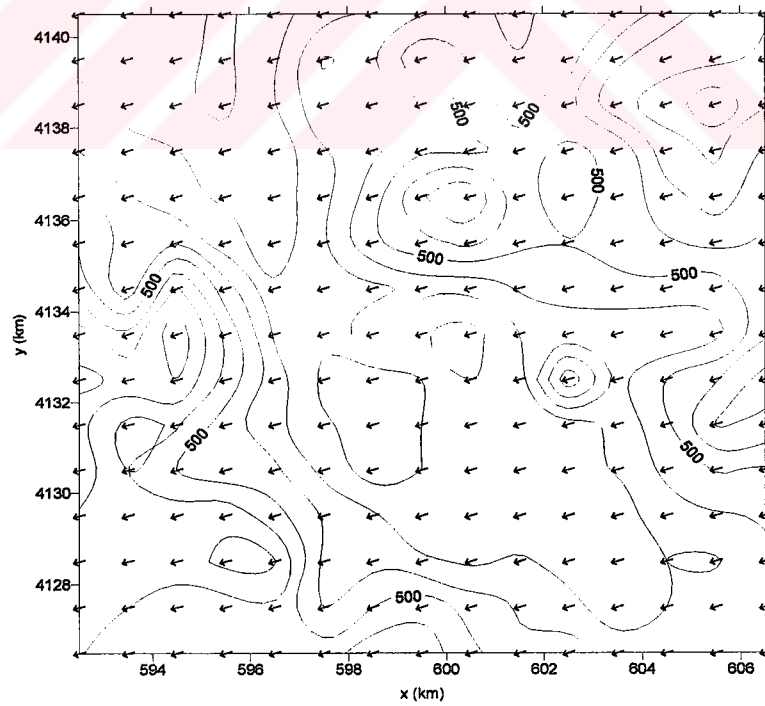


Figure 5.90. Wind field for the modeling area at 23:00 on December 1, 2000

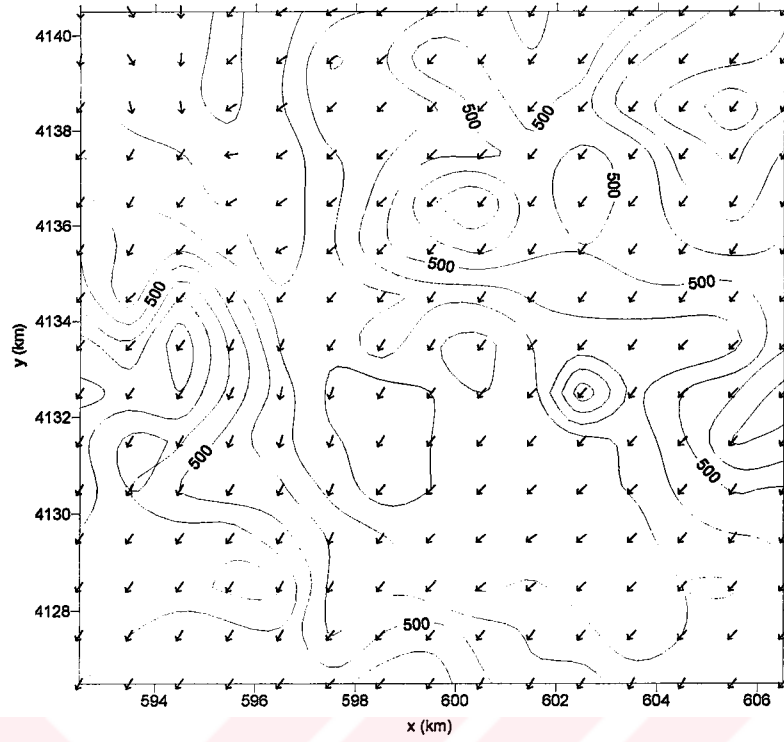


Figure 5.91. Wind field for the modeling area at 07:00 on December 2, 2000

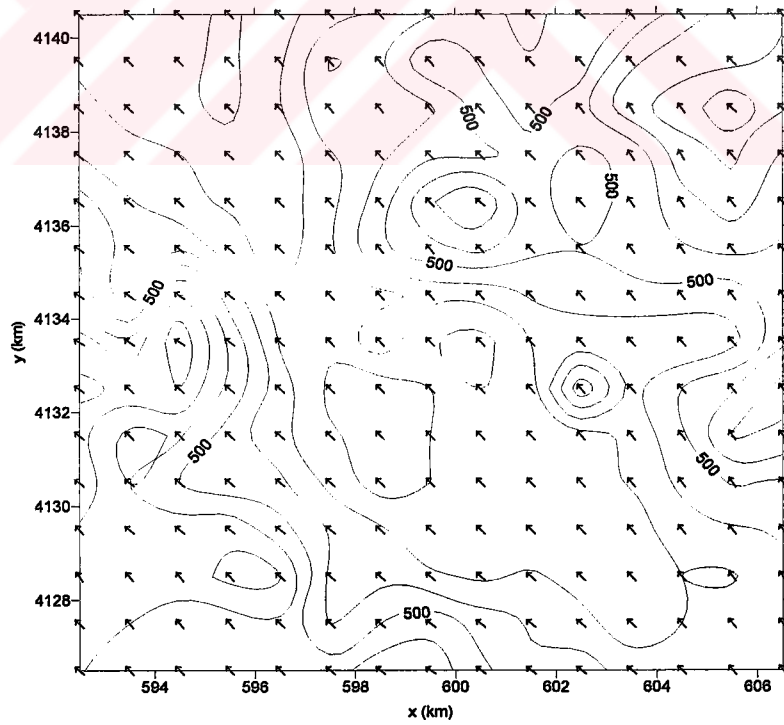


Figure 5.92. Wind field for the modeling area at 15:00 on December 2, 2000

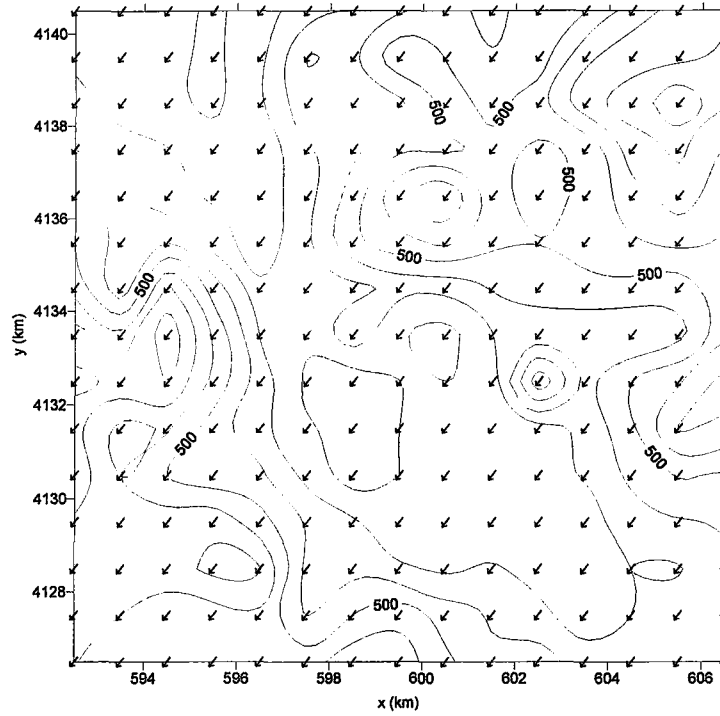


Figure 5.93. Wind field for the modeling area at 23:00 on December 2, 2000

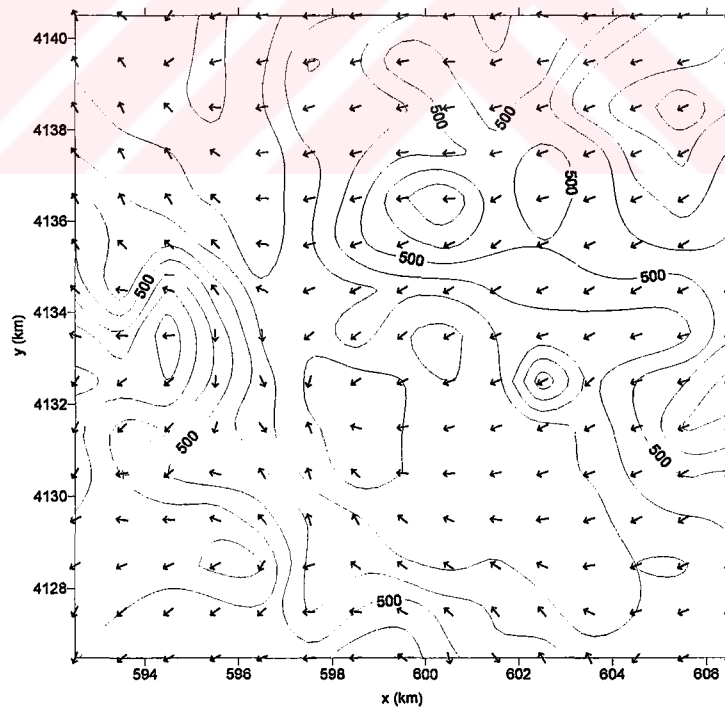


Figure 5.94. Wind field for the modeling area at 07:00 on December 3, 2000

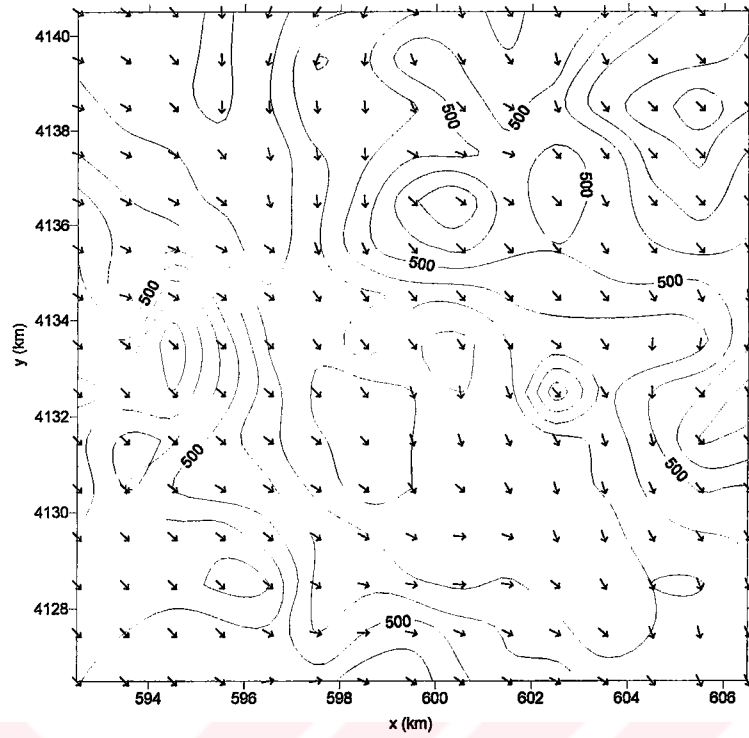


Figure 5.95. Wind field for the modeling area at 15:00 on December 3, 2000

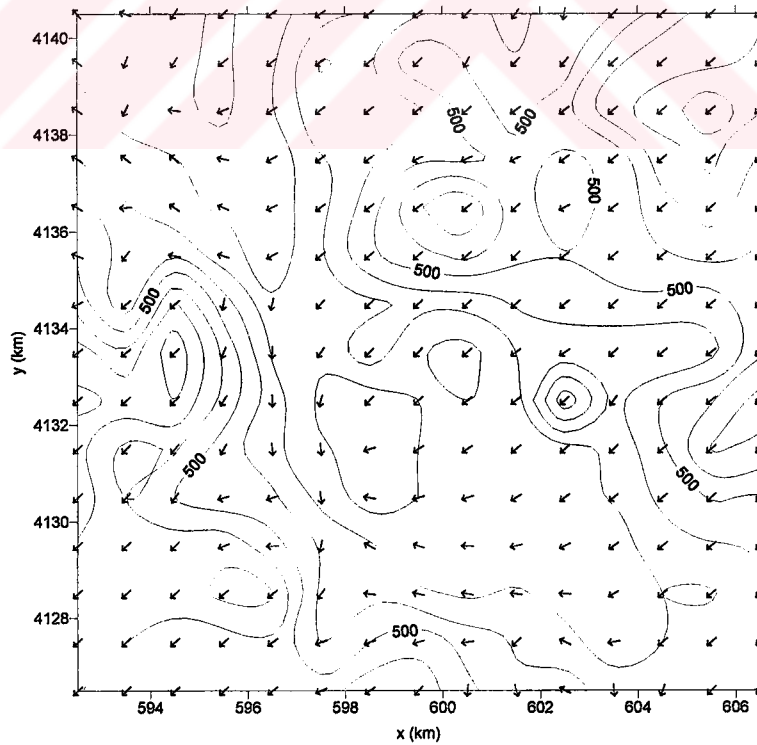


Figure 5.96. Wind field for the modeling area at 23:00 on December 3, 2000

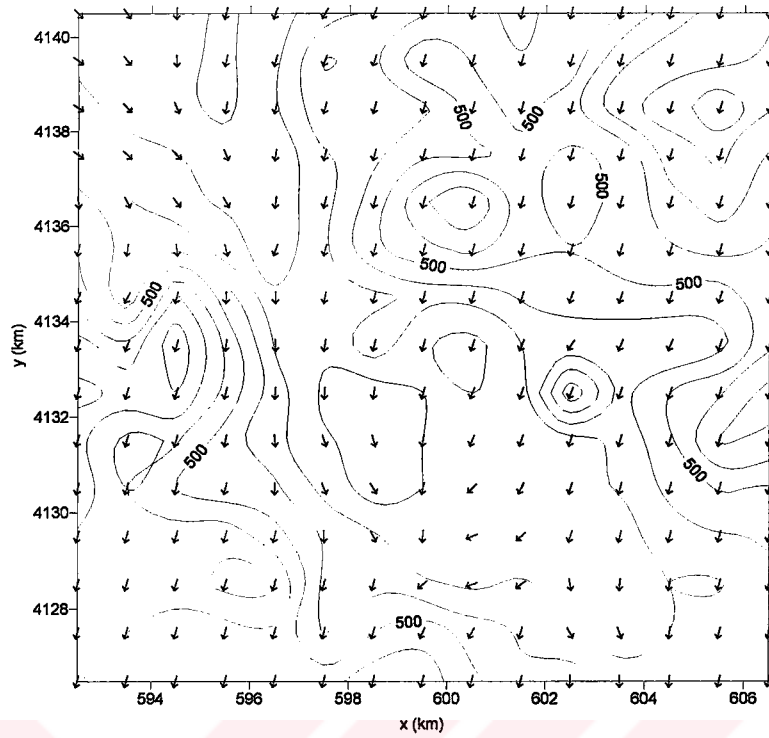


Figure 5.97. Wind field for the modeling area at 07:00 on December 4, 2000

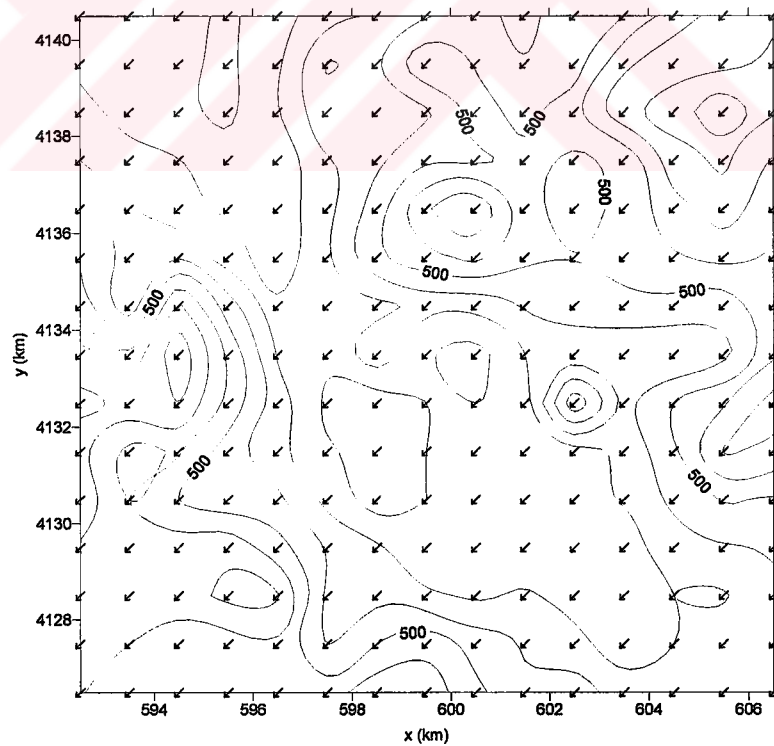


Figure 5.98. Wind field for the modeling area at 15:00 on December 4, 2000

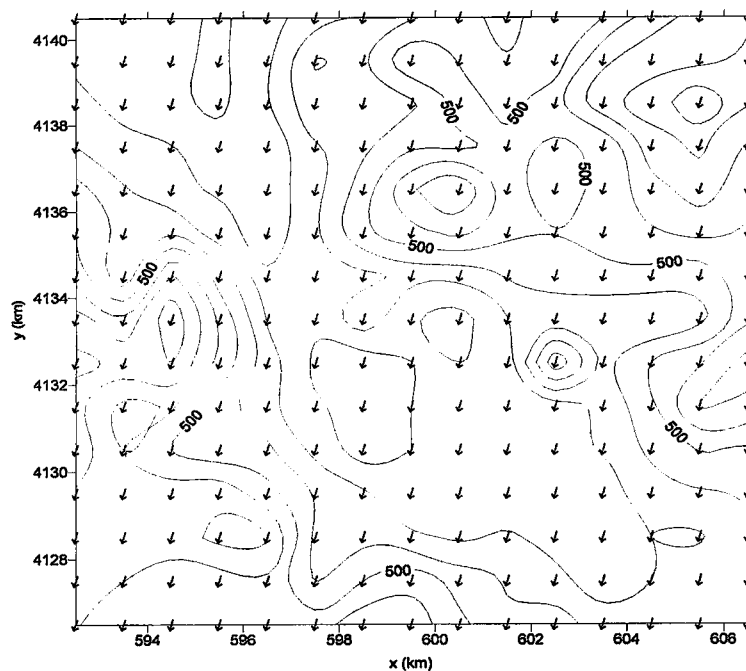


Figure 5.99. Wind field for the modeling area at 23:00 on December 4, 2000

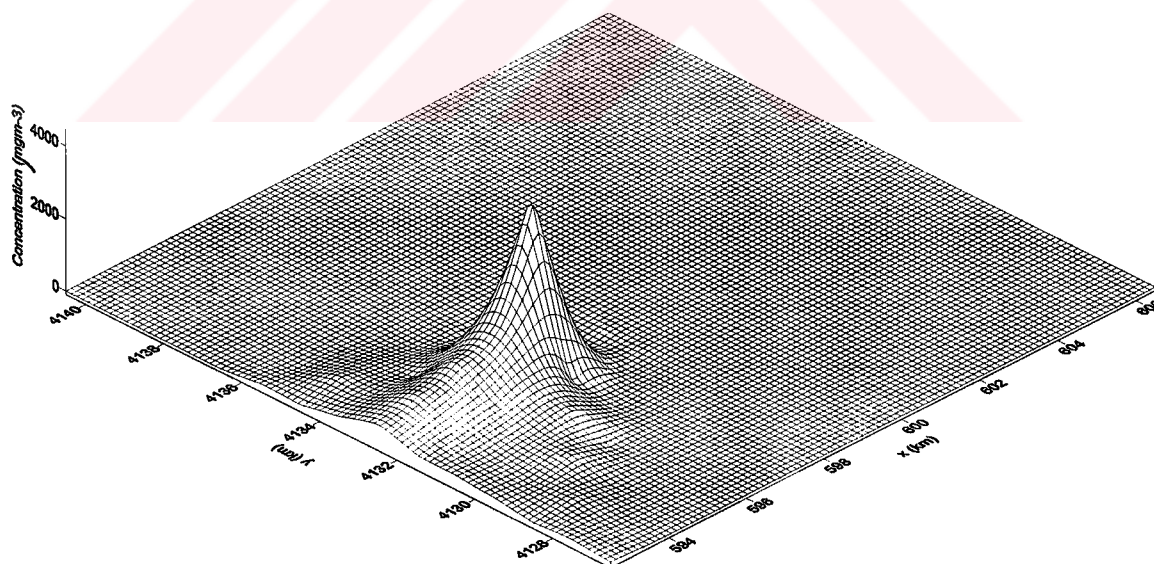


Figure 5.100. Concentration distribution for the modeling area at 07:00 on December 1, 2000.

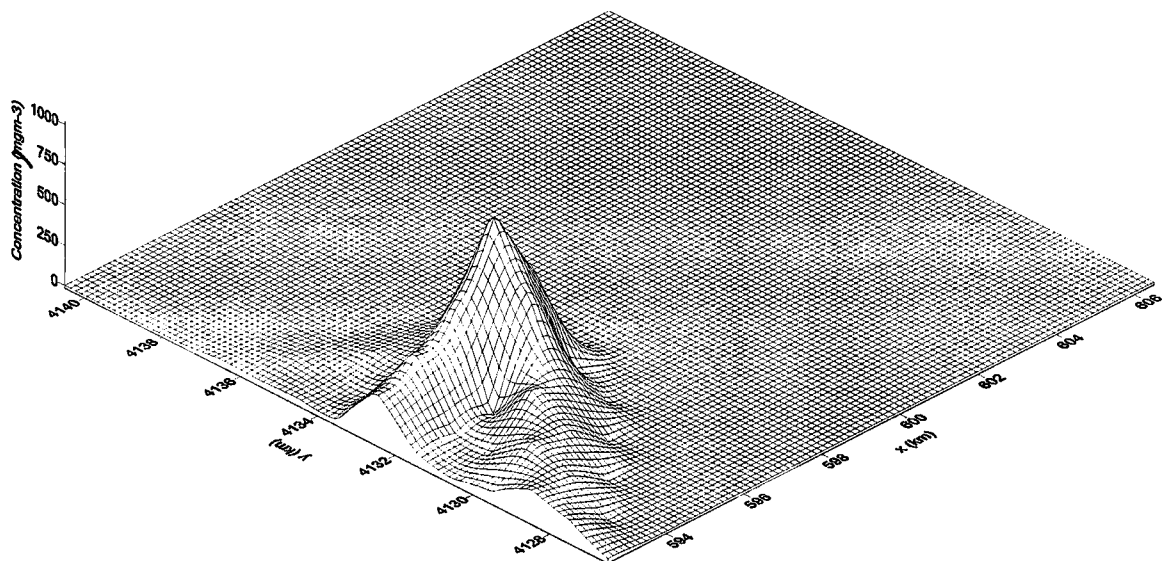


Figure 5.101. Concentration distribution for the modeling area at 15:00 on December 1, 2000.

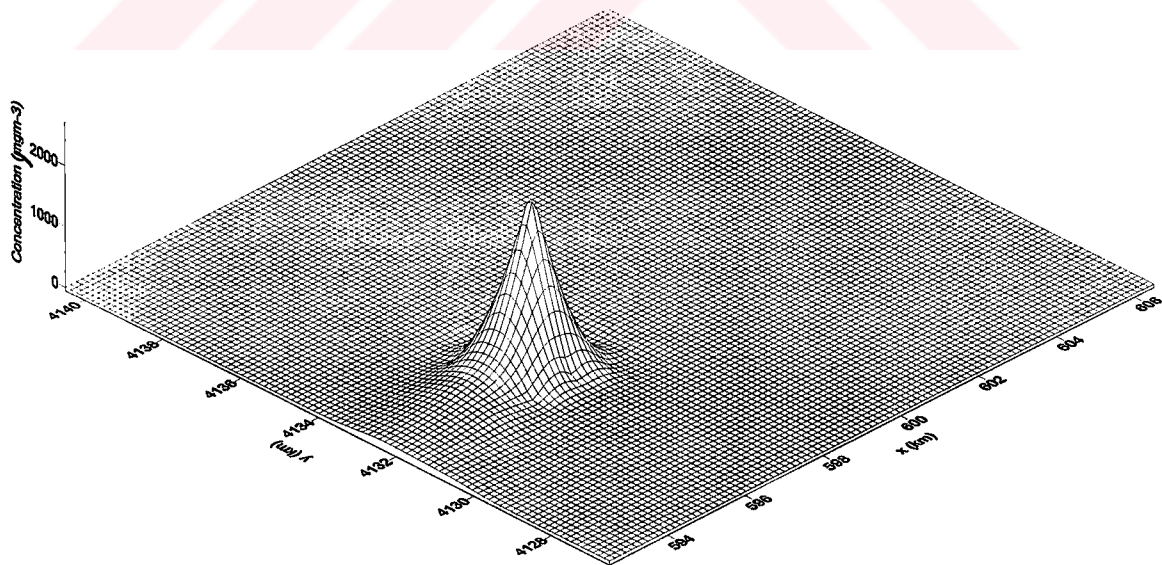


Figure 5.102. Concentration distribution for the modeling area at 23:00 on December 1, 2000.

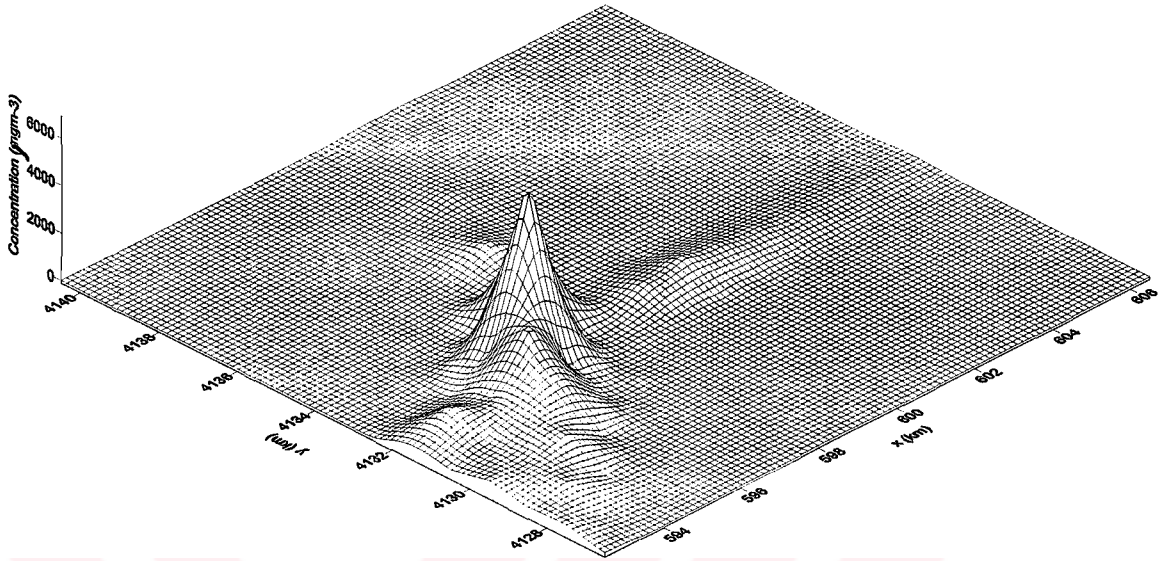


Figure 5.103. Concentration distribution for the modeling area at 07:00 on December 2, 2000.

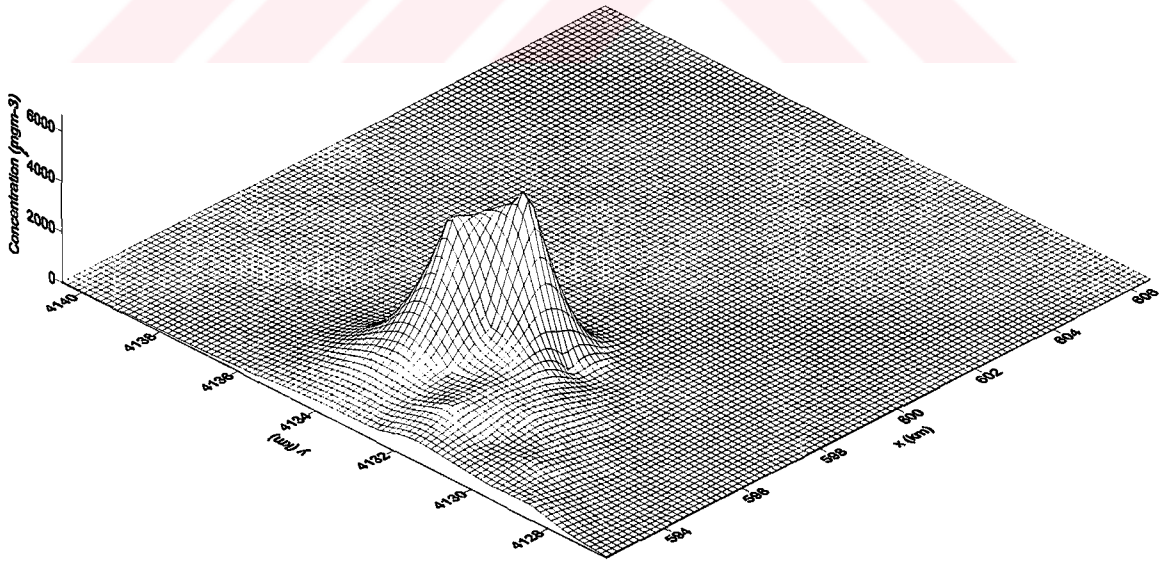


Figure 5.104. Concentration distribution for the modeling area at 15:00 on December 2, 2000.

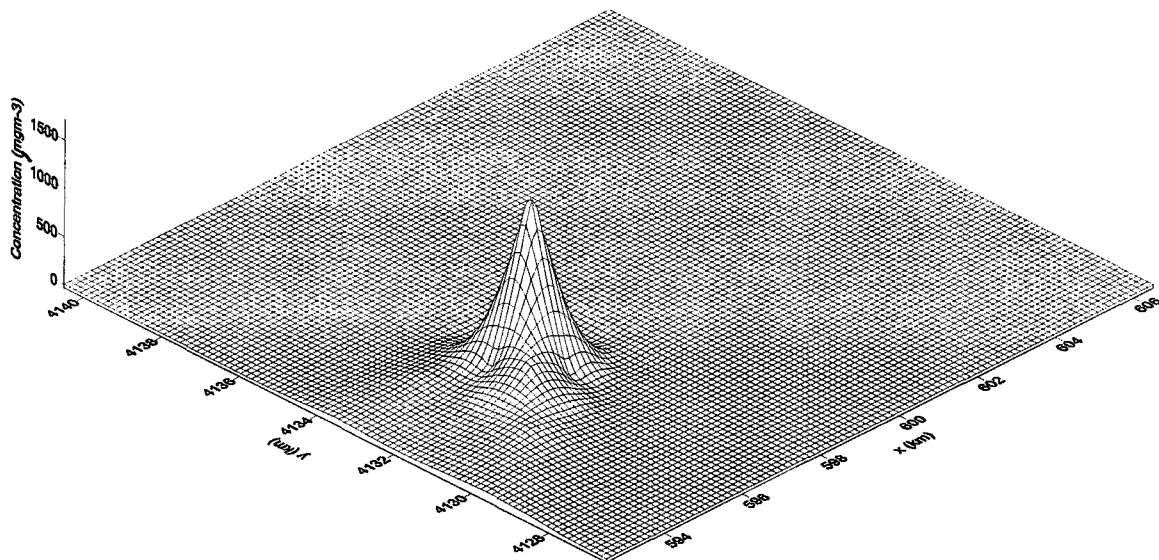


Figure 5.105. Concentration distribution for the modeling area at 23:00 on December 2, 2000.

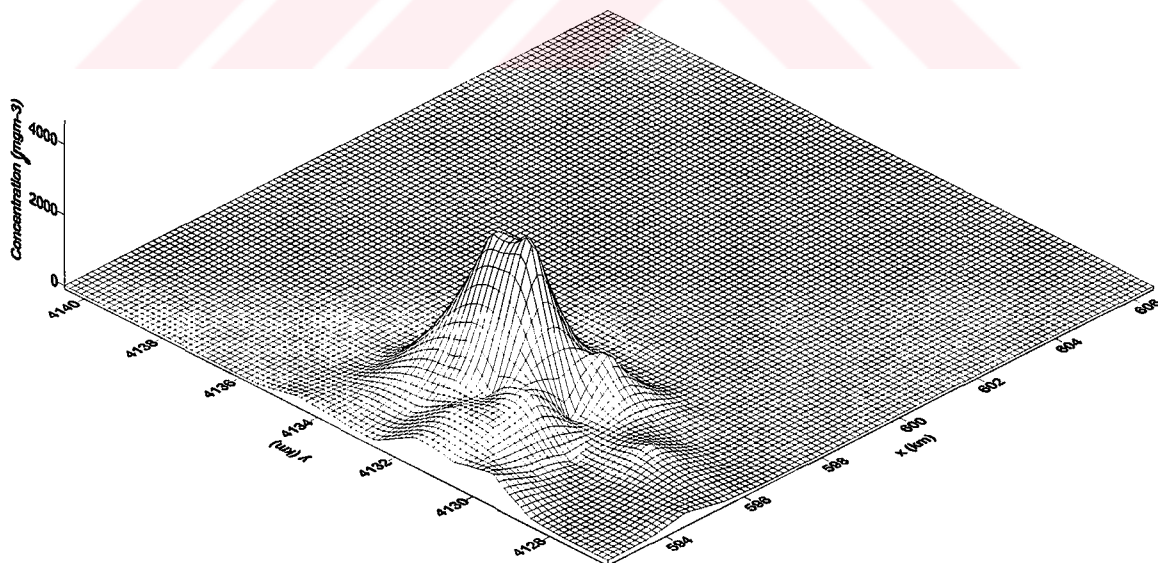


Figure 5.106. Concentration distribution for the modeling area at 07:00 on December 3, 2000.

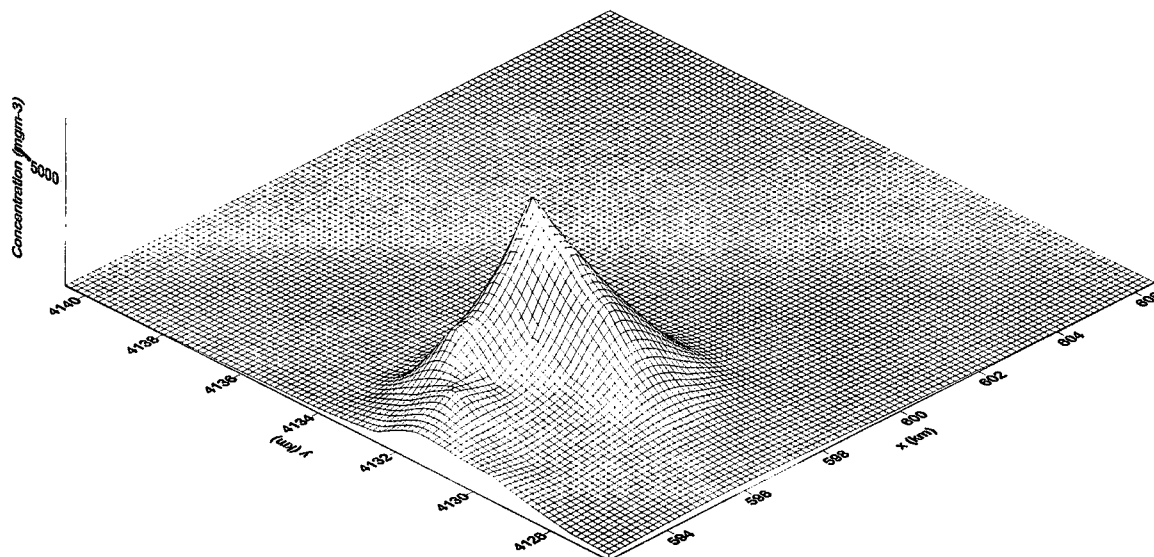


Figure 5.107. Concentration distribution for the modeling area at 15:00 on December 3, 2000.

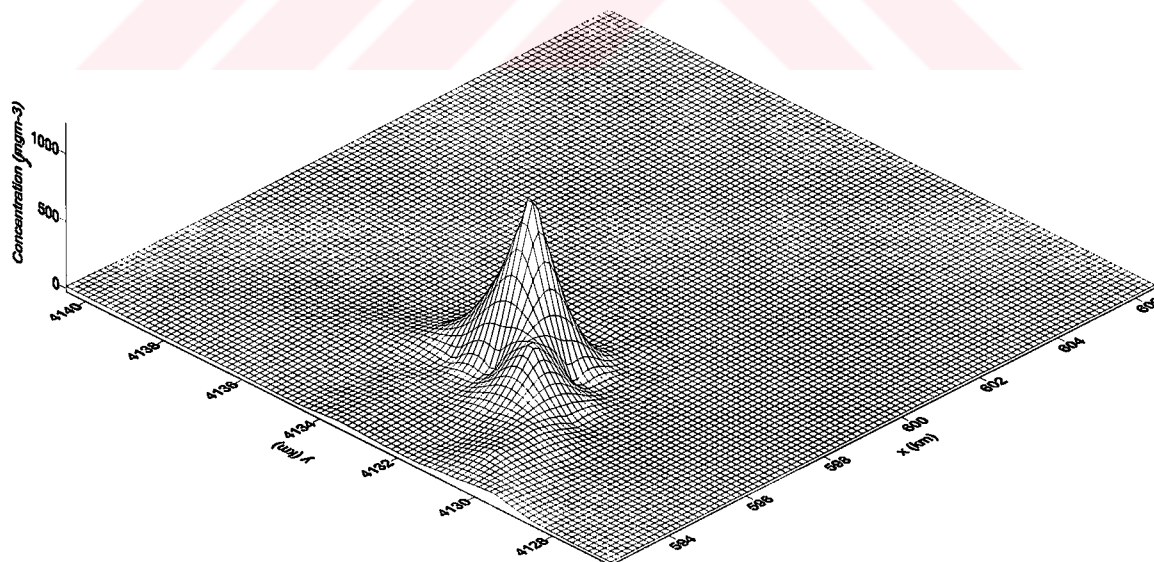


Figure 5.108. Concentration distribution for the modeling area at 23:00 on December 3, 2000.

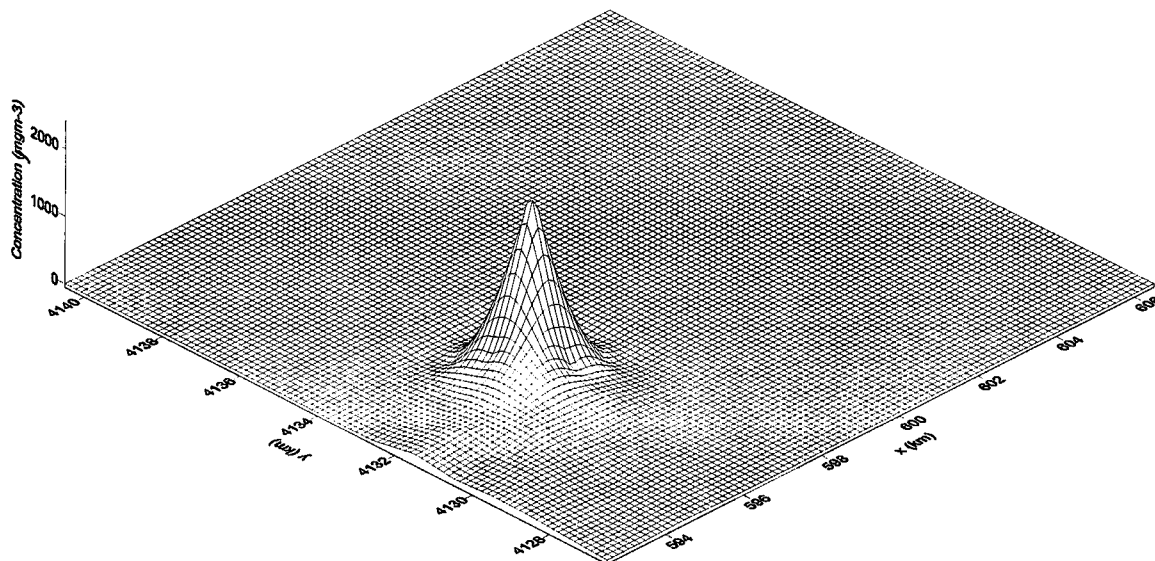


Figure 5.109. Concentration distribution for the modeling area at 07:00 on December 4, 2000.

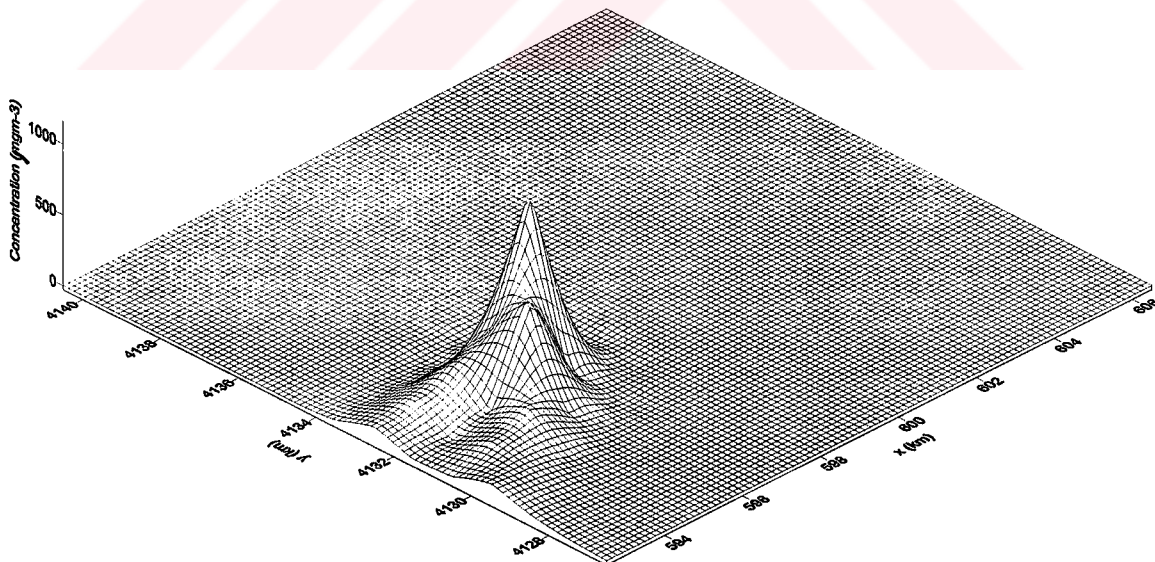


Figure 5.110. Concentration distribution for the modeling area at 15:00 on December 4, 2000.

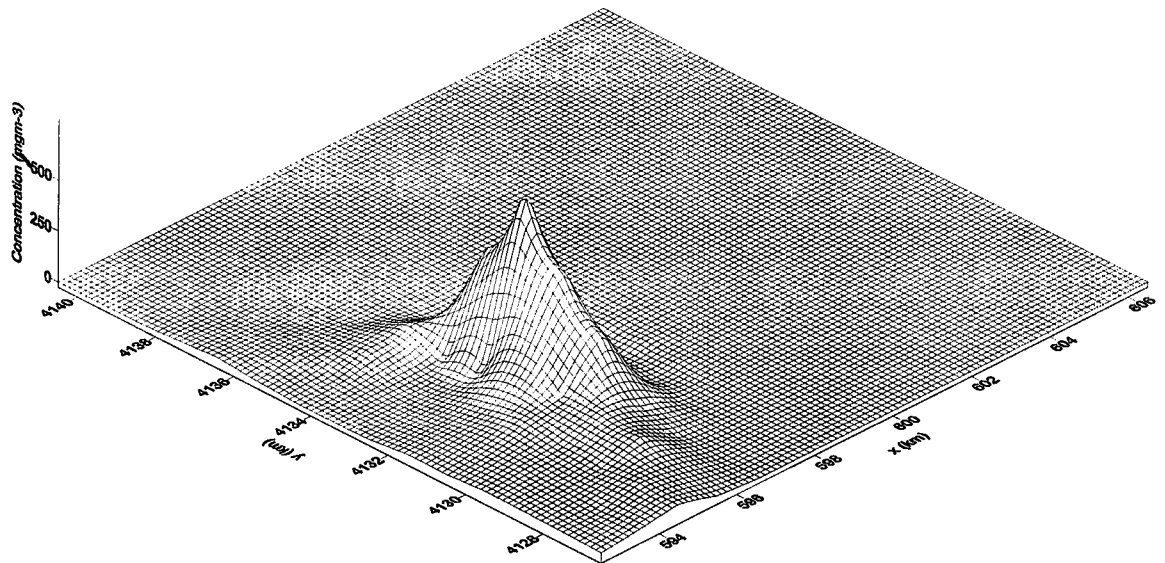


Figure 5.111. Concentration distribution for the modeling area at 23:00 on December 4, 2000.

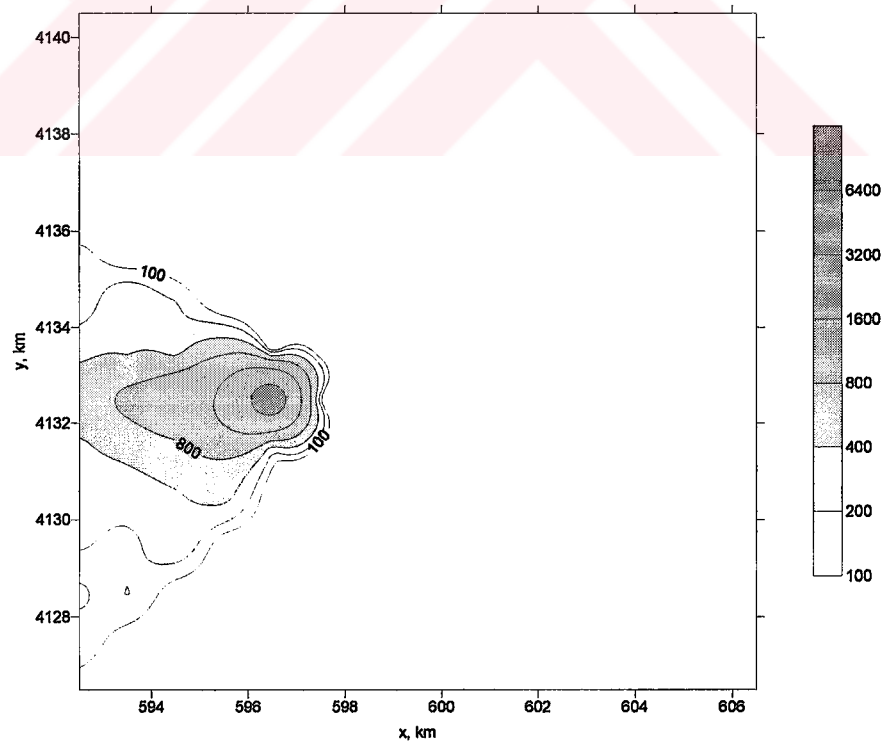


Figure 5.112. Concentration distribution (μgm^{-3}) at 07:00 on December 1, 2000.

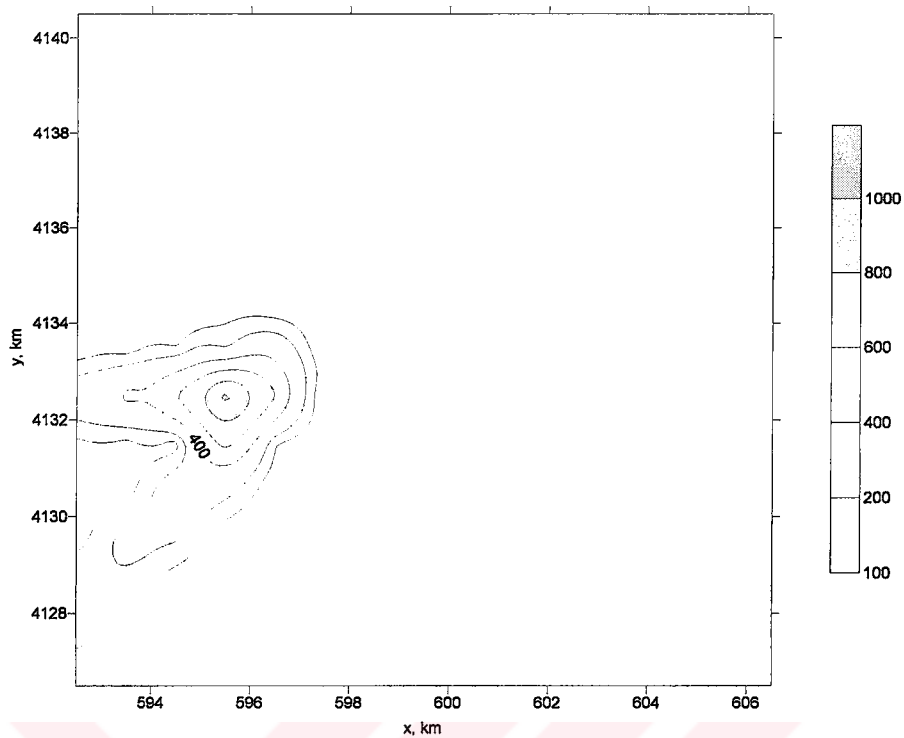


Figure 5.113. Concentration distribution ($\mu\text{g m}^{-3}$) at 15:00 on December 1, 2000.

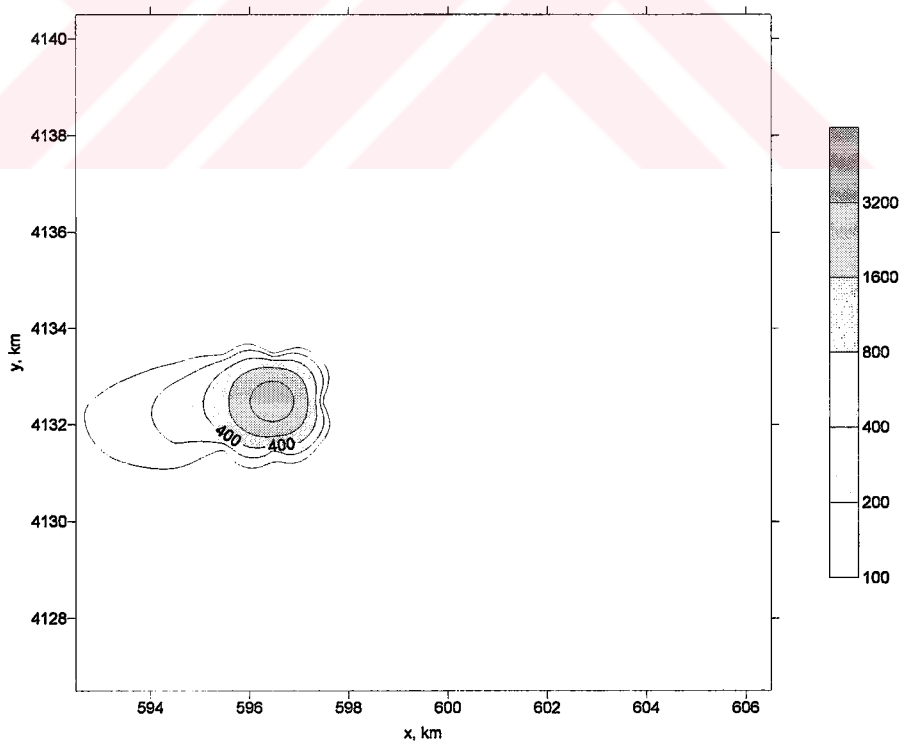


Figure 5.114. Concentration distribution ($\mu\text{g m}^{-3}$) at 23:00 on December 1, 2000.

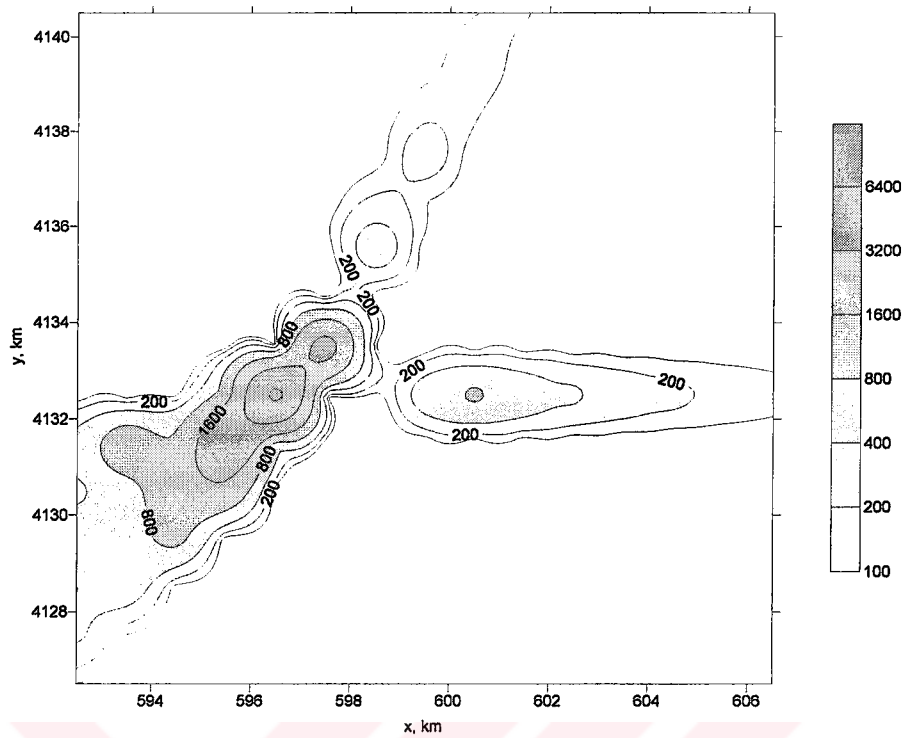


Figure 5.115. Concentration distribution ($\mu\text{g m}^{-3}$) at 07:00 on December 2, 2000.

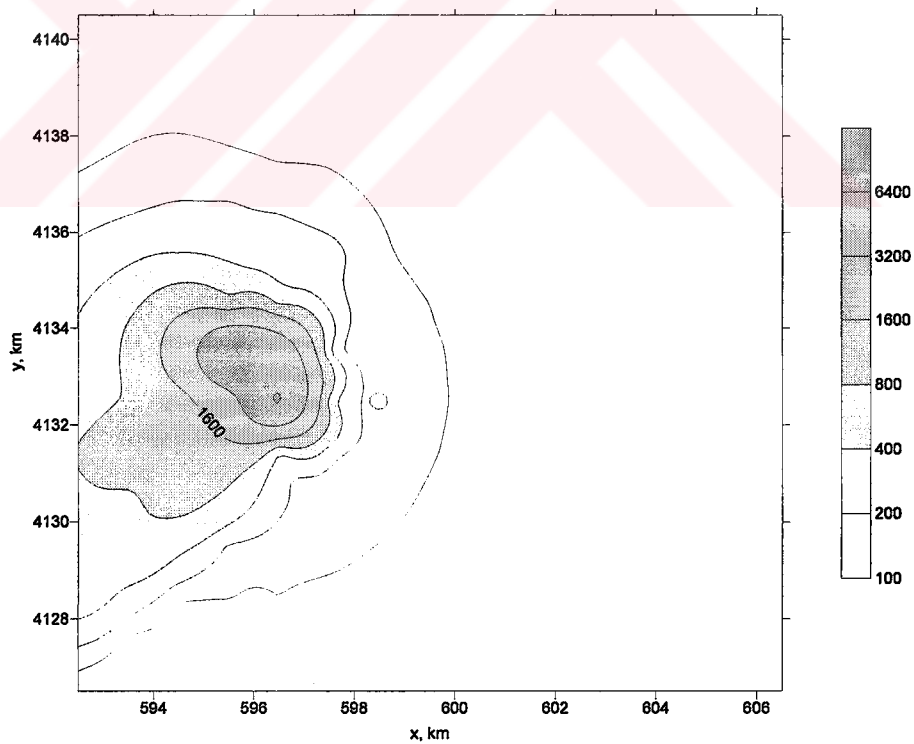


Figure 5.116. Concentration distribution ($\mu\text{g m}^{-3}$) at 15:00 on December 2, 2000.

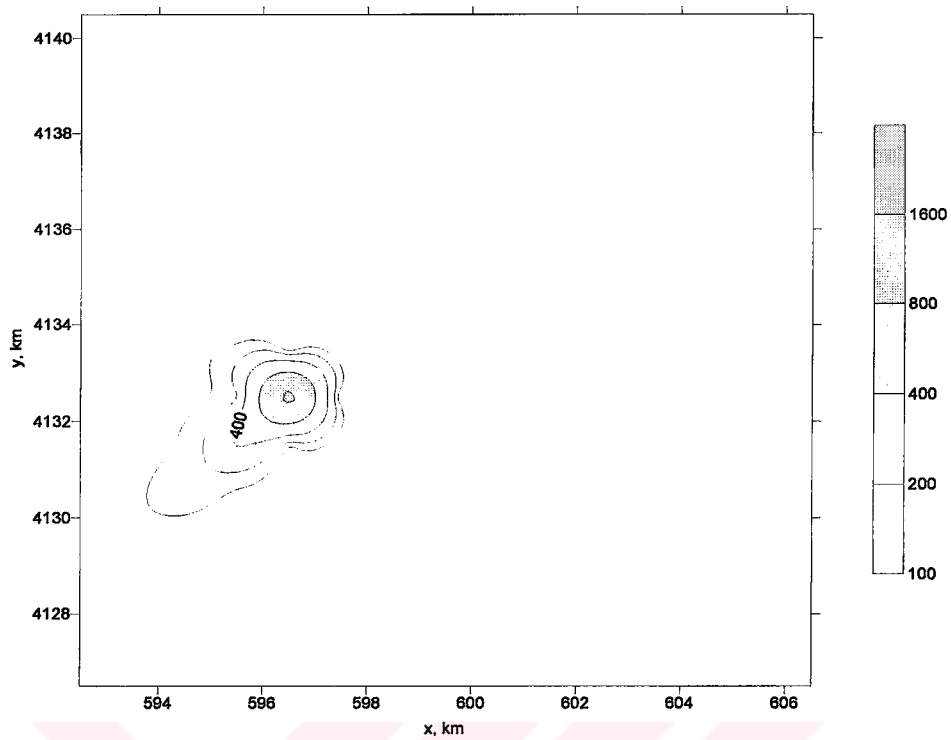


Figure 5.117. Concentration distribution ($\mu\text{g m}^{-3}$) at 23:00 on December 2, 2000.

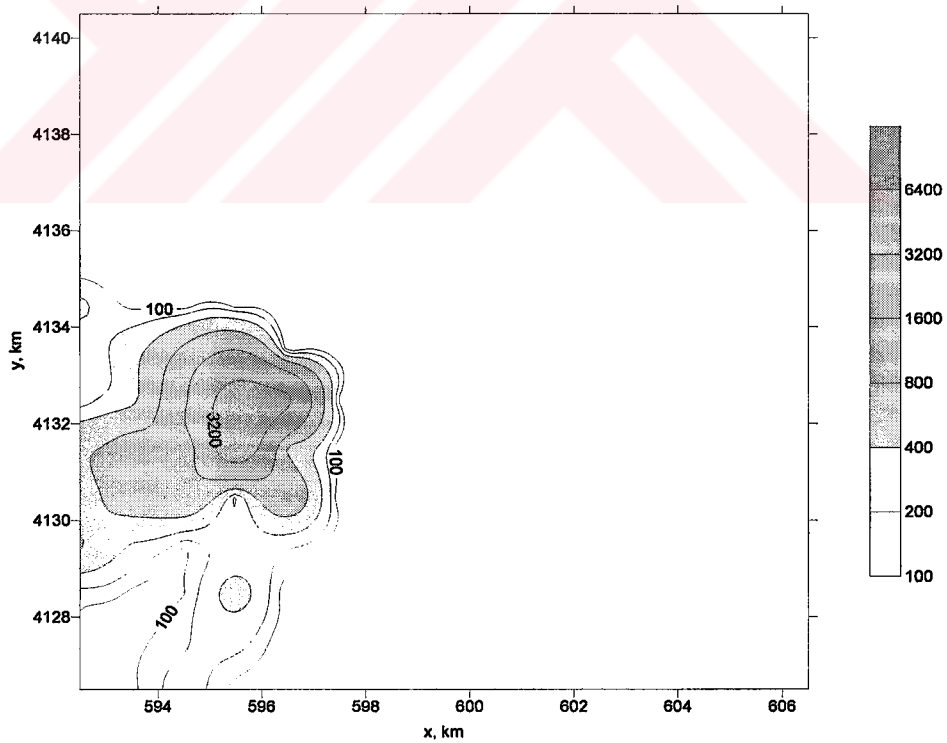


Figure 5.118. Concentration distribution ($\mu\text{g m}^{-3}$) at 07:00 on December 3, 2000.

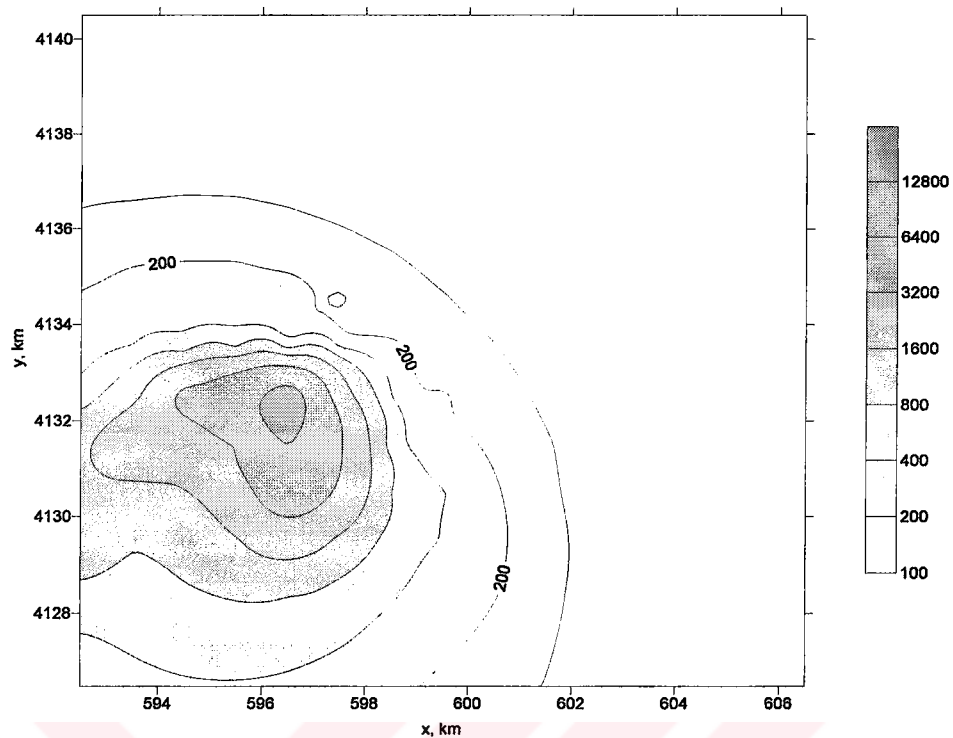


Figure 5.119. Concentration distribution ($\mu\text{g m}^{-3}$) at 15:00 on December 3, 2000.

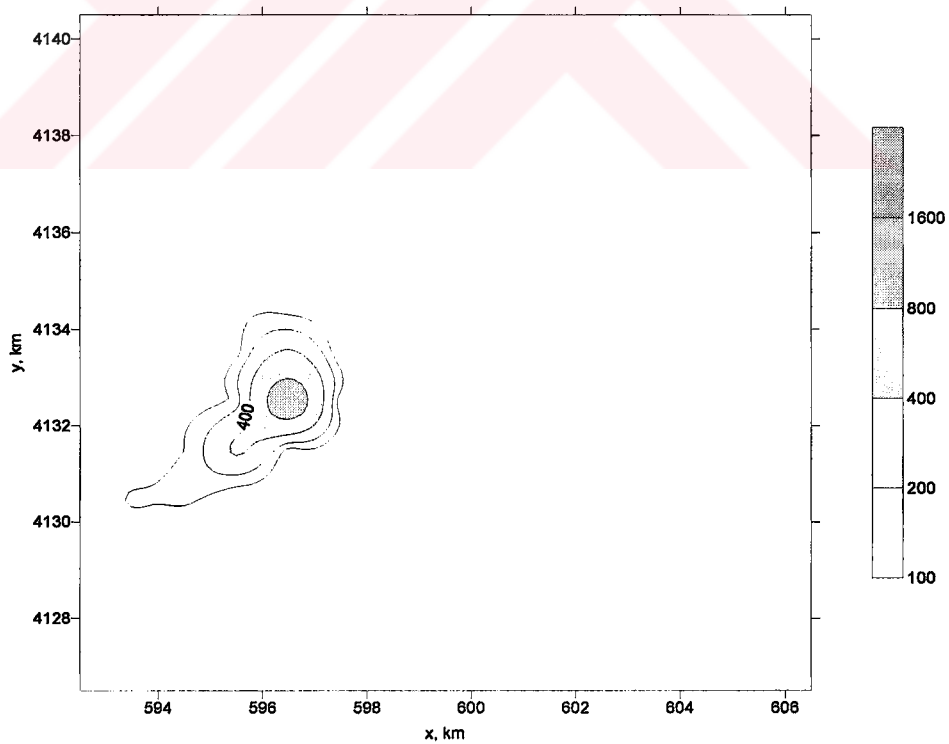


Figure 5.120. Concentration distribution ($\mu\text{g m}^{-3}$) at 23:00 on December 3, 2000.

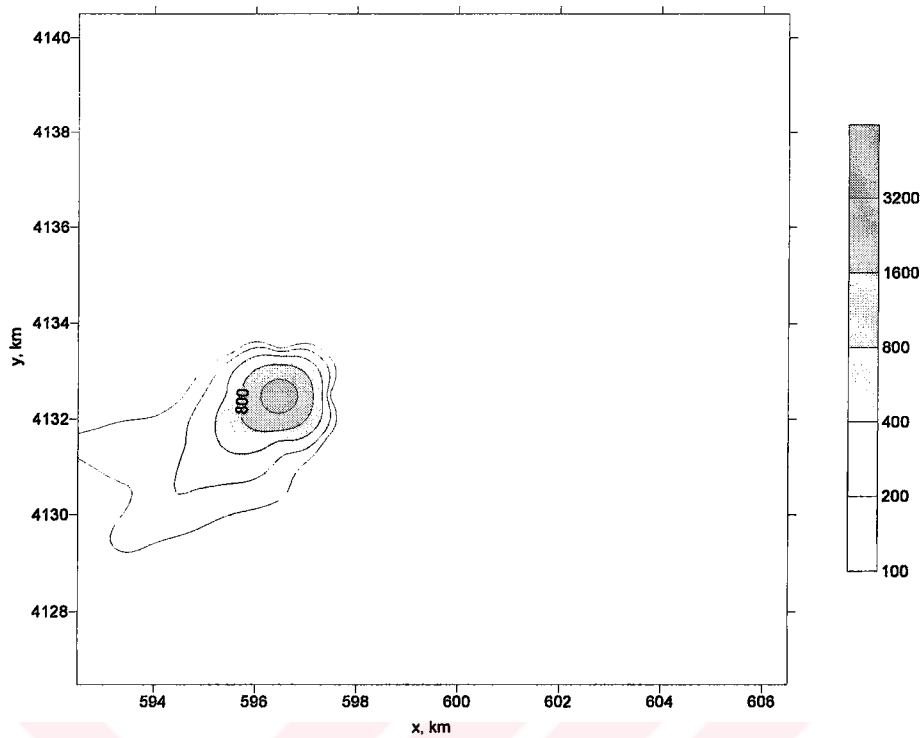


Figure 5.121. Concentration distribution ($\mu\text{g m}^{-3}$) at 07:00 on December 4, 2000.

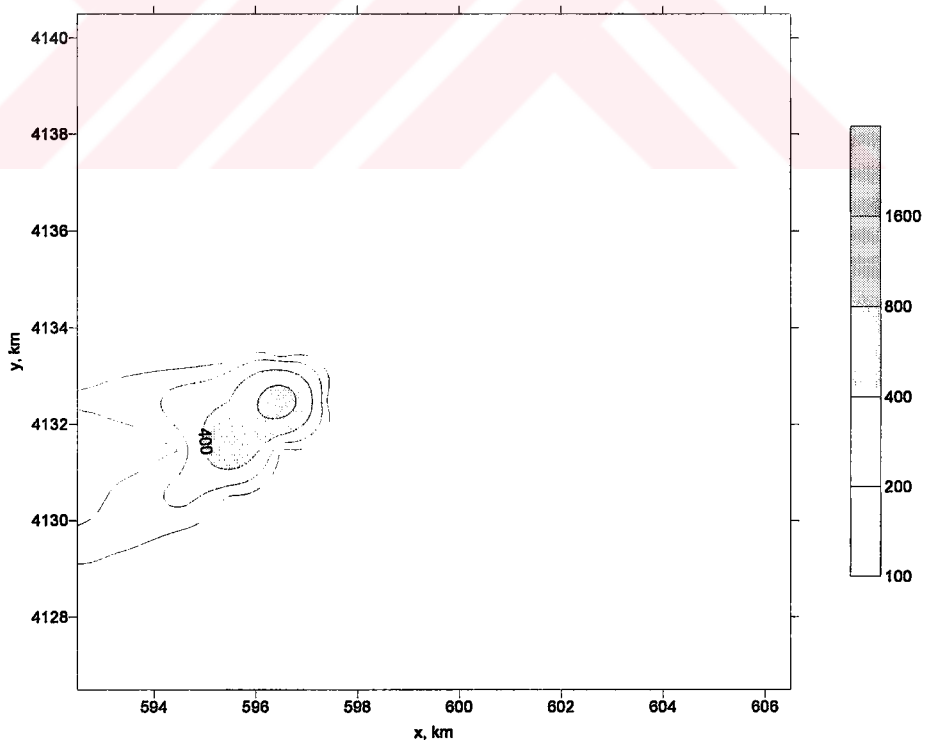


Figure 5.122. Concentration distribution ($\mu\text{g m}^{-3}$) at 15:00 on December 4, 2000.

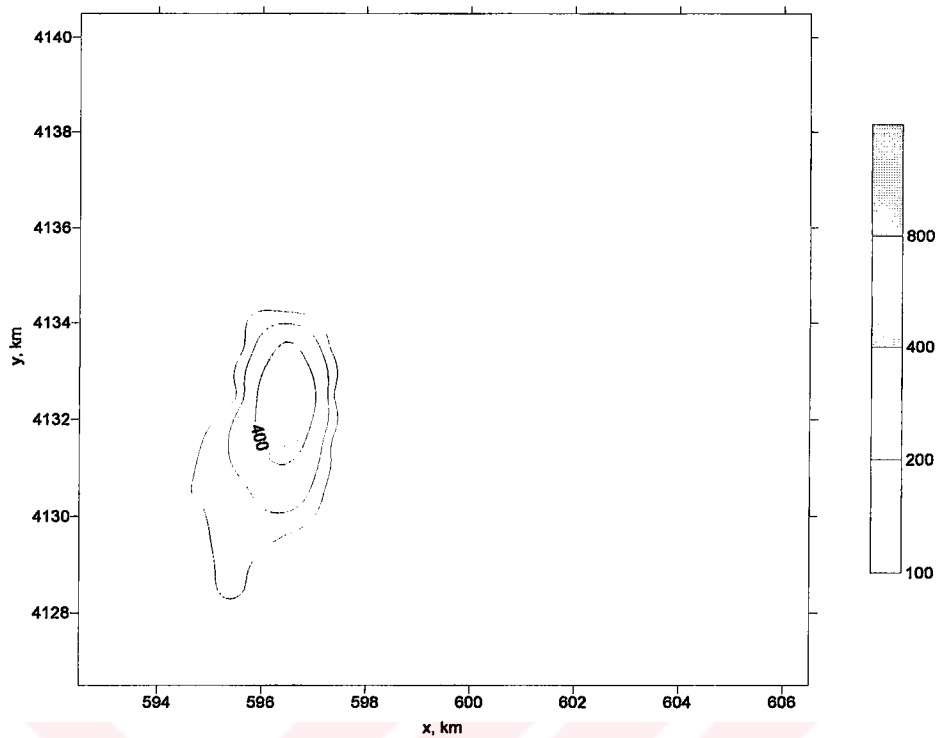


Figure 5.123. Concentration distribution (μgm^{-3}) at 23:00 on December 4, 2000.

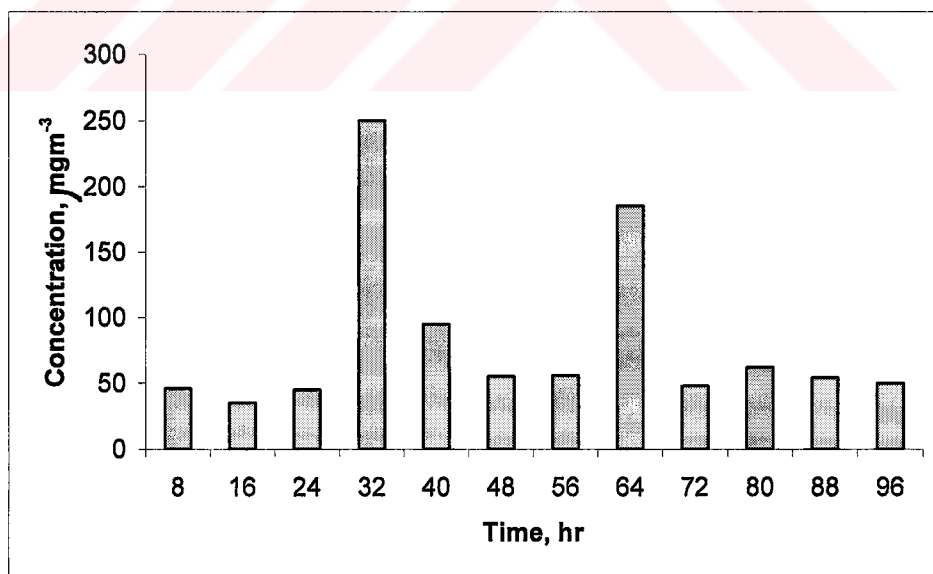


Figure 5.124. Maximum concentrations levels over Yatağan for Scenario 3.

5.3. Sensitivity Analysis

In order to be able to measure the sensitivity of the CALPUFF Modeling System the responses of the model to changes in surface temperature, wind speed, wind direction and emission rates were tested. The results are presented in Tables 5.1 to 5.4.

For the sensitivity analysis of the model, Yatağan district is chosen as a fixed location and December 2, 15:00 is selected as the reference time. In each of the test simulations all other parameters except for the considered parameter are kept the same as in the original case.

Table 5.1. Concentration levels over Yatağan district for surface temperatures on December 2, 2000 at 15:00

Surface Temperature (°C)	Concentration (μgm^{-3})
0	3137
10	3140
20	3142
30	3143
40	3147

Table 5.2. Concentration levels over Yatağan district for different wind speeds on December 2, 2000 at 15:00

Wind Speed (ms^{-1})	Concentration (μgm^{-3})
0	610
2	1193
4	418
6	285
8	127

Table 5.3. Concentration levels over Yatağan district for different wind directions on December 2, 2000 at 15:00

Wind Direction (degree)	Concentration (μgm^{-3})
0	98
45	105
90	48
135	78
180	230
225	3412
270	2758
315	510
360	187

Table 5.4. Concentration levels over Yatağan district for different emission rates on December 2, 2000 at 15:00

Emission Rate (gs^{-1})	Concentration (μgm^{-3})
500	257
1000	418
2000	874
3000	1490
4000	3279
5000	4180

For the first simulation considering the effect of surface temperature on the ground level concentrations, as can be seen from Table 5.1. and Figure 5.125., the ground level concentrations increases with the increasing temperature but the magnitudes of these concentrations do not increase in the same order as the emission rates, but increase very slightly.

In Table 5.2., it can be seen that there is no regular pattern between the wind speed and concentration. On the other hand, it can be concluded that for calm wind speeds, below 2 ms^{-1} , the concentrations tend to increase because the light winds can not carry the pollutants away from the modeling domain, thus, lead to accumulation over Yatağan district. As can be seen in Figure 5.126., when the wind speeds become stronger such as 6 and 8 ms^{-1} , the concentrations decrease with the increasing wind speeds because the pollutants are carried away and dispersed better with the better mixing conditions.

Table 5.3. gives the concentration levels over Yatağan for different wind directions. As expected, the concentrations increase as the winds turn south westerly and westerly. This can be explained by the location of Yatağan district being on north east of the power plant and thus, the pollutants are carried directly towards the district (Figure 5.127.).

Finally, the last simulation test considering the effect of emission rates shows that, as expected, there is a close to linear relationship between emission rates and concentrations. As can be seen from Table 5.4. and Figure 5.128., the concentrations increase directly proportional to the increasing emission rates.

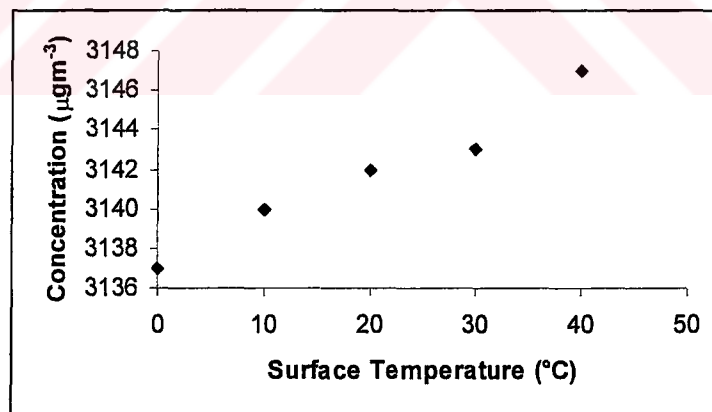


Figure 5.125. Concentration levels over Yatağan district for different surface temperatures on December 2, 2000 at 15:00

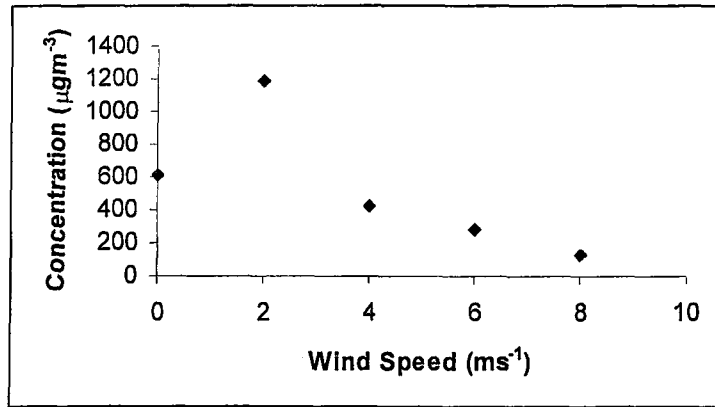


Figure 5.126. Concentration levels over Yatağan district for different wind speeds on December 2, 2000 at 15:00

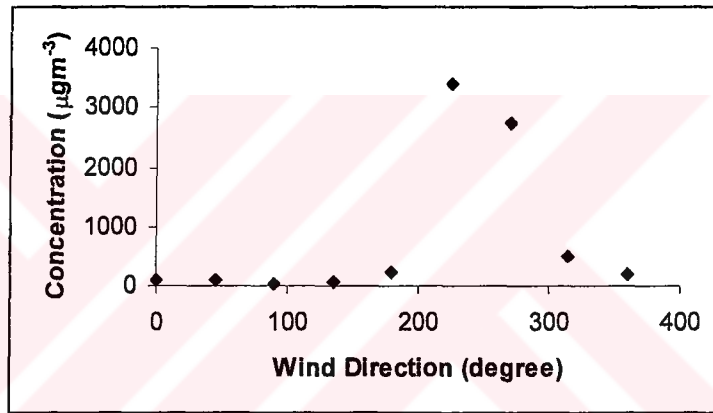


Figure 5.127. Concentration levels over Yatağan district for different wind directions on December 2, 2000 at 15:00

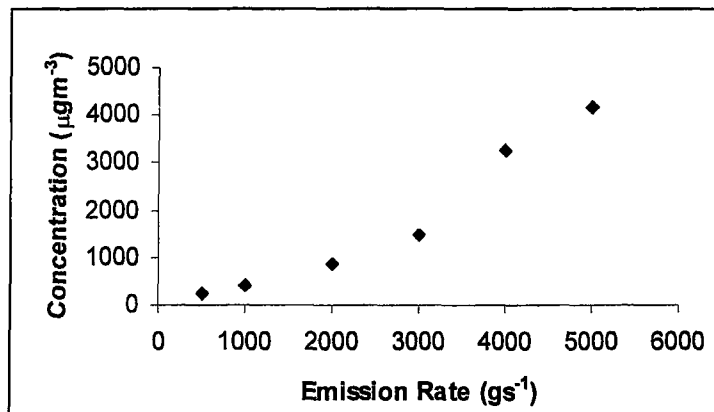


Figure 5.128. Concentration levels over Yatağan district for different emission rates on December 2, 2000 at 15:00

6. CONCLUSIONS AND RECOMMENDATIONS

In this study, the CALMET Meteorological Model and the CALPUFF Dispersion Model are used to simulate the effects of the SO₂ pollution produced by Yatağan Power Plant over the Yatağan district in an episodic event that has occurred on December 2 and 3, 2000. CALMET computed the hourly wind fields and CALPUFF used these wind fields as input in order to calculate the hourly SO₂ concentrations in the model domain. These concentrations are then compared with the measurements done by the Local Environmental Authority of Muğla (Muğla İl Çevre Müdürlüğü).

The meteorological data show that daytime winds were moderate winds with speeds around 5 ms⁻¹ on average during the simulation period. On 2nd and 3rd of December, nighttime winds changed to light winds with speeds below 2 ms⁻¹ and turned to north east direction. Under stable conditions and with the existence of surface inversion layers of 300 m on average, starting from early hours of the night, mixing in the atmosphere became very poor and led the pollutants not to disperse, but accumulate over the region until noon hours of the following day.

The maximum ground level concentrations are found northeast from the source, which agrees with experimental recordings and meteorological data. On the other hand, these concentrations differed from measurements in terms of magnitude. The maximum concentration during the simulation period over Yatağan is calculated as 3140 µgm⁻³ on the 38th hour of the period, on December 2, 2000, at 13:00, whereas according to on site measurements, the highest ground level concentration measured at Yatağan during the simulation period was 4100 µgm⁻³.

The differences between the modeled concentration levels and measured concentration levels may originate from the insufficiencies with meteorological data incorporated into the model. The surface meteorological data incorporated to the model is taken from only one meteorological station. Isparta meteorological station, where the upper air data were taken, is not inside the modeling domain and is around 300 km from the power plant. Besides, Isparta

is located in a lake district and the meteorological parameters are influenced by the lakes. Therefore, the upper air data from this station do not adequately reflect the topographical effects of the modeled area on the meteorological variables. Additionally, the predicted concentrations are calculated as the maximum average values within 1 hour intervals inside a 1 km x 1 km resolution whereas the on site observations represent the conditions at the particular moment at a particular point. Therefore, a one to one match between the predicted and observed concentrations was not expected. As a result, it is concluded that wind data should be available at more than a single station within the modeled domain and upper air meteorological data should be from a station within or very close to the modeled region.

The sensitivity analysis showed that the concentrations are directly proportional to the emission rates, but wind speed is the most significant meteorological parameter on air pollution modeling compared to other meteorological parameters. Light winds cannot carry the pollutants away and causes them to accumulate over Earth's surface. The wind direction plays an important role in where the pollutants are carried and becomes more critical when the governing wind direction is towards urban areas and winds are calm. Surface temperatures do not affect the ground level concentrations alone but with the sharp decrease in ambient temperature, inversion layers trap the pollutants in shallow heights from the surface and concentrations increase significantly.

As a conclusion, it can be suggested that CALPUFF Modeling System can be used in further air pollution studies involving the effects of power plants on environment and management of emission rates of these plants. On the other hand, it should be stated that the modeling studies should be conducted with sufficient and accurate data.

REFERENCES

- Allwine, K. J., Whitemann, C. D., *MELSAR: A Mesoscale Air Quality Model for Complex Terrain*, Vol. 1 – Overview, Technical Description and User's Guide, Pacific Northwest Laboratory, Richland, Washington, 1985
- Douglas, S., Kessler, R., *User Guide to the Diagnostic Wind Field Model*, Version 1.0, System Applications Inc., San Rafael, CA, pp. 48, 1988
- Garcia, M. M., Leon, H.R., "Numerical and Experimental Study on the SO₂ Pollution produced by Lerdo Thermal Power Plant, Mexico", *Atmospheric Environment*, Vol 33, pp. 3723 – 3728, 1999
- Hewitt, C. N., "The Atmospheric Chemistry Of Sulphur And Nitrogen In Power Station Plumes," *Atmospheric Environment*, Vol 35, pp. 1155 – 1170, 2001
- Holstag, A. A. N., van Ulden, A. P., "A Simple Scheme for Daytime Estimates of the Surface Fluxes from Routine Weather Data", *Journal of Climate and Applied Meteorology*, Vol. 22, pp. 517 – 529, 1983
- Lavery, T. F., Goss, R. S., Fabrick, A., Rogers, C. M., "Application Of Micrometeorological Model To Simulate Long – Term Deposition Of Atmospheric Gases And Aerosols", *Air Pollution Modeling and Its Application XIV*, Kluwer Academic / Plenum Publishers, New York, 2001
- Nicholson, K. W., "The Dry Deposition of Small Particles: A Review of Experimental Measurements", *Atmospheric Environment*, Vol. 22, pp. 2653 – 2666, 1998
- Scire, J. S., Robe, F. R., Fernau, M. E., Yamartino, R. J., *A User's Guide for the CALMET Meteorological Model*, Version 5, Earth Tech Inc. 2000

Seinfeld, J.H., Pandis, S.N., ATMOSPHERIC CHEMISTRY AND PHYSICS: *From Air Pollution to Climate Change*, Wiley – Interscience Publication, JOHN WILEY & SONS, INC., New York, 1998

Sharan, M., Yadav, A. K., Singh, M. P., Agarwal, P., Nigam, S., “A Mathematical Model for the Dispersion of Air Pollutants in Low Wind Conditions”, *Atmospheric Environment*, Vol. 30, pp. 1209 – 1220, 1996

Stern, A.C., Boubel, R.W., Turner, D.B., Fox, D.L., FUNDAMENTALS OF AIR POLLUTION; *Second Edition*, Academic Press, Inc., Florida, 1984

Stull R.B., *An Introduction To Boundary Layer Meteorology*, Kluwer Academic Publishers, Dordrecht, 1988

Turner, D. B., Workbook of Atmospheric Estimates: *An Introduction to Dispersion Modeling*, Lewis Publishers, 1994

Venkatram, A., “Estimating the Monin – Obukhov Length in the Stable Boundary for Dispersion Calculations”, *Boundary Layer Meteorology*, Vol. 19, pp. 481 – 485, 1980

Weil, J. C., Brower, R. P., Estimating Convective Layer Parameters for Diffusion Application, Draft Report Prepared by Environmental Center, Martin Marietta Corp. for Maryland Dept. of Natural Resources, 1983

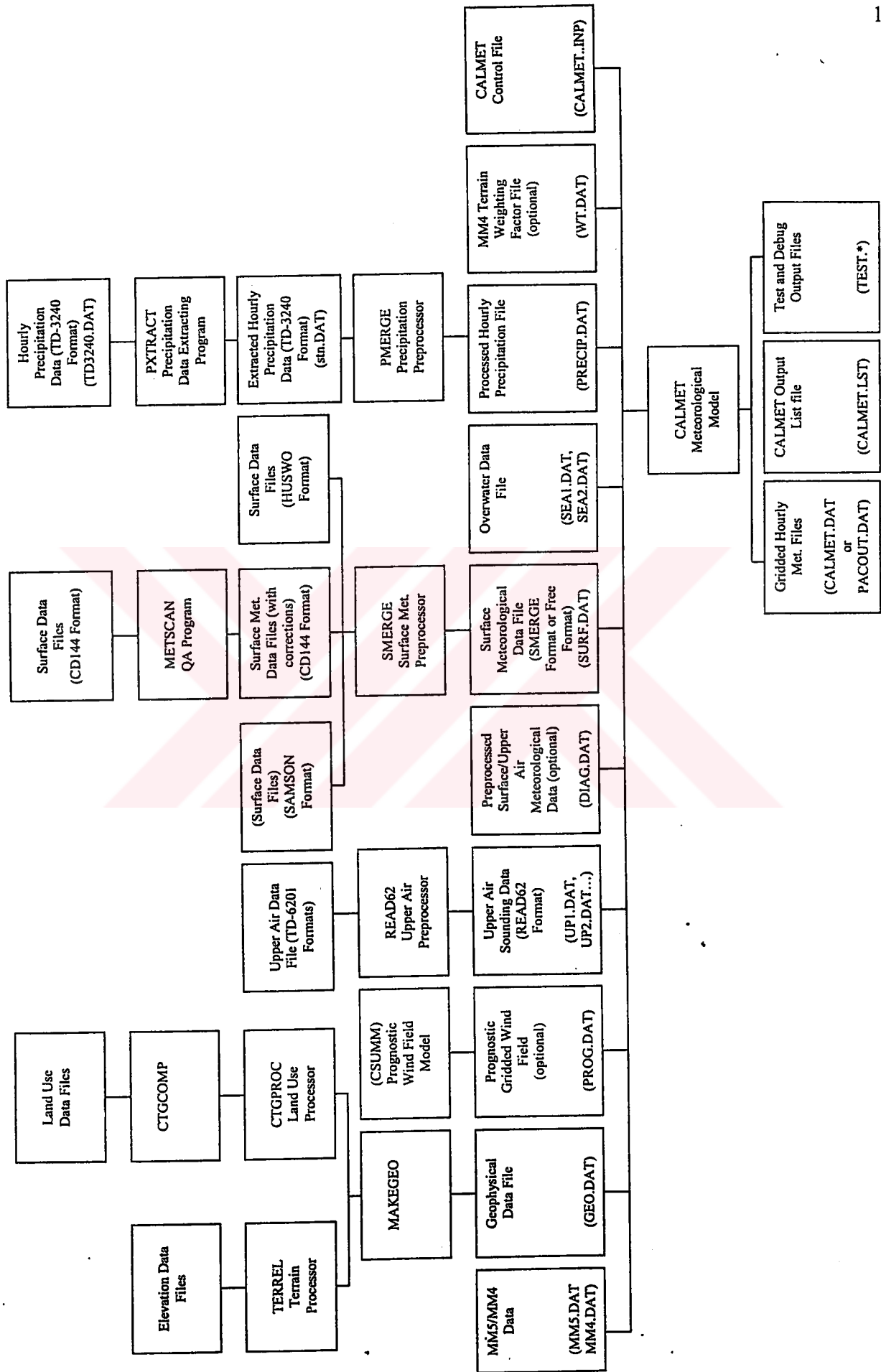
Zannetti, P., Air Pollution Modeling: *Theories, Computational Methods And Available Software*, Computational Mechanics Publications, Southampton, Boston, 1990

REFERENCES NOT CITED

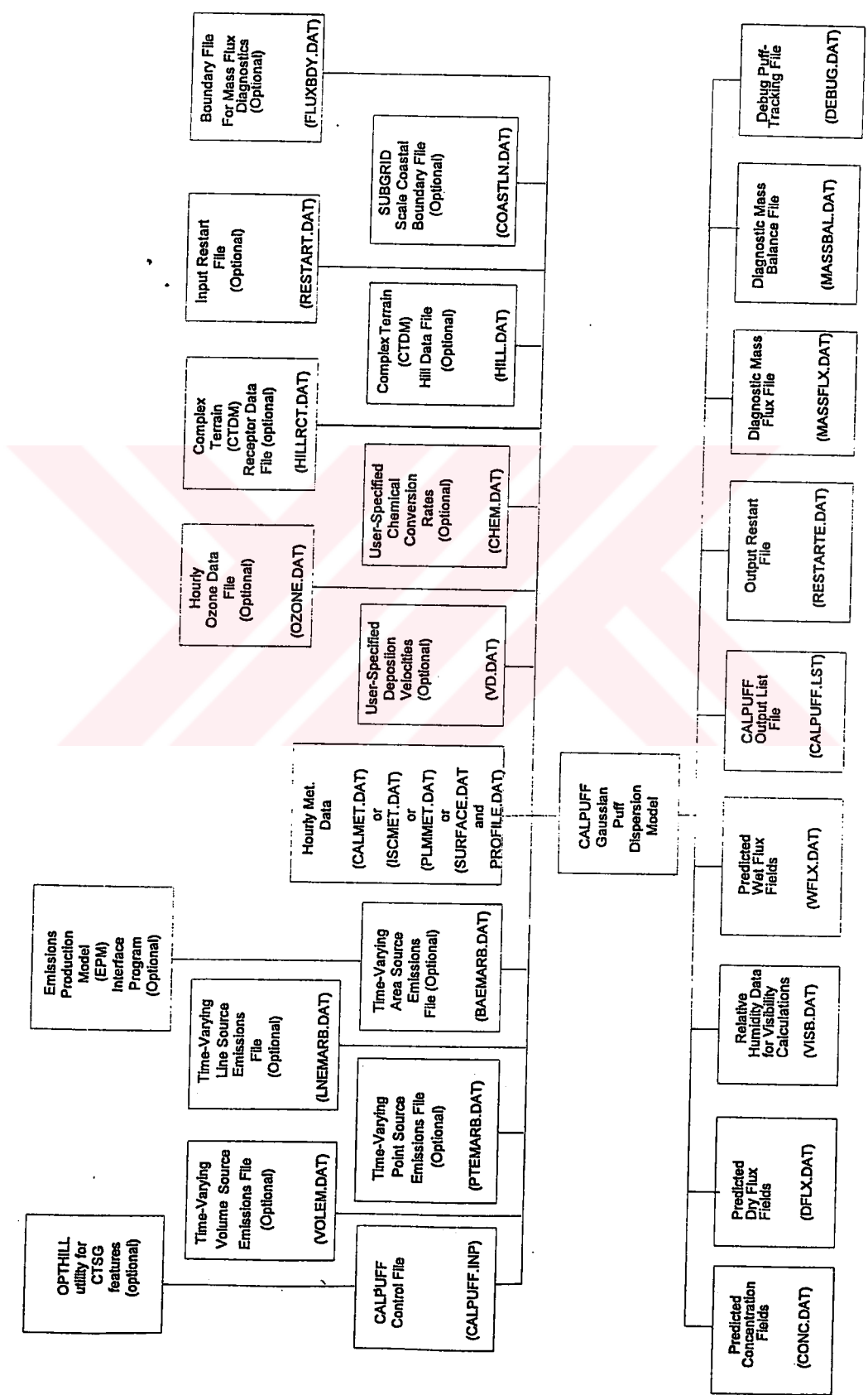
- Ames, M. R., Zemba, S. G., Yamartino, R. J., Valberg, P. A., Green, L. C., "Comments on: Using CALPUFF to Evaluate the Impacts of Power Plant Emissions in Illinois: Model Sensitivity and Implications", *Atmospheric Environment*, Vol. 36, pp. 2263-2265, 2002
- Builtjes, P. J. H., "Major Twentieth Century Milestones in Air Pollution Modeling and Its Application", *Air Pollution and Its Application XIV*, Kluwer Academic/Plenum Publishers, New York, 2001
- Buzcu, B., "Mathematical Modeling of Plume Dispersion in Tüpraş Fire of August 1999", M.S. Thesis, Boğaziçi University, 2001
- Degrazia, G. A., Anfossi, D., Carvalho, J. C., Tirabassi, T., Velho, H. F. C., "Turbulence Parameterisation for PBL Dispersion Models in All Stability Conditions", *Atmospheric Environment*, Vol. 34, pp. 3575-3583, 2000
- İncecik, S., "Investigation of Atmospheric Conditions in İstanbul Leading to Air Pollution Episodes", *Atmospheric Environment*, Vol. 30, pp. 2739-2749, 1996
- Lalas, D. P., Ratto, C. F. (Eds), *Modeling of Atmospheric Flow Fields*, World Scientific Publishing Co., 1996
- Seibert, P., Beyrich, F., Gryning, S., Joffre, S., Rasmussen, A., Tercier, P., "Review and Intercomparison of Operational Methods for the Determination of the Mixing Height", *Atmospheric Environment*, Vol. 34, pp. 1001-1027, 2000



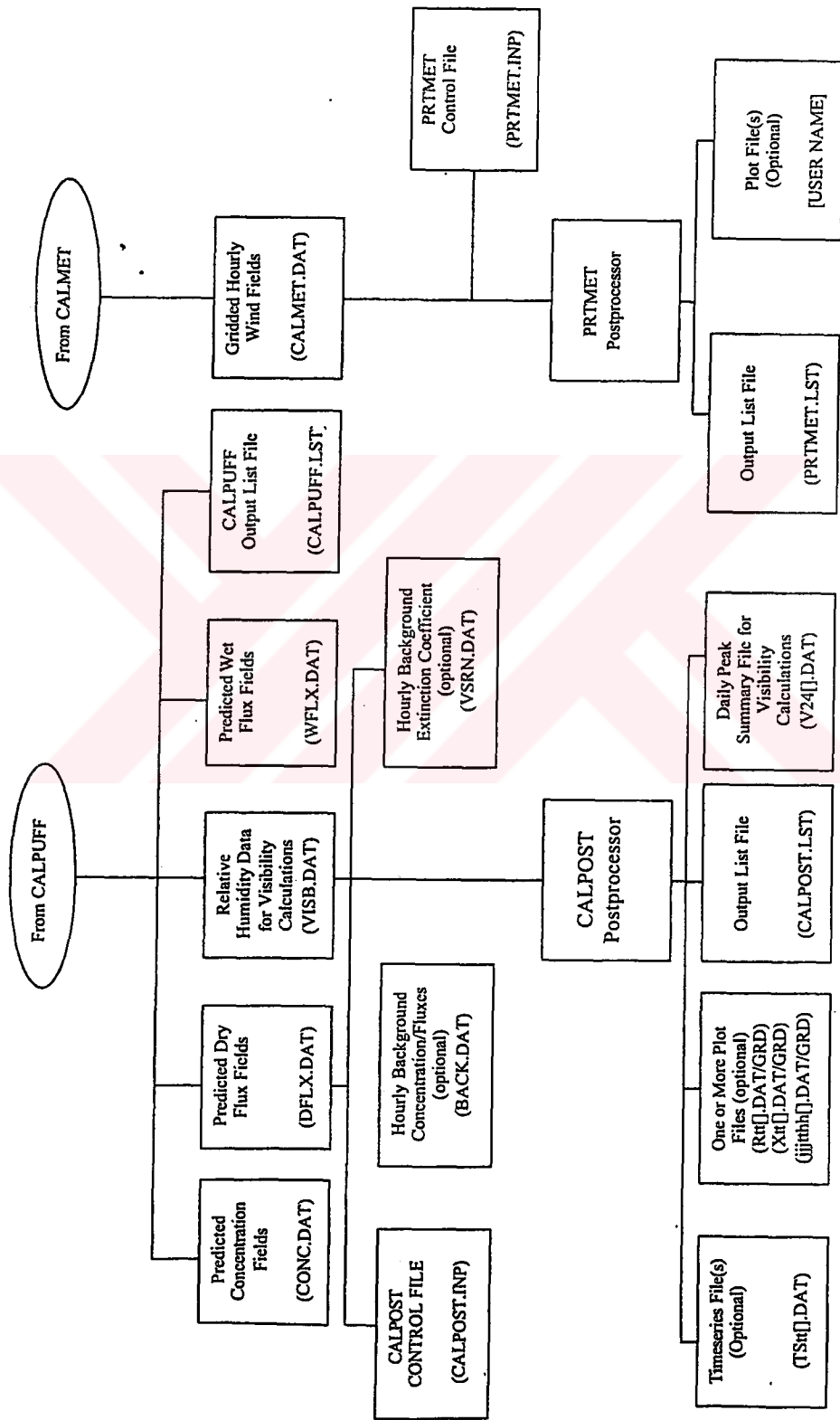
APPENDIX I
FLOW DIAGRAMS OF CALMET, CALPUFF, AND CALPOST



Meteorological modeling: CALMET modeling flow diagram.



Dispersion Modeling: CALPUFF modeling flow diagram.



Postprocessing: CALPOST/PRTMET postprocessing flow diagram.



APPENDIX II
CALMET MODEL CONTROL FILE

CALMET MODEL CONTROL FILE

INPUT GROUP: 0 -- Input and Output File Names

Subgroup (a)

Default Name	Type	File Name
GEO.DAT	input	! GEODAT=C:\CALPUFF\DEMO\MODELS\CALMET\GEOIKM-1.TXT !
SURF.DAT	input	! SRFDAT=C:\CALPUFF\DEMO\MODELS\CALMETSURFDE-1.TXT !
CLOUD.DAT	input	* CLDDAT= *
PRECIP.DAT	input	* PRCDAT= *
MM4.DAT	input	* MM4DAT= *
WT.DAT	input	* WTDAT= *
CALMET.LST	output	! METLST=C:\CALPUFF\DEMO\MODELS\CALMET\BIRNUR.LST !
CALMET.DAT	output	! METDAT=C:\CALPUFF\DEMO\MODELS\CALPUFF\BIRNUR.DAT !
PACOUT.DAT	output	* PACDAT= *

All file names will be converted to lower case if LCFILES = T
 Otherwise, if LCFILES = F, file names will be converted to UPPER CASE
 T = lower case ! LCFILES = F !
 F = UPPER CASE

NUMBER OF UPPER AIR & OVERWATER STATIONS:

Number of upper air stations (NUSTA) No default ! NUSTA = 1 !
 Number of overwater met stations
 (NOWSTA) No default ! NOWSTA = 1 !

!END!

Subgroup (b)

Upper air files (one per station)

Default Name	Type	File Name
UPI.DAT	input	! UPDAT=C:\CALPUFF\DEMO\MODELS\CALMET\UPALBR-1.TXT! !END!

Subgroup (c)

Overwater station files (one per station)

Default Name	Type	File Name
SEA1.DAT	input	! SEADAT=C:\CALPUFF\DEMO\MODELS\CALMET\SEADEN-1.TXT! !END!

Subgroup (d)

Other file names

Default Name	Type	File Name
DIAG.DAT	input	* DIADAT= *
PROG.DAT	input	* PRGDAT= *
TEST.PRT	output	* TSTPRT= *
TEST.OUT	output	* TSTOUT= *
TEST.KIN	output	* TSTKIN= *
TEST.FRD	output	* TSTFRD= *
TEST.SLP	output	* TSTSLP= *

NOTES: (1) File/path names can be up to 70 characters in length
 (2) Subgroups (a) and (d) must have ONE 'END' (surround by delimiters) at the end of the group
 (3) Subgroups (b) and (c) must have an 'END' (surround by delimiters) at the end of EACH LINE

!END!

INPUT GROUP: 1 -- General run control parameters

Starting date: Year (IBYR) -- No default !IBYR= 1999 !
 Month (IBMO) -- No default !IBMO= 8 !
 Day (IBDY) -- No default !IBDY= 17 !
 Hour (IBHR) -- No default !IBHR= 3 !

Base time zone (IBTZ) -- No default !IBTZ= -2 !
 PST = 08, MST = 07
 CST = 06, EST = 05

Length of run (hours) (IRLG) -- No default !IRLG= 82 !

Run type (IRTYPE) -- Default: 1 !IRTYPE= 1 !

0 = Computes wind fields only
 1 = Computes wind fields and micrometeorological variables
 (u*, w*, L, zi, etc.)
 (IRTYPE must be 1 to run CALPUFF or CALGRID)

Compute special data fields required
 by CALGRID (i.e., 3-D fields of W wind
 components and temperature)
 in addition to regular Default: T !LCALGRD = T !
 fields ? (LCALGRD)
 (LCALGRD must be T to run CALGRID)

Flag to stop run after
 SETUP phase (ITEST) Default: 2 !ITEST= 2 !
 (Used to allow checking
 of the model inputs, files, etc.)
 ITEST = 1 - STOPS program after SETUP phase
 ITEST = 2 - Continues with execution of
 COMPUTATIONAL phase after SETUP

!END!

INPUT GROUP: 2 -- Grid control parameters

HORIZONTAL GRID DEFINITION:

No. X grid cells (NX) No default !NX = 33 !
 No. Y grid cells (NY) No default !NY = 26 !

GRID SPACING (DGRIDKM) No default !DGRIDKM = 1. !
 Units: km

REFERENCE COORDINATES
of SOUTHWEST corner of grid cell (1,1)

X coordinate (XORIGKM) No default !XORIGKM = 721.000 !
 Y coordinate (YORIGKM) No default !YORIGKM = 4502.000 !
 Units: km

Latitude (XLAT0) No default !XLAT0 = 40.370 !
 Longitude (XLON0) No default !XLON0 = -29.380 !

UTM ZONE (IUTMZN) Default: 0 !IUTMZN = 35 !

LAMBERT CONFORMAL PARAMETERS

Rotate input winds from true north to
 map north using a Lambert conformal
 projection? (LLCONF) Default: F !LLCONF = F !

Latitude of 1st standard parallel Default: 30. !XLAT1 = 30.000 !
 Latitude of 2nd standard parallel Default: 60. !XLAT2 = 60.000 !

(XLAT1 and XLAT2; + in NH, - in SH)

Longitude (RLON0) Default = 90. ! RLON0 = 90.000 !
 (used only if LLCONF = T)
 (Positive = W. Hemisphere;
 Negative = E. Hemisphere)
 Origin Latitude (RLAT0) Default = 40. ! RLAT0 = 40.000 !
 (used only if IPROG > 2)
 (Positive = N. Hemisphere;
 Negative = S. Hemisphere)

Vertical grid definition:

No. of vertical layers (NZ) No default ! NZ = 10 !
 Cell face heights in arbitrary
 vertical grid (ZFACE(NZ+1)) No defaults
 Units: m
 ! ZFACE = 0.,20.,40.,80.,160.,300.,600.,1000.,1500.,2200.,2800. !

!END!

INPUT GROUP: 3 -- Output Options

DISK OUTPUT OPTION

Save met. fields in an unformatted
 output file ? (LSAVE) Default: T ! LSAVE = T !
 (F = Do not save, T = Save)

Type of unformatted output file:
 (IFORMO) Default: 1 ! IFORMO = 1 !

1 = CALPUFF/CALGRID type file (CALMET.DAT)
 2 = MESOPUFF-II type file (PACOUT.DAT)

LINE PRINTER OUTPUT OPTIONS:

Print met. fields ? (LPRINT) Default: F ! LPRINT = F !
 (F = Do not print, T = Print)
 (NOTE: parameters below control which
 met. variables are printed)

Print interval
 (IPRINF) in hours Default: 1 ! IPRINF = 1 !
 (Meteorological fields are printed
 every 1 hours)

Specify which layers of U, V wind component
 to print (IUVOU(NZ)) -- NOTE: NZ values must be entered
 (0=Do not print, 1=Print)
 (used only if LPRINT=T) Defaults: NZ*0
 ! IUVOU = 0, 0, 0, 0, 0, 0, 0, 0, 0, 0 !

Specify which levels of the W wind component to print
 (NOTE: W defined at TOP cell face -- 10 values)
 (IWOUT(NZ)) -- NOTE: NZ values must be entered
 (0=Do not print, 1=Print)
 (used only if LPRINT=T & LCALGRD=T)

Defaults: NZ*0
 ! IWOUT = 0, 0, 0, 0, 0, 0, 0, 0, 0, 0 !

Specify which levels of the 3-D temperature field to print
 (ITOUT(NZ)) -- NOTE: NZ values must be entered
 (0=Do not print, 1=Print)
 (used only if LPRINT=T & LCALGRD=T)

Defaults: NZ*0
 ! ITOUT = 0, 0, 0, 0, 0, 0, 0, 0, 0, 0 !

Specify which meteorological fields
to print
(used only if LPRINT=T) Defaults: 0 (all variables)

Variable	Print ?	
(0 = do not print, 1 = print)		
! STABILITY =	0	! - PGT stability class
! USTAR =	0	! - Friction velocity
! MONIN =	0	! - Monin-Obukhov length
! MIXHT =	0	! - Mixing height
! WSTAR =	0	! - Convective velocity scale
! PRECIP =	0	! - Precipitation rate
! SENSHEAT =	0	! - Sensible heat flux
! CONVZI =	0	! - Convective mixing ht.

Testing and debug print options for micrometeorological module

Print input meteorological data and
internal variables (LDB) Default: F ! LDB = F !
(F = Do not print, T = print)
(NOTE: this option produces large amounts of output)

First time step for which debug data
are printed (NN1) Default: 1 ! NN1 = 1 !

Last time step for which debug data
are printed (NN2) Default: 1 ! NN2 = 2 !

Testing and debug print options for wind field module
(all of the following print options control output to
wind field module's output files: TEST.PRT, TEST.OUT,
TEST.KIN, TEST.FRD, and TEST.SLP)

Control variable for writing the test/debug
wind fields to disk files (IOUTD)
(0=Do not write, 1=write) Default: 0 ! IOUTD = 0 !

Number of levels, starting at the surface,
to print (NZPRN2) Default: 1 ! NZPRN2 = 1 !

Print the INTERPOLATED wind components ?
(IPR0) (0=no, 1=yes) Default: 0 ! IPR0 = 0 !

Print the TERRAIN ADJUSTED surface wind
components ?
(IPR1) (0=no, 1=yes) Default: 0 ! IPR1 = 0 !

Print the SMOOTHED wind components and
the INITIAL DIVERGENCE fields ?
(IPR2) (0=no, 1=yes) Default: 0 ! IPR2 = 0 !

Print the FINAL wind speed and direction
fields ?
(IPR3) (0=no, 1=yes) Default: 0 ! IPR3 = 0 !

Print the FINAL DIVERGENCE fields ?
(IPR4) (0=no, 1=yes) Default: 0 ! IPR4 = 0 !

Print the winds after KINEMATIC effects
are added ?
(IPR5) (0=no, 1=yes) Default: 0 ! IPR5 = 0 !

Print the winds after the FROUDE NUMBER
adjustment is made ?
(IPR6) (0=no, 1=yes) Default: 0 ! IPR6 = 0 !

Print the winds after SLOPE FLOWS
are added ?
(IPR7) (0=no, 1=yes) Default: 0 ! IPR7 = 0 !

Print the FINAL wind field components ?

(IPR8) (0=no, 1=yes) Default: 0 ! IPR8 = 0 !

!END!

 INPUT GROUP: 4 -- Meteorological data options

 NUMBER OF SURFACE & PRECIP. METEOROLOGICAL STATIONS

Number of surface stations (NSSTA) No default ! NSSTA = 2 !
 Number of precipitation stations
 (NPSTA) No default ! NPSTA = 0 !

FILE FORMATS

Surface meteorological data file format
 (IFORMS) Default: 2 ! IFORMS = 2 !
 (1 = unformatted (e.g., SMERGE output))
 (2 = formatted (free-formatted user input))

Precipitation data file format
 (IFORMP) Default: 2 ! IFORMP = 2 !
 (1 = unformatted (e.g., PMERGE output))
 (2 = formatted (free-formatted user input))

Cloud data file format
 (IFORMC) Default: 2 ! IFORMC = 2 !
 (1 = unformatted - CALMET unformatted output)
 (2 = formatted - free-formatted CALMET output or user input)

!END!

 INPUT GROUP: 5 -- Wind Field Options and Parameters

 WIND FIELD MODEL OPTIONS

Model selection variable (IWFCOD) Default: 1 ! IWFCOD = 1 !
 0 = Objective analysis only
 1 = Diagnostic wind module

Compute Froude number adjustment
 effects ? (IFRADJ) Default: 1 ! IFRADJ = 1 !
 (0 = NO, 1 = YES)

Compute kinematic effects ? (IKINE) Default: 0 ! IKINE = 0 !
 (0 = NO, 1 = YES)

Use O'Brien procedure for adjustment
 of the vertical velocity ? (IOBR) Default: 0 ! IOBR = 0 !
 (0 = NO, 1 = YES)

Compute slope flow effects ? (ISLOPE) Default: 1 ! ISLOPE = 1 !
 (0 = NO, 1 = YES)

Extrapolate surface wind observations
 to upper layers ? (IEXTRP) Default: -4 ! IEXTRP = -1 !
 (1 = no extrapolation is done,
 2 = power law extrapolation used,
 3 = user input multiplicative factors
 for layers 2 - NZ used (see FEXTRP array)
 4 = similarity theory used
 -1, -2, -3, -4 = same as above except layer 1 data
 at upper air stations are ignored

Extrapolate surface winds even
 if calm? (ICALM) Default: 0 ! ICALM = 0 !
 (0 = NO, 1 = YES)

Layer-dependent biases modifying the weights of
 surface and upper air stations (BIAS(NZ))
 -1 <= BIAS <= 1
 Negative BIAS reduces the weight of upper air stations
 (e.g. BIAS=-0.1 reduces the weight of upper air stations

by 10%; BIAS=-1, reduces their weight by 100 %)
 Positive BIAS reduces the weight of surface stations
 (e.g. BIAS= 0.2 reduces the weight of surface stations
 by 20%; BIAS=1 reduces their weight by 100%)
 Zero BIAS leaves weights unchanged (1/R**2 interpolation)
 Default: NZ*0

! BIAS = 0, 0, 0, 0, 0, 0, 0, 0, 0, 0, 0 !

Minimum distance from nearest upper air station
 to surface station for which extrapolation
 of surface winds at surface station will be allowed
 (RMIN2: Set to -1 for IEXTRP = 4 or other situations
 where all surface stations should be extrapolated)

Default: 4. ! RMIN2 = 4.0 !

Use gridded prognostic wind field model
 output fields as input to the diagnostic
 wind field model (IPROG) Default: 0 ! IPROG = 0 !
 (0 = No, [IWFCOD = 0 or 1])

- 1 = Yes, use CSUMM prog. winds as Step 1 field, [IWFCOD = 0]
- 2 = Yes, use CSUMM prog. winds as initial guess field [IWFCOD = 1]
- 3 = Yes, use winds from MM4.DAT file as Step 1 field [IWFCOD = 0]
- 4 = Yes, use winds from MM4.DAT file as initial guess field [IWFCOD = 1]
- 5 = Yes, use winds from MM4.DAT file as observations [IWFCOD = 1]
- 13 = Yes, use winds from MM5.DAT file as Step 1 field [IWFCOD = 0]
- 14 = Yes, use winds from MM5.DAT file as initial guess field [IWFCOD = 1]
- 15 = Yes, use winds from MM5.DAT file as observations [IWFCOD = 1]

RADIUS OF INFLUENCE PARAMETERS

Use varying radius of influence Default: F ! LVARY = F!
 (if no stations are found within RMAX1,RMAX2,
 or RMAX3, then the closest station will be used)

Maximum radius of influence over land
 in the surface layer (RMAX1) No default ! RMAX1 = 17. !
 Units: km

Maximum radius of influence over land
 aloft (RMAX2) No default ! RMAX2 = 17. !
 Units: km

Maximum radius of influence over water
 (RMAX3) No default ! RMAX3 = 17. !
 Units: km

OTHER WIND FIELD INPUT PARAMETERS

Minimum radius of influence used in
 the wind field interpolation (RMIN) Default: 0.1 ! RMIN = 0.1 !
 Units: km

Radius of influence of terrain
 features (TERRAD) No default ! TERRAD = 12. !
 Units: km

Relative weighting of the first
 guess field and observations in the
 SURFACE layer (R1) No default ! R1 = 1. !
 (R1 is the distance from an Units: km
 observational station at which the
 observation and first guess field are
 equally weighted)

Relative weighting of the first
 guess field and observations in the
 layers ALOFT (R2) No default ! R2 = 1. !
 (R2 is applied in the upper layers Units: km
 in the same manner as R1 is used in
 the surface layer).

Relative weighting parameter of the
 prognostic wind field data (RPROG) No default ! RPROG = 0. !
 (Used only if IPROG = 1) Units: km

Maximum acceptable divergence in the
 divergence minimization procedure
 (DIVLIM) Default: 5.E-6 ! DIVLIM= 5.0E-06 !

Maximum number of iterations in the
divergence min. procedure (NITER) Default: 50 ! NITER = 50 !

Number of passes in the smoothing
procedure (NSMTH(NZ))
NOTE: NZ values must be entered
Default: 2,(mxnz-1)*4 ! NSMTH =

2 . 4 . 4 . 4 . 4 . 4 . 4 . 4 . 4 . 4 !

Maximum number of stations used in
each layer for the interpolation of
data to a grid point (NINTR2(NZ))
NOTE: NZ values must be entered Default: 99. ! NINTR2 =

2 , 2 , 2 , 2 , 2 , 2 , 2 , 2 , 2 , 2 !

Critical Froude number (CRITFN) Default: 1.0 ! CRITFN = 1. !

Empirical factor controlling the
influence of kinematic effects
(ALPHA) Default: 0.1 ! ALPHA = 0.1 !

Multiplicative scaling factor for
extrapolation of surface observations
to upper layers (FEXTR2(NZ)) Default: NZ*0.0
! FEXTR2 = 0., 0., 0., 0., 0., 0., 0., 0., 0. !
(Used only if IEXTRP = 3 or -3)

DIAGNOSTIC MODULE DATA INPUT OPTIONS

Surface temperature (IDIOPT1) Default: 0 ! IDIOPT1 = 0 !
0 = Compute internally from
hourly surface observations
1 = Read preprocessed values from
a data file (DIAG.DAT)

Surface met. station to use for
the surface temperature (ISURFT) No default ! ISURFT = 1 !
(Must be a value from 1 to NSSTA)
(Used only if IDIOPT1 = 0)

Domain-averaged temperature lapse
rate (IDIOPT2) Default: 0 ! IDIOPT2 = 0 !
0 = Compute internally from
twice-daily upper air observations
1 = Read hourly preprocessed values
from a data file (DIAG.DAT)

Upper air station to use for
the domain-scale lapse rate (IUPT) No default ! IUPT = 1 !
(Must be a value from 1 to NUSTA)
(Used only if IDIOPT2 = 0)

Depth through which the domain-scale
lapse rate is computed (ZUPT) Default: 200. ! ZUPT = 200. !
(Used only if IDIOPT2 = 0) Units: meters

Domain-averaged wind components
(IDIOPT3) Default: 0 ! IDIOPT3 = 0 !
0 = Compute internally from
twice-daily upper air observations
1 = Read hourly preprocessed values
a data file (DIAG.DAT)

Upper air station to use for
the domain-scale winds (IUPWND) Default: -1 ! IUPWND = -1 !
(Must be a value from -1 to NUSTA)
(Used only if IDIOPT3 = 0)

Bottom and top of layer through
which the domain-scale winds

are computed
 (ZUPWND(1), ZUPWND(2)) Defaults: 1., 1000. ! ZUPWND= 1., 1000. !
 (Used only if IDIOPT3 = 0) Units: meters

Observed surface wind components
 for wind field module (IDIOPT4) Default: 0 ! IDIOPT4 = 0 !
 0 = Read WS, WD from a surface
 data file (SURF.DAT)
 1 = Read hourly preprocessed U, V from
 a data file (DIAG.DAT)

Observed upper air wind components
 for wind field module (IDIOPT5) Default: 0 ! IDIOPT5 = 0 !
 0 = Read WS, WD from an upper
 air data file (UPI.DAT, UP2.DAT, etc.)
 1 = Read hourly preprocessed U, V from
 a data file (DIAG.DAT)

 INPUT GROUP: 6 -- Mixing Height, Temperature and Precipitation Parameters

 EMPIRICAL MIXING HEIGHT CONSTANTS

Neutral, mechanical equation
 (CONSTB) Default: 1.41 ! CONSTB = 1.41 !
 Convective mixing ht. equation
 (CONSTE) Default: 0.15 ! CONSTE = 0.15 !
 Stable mixing ht. equation
 (CONSTN) Default: 2400. ! CONSTN = 2400. !
 Overwater mixing ht. equation
 (CONSTW) Default: 0.16 ! CONSTW = 0.16 !
 Absolute value of Coriolis
 parameter (FCORIO) Default: 1.E-4 ! FCORIO = 1.0E-04!
 Units: (1/s)

SPATIAL AVERAGING OF MIXING HEIGHTS

Conduct spatial averaging
 (IAVEZI) (0=no, 1=yes) Default: 1 ! IAVEZI = 1 !
 Max. search radius in averaging
 process (MNMDAV) Default: 1 ! MNMDAV = 10 !
 Units: Grid
 cells
 Half-angle of upwind looking cone
 for averaging (HAFANG) Default: 30. ! HAFANG = 30. !
 Units: deg.
 Layer of winds used in upwind
 averaging (ILEVZI) Default: 1 ! ILEVZI = 1 !
 (must be between 1 and NZ)

OTHER MIXING HEIGHT VARIABLES

Minimum potential temperature lapse
 rate in the stable layer above the
 current convective mixing ht. Default: 0.001 ! DPTMIN = 0.001 !
 (DPTMIN) Units: deg. K/m
 Depth of layer above current conv.
 mixing height through which lapse Default: 200. ! DZZI = 200. !
 rate is computed (DZZI) Units: meters
 Minimum overland mixing height Default: 50. ! ZIMIN = 50. !
 (ZIMIN) Units: meters
 Maximum overland mixing height Default: 3000. ! ZIMAX = 2600. !
 (ZIMAX) Units: meters
 Minimum overwater mixing height Default: 50. ! ZIMINW = 50. !
 (ZIMINW) -- (Not used if observed Units: meters
 overwater mixing hts. are used)
 Maximum overwater mixing height Default: 3000. ! ZIMAXW = 2600. !
 (ZIMAXW) -- (Not used if observed Units: meters
 overwater mixing hts. are used)

TEMPERATURE PARAMETERS

Interpolation type
 (1 = 1/R ; 2 = 1/R**2) Default: 1 ! IRAD = 1 !

Radius of influence for temperature
 interpolation (TRADKM) Default: 500. ! TRADKM = 20. !
 Units: km

Maximum Number of stations to include
 in temperature interpolation (NUMTS) Default: 5 ! NUMTS = 2 !

Conduct spatial averaging of temp-
 eratures (IAVET) (0=no, 1=yes) Default: 1 ! IAVET = 1 !
 (will use mixing ht MNMDAV,HAFANG
 so make sure they are correct)

Default temperature gradient Default: -.0098 ! TGDEFB = -0.0098 !
 below the mixing height over
 water (K/m) (TGDEFB)

Default temperature gradient Default: -.0045 ! TGDEFA = -0.0045 !
 above the mixing height over
 water (K/m) (TGDEFA)

Beginning (JWAT1) and ending (JWAT2)
 land use categories for temperature
 interpolation over water -- Make ! JWAT1 = 55 !
 bigger than largest land use to disable ! JWAT2 = 55 !

 INPUT GROUP: 7 -- Surface meteorological station parameters

SURFACE STATION VARIABLES
 (One record per station -- 2 records in all)

Name	ID	X coord. (km)	Y coord. (km)	Time zone	Anem. Ht.(m)
! SS1 = 'KOCA'	17066	742.000	4528.000	-2	10 !
! SS2 = 'GOZT'	17062	680.000	4538.000	-2	10 !

1
 Four character string for station name
 (MUST START IN COLUMN 9)

2
 Five digit integer for station ID

!END!

 INPUT GROUP: 8 -- Upper air meteorological station parameters

UPPER AIR STATION VARIABLES
 (One record per station -- 1 records in all)

Name	ID	X coord. (km)	Y coord. (km)	Time zone
! US1 = 'GOZT'	17062	680.000	4538.000	-2 !

1
 Four character string for station name
 (MUST START IN COLUMN 9)

2
 Five digit integer for station ID

!END!

CALMET Control File Input Groups

<u>Input Group</u>	<u>Description</u>
*	Run Title First three lines of control file (up to 80 characters/line)
0	Input and Output File Names
1	General Run Control Parameters Starting date and hour, run length, base time zone, and run type options
2	Grid Control Parameters Grid spacing, number of cells, vertical layer structure, and reference coordinates
3	Output Options Printer control variables, and disk output control variables
4	Meteorological Data Options Number of surface, upper air, over water, and precipitation stations, input file formats, and precipitation options
5	Wind Field Options and Parameters Model option flags, radius of influence parameters, weighting factors, barrier data, diagnostic module input flags, and lake breeze information
6	Mixing Height, Temperature, and Precipitation Parameters Empirical constants for the mixing height scheme, spatial averaging parameters, minimum/maximum overland and overwater mixing heights, temperature options, and precipitation interpolation options
7	Surface Meteorological Station Parameters Station name, coordinates, time zone, and anemometer height
8	Upper Air Station Parameters Station name, coordinates, and time zone
9	Precipitation Station Parameters Station name, station code, and coordinates

CALMET Input and Output Files

<u>Unit</u>	<u>Default File Name</u>	<u>Type</u>	<u>Format</u>	<u>Description</u>
IO2	DIAG.DAT	input	formatted	File containing preprocessed meteorological data for diagnostic wind field module. (Used only if IDIOPT1, IDIOPT2, IDIOPT3, IDIOPT4, or IDIOPT5 = 1.)
IO5	CALMET.INP	input	formatted	Control file containing user inputs.
IO6	CALMET.LST	output	formatted	List file (line printer output file) created by CALMET.
IO7	CALMET.DAT or PACOUT.DAT	output	unformatted	Output data file created by CALMET containing hourly gridded fields of meteorological data. (Created only if LSAVE=T.)
IO8	GEO.DAT	input	formatted	Geophysical data fields (land use, elevation, surface characteristics, anthropogenic heat fluxes).
IO10	SURF.DAT	input	unformatted (if IFORMS=1) or formatted (if IFORMS=2)	Hourly surface observations (Used only if IDIOPT4=0.) If IFORMS=1, use the unformatted output file of the SMERGE program. If IFORMS=2, use a free-formatted input file generated either by SMERGE or the user.
IO12	PRECIP.DAT	input	unformatted (if IFORMP=1) or formatted (if IFORMP=2)	Hourly precipitation data (used if NPSTA > 0). If IFORMP=1, PRECIP.DAT is the unformatted output file of the PMERGE program. If IFORMP=2, PRECIP.DAT is a free-formatted input file generated either by PMERGE or the user.
IO14	WT.DAT	input	formatted	Gridded fields of terrain weighting factors used to weight the observed winds and the MM4 winds in the interpolation process

(CALMET Input and Output Files Continued)

CALMET Input and Output Files

<u>Unit</u>	<u>Default File Name</u>	<u>Type</u>	<u>Format</u>	<u>Description</u>
IO30	UP1.DAT	input	formatted	Upper air data (READ56/READ62 output) for upper air station #n. (Used only if IDIOPT5=0.)
IO30+1	UP2.DAT			
IO30+2	UP3.DAT			
.	.			
.	.			
.	UPn.DAT			

(Up to "MAXUS" upper air stations allowed. MAXUS currently = 50).


IO80	SEA1.DAT	input	formatted	Overwater meteorological data for station #n. (Used only if NOWSTA > 0).
IO80+1	SEA2.DAT			
IO80+2	SEA3.DAT			
.	.			
.	.			
.	SEAn.DAT			

(Up to "MXOWS" overwater stations allowed. MXOWS currently = 15).

IO20	PROG.DAT (CSUMM)	input	unformatted	Gridded fields of prognostic wind data to use as input to the diagnostic wind field module. (Used only if IPROG > 0.)
	or			
IO20	MM4.DAT (MM4/MM5)	input	formatted	

Wind Field Module Test and Debug Files

IO21	TEST.PRT	output	unformatted	Intermediate winds and misc. input and internal variables. (Created only if at least one wind field print option activated (IPR0-IPR8).)
IO22	TEST.OUT	output	formatted	Final wind fields. (Created only if IPR8=1 and IOUTD=1.)
IO23	TEST.KIN	output	formatted	Wind fields after kinematic effects. (Created only if IPR5=1 and IOUTD=1.)
IO24	TEST.FRD	output	formatted	Wind fields after Froude No. effects. (Created only if IPR6=1 and IOUTD=1.)
IO25	TEST.SLP	output	formatted	Wind fields after slope flow effects. (Created only if IPR7=1 and IOUTD=1.)



APPENDIX III
CALPUFF MODEL CONTROL FILE

CALPUFF MODEL CONTROL FILE

INPUT GROUP: 0 -- Input and Output File Names

```

-----
Default Name Type      File Name
-----
CALMET.DAT  input  ! METDAT =C:\CALPUFF\DEMOMODELS\CALPUFF\BIRNUR.DAT !
or
ISCMET.DAT  input  * ISCDAT =      *
or
PLMMET.DAT  input  * PLMDAT =      *
or
PROFILE.DAT input  * PRFDAT =      *
SURFACE.DAT input  * SFCDAT =      *
RESTARTB.DAT input  * RSTARTB=      *
-----
CALPUFF.LST output ! PUFLST=C:\CALPUFF\DEMOMODELS\CALPUFF\BIRNUR.LST !
CONC.DAT    output ! CONDAT =C:\CALPUFF\DEMOMODELS\CALPUFF\BIRNUR.CON !
DFLX.DAT    output ! DFDAT =C:\CALPUFF\DEMOMODELS\CALPUFF\BIRNUR.DRY !
WFLX.DAT    output * WFDAT =      *
-----
VISB.DAT    output ! VISDAT =C:\CALPUFF\DEMOMODELS\CALPUFF\BIRNUR.VIS !
RESTARTE.DAT output * RSTARTE=      *
-----

```

Emission Files

```

-----
PTEMARB.DAT input  * PTDAT =      *
VOLEMARB.DAT input  * VOLDAT =      *
BAEMARB.DAT input  * ARDAT =      *
LNEMARB.DAT input  * LNDAT =      *
-----

```

Other Files

```

-----
OZONE.DAT  input  * OZDAT =      *
VD.DAT     input  * VDDAT =      *
CHEM.DAT   input  * CHEMDAT=      *
HILL.DAT   input  * HILDAT=      *
HILLRCT.DAT input  * RCTDAT=      *
COASTLN.DAT input  * CSTDAT=      *
FLUXBDY.DAT input  * BDYDAT=      *
BCON.DAT   input  * BCNDAT=      *
DEBUG.DAT  output  * DEBUG=      *
MASSFLX.DAT output  * FLXDAT=      *
MASSBAL.DAT output  * BALDAT=      *
FOG.DAT    output  * FOGDAT=      *
-----

```

All file names will be converted to lower case if LCFILES = T
 Otherwise, if LCFILES = F, file names will be converted to UPPER CASE
 T = lower case ! LCFILES = F !
 F = UPPER CASE

NOTE: (1) file/path names can be up to 70 characters in length
 Provision for multiple input files

```

-----
Number of CALMET.DAT files for run (NMETDAT)
Default: 1 ! NMETDAT = 1 !

```

```

Number of PTEMARB.DAT files for run (NPTDAT)
Default: 0 ! NPTDAT = 0 !

```

```

Number of BAEMARB.DAT files for run (NARDAT)
Default: 0 ! NARDAT = 0 !

```

```

Number of VOLEMARB.DAT files for run (NVOLDAT)
Default: 0 ! NVOLDAT = 0 !

```

!END!

Subgroup (0a)

The following CALMET.DAT filenames are processed in sequence if NMETDAT>1

```

-----
Default Name Type      File Name
-----

```

 none input * METDAT= * *END*

INPUT GROUP: 1 -- General run control parameters

Option to run all periods found
 in the met. file (METRUN) Default: 0 ! METRUN = 0 !

METRUN = 0 - Run period explicitly defined below
 METRUN = 1 - Run all periods in met. file

Starting date: Year (IBYR) -- No default ! IBYR = 1999 !
 (used only if Month (IBMO) -- No default ! IBMO = 8 !
 METRUN = 0) Day (IBDY) -- No default ! IDBY = 17 !
 Hour (IBHR) -- No default ! IBHR = 3 !

Length of run (hours) (IRLG) -- No default ! IRLG = 82 !

Number of chemical species (NSPEC)
 Default: 5 ! NSPEC = 1 !

Number of chemical species
 to be emitted (NSE) Default: 3 ! NSE = 1 !

Flag to stop run after
 SETUP phase (ITEST) Default: 2 ! ITEST = 2 !
 (Used to allow checking
 of the model inputs, files, etc.)
 ITEST = 1 - STOPS program after SETUP phase
 ITEST = 2 - Continues with execution of program
 after SETUP

Restart Configuration:

Control flag (MRESTART) Default: 0 ! MRESTART = 0 !

0 = Do not read or write a restart file
 1 = Read a restart file at the beginning of
 the run
 2 = Write a restart file during run
 3 = Read a restart file at beginning of run
 and write a restart file during run

Number of periods in Restart
 output cycle (NRESPD) Default: 0 ! NRESPD = 0 !

0 = File written only at last period
 >0 = File updated every NRESPD periods

Meteorological Data Format (METFM)
 Default: 1 ! METFM = 1 !

METFM = 1 - CALMET binary file (CALMET.MET)
 METFM = 2 - ISC ASCII file (ISCMET.MET)
 METFM = 3 - AUSPLUME ASCII file (PLMMET.MET)
 METFM = 4 - CTDM plus tower file (PROFILE.DAT) and
 surface parameters file (SURFACE.DAT)

PG sigma-y is adjusted by the factor (AVET/PGTIME)**0.2
 Averaging Time (minutes) (AVET)
 Default: 60.0 ! AVET = 60. !
 PG Averaging Time (minutes) (PGTIME)
 Default: 60.0 ! PGTIME = 60. !

!END!

 INPUT GROUP: 2 -- Technical options

Vertical distribution used in the
 near field (MGAUSS) Default: 1 ! MGAUSS = 1 !
 0 = uniform
 1 = Gaussian

Terrain adjustment method
 (MCTADJ) Default: 3 ! MCTADJ = 3 !

0 = no adjustment
 1 = ISC-type of terrain adjustment
 2 = simple, CALPUFF-type of terrain adjustment
 3 = partial plume path adjustment

Subgrid-scale complex terrain flag (MCTSG) Default: 0 ! MCTSG = 0 !
 0 = not modeled
 1 = modeled

Near-field puffs modeled as elongated 0 (MSLUG) Default: 0 ! MSLUG = 0 !
 0 = no
 1 = yes (slug model used)

Transitional plume rise modeled ? (MTRANS) Default: 1 ! MTRANS = 1 !
 0 = no (i.e., final rise only)
 1 = yes (i.e., transitional rise computed)

Stack tip downwash? (MTIP) Default: 1 ! MTIP = 1 !
 0 = no (i.e., no stack tip downwash)
 1 = yes (i.e., use stack tip downwash)

Vertical wind shear modeled above stack top? (MSHEAR) Default: 0 ! MSHEAR = 0 !
 0 = no (i.e., vertical wind shear not modeled)
 1 = yes (i.e., vertical wind shear modeled)

Puff splitting allowed? (MSPLIT) Default: 0 ! MSPLIT = 0 !
 0 = no (i.e., puffs not split)
 1 = yes (i.e., puffs are split)

Chemical mechanism flag (MCHEM) Default: 1 ! MCHEM = 0 !
 0 = chemical transformation not modeled
 1 = transformation rates computed internally (MESOPUFF II scheme)
 2 = user-specified transformation rates used
 3 = transformation rates computed internally (RIVAD/ARM3 scheme)
 4 = secondary organic aerosol formation computed (MESOPUFF II scheme for OH)

Wet removal modeled ? (MWET) Default: 1 ! MWET = 0 !
 0 = no
 1 = yes

Dry deposition modeled ? (MDRY) Default: 1 ! MDRY = 1 !
 0 = no
 1 = yes
 (dry deposition method specified for each species in Input Group 3)

Method used to compute dispersion coefficients (MDISP) Default: 3 ! MDISP = 3 !
 1 = dispersion coefficients computed from measured values of turbulence, σ_v , σ_w
 2 = dispersion coefficients from internally calculated σ_v , σ_w using micrometeorological variables (u^* , w^* , L , etc.)
 3 = PG dispersion coefficients for RURAL areas (computed using the ISCST multi-segment approximation) and MP coefficients in urban areas
 4 = same as 3 except PG coefficients computed using the MESOPUFF II eqns.
 5 = CTDM sigmas used for stable and neutral conditions. For unstable conditions, sigmas are computed as in MDISP = 3, described above. MDISP = 5 assumes that measured values are read

Sigma-v/sigma-theta, sigma-w measurements used? (MTURBVW)
(Used only if MDISP = 1 or 5) Default: 3 ! MTURBVW = 3 !

- 1 = use sigma-v or sigma-theta measurements
from PROFILE.DAT to compute sigma-y
(valid for METFM = 1, 2, 3, 4)
- 2 = use sigma-w measurements
from PROFILE.DAT to compute sigma-z
(valid for METFM = 1, 2, 3, 4)
- 3 = use both sigma-(v/theta) and sigma-w
from PROFILE.DAT to compute sigma-y and sigma-z
(valid for METFM = 1, 2, 3, 4)
- 4 = use sigma-theta measurements
from PLMMET.DAT to compute sigma-y
(valid only if METFM = 3)

Back-up method used to compute dispersion
when measured turbulence data are
missing (MDISP2) Default: 3 ! MDISP2 = 3 !
(used only if MDISP = 1 or 5)

- 2 = dispersion coefficients from internally calculated
sigma v, sigma w using micrometeorological variables
(u*, w*, L, etc.)
- 3 = PG dispersion coefficients for RURAL areas (computed using
the ISCST multi-segment approximation) and MP coefficients in
urban areas
- 4 = same as 3 except PG coefficients computed using
the MESOPUFF II eqns.

PG sigma-y,z adj. for roughness? Default: 0 ! MROUGH = 0 !
(MROUGH)

- 0 = no
- 1 = yes

Partial plume penetration of elevated inversion? Default: 1 ! MPARTL = 1 !
(MPARTL)

- 0 = no
- 1 = yes

Strength of temperature inversion provided in PROFILE.DAT extended records? Default: 0 ! MTINV = 0 !
(MTINV)

- 0 = no (computed from measured/default gradients)
- 1 = yes

PDF used for dispersion under convective conditions? Default: 0 ! MPDF = 0 !
(MPDF)

- 0 = no
- 1 = yes

Sub-Grid TIBL module used for shore line? Default: 0 ! MSGTIBL = 0 !
(MSGTIBL)

- 0 = no
- 1 = yes

Boundary conditions (concentration) modeled? Default: 0 ! MBCON = 0 !
(MBCON)

- 0 = no
- 1 = yes

Analyses of fogging and icing impacts due to emissions from arrays of mechanically-forced cooling towers can be performed using CALPUFF in conjunction with a cooling tower emissions processor (CTEMISS) and its associated postprocessors. Hourly emissions of water vapor and temperature from each cooling tower cell are computed for the current cell configuration and ambient conditions by CTEMISS. CALPUFF models the dispersion of these emissions and provides cloud information in a specialized format for further analysis. Output to FOG.DAT is provided in either 'plume mode' or 'receptor mode' format.

Configure for FOG Model output? Default: 0 ! MFQG = 0 !

(MFOG)
 0 = no
 1 = yes - report results in PLUME Mode format
 2 = yes - report results in RECEPTOR Mode format
 Test options specified to see if
 they conform to regulatory
 values? (MREG) Default: 1 ! MREG = 0 !

0 = NO checks are made
 1 = Technical options must conform to USEPA values
 METFM 1
 AVET 60. (min)
 MGAUSS 1
 MCTADJ 3
 MTRANS 1
 MTIP 1
 MCHEM 1 (if modeling SOx, NOx)
 MWET 1
 MDRY 1
 MDISP 3
 MRQUGH 0
 MPARTL 1
 SYTDEP 550. (m)
 MHFTSZ 0

!END!

 INPUT GROUP: 3a, 3b -- Species list

 Subgroup (3a)

The following species are modeled:

! CSPEC = SO2 ! !END!

SPECIES NAME (Limit: 12 Characters in length)	MODELED (0=NO, 1=YES)	Dry		OUTPUT GROUP DEPOSITED (0=NO, 1=1st CGRUP, 2=2nd CGRUP, 3=etc.)	NUMBER (0=NONE, 1=1st CGRUP, 2=2nd CGRUP, 3=etc.)
		EMITTED (0=NO, 1=YES)	DEPOSITED (0=NO, 1=YES)		

! SO2 =	1,	1,	1,	0 !
---------	----	----	----	-----

!END!

 Subgroup (3b)

The following names are used for Species-Groups in which results
 for certain species are combined (added) prior to output. The
 CGRUP name will be used as the species name in output files.
 Use this feature to model specific particle-size distributions
 by treating each size-range as a separate species.
 Order must be consistent with 3(a) above.

 INPUT GROUP: 4 -- Grid control parameters

METEOROLOGICAL grid:

No. X grid cells (NX) No default ! NX = 33 !
 No. Y grid cells (NY) No default ! NY = 26 !
 No. vertical layers (NZ) No default ! NZ = 10 !

Grid spacing (DGRIDKM) No default ! DGRIDKM = 1. !
 Units: km

Cell face heights
 (ZFACE(nz+1)) No defaults
 Units: m

! ZFACE = 0., 20., 40., 80., 160., 300., 600., 1000., 1500., 2200.,
 2800. !

Reference Coordinates
 of SOUTHWEST corner of

grid cell(1, 1):

X coordinate (XORIGKM) No default ! XORIGKM = 721. !
 Y coordinate (YORIGKM) No default ! YORIGKM = 4502. !
 Units: km

UTM zone (IUTMZN) No default ! IUTMZN = 35 !

Reference coordinates of CENTER
 of the domain (used in the
 calculation of solar elevation
 angles)

Latitude (deg.) (XLAT) No default ! XLAT = 40.45 !
 Longitude (deg.) (XLONG) No default ! XLONG = -29.49 !
 Time zone (XTZ) No default ! XTZ = -2.0 !
 (PST=8, MST=7, CST=6, EST=5)

Computational grid:

The computational grid is identical to or a subset of the MET. grid.
 The lower left (LL) corner of the computational grid is at grid point
 (IBCOMP, JBCOMP) of the MET. grid. The upper right (UR) corner of the
 computational grid is at grid point (IECOMP, JECOMP) of the MET. grid.
 The grid spacing of the computational grid is the same as the MET. grid.

X index of LL corner (IBCOMP) No default ! IBCOMP = 1 !
 (1 <= IBCOMP <= NX)

Y index of LL corner (JBCOMP) No default ! JBCOMP = 1 !
 (1 <= JBCOMP <= NY)

X index of UR corner (IECOMP) No default ! IECOMP = 33 !
 (1 <= IECOMP <= NX)

Y index of UR corner (JECOMP) No default ! JECOMP = 26 !
 (1 <= JECOMP <= NY)

SAMPLING GRID (GRIDDED RECEPTORS):

The lower left (LL) corner of the sampling grid is at grid point
 (IBSAMP, JBSAMP) of the MET. grid. The upper right (UR) corner of the
 sampling grid is at grid point (IESAMP, JESAMP) of the MET. grid.
 The sampling grid must be identical to or a subset of the computational
 grid. It may be a nested grid inside the computational grid.
 The grid spacing of the sampling grid is DGRIDKM/MESHDN.

Logical flag indicating if gridded
 receptors are used (LSAMP) Default: T ! LSAMP = T !
 (T=yes, F=no)

X index of LL corner (IBSAMP) No default ! IBSAMP = 10 !
 (IBCOMP <= IBSAMP <= IECOMP)

Y index of LL corner (JBSAMP) No default ! JBSAMP = 10 !
 (JBCOMP <= JBSAMP <= JECOMP)

X index of UR corner (IESAMP) No default ! IESAMP = 13 !
 (IBCOMP <= IESAMP <= IECOMP)

Y index of UR corner (JESAMP) No default ! JESAMP = 13 !
 (JBCOMP <= JESAMP <= JECOMP)

Nesting factor of the sampling
 grid (MESHDN) Default: 1 ! MESHDN = 1 !
 (MESHDN is an integer >= 1)

IEND!

 INPUT GROUP: 5 -- Output Options

FILE	DEFAULT VALUE	VALUE THIS RUN
------	---------------	----------------

```

Concentrations (ICON)      I      ! ICON = 1 !
Dry Fluxes (IDRY)         I      ! IDRY = 1 !
Wet Fluxes (IWET)        I      ! IWET = 0 !
Relative Humidity (IVIS)  I      ! IVIS = 1 !
(relative humidity file is
required for visibility
analysis)
Use data compression option in output file?
(L.COMPRS)                Default: T  ! LCOMPRS = T !

```

*

0 = Do not create file, 1 = create file
DIAGNOSTIC MASS FLUX OUTPUT OPTIONS:

Mass flux across specified boundaries
for selected species reported hourly?
(IMFLX) Default: 0 ! IMFLX = 0 !
0 = no
1 = yes (FLUXBDY.DAT and MASSFLX.DAT filenames
are specified in Input Group 0)

Mass balance for each species
reported hourly?
(IMBAL) Default: 0 ! IMBAL = 0 !
0 = no
1 = yes (MASSBAL.DAT filename is
specified in Input Group 0)

LINE PRINTER OUTPUT OPTIONS:

Print concentrations (ICPRT) Default: 0 ! ICPRT = 1 !
Print dry fluxes (IDPRT) Default: 0 ! IDPRT = 0 !
Print wet fluxes (IWPRRT) Default: 0 ! IWPRRT = 0 !
(0 = Do not print, 1 = Print)

Concentration print interval
(ICFRQ) in hours Default: 1 ! ICFRQ = 1 !
Dry flux print interval
(IDFRQ) in hours Default: 1 ! IDFRQ = 1 !
Wet flux print interval
(IWFRQ) in hours Default: 1 ! IWFRQ = 1 !

Units for Line Printer Output
(IPRTU) Default: 1 ! IPRTU = 1 !
for for
Concentration Deposition
1 = g/m**3 g/m**2/s
2 = mg/m**3 mg/m**2/s
3 = ug/m**3 ug/m**2/s
4 = ng/m**3 ng/m**2/s
5 = Odour Units

Messages tracking progress of run
written to the screen ?
(IMESG) Default: 2 ! IMESG = 2 !
0 = no
1 = yes (advection step, puff ID)
2 = yes (YYYYJJHH, # old puffs, # emitted puffs)

SPECIES (or GROUP for combined species) LIST FOR OUTPUT OPTIONS

```

---- CONCENTRATIONS ---- ----- DRY FLUXES ----- ----- WET FLUXES ----- -- MASS FLUX --
SPECIES
/GROUP PRINTED? SAVED ON DISK? PRINTED? SAVED ON DISK? PRINTED? SAVED ON DISK? SAVED ON
DISK?
-----
! SO2 = 1, 1, 0, 1, 0, 0, 0 !

```

OPTIONS FOR PRINTING "DEBUG" QUANTITIES (much output)

Logical for debug output
(LDEBUG) Default: F ! LDEBUG = F !
First puff to track

(IPFDEB) Default: 1 ! IPFDEB = 1 !
 Number of puffs to track (NPFDEB) Default: 1 ! NPFDEB = 1 !
 Met. period to start output (NN1) Default: 1 ! NN1 = 1 !
 Met. period to end output (NN2) Default: 10 ! NN2 = 10 !

!END!

 INPUT GROUP: 6a, 6b, & 6c -- Subgrid scale complex terrain inputs

 Subgroup (6a)

Number of terrain features (NHILL) Default: 0 ! NHILL = 0 !

Number of special complex terrain receptors (NCTREC) Default: 0 ! NCTREC = 0 !

Terrain and CTSG Receptor data for CTSG hills input in CTDM format ? (MHILL) No Default ! MHILL = 2 !

- 1 = Hill and Receptor data created by CTDM processors & read from HILL.DAT and HILLRCT.DAT files
- 2 = Hill data created by OPTHILL & input below in Subgroup (6b); Receptor data in Subgroup (6c)

Factor to convert horizontal dimensions to meters (MHILL=1) Default: 1.0 ! XHILL2M = 1.0 !

Factor to convert vertical dimensions to meters (MHILL=1) Default: 1.0 ! ZHILL2M = 1.0 !

X-origin of CTDM system relative to CALPUFF coordinate system, in Kilometers (MHILL=1) No Default ! XCTDMKM = 0.0E00 !

Y-origin of CTDM system relative to CALPUFF coordinate system, in Kilometers (MHILL=1) No Default ! YCTDMKM = 0.0E00 !

! END !

 INPUT GROUP: 7 -- Chemical parameters for dry deposition of gases

SPECIES NAME	DIFFUSIVITY (cm**2/s)	ALPHA STAR	REACTIVITY (s/cm)	MESOPHYLL RESISTANCE (dimensionless)	HENRY'S LAW COEFFICIENT
! SO2 =	0.1509,	1000.,	8.,	0.,	0.04 !

!END!

 INPUT GROUP: 8 -- Size parameters for dry deposition of particles

For SINGLE SPECIES, the mean and standard deviation are used to compute a deposition velocity for NINT (see group 9) size-ranges, and these are then averaged to obtain a mean deposition velocity.

For GROUPED SPECIES, the size distribution should be explicitly specified (by the 'species' in the group), and the standard deviation for each should be entered as 0. The model will then use the deposition velocity for the stated mean diameter.

SPECIES NAME	GEOMETRIC MASS MEAN DIAMETER (microns)	GEOMETRIC STANDARD DEVIATION (microns)
-----	-----	-----

!END!

 INPUT GROUP: 9 -- Miscellaneous dry deposition parameters

Reference cuticle resistance (s/cm)
(RCUTR) Default: 30 ! RCUTR = 30.0 !
Reference ground resistance (s/cm)
(RGR) Default: 10 ! RGR = 10.0 !
Reference pollutant reactivity
(REACTR) Default: 8 ! REACTR = 8.0 !

Number of particle-size intervals used to
evaluate effective particle deposition velocity
(NINT) Default: 9 ! NINT = 9 !

Vegetation state in unirrigated areas
(IVEG) Default: 1 ! IVEG = 1 !
IVEG=1 for active and unstressed vegetation
IVEG=2 for active and stressed vegetation
IVEG=3 for inactive vegetation

!END!

INPUT GROUP: 10.-- Misc. Dispersion and Computational Parameters

Horizontal size of puff (m) beyond which
time-dependent dispersion equations (Heffter)
are used to determine sigma-y and
sigma-z (SYTDEP) Default: 550. ! SYTDEP = 5.5E02 !

Switch for using Heffter equation for sigma z
as above (0 = Not use Heffter; 1 = use Heffter
(MHFTSZ) Default: 0 ! MHFTSZ = 0 !

Stability class used to determine plume
growth rates for puffs above the boundary
layer (JSUP) Default: 5 ! JSUP = 5 !

Vertical dispersion constant for stable
conditions (k1 in Eqn. 2.7-3) (CONK1) Default: 0.01 ! CONK1 = .01 !

Vertical dispersion constant for neutral/
unstable conditions (k2 in Eqn. 2.7-4)
(CONK2) Default: 0.1 ! CONK2 = .1 !

Factor for determining Transition-point from
Schulman-Scire to Huber-Snyder Building Downwash
scheme (SS used for $H_s < H_b + TBD * HL$)
(TBD) Default: 0.5 ! TBD = .5 !
TBD < 0 ==> always use Huber-Snyder
TBD = 1.5 ==> always use Schulman-Scire
TBD = 0.5 ==> ISC Transition-point

Range of land use categories for which
urban dispersion is assumed
(IURB1, IURB2) Default: 10 ! IURB1 = 10 !
19 ! IURB2 = 19 !

Site characterization parameters for single-point Met data files -----
(needed for METFM = 2,3,4)

Land use category for modeling domain
(ILANDUIN) Default: 20 ! ILANDUIN = 20 !

Roughness length (m) for modeling domain
(Z0IN) Default: 0.25 ! Z0IN = .25 !

Leaf area index for modeling domain
(XLAIN) Default: 3.0 ! XLAIN = 3.0 !

Elevation above sea level (m)
(ELEVIN) Default: 0.0 ! ELEVIN = .0 !

Latitude (degrees) for met location
(XLATIN) Default: -999. ! XLATIN = -999.0 !

Longitude (degrees) for met location
(XLONIN) Default: -999. ! XLONIN = -999.0 !

Specialized information for interpreting single-point Met data files ----

Anemometer height (m) (Used only if METFM = 2,3)
(ANEMHT) Default: 10. ! ANEMHT = 10.0 !

Form of lateral turbulence data in PROFILE.DAT file
(Used only if METFM = 4 or MTURBVW = 1 or 3)
(ISIGMAV) Default: 1 ! ISIGMAV = 1 !
0 = read sigma-theta
1 = read sigma-v

Choice of mixing heights (Used only if METFM = 4)
(IMIXCTDM) Default: 0 ! IMIXCTDM = 0 !
0 = read PREDICTED mixing heights
1 = read OBSERVED mixing heights

Maximum length of a slug (met. grid units)
(XMXLEN) Default: 1.0 ! XMXLEN = 1.0 !

Maximum travel distance of a puff/slug (in
grid units) during one sampling step
(XSAMLEN) Default: 1.0 ! XSAMLEN = 1.0 !

Maximum Number of slugs/puffs release from
one source during one time step
(MXNEW) Default: 99 ! MXNEW = 99 !

Maximum Number of sampling steps for
one puff/slug during one time step
(MXSAM) Default: 99 ! MXSAM = 99 !

Number of iterations used when computing
the transport wind for a sampling step
that includes gradual rise (for CALMET
and PROFILE winds)
(NCOUNT) Default: 2 ! NCOUNT = 2 !

Minimum sigma y for a new puff/slug (m)
(SYMIN) Default: 1.0 ! SYMIN = 1.0 !

Minimum sigma z for a new puff/slug (m)
(SZMIN) Default: 1.0 ! SZMIN = 1.0 !

Default minimum turbulence velocities
sigma-v and sigma-w for each
stability class (m/s)
(SVMIN(6) and SWMIN(6)) Default SVMIN : .50, .50, .50, .50, .50, .50
Default SWMIN : .20, .12, .08, .06, .03, .016

Stability Class : A B C D E F

! SVMIN = 0.500, 0.500, 0.500, 0.500, 0.500, 0.500!
! SWMIN = 0.200, 0.120, 0.080, 0.060, 0.030, 0.016!

Divergence criterion for dw/dz across puff
used to initiate adjustment for horizontal
convergence (1/s)
Partial adjustment starts at CDIV(1), and
full adjustment is reached at CDIV(2)
(CDIV(2)) Default: 0.0,0.0 ! CDIV = .0, .0 !

Minimum wind speed (m/s) allowed for
non-calm conditions. Also used as minimum
speed returned when using power-law
extrapolation toward surface
(WSCALM) Default: 0.5 ! WSCALM = .5 !

Maximum mixing height (m)
(XMAXZI) Default: 3000. ! XMAXZI = 3000.0 !

Minimum mixing height (m)
(XMINZI) Default: 50. ! XMINZI = 50.0 !

Default wind speed classes --
 5 upper bounds (m/s) are entered;
 the 6th class has no upper limit
 (WSCAT(5)) Default :
 ISC RURAL : 1.54, 3.09, 5.14, 8.23, 10.8 (10.8+)

Wind Speed Class : 1 2 3 4 5 6
 --- --- --- --- --- ---
 ! WSCAT = 1.54, 3.09, 5.14, 8.23, 10.80 !

Default wind speed profile power-law
 exponents for stabilities 1-6
 (PLX0(6)) Default : ISC RURAL values
 ISC RURAL : .07, .07, .10, .15, .35, .55
 ISC URBAN : .15, .15, .20, .25, .30, .30

Stability Class : A B C D E F
 --- --- --- --- --- ---
 ! PLX0 = 0.07, 0.07, 0.10, 0.15, 0.35, 0.55 !

Default potential temperature gradient
 for stable classes E, F (degK/m)
 (PTG0(2)) Default: 0.020, 0.035
 ! PTG0 = 0.020, 0.035 !

Default plume path coefficients for
 each stability class (used when option
 for partial plume height terrain adjustment
 is selected -- MCTADJ=3)
 (PPC(6)) Stability Class : A B C D E F
 Default PPC : .50, .50, .50, .50, .35, .35
 --- --- --- --- --- ---
 ! PPC = 0.50, 0.50, 0.50, 0.50, 0.35, 0.35 !

Slug-to-puff transition criterion factor
 equal to sigma-y/length of slug
 (SL2PF) Default: 10. ! SL2PF = 10.0 !

Puff-splitting control variables -----
 VERTICAL SPLIT

 Number of puffs that result every time a puff
 is split - nsplit=2 means that 1 puff splits
 into 2
 (NSPLIT) Default: 3 ! NSPLIT = 3 !

Time(s) of a day when split puffs are eligible to
 be split once again; this is typically set once
 per day, around sunset before nocturnal shear develops.
 24 values: 0 is midnight (00:00) and 23 is 11 PM (23:00)
 0=do not re-split 1=eligible for re-split
 (IRESPLIT(24)) Default: Hour 17 = 1
 ! IRESPLIT = 0,0 !

Split is allowed only if last hour's mixing
 height (m) exceeds a minimum value
 (ZISPLIT) Default: 100. ! ZISPLIT = 100.0 !

Split is allowed only if ratio of last hour's
 mixing ht to the maximum mixing ht experienced
 by the puff is less than a maximum value (this
 postpones a split until a nocturnal layer develops)
 (ROLDMAX) Default: 0.25 ! ROLDMAX = 0.25 !
 HORIZONTAL SPLIT

Number of puffs that result every time a puff
 is split - nsplith=5 means that 1 puff splits
 into 5
 (NSPLITH) Default: 5 ! NSPLITH = 5 !

Minimum sigma-y (Grid Cells Units) of puff
 before it may be split
 (SYSPLITH) Default: 1.0 ! SYSPLITH = 1.0 !

Minimum puff elongation rate (SYSPLITH/hr) due to

wind shear, before it may be split
(SHSPLITH) Default: 2. !SHSPLITH = 2.0!

Minimum concentration (g/m^3) of each
species in puff before it may be split
Enter array of NSPEC values; if a single value is
entered, it will be used for ALL species
(CNSPLITH) Default: 1.0E-07 !CNSPLITH = 1.0E-07!

Integration control variables -----

Fractional convergence criterion for numerical SLUG
sampling integration
(EPSSLUG) Default: 1.0e-04 !EPSSLUG = 1.0E-04!

Fractional convergence criterion for numerical AREA
source integration
(EPSAREA) Default: 1.0e-06 !EPSAREA = 1.0E-06!

Trajectory step-length (m) used for numerical rise
integration
(DSRISE) Default: 1.0 !DSRISE = 1.0!

!END!

INPUT GROUPS: 11a, 11b, 11c, 11d -- Point source parameters

Subgroup (11a)

Number of point sources with
parameters provided below (NPT1) No default ! NPT1 = 1 !

Units used for point source
emissions below (IPTU) Default: 1 ! IPTU = 1 !

- 1 = g/s
- 2 = kg/hr
- 3 = lb/hr
- 4 = tons/yr
- 5 = Odour Unit * m^3/s (vol. flux of odour compound)
- 6 = Odour Unit * m^3/min
- 7 = metric tons/yr

Number of source-species
combinations with variable
emissions scaling factors
provided below in (11d) (NSPT1) Default: 0 ! NSPT1 = 0 !

Number of point sources with
variable emission parameters
provided in external file (NPT2) No default ! NPT2 = 0 !

(If NPT2 > 0, these point
source EMISSIONS are read from
the file: PTEMARB.DAT)

!END!

Subgroup (11b)

a
POINT SOURCE: CONSTANT DATA

Source No.	X UTM Coordinate (km)	Y UTM Coordinate (km)	Stack Height (m)	Base Elevation (m)	Stack Diameter (m)	Exit Vel. (m/s)	Exit Temp. (deg. K)	Bldg. Dwash Rates	Emission Rates
------------	-----------------------------	-----------------------------	------------------------	--------------------------	--------------------------	-----------------------	---------------------------	-------------------------	-------------------

! ! SRCNAM = P1 !
! ! X = 738.0, 4516.0, 20.0, 10.0, 30.0, 5.0, 350.0, .0,9.07E02 !
! ! FMFAC = 1.0 ! !END!

a
Data for each source are treated as a separate input subgroup
and therefore must end with an input group terminator.

SRCNAM is a 12-character name for a source
 (No default)
 X is an array holding the source data listed by the column headings
 (No default)
 SIGYZI is an array holding the initial sigma-y and sigma-z (m)
 (Default: 0.,0.)
 FMFAC is a vertical momentum flux factor (0. or 1.0) used to represent
 the effect of rain-caps or other physical configurations that
 reduce momentum rise associated with the actual exit velocity.
 (Default: 1.0 -- full momentum used)

b
 0. = No building downwash modeled, 1. = downwash modeled
 NOTE: must be entered as a REAL number (i.e., with decimal point)

c
 An emission rate must be entered for every pollutant modeled.
 Enter emission rate of zero for secondary pollutants that are
 modeled, but not emitted. Units are specified by IPTU
 (e.g. 1 for g/s).

 Subgroup (11c)

BUILDING DIMENSION DATA FOR SOURCES SUBJECT TO DOWNWASH

Source a
 No. Effective building width and height (in meters) every 10 degrees

a
 Each pair of width and height values is treated as a separate input
 subgroup and therefore must end with an input group terminator.

 Subgroup (11d)

a
 POINT SOURCE: VARIABLE EMISSIONS DATA

Use this subgroup to describe temporal variations in the emission
 rates given in 13b. Factors entered multiply the rates in 13b.
 Skip sources here that have constant emissions. For more elaborate
 variation in source parameters, use PTEMARB.DAT and NP12 > 0.

IVARY determines the type of variation, and is source-specific:
 (IVARY) Default: 0

- 0 = Constant
- 1 = Diurnal cycle (24 scaling factors: hours 1-24)
- 2 = Monthly cycle (12 scaling factors: months 1-12)
- 3 = Hour & Season (4 groups of 24 hourly scaling factors,
 where first group is DEC-JAN-FEB)
- 4 = Speed & Stab. (6 groups of 6 scaling factors, where
 first group is Stability Class A,
 and the speed classes have upper
 bounds (m/s) defined in Group 12)
- 5 = Temperature (12 scaling factors, where temperature
 classes have upper bounds (C) of:
 0, 5, 10, 15, 20, 25, 30, 35, 40,
 45, 50, 50+)

a
 Data for each species are treated as a separate input subgroup
 and therefore must end with an input group terminator.

 INPUT GROUPS: 12a & 12b -- Non-gridded (discrete) receptor information

 Subgroup (12a)

Number of non-gridded receptors (NREC) No default ! NREC = 1 !

!END!

 Subgroup (12b)

a
NON-GRIDDED (DISCRETE) RECEPTOR DATA

Receptor No.	X UTM Coordinate (km)	Y UTM Coordinate (km)	Ground Elevation (m)	Height b Above Ground (m)
1	742.0,	4528.0,	350.000,	1.500!

!END!

a
Data for each receptor are treated as a separate input subgroup and therefore must end with an input group terminator.

b
Receptor height above ground is optional. If no value is entered, the receptor is placed on the ground.



Input Groups in the CALPUFF Control File

<u>Input Group</u>	<u>Description</u>
*	<p>Run title</p> <p style="padding-left: 20px;">First three lines of control file (up to 80 characters/line)</p>
0	<p>Input and Output filenames</p>
1	<p>General run control parameters</p> <p style="padding-left: 20px;">Starting date and hour, run length, time step.</p> <p style="padding-left: 20px;">Number of species.</p> <p style="padding-left: 20px;">Model restart configuration for making a series of continuation runs.</p> <p style="padding-left: 20px;">Meteorological data format and averaging time adjustment.</p>
2	<p>Technical options</p> <p style="padding-left: 20px;">Control variables determining methods for treating chemistry, wet deposition, dry deposition, dispersion, plume rise, complex terrain, and near-field puff sampling methods</p>
3 a,b	<p>Species list</p> <p style="padding-left: 20px;">Species names, flags for determining which species are modeled, advected, emitted, and dry deposited</p>
4	<p>Grid control parameters</p> <p style="padding-left: 20px;">Specification of meteorological, computational, and sampling grids, number of cells, vertical layers, and reference coordinates.</p>
5	<p>Output options</p> <p style="padding-left: 20px;">Printer control variables, disk output control variables</p>
6a,b,c	<p>Subgrid scale complex terrain (CTSG) inputs</p> <p style="padding-left: 20px;">Information describing subgrid scale hill location, shape and height. Complex terrain receptor locations and elevations.</p>
7	<p>Dry deposition parameters - Gases</p> <p style="padding-left: 20px;">Pollutant diffusivity, dissociation constant, reactivity, mesophyll resistance, Henry's law coefficient</p>

Input Groups in the CALPUFF Control File

<u>Input Group</u>	<u>Description</u>
8	Dry deposition parameters - Particles Geometric mass mean diameter, geometric standard deviation
9	Miscellaneous dry deposition parameters Reference cuticle and ground resistances, reference pollutant reactivity, vegetation state
10	Wet deposition parameters Scavenging coefficients for each pollutant and precipitation type (liquid and frozen precipitation)
11	Chemistry parameters Control variables for input of ozone data, background ozone and ammonia concentrations, nighttime transformation rates
12	Miscellaneous dispersion parameters and computational parameters Vertical dispersion constants, dispersion rate above the boundary layer, crossover distance to time-dependent dispersion coefficients, land use associated with urban dispersion, site characterization parameters for single-point meteorological data files, sampling constraints, puff-splitting controls, plume path coefficients, wind speed power-law exponents, default temperature gradients and wind speed classes
13a,b,c,d	Point source parameters Point source data including source location, elevation, stack parameters, emissions, units, building dimensions, variable emissions cycle
14a,b,c,d	Area source parameters Area source data including source location, effective height, elevation, initial sigmas, emissions, units, variable emissions cycle
15a,b,c	Line source parameters Buoyant line source data including source location, elevation, line length, buoyancy parameters, release height, emissions, units, variable emissions cycle
16a,b,c	Volume source parameters Volume source data including source location, elevation, effective height, initial size data, emissions, units, variable emissions cycle
17a,b	Non-gridded (discrete) receptor information Receptor coordinates and ground elevation

Summary of CALPUFF Output Files

Default File Name	Contents	Unit* Number	Type
RESTARTE.DAT	Output restart file containing a dump of all puff parameters sufficient to allow a model run to continue (optional)	IO4	Unformatted
CALPUFF.LST	List file produced by CALPUFF	IO6	Formatted
CONC.DAT	One-hour averaged concentrations (g/m^3) at the gridded and discrete receptors for species selected by the user in the control file (optional)	IO8	Unformatted
DFLX.DAT	One-hour averaged dry deposition fluxes ($\text{g}/\text{m}^2/\text{s}$) at the gridded and discrete receptors for species selected by the user in the control file (optional)	IO9	Unformatted
WFLX.DAT	One-hour averaged wet deposition fluxes ($\text{g}/\text{m}^2/\text{s}$) at the gridded and discrete receptors for species selected by the user in the control file (optional)	IO10	Unformatted
VISB.DAT	Relative humidity data required for visibility-related postprocessing (optional)	IO11	Unformatted
DEBUG.DAT	Tables of detailed puff/slug data useful for debugging (optional)	IO30	Formatted
MASSFLX.DAT	Hourly report of mass flux into and out of regions defined by the boundaries in the FLUXBDY.DAT file	IO36	Formatted
MASSBAL.DAT	Hourly report of changes in mass of all species modeled	IO37	Formatted

* Variable shown is the parameter controlling the FORTRAN unit number associated with the file. Usually, the value assigned to the parameter is consistent with the name (i.e., IO8 = 8). However, the value can be easily changed in the parameter file to accommodate reserved unit numbers on a particular system.

APPENDIX IV

EXAMPLE OF SURF.DAT FILE FOR SURFACE METEOROLOGICAL DATA OF
YATAĞAN

```

00 336 0 00 339 23 2 1
17886
00 336 0
3.700000 145.000000 9998 0 279.300000 77 980.800000 9999
00 336 1
4.700000 55.000000 9998 0 279.000000 77 980.800000 9999
00 336 2
4.800000 145.000000 9998 0 278.900000 77 980.800000 9999
00 336 3
4.600000 45.000000 9998 0 278.300000 77 980.800000 9999
00 336 4
4.700000 102.500000 9998 0 277.300000 77 980.900000 9999
00 336 5
4.500000 102.500000 9998 0 277.000000 77 980.900000 9999
00 336 6
4.600000 112.500000 9998 0 277.000000 77 981.400000 9999
00 336 7
4.800000 132.500000 9998 0 277.300000 77 981.700000 9999
00 336 8
4.900000 137.500000 9998 0 280.500000 77 981.800000 9999
00 336 9
5.500000 15.000000 9998 0 281.500000 77 981.900000 9999
00 336 10
6.400000 65.000000 9998 0 285.000000 77 981.500000 9999

```


APPENDIX V

EXAMPLE OF UP.DAT UPPER AIR METEOROLOGICAL DATA FOR YATAĞAN

```

00 336  0  00 339  12  750
  F  F  F  F
9999      17240      001201 0      72
901.0/ 997./281.6/246/ 7  900.0/1006./282.6/999/999
899.0/1015./281.3/246/ 7  898.0/1024./281.8/245/ 7
897.0/1033./281.8/245/ 7  896.0/1042./281.9/245/ 8
893.0/1070./281.9/244/ 8  892.0/1079./281.8/244/ 8
891.0/1089./281.7/244/ 8  888.0/1116./281.7/244/ 8
887.0/1126./281.6/245/ 8  886.0/1135./281.6/245/ 8
885.0/1144./281.5/245/ 8  883.0/1163./281.3/245/ 8
882.0/1172./281.3/245/ 8  881.0/1182./281.2/245/ 8
880.0/1191./281.2/245/ 8  879.0/1200./281.0/245/ 13
878.0/1210./281.0/245/ 13  877.0/1219./280.9/245/ 13
874.0/1247./280.6/246/ 13  873.0/1257./280.5/246/ 13
872.0/1266./280.5/246/ 13  871.0/1276./280.4/246/ 13
869.0/1294./280.4/246/ 13  868.0/1304./280.3/246/ 9
857.0/1408./279.3/247/ 13  856.0/1418./279.2/247/ 13
855.0/1428./279.2/247/ 13  854.0/1437./279.1/247/ 13
853.0/1447./279.1/247/ 13  852.0/1456./279.0/247/ 13
851.0/1466./279.0/247/ 13  850.0/1475./278.9/246/ 13
845.0/1524./278.5/248/ 10  840.0/1572./278.2/248/ 14
835.0/1621./278.3/248/ 14  830.0/1670./277.9/248/ 14
825.0/1719./277.4/249/ 12  820.0/1768./278.0/249/ 12
810.0/1867./276.0/250/ 13  805.0/1917./275.6/251/ 13
800.0/1968./275.0/252/ 13  795.0/2018./274.6/253/ 13
790.0/2069./274.2/254/ 14  785.0/2120./274.4/254/ 14
775.0/2223./274.0/254/ 14  770.0/2275./273.7/254/ 15
765.0/2327./273.3/254/ 15  760.0/2379./272.8/254/ 16
755.0/2432./272.4/254/ 16  750.0/2485./271.9/253/ 16
700.0/3485./271.9/253/ 16

```

53

APPENDIX VI
EXAMPLE OF GEO.DAT FILE FOR THE GEOPHYSICAL PARAMETERS FOR
YATAĞAN

```
GEO.DAT 1 km grid 15x15 subset from ll corner
15, 15, 1.0, 592.0, 4126.0, 35
0 - LAND USE DATA - (0 = default categories)
41 41 41 41 43 43 32 32 32 32 32 42 32 32 32
41 31 31 41 41 32 32 32 32 32 32 32 32 32 32
31 22 22 41 41 32 43 30 22 41 32 32 32 32 32
22 31 32 41 31 32 32 43 32 32 32 32 32 32 32
41 41 32 31 41 32 41 32 32 32 41 32 32 32 42
22 41 41 31 41 41 32 32 32 32 32 32 32 32 42
22 41 43 42 32 41 32 32 11 11 32 32 43 42 42
43 42 33 42 43 13 32 -20 11 11 41 32 42 42 32
42 41 32 32 11 13 -20 -20 31 41 11 42 41 32 32
32 32 22 32 42 31 31 31 41 32 41 41 11 32 32
41 11 11 32 42 42 41 41 41 41 41 11 43 42
42 32 42 32 32 42 11 -20 31 41 11 11 11 42 42
31 32 31 32 31 32 32 31 11 -20 41 -20 11 41 32
31 42 43 43 42 42 32 31 32 32 32 41 21 41 42
43 22 42 42 42 32 32 32 32 11 11 41 42 42
1.00000
326.0 310.0 318.4 290.0 330.0 378.6 410.0 445.0 479.5
519.8 459.1 500.0 575.0 620.5 640.0
340.0 320.0 310.0 290.0 340.0 452.9 440.0 541.2 497.0
495.0 475.0 590.0 632.9 635.0 662.5
365.0 335.0 310.0 290.0 345.3 438.9 401.1 440.0 519.5
484.0 531.5 634.7 671.4 739.9 655.0
400.0 365.0 351.8 320.0 315.0 395.0 440.0 489.3 490.0
514.5 492.2 510.0 630.0 660.0 595.7
470.0 405.0 365.0 342.9 320.0 385.0 474.2 595.0 642.9
515.0 480.0 511.7 580.0 627.5 564.6
500.0 430.3 445.0 374.4 320.0 391.7 489.0 535.0 561.9
511.0 502.0 526.3 545.0 563.0 544.7
530.0 415.5 610.0 475.0 359.5 358.3 386.7 415.0 415.0
455.0 475.0 482.0 485.0 471.7 540.0
620.0 565.0 685.0 540.0 395.0 360.0 429.7 355.0 330.0
400.0 415.0 412.7 400.0 435.0 540.0
665.0 635.0 648.5 534.3 422.5 340.0 320.0 350.0 350.0
375.0 585.0 433.8 500.0 545.0 619.9
615.0 535.0 555.0 474.7 414.8 355.0 332.3 350.0 350.0
360.0 380.0 412.0 490.5 605.0 590.0
627.5 550.0 500.0 465.6 460.0 385.4 325.0 350.0 350.0
350.0 380.0 403.9 462.4 505.0 495.0
594.5 592.9 574.9 588.1 520.0 443.8 408.3 350.0 351.0
350.0 370.0 380.0 425.0 445.0 455.0
560.0 595.0 575.0 613.4 604.8 437.5 433.6 410.0 391.1
408.3 379.9 380.0 400.0 395.0 440.0
575.0 550.0 525.0 525.0 540.0 450.0 500.0 532.9 480.0
444.4 415.0 373.0 400.0 424.5 440.0
555.5 500.0 544.5 520.0 545.0 525.0 583.1 580.0 512.0
460.0 475.0 425.0 400.0 400.0 425.0
```

Extended CALMET Land Use Categories Based on the U.S. Geological Survey Land Use and Land
Cover Classification System (52-Category System)

Level I		Level II	
10	Urban or Built-up Land	11	Residential
		12	Commercial and Services
		13	Industrial
		14	Transportation, Communications and Utilities
		15	Industrial and Commercial Complexes
		16	Mixed Urban or Built-up Land
		17	Other Urban or Built-up Land
20	Agricultural Land — Unirrigated	21	Cropland and Pasture
		22	Orchards, Groves, Vineyards, Nurseries, and Ornamental Horticultural Areas
		23	Confined Feeding Operations
		24	Other Agricultural Land
-20	Agricultural Land — Irrigated	-21	Cropland and Pasture
		-22	Orchards, Groves, Vineyards, Nurseries, and Ornamental Horticultural Areas
		-23	Confined Feeding Operations
		-24	Other Agricultural Land
30	Rangeland	31	Herbaceous Rangeland
		32	Shrub and Brush Rangeland
		33	Mixed Rangeland
40	Forest Land	41	Deciduous Forest Land
		42	Evergreen Forest Land
		43	Mixed Forest Land
50	Water	51	Streams and Canals
		52	Lakes
		53	Reservoirs
		54	Bays and Estuaries
		55	Oceans and Seas
60	Wetland	61	Forested Wetland
		62	Nonforested Wetland
70	Barren Land	71	Dry Salt Flats
		72	Beaches
		73	Sandy Areas Other than Beaches
		74	Bare Exposed Rock
		75	Strip Mines, Quarries, and Gravel Pits
		76	Transitional Areas
		77	Mixed Barren Land
80	Tundra	81	Shrub and Brush Tundra
		82	Herbaceous Tundra
		83	Bare Ground
		84	Wet Tundra
		85	Mixed Tundra
90	Perennial Snow or Ice	91	Perennial Snowfields
		92	Glaciers

Note: Negative values indicate irrigated land use.

* Values used for JWAT (Input Group 6) or IWAT (GEO.DAT Input File)

UTM (Universal Transverse Mercator) Coordinates

The Universal Transverse Mercator projection and grid system was adopted by the U.S. Army in 1947 for designating rectangular coordinates on large scale military maps. UTM is currently used by the United States and NATO armed forces. With the advent of inexpensive GPS receivers, many other map users are adopting the UTM grid system for coordinates that are simpler to use than latitude and longitude.

The UTM system divides the earth into 60 zones each 6 degrees of longitude wide. These zones define the reference point for UTM grid coordinates within the zone. UTM zones extend from a latitude of 80° S to 84° N. In the Polar Regions the Universal Polar Stereographic (UPS) grid system is used.

UTM zones are numbered 1 through 60, starting at the International Date Line, longitude 180°, and proceeding east. Zone 1 extends from 180° W to 174° W and is centered on 177° W. Each zone is divided into horizontal bands spanning 8 degrees of latitude. These bands are lettered, south to north, beginning at 80° S with the letter C and ending with the letter X at 84° N. The letters I and O are skipped to avoid confusion with the numbers one and zero. The band lettered X spans 12° of latitude.

A square grid is superimposed on each zone. It is aligned so that vertical grid lines are parallel to the center of the zone, called the central meridian.

UTM grid coordinates are expressed as a distance in meters to the east, referred to as the “easting” and a distance in meters to the north, referred to as the “northing”.

(Source: <http://www.maptools.com/UsingUTM/UTMdetails.html>)